The Stellate Cancer-Associated Fibroblast in Pancreatic Ductal Adenocarcinoma; Its role in Chemoresistance

Miss Natalie Georgette Johnson

A thesis presented for the degree of Doctor of Philosophy

(PhD)

Imperial College London

Hammersmith Campus

Du Cane road, London

W12 ONN

Institute of Cancer Research

237, Fulham road, London

SW3 6JB

Declaration

This thesis was completed under the supervision of Mr Duncan Spalding, Dr Chris Lord, Professor Alan Ashworth, Professor Gordon Stamp and Dr. Andrew Thillainayagam. The work described was carried out at Imperial College, Hammersmith campus, Investigative sciences department, Du Cane road, London, W12 ONN; at Cancer Research UK, 61 Lincoln's Inn Fields, London WC2A 3PX; and the Institute of Cancer Research, 237 Fulham road, Chelsea, London, SW3 6JB.

I, Natalie G Johnson, confirm that the work presented in this thesis is my own. Where information has been derived from other sources, I confirm this has been indicated in the thesis.

Date: 28.12. 2012

Abstract

Introduction: The tumour microenvironment has been found to contribute to cancer survival and progression, and more specifically, the stromal microenvironment has been implicated in the drug resistant nature of cancers such as pancreatic cancer. This microenvironment consists of fibroblasts, pericytes, endothelial cells and the extracellular matrix, with the stellate cancer-associated fibroblast (CAF) being the most predominant cell type present. The aim of this study was to investigate the role of the cancer associated fibroblast in tumourigenesis in Pancreatic Ductal Adenocarcinoma (PDA) with specific reference to the mechanisms involved in chemoresistance via the stellate cancer associated fibroblast.

Methods: I investigated the molecular pathogenesis of PDA assessing DNA copy number alterations (CNA) in selection of clinically relevant PDA cell lines (PANC-1, MiaPaCa-2, ASPC-1, SU86.86, HPAC, HS776T, PL5 and PL45), seven primary resected, non immortalised samples (PF3, PF7, PF8, PF9, PF16, PF18 and PF20) and an immortalised stellate cell line using array comparative genomic hybridization (aCGH). All cultures and cell lines were then screened in order to determine their sensitivity to currently used therapeutic compounds. Analysis was done using R software and Graph Pad Prism 5.

Results: The non-immortalised stellate CAFs and formalin fixed paraffin embedded stromal fibroblast samples showed no homozygous genomic CNAs. The stellate cancer associated fibroblasts both primary and immortalised appear more responsive to the chemotherapeutic drugs in the compound library compared to the PDA cell lines.

Conclusions: This study suggests the absence of homozygous deletions that may lead to a change in phenotype in the stellate CAF. However, the presence of heterozygous deletions and epigenetic changes has not yet been excluded. Further experiments such as micro RNA and epigenetic studies, such as SNP arrays, may identify the presence of aberrations that have aetiological significance in carcinogenesis even if they do not result in CNVs. This higher sensitivity of the stellate CAF to the drugs in the chemotherapy library may favour them as potential targets for management of this hard to street subtype of disease.

Acknowledgements

I would like to thank my supervisor, Mr Duncan Spalding who graciously took over my academic supervision during the second half of this PhD and patiently guided it to its completion. I am grateful for all your invaluable support and accessibility. I would like to thank Professor Gordon Stamp and Dr Andrew Thillainayagam for their supervision during the first half of this PhD. I gained valuable experience and developed skills that were utilised throughout the research process.

I am indebted to Mr Alan Ashworth, Dr Chris Lord and Dr Claus Jorgensen who generously took me under their wing for the second half of this PhD and thoroughly guided it to success. I am grateful to them for giving me the opportunity to continue research at the Institute of cancer research and for generously providing resources, technical support and guidance for me to complete this research.

I would also like to thank Dr Jayson Wang and Ms Mahrokh Nohadani for their, supervision throughout the first half of this PhD; Dr Vikash Reebye of the Francis Fraser Lab at Imperial College Hammersmith for his assistance with protein gel work, continued support with lab resources and his invaluable and patient editing of written work; Dr William Mathieson for his help on protein gel work and Professor Gerry Thomas and her group at Imperial College Hammersmith Campus.

I am especially grateful to Emma Nye, Richard Stone and Bradley Spencer-Dene at the Cancer Research UK experimental pathology lab, for their generous cutting and preparation of samples and for the use of their Laser Capture Micro-dissection microscope and their continued moral support throughout this PhD.

I also need to thank Professor Jorge Reis-Filho, Maryou Lambros, Daniel Wetterskog, Radost Vatcheva and the rest of the team at the Breakthrough Breast lab at the Institute of Cancer Research for their invaluable scientific support and their generosity of time and resources towards the completion of the array CGH, F.I.S.H and Western Blot techniques in the first stage of this PhD. I thank the London Clinic and Imperial College for providing funding during this period of research.

Finally I would like to thank my parents, especially my mother, Catherine Johnson, and sisters Corrinne and Amanda for their continued support during this trying time and for their continuous prayers, optimism, tolerance and encouragement.

Table of Contents

Title page **1**

Declaration **2**

Abstract **3**

Acknowledgements **5**

Table of contents **7**

List of figures **14**

List of tables **17**

Abbreviations **19**

Chapter 1 Introduction

1.1 General introduction…..... 21

1.2 Pancreatic Ductal Adenocarcinoma 23

1.2.1 Pancreatic cancer morbidity and mortality 23

1.2.1.1 Risk factors 25

1.2.1.2 Symptoms..... 26

1.2.1.3 Prognosis..... 26

1.2.1.4 Management..... 27

1.2.2 Pancreatic cancer current treatment modalities 28

1.2.2.1 Clinical trials 30

1.2.2.1.1 Adjuvant therapy 30

1.2.2.1.2 Neoadjuvant therapy 32

1.2.2.1.3 Targeted therapy 33

1.2.3 Pancreatic cancer and the stroma 34

1.3 The Cancer-associated fibroblast 37

1.3.1 The Cancer-associated fibroblasts (CAF) 37

1.3.2 Origins of the Cancer-associated fibroblast 40

1.3.3 Crosstalk between the CAF and tumour 43
1.3.4 Genetic changes 48
1.3.4.1 Somatic mutations 49
1.3.4.2 Loss of heterozygosity and SNPs 50
1.3.4.3 Gene expression 52
1.3.4.4 Pluripotency in CAFs…….....54
1.4 Chemo-resistance in pancreatic cancer 55
1.4.1 Genetic mutations 56
1.4.1.1 Micro RNA gene expression profiling……...58
1.4.2 Upregulated survival pathways /downregulated apoptosis and protein secretion 62
1.4.3 Gene products involved in Gemcitabine uptake 62
1.4.4 The Pancreatic Stellate cells (PSC) and chemoresistance 64
1.4.5 The hedgehog signalling pathway 65
1.4.6 Stromal density and chemoresistance 67
1.5 Aims 68
Chapter 2 Materials and Methods
2.1 Materials 69
2.1.1 General use reagents 69
2.1.2 Reagents used for cell culture 70
2.1.3 Reagents used for Immunohistochemistry 71
2.1.4 Reagents used for Gel Analysis.....72
2.1.5 Reagents used for Laser capture microdissection.....73
2.1.6 Reagents used for Pico green 74
2.1.7 Reagents used for Multiplex PCR 75

2.1.8 Reagents used for Array CGH 76
2.1.9 Reagents used for FISH 77
2.1.10 Reagents used for CTG 78
2.1.11 Reagents used for plasmid DNA transfection 78
2.2 Methods
2.2.1 Ethics approval 79
2.2.2 Tissue collection 79
2.2.3 Cell culture 79
2.2.4 Immunohistochemistry 83
2.2.5 Laser capture micro-dissection of FFPE 85
2.2.6 Array CGH of cell lines and FFPE 90
2.2.7 Fluorescent in Situ Hybridisation FISH 97
2.2.8 Cell titre Glo 102
2.2.8.1 Cell titration for Gemcitabine curves 102
2.2.8.1.1 Gemcitabine resistance after 72 hours 102
2.2.8.1.2 Gemcitabine resistance after 6 days 103
2.2.8.2 Cell titre Glo (CTG) survival readings 103
2.2.8.3 High throughput screening 104
2.2.9 Luciferase marking of PDA and stellate cell lines 105
2.2.9.1 Generating Renilla and Firefly luciferase plasmid 105
2.2.9.2 Plasmid purification using Gen-Elute™ HP plasmid Miniprep kit and protocol 107
2.2.9.3 Digestion 108
2.2.9.4 Agarose gel purification and DNA extraction 110
2.2.9.5 Ligation of luciferase insert into vector 112

2.2.9.6 Transformation of the DNA 113
2.2.9.7 Amplification of colonies 114
Chapter 3 Cancer associated fibroblasts cultured from primary pancreatic specimen and formalin fixed paraffin embedded pancreatic LCM tissue stroma display no copy number changes
3.1 Introduction 116
3.2 Cell culture 118
3.3 DNA yield and quality 120
3.3.1 Pico green assay of DNA LCM samples 122
3.4 ArrayCGH analysis results 124
3.4.1 Genome plots for primary cultured fibroblasts 126
3.4.2 Genome plots for FFPE samples 126
3.5 Fluorescent in situ hybridisation (FISH) analysis of copy number Alterations 132
3.6 Discussion 135
Chapter 4 The pancreatic cancer cell and Chemo-resistance
4.1 Introduction 140
4.1.1 Chemoresistance in pancreatic ductal adenocarcinoma (PDA) has been the limiting factor to disease management 140
4.1.2 Chemoresistance is multifactorial 140
4.1.2.1 Cancer cell mutations, poor drug delivery, anti apoptotic factors, activated tumour-stromal cell interactions and signalling pathways 141
4.1.2.1.1 Cancer cell mutations 141
4.1.2.1.2 Drug delivery: Gemcitabine transport, uptake and

Metabolism 142
4.1.2.1.2.1 Gemcitabine transport and uptake 142
4.1.2.1.2.2 Gemcitabine Metabolism 143
4.1.2.1.3 Acquired chemoresistance due to downregulation of proapoptotic genes and upregulation of anti apoptotic genes 145
4.1.2.1.4 Activated tumour-stromal cell interactions and signalling pathways.....146
4.2 Compound library High throughput screening (HTS) of PDA cell lines 147
4.2.1 Ashworth plate 10 compound library 147
4.2.1.1 Map of the sample layout for HTS 148
4.2.1.2 Cell titre Glo (CTG) survival readings 151
4.2.2 Cell titration for PDA cell lines 151
4.2.3 Baseline Gemcitabine resistance curves for PDA cell lines 153
4.2.3.1 Gemcitabine resistance after 72 hours of treatment 153
4.2.3.2 Gemcitabine resistance after 6 days of treatment 155
4.2.4 HTS Screen results of all PDA models 157
4.2.4.1 Cell Survival HTS results for AsPC-1 158
4.2.4.2 Cell Survival HTS results for HPAC 160
4.2.4.3 Cell Survival HTS results for Hs776T 162
4.2.4.4 Cell Survival HTS results for PANC-1 164
4.2.4.5 Cell Survival HTS results for PL5.....166
4.2.4.6 Cell Survival HTS results for PL45 168
4.2.4.7 Cell Survival HTS results for MiaPaCa-2 170
4.2.4.7.1 HTS results for clone 2 of luciferase marked MiaPaCa-2 172

4.2.4.7.2 HTS results for clone 3 of luciferase marked MiaPaCa-2 174
4.2.4.7.3 HTS results for parent MiaPaca2 and luciferase clones...176
4.2.4.8 Cell Survival HTS results for Su86.86 177
4.2.5 Comparison of cell survival at low concentrations 10nM 179
4.2.6 Comparison of cell survival at higher concentration 100nM 181
4.3 Discussion 183
Chapter 5 The pancreatic stellate cell and Chemo-resistance
5.1 Introduction 188
5.1.1 Crosstalk and chemoresistance 189
5.1.2 Hedgehog (Hh) signaling and chemoresistance 191
5.1.3 Stromal density and chemoresistance 193
5.2 High throughput screen results of stellate cancer associated fibroblasts 194
5.2.1 Cell survival HTS results for PF3 196
5.2.2 Cell survival HTS results for PF18 198
5.2.3 Cell survival HTS results for PF20 200
5.2.4 Cell survival HTS results for Immortalised human pancreatic Stellate cells 202
5.2.5 Repeat cell survival HTS results for Immortalised human pancreatic Stellate cells 204
5.2.6 Comparison of cell survival at low concentration of10nM 205
5.2.7 Comparison of cell survival at higher concentration of 100nM 207
5.3 Discussion 209
Chapter 6 Conclusion.....211
Chapter 7 Future Work 214
Appendix 1 Quality control Z factor scores for PDA and Stellate cells.....220

Bibliography.....233

List of Figures

Chapter 1

Figure 1.1 The Anatomy of the Pancreas

Figure 1.2 The quiescent and activated cancer-associated fibroblast

Figure 1.3 Factors involved in crosstalk between the CAF and the stroma

Figure 1.4 The Hedgehog signalling pathway

Chapter 2

Figure 2.1 Electron microscopy of primary fibroblasts at 10X magnification

Figure 2.2 Immunohistochemistry of primary fibroblasts

Figure 2.3 Zeiss P.A.L.M. Laser Capture Micro-dissection station

Figure 2.4 H and E stained and LCM methyl green cut sample of FFPE

Figure 2.5 Principle of ArrayCGH

Figure 2.6 Region overview of Chromosome 19P 13.2 showing a possible gain

Figure 2.7 Luciferase plasmid containing the synthetic Renilla and Firefly insert

Figure 2.8 Steps in Luciferase cloning

Figure 2.9 Agarose Gel purification and extraction of Renilla and Firefly luciferase

Figure 2.10 Agarose gel showing the 5 colonies with the Renilla insert

Chapter 3

Figure 3.1 Genome plots for primary cultured stellate cells

Figure 3.2 Genome plots for FFPE stroma C33 and 3KS

Figure 3.3 Region overview of Ch19p13.2

Figure 3.4 FISH analysis of Copy Number Variations in a Normal lymphocyte cell

Figure 3.5 FISH Probe analyses for PF3, PF7, PF9, and PF16

Chapter 4

Figure 4.1 Gemcitabine metabolism, activation and excretion

Figure 4.2 Heat map of the 384 well High Throughput Screen

Figure 4.3 Schematic of High throughput screening

Figure 4.4 Simple cell titration of PDA cell lines

Figure 4.5 Gemcitabine survival curves at 72 hours

Figure 4.6 Gemcitabine survival curves at 6 days

Figure 4.7 Quality control heat map, bar graph and box plot for ASPC-1

Figure 4.8 Cell Survival HTS results for ASPC-1

Figure 4.9 Quality control heat map, bar graph and box plot for HPAC

Figure 4.10 Cell Survival HTS results for HPAC

Figure 4.11 Quality control heat map, bar graph and box plot for Hs776T

Figure 4.12 Cell Survival HTS results for Hs776T

Figure 4.13 Quality control heat map, bar graph and box plot for PANC-1

Figure 4.14 Cell Survival HTS results for PANC-1

Figure 4.15 Quality control heat map, bar graph and box plot for PL5

Figure 4.16 Cell Survival HTS results for PL5

Figure 4.17 Quality control heat map, bar graph and box plot for PL45

Figure 4.18 Cell Survival HTS results for PL45

Figure 4.19 Quality control heat map, bar graph and box plot for MiaPaca2

Figure 4.20 Cell Survival HTS results for MiaPaca2

Figure 4.21 Quality control heat map, bar graph and box plot for clone 2 of luciferase marked MiaPaca2

Figure 4.22 Cell Survival HTS results for clone 3 of luciferase marked MiaPaca2

Figure 4.23 Quality control heat map, bar graph and box plot for clone 3 of luciferase marked MiaPaca2

Figure 4.24 Cell Survival HTS results for clone 3 of luciferase marked MiaPaca2

Figure 4.25 Cell Survival HTS results for clone MiaPaca2 and its clones

Figure 4.26 Quality control heat map, bar graph and box plot for Su86.86

Figure 4.27 Cell Survival HTS results for Su86.86

Chapter 5

Figure 5.1 Quality control heat map, bar graph and box plot for PF3

Figure 5.2 Cell Survival HTS results for primary stellate cell line PF3

Figure 5.3 Quality control heat map, bar graph and box plot for PF18

Figure 5.4 Cell Survival HTS results for Immortalized PF18

Figure 5.5 Quality control heat map, bar graph and box plot for PF20

Figure 5.6 Cell Survival HTS results for Immortalized PF20

Figure 5.7 Quality control heat map, bar graph and box plot for HPSC

Figure 5.8 Quality control heat map, bar graph and box plot for HPSC screen 2

Figure 5.9 Cell Survival HTS results for Immortalized HPSCs

List of Tables

Chapter 1

Table 1.1 Studies of chromosomes/gene copy number changes in CAFs

Table 1.2 Studies using gene expression microarrays on CAFs

Table 1.3 The common genetic changes found pancreatic cancer cell lines

Table 1.4 MicroRNA expression in PDAC

Chapter 2

Table 2.1 The low range standard curve used for Pico Green quantification

Table 2.2 DNA concentrations and volumes added for initial labelling step

Table 2.3 DNA concentrations of the BAC clones chosen

Table 2.4 Nanodrop quantification of Plasmid DNA

Table 2.5 Enzymes and buffers needed for luciferase digestion

Table 2.6 Reagent mix for digestion step

Table 2.7 Molecular weights of Gel bands

Table 2.8 Nanodrop quantification of DNA extracted from the Agarose gel

Table 2.9 Average concentrations of colonies formed

Table 2.10 Reagent mix for digestion of colonised DNA and negative control

Chapter 3

Table 3.1 Cell culture library from primary wedge resections

Table 3.2 Archival FFPE specimens obtained from LCM Initial specimen blocks

Table 3.3 Pico green quantification of double stranded DNA in LCM tissues

Table 3.4 Variation loci found at 19p13.2

Chapter 4

Table 4.1 Ashworth plate 10 compound library

Table 4.2 Cell survival for PDA cell lines at 10nM of compound

Table 4.3 Cell survival for PDA cell lines at 100nM of compound

Chapter 5

Table 5.1 Cell survival for stellate cell lines at 10nM concentrations

Table 5.2 Cell survival for stellate cell lines at 100nM concentrations

List of abbreviations

AKT	protein kinase B
αSMA	α smooth muscle actin
β-catenin	Beta catenin
BSA	Biotinylated secondary antibody
CAF	Cancer-associated fibroblasts
CO_2	Carbon dioxide
Cy3	Cyanine 3
Cy5	Cyanine 5
ddH2O	Distilled and deionised water
DMEM	Dulbecco's Modified Eagles Medium
DMSO	Dimethylsulfoxide
DNA	Deoxyribonucleic acid
dNTP	Deoxynucleotide triphosphate
ECM	Extra-cellular matrix
EMT	Epithelial to Mesenchymal transition
FCS	Foetal Calf Serum
FFPE	Formalin fixed paraffin embedded
FSP-1	Fibroblast specific protein-1
IL	Interleukin
ILGF	Insulin like growth factor
LCM	Laser capture microdissection
L-GLUT	L- glutamine
LOH	Loss of Heterozygosity
MAPK	Mitogen-activated protein kinase

MgCl2	Magnesium chloride
NASCN	Sodium Thiocyanate
PAGE	Polyacrylamide gel electrophoresis
PBS	Phosphate buffered saline
PCR	Polymerase chain reaction
PI3K	Phosphoinositide 3- kinase
Pen/Strep	Penicillin /streptomycin
PSC	Pancreatic stellate cells
RNA	Ribonucleic acid
Rpm	Revolutions per minute
RPMI	Roswell Park Memorial Institute
RT	Room temperature
SSC	Saline-sodium citrate
SDF1	Stromal cell derived factor 1
SDS	Sodium dodecyl sulphate
siRNA	Small interfering RNA
TE	Tris ((hydroxymethyl) aminomethane) and EDTA (ethylenediaminetetraacetic acid)
TBE	Tris/Borate/EDTA
TGF-β	Transforming growth factor β
TNF	Tumour necrosis factor
Tris	Tris (hydroxymethyl) methylamine
VEGF	Vascular endothelial growth factor

Chapter 1: Introduction

1.1 General Introduction

Pancreatic cancer is known for its poor morbidity and high mortality rates. Its surgical management is complicated by its late presentation, early local invasion, distant metastasis of the tumour, and its resistance to the current chemotherapeutic agents. Despite the use of Gemcitabine as adjuvant therapy, the average survival still only ranges around 6 months for those with metastatic disease and 10 months for those with locally advanced disease (*Benson et al 2011*).

Neither clinical response nor quality of life was improved with the Gemcitabine/Capecitabine combination when compared to Gemcitabine alone, (*Bernhard et al, 2008)*. For those trials in which patients experienced an improved response rate or better median survival, the toxicity of the combinations regimes was too severe as was seen in Gemcitabine/ Erlotinib *vs.* Gemcitabine alone, (*Vervenne et al ,2008*).

The non-Gemcitabine regimen of Folforinox, Oxaliplatin and Irinotecan improved median survival but was toxic and patients presented with other complications such as febrile neutropenia, (*Conroy et al, 2011*). Most trials using combination therapy have failed due to the severe toxicity and therefore Gemcitabine is still considered the mainstay therapy for metastatic and unresectable disease. As yet, radiotherapy has not proved beneficial and has added toxicity (*Loehrer et al, 2008*). These and further trials are discussed in detail in section 1.2.2.

The development of chemo-resistant tumours can be attributed to numerous factors including mutated signalling pathways such as the hedgehog signalling pathway, and selective clonal expansion of transformed cells. Although these factors are not mutually exclusive, it is becoming more evident that the stromal microenvironment plays a significant role in this setting. It was previously believed that tumour epithelial cells displayed the up-regulated pathways that stimulated stromal development, (*Bailey et al, 2008)*. It has since been shown that these pathways are indeed upregulated in the stromal compartment and have an effect on tumour growth and development.

The stromal desmoplasia is a dense proliferation of multiple cell types and vasculature that affects drug delivery to tumour sites. The most prominent cell type found, the cancer associated-Fibroblast (CAF) or activated fibroblast is a stellate cell that is suspected to play a role in chemo-resistance via multiple signalling pathways between the stroma and tumour. Pancreatic cancer specimens have been shown to be made up of more than 90% representation by these pancreatic stellate cells within the stromal microenvironment. This therefore makes it a suitable vehicle to study their role in tumour progression, metastasis and chemoresistance.

1.2 Pancreatic Ductal Adenocarcinoma

1.2.1 The Pancreas, cancer, morbidity and mortality

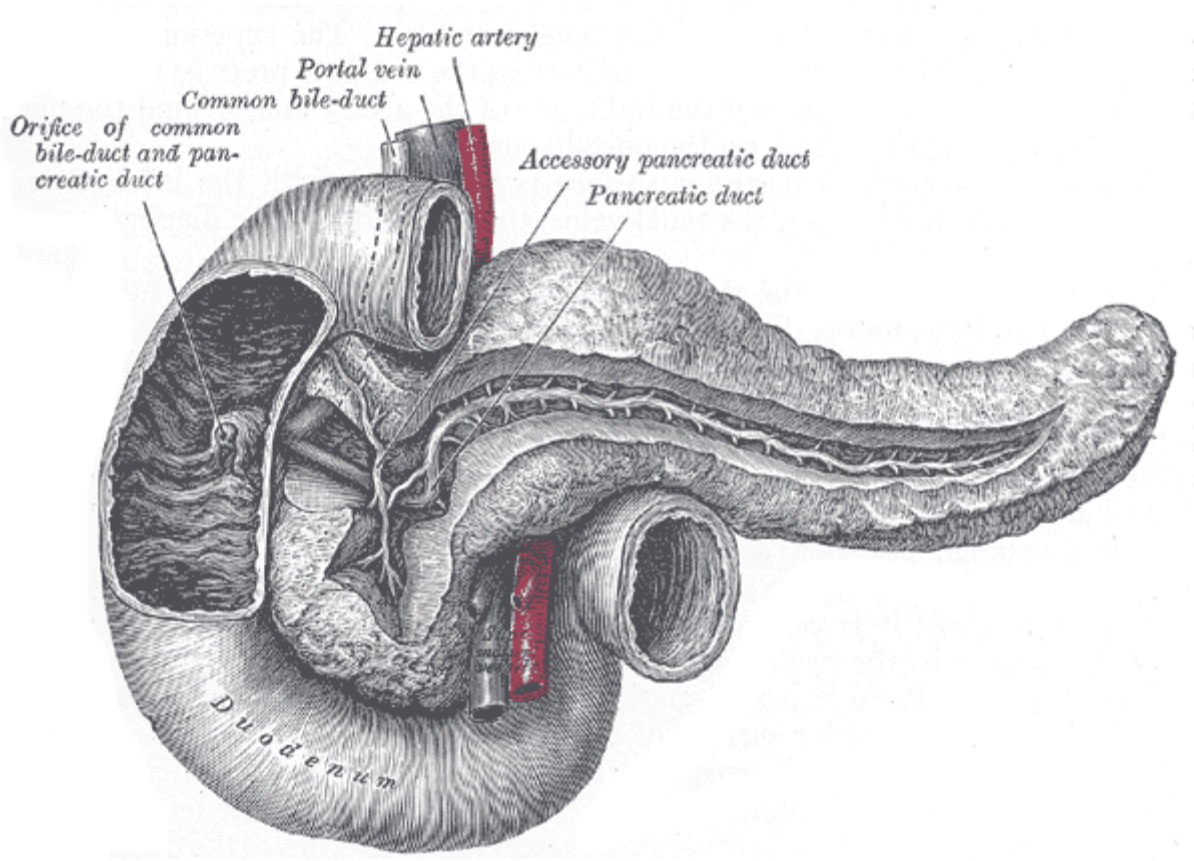


Figure 1.1 The Pancreas.

The Pancreas, as represented in figure 1.1, is situated transversely across the posterior wall of the abdomen. It has a long irregular prismatic shape with a head (the broadest portion), neck, body and tail. Its length varies from 12.5 to 15cm and its weight from 60gms to 100gms. In the digestive system it is the organ responsible for the production of insulin and digestive juices containing digestive enzymes. Pancreatic adenocarcinoma is a malignant exocrine neoplasm of the pancreas. It is the tenth most common site of new cancers and the fourth leading cause of cancer deaths among men and women, being responsible for 6% of all cancer-related deaths, (*Anderson et al, 2006*).

Internationally, pancreatic cancer ranks 13th in incidence and 8th as a cause of cancer death with an incidence rate of 8-12/100,000 people per year, (*Anderson et al, 2006*). Endocrine tumours of the pancreas or pancreatic neuroendocrine tumours (PNETs) as they are called, account for only 1% of pancreatic cancers. They arise from the amine precursor and uptake cells (APUD) of the pancreas. These stem cells are pluripotent cell found in the ducal epithelium of the pancreas and areas of the distal foregut. They are characterised into functional, if they produce clinical symptoms due to hypersecretion of hormones or non-functional.

The majority of PNETs are non–functional (*Halfdanarson et al 2008*). Although they secrete pancreatic peptide (PP), this does not result in any syndrome related to its hypersecretion. The annual clinical incidence is low and most are benign. According to British Society of Gastroenterology, the incidence of PNETs is around 0.2-0.4 per 100,000. Insulinomas and Gastrinomas account for over 50% of cases. Vasoactive intestinal polypeptide-secreting tumours, (VIPomas) are one eighth and glucagonomas (secretes glucagon) are one seventeenth as common. Somatostatinomas, (secretes somatostatin), are rare and non-functional tumours account for 14-48% of all recognised PNETs (*British Society of Gastroenterology,* 2012).

The remaining 99% of tumours however, arise from the exocrine pancreas. Of these, 95% are adenocarcinomas and the remaining 5% include adenosquamous carcinomas, signet ring cell carcinomas, hepatoid carcinomas, colloid carcinomas, undifferentiated carcinomas and undifferentiated carcinomas with osteoclast-like giant cells*, (WHO Cancer, 2009).* Most carcinomas of the pancreas occur within the head and neck, accounting for 75% of these tumours. About 15-20% occur in the body and the remaining 5-10% occur in the tail, (*Dragovich et al, 2012)*.

1.2.1.1 Risk factors

Suspected risk factors include smoking 30%, dietary factors and obesity 20%. About 40% of cases are estimated to be sporadic and only 5-10% of patients with pancreatic cancer are believed to be hereditary, (*Raimondi et al 2009*). The risk associated with alcohol is controversial but the risk increases significantly with longstanding chronic pancreatitis, (*Lowenfels et al, 1993*), which can occur as a result of excessive alcohol consumption.

The molecular genetics of pancreatic adenocarcinoma have been well studied. Of these tumours, 80-95% have mutations in the *KRAS2* gene; 85-98% have mutations, deletions, or hypermethylation in the *CDKN2* gene; 50% have mutations in *p53*; and about 55% have homozygous deletions or mutations in *Smad4,* (*Soto et al, 2006, Hahn et al, 1995, Shi et al, 2008).* Some of these mutations can also be found in high-risk precursors of pancreatic cancer. For example, in chronic pancreatitis, 30% of patients have detectable mutations in *p16* and 10% have K-*ras* mutations, (*Dragovich et al, 2012).*

1.2.1.2 Symptoms

Symptoms of pancreatic cancer include epigastric and back pain, which is seen in up to 85% of patients with locally advanced disease, loss of appetite, nausea and vomiting, significant weight loss, painless jaundice and thrombophlebitis (Trousseau's sign). Painless obstructive jaundice is present in 50% of patients with locally unresectable disease. Many patients develop diabetes mellitus in advance of the diagnosis of pancreatic cancer but this is not a definitive screening test. Patients diagnosed with pancreatic cancer have a very poor prognosis owing to the late presentation of symptoms at the time of diagnosis.

1.2.1.3 Prognosis

The median survival for patients with pancreatic cancer without treatment is 3-6 months from the time of diagnosis. The 1 year relative survival rate for all stages combined is 24% (*American Cancer society, 2009*) and the overall 5 year survival is less than 5%, (*Carpelan-Holmstrom et al, 2005).* In the UK, 8364 people were diagnosed with pancreatic cancer in 2009 and around 7900 died from this disease in 2010. Between 2005 and 2009 the 5 year survival rate was 4%, (*Cancer Research UK, 2012*). In about 20% of patients that have had a successful potentially curative resection, the median survival time ranges from 12-19 months, and the 5-year survival rate is 15-20%, (*Dragovich et al, 2012).*

1.2.1.4 Management

Surgical resection of the tumour is the current treatment modality for pancreatic cancer depending on the stage at presentation. Only about 15% of patients present early enough to be considered for resection and more than 80% of these re-present with local or metastatic disease within 2 years (*Stathis/Moore*, 2010; *Sperti et al, 2007*). Currently the best predictors of long-term survival after surgery are a tumour diameter of less than 3 cm, no nodal involvement, negative resection margins, and diploid tumour deoxyribonucleic acid (DNA) content, (*Allison et al, 1991)*.

Most patients present at the stage of locally advanced or metastatic disease. For patients with extra-peritoneal disease, surgery can only be considered as palliative intervention. For those whom curative or palliative surgery is not an option, palliative chemotherapy, Gemcitabine being the gold standard since 1997, provides an alternative in order to improve quality of life and possibly gain a marginal survival benefit *(Burris et al, 1997).*

The current deterrent in management of pancreatic cancer resulting in its poor clinical outcome is the late stage at which patients present as well as the resistance of pancreatic cancer to the current treatment modalities. This drug resistance is proposed to be due to its aggressive desmoplastic reaction surrounding the tumour which appears to affect suitable drug delivery. Notably, the CAF is the most prominent cell found in this area of desmoplasia, (*Armstrong et al, 2004, Watanabe et al, 2003)*.

1.2.2 Pancreatic cancer and current treatment modalities

Surgical resection followed by adjuvant therapy is the standard management for patients with early stage or localised disease. This is usually about 10 -15 % of patients (*Heinemann et al, 2008*). For those with unresectable disease, chemotherapy is necessary adjuvant treatment. Over the last 14 years pharmaceutical companies and collaborative groups have embarked on clinical research to improve survival and prognosis of pancreatic cancer sufferers. This involved trials with Gemcitabine and a number of combination therapies.

Currently, the response rate to first line treatment with Gemcitabine is only 20% (*Funamizu* et al., 2009). Despite the anti-tumour activity seen with several chemotherapeutic agents and novel molecular targeted therapies, these drugs have thus far failed to show significant effects against epithelial tumour cells in the clinical setting without toxic or deleterious effects to the patients.

In patients with metastatic disease, combination therapy with Erlotinib has seen higher median and 1-year survival rates when compared to the use of Gemcitabine alone, (*Vervenne et al, 2008),* and has since been used in combination with Gemcitabine in advanced, unresectable pancreatic cancer. However, due to significant toxicity and only a small improvement in response rate, cautious use is recommended.

A randomised, multicenter, phase III clinical trial in 319 patients by the Central European Cooperative Oncology Group (ECOG) found that neither clinical response nor quality of life were improved when the Gemcitabine/Capecitabine combination was compared to Gemcitabine alone, (*Bernhard et al, 2008)*. This contrasted with the results of the phase III National Cancer Research Institute GEMCAP trial in the UK, an open-label (both researchers and participants know which treatment is being administered). This randomised study of Gemcitabine alone versus Gemcitabine combined with Capecitabine involved 533 patients. Compared with Gemcitabine alone, treatment with the Gemcitabine/Capecitabine combination produced a significantly higher objective response rate (12.4% *vs.* 19.1%, respectively) and progression-free survival. (*Cunningham et al, 2009)*.

Other phase III trials have ruled out the benefits of combination therapy with Cisplatin, Oxaliplatin, Irinotecan and Docetaxel when compared to Gemcitabine alone. Therefore Gemcitabine remains the mainstay therapy for patients with metastatic disease. For those refractory to Gemcitabine, Capecitabine alone or Capecitabine plus Erlotinib may provide some benefit as second line therapy, (*Kulke et al, 2007).*

In 2011 the NCCN made several recommendations with respect to the management of patients with unresectable disease. This included Gemcitabine monotherapy or patients with locally advanced or metastatic disease, the use of the GTX regimen (Gemcitabine, Docetaxel and Capecitabine) and the Gemcitabine/nab-paclitaxel combination regimen*)* for metastatic disease, (*NCCN, 2011*.

1.2.2.1 Clinical trials

1.2.2.1.1 Adjuvant therapy

Adjuvant therapy is treatment that is used following primary treatment, which is surgery in the case of pancreatic cancer, in order to reduce the risk of disease recurrence. It may be in the form of chemotherapy, hormone therapy, radiotherapy, targeted or biological therapy**.**

The phase III National Cancer Research Institute GEMCAP trial in the UK was a randomised study of Gemcitabine versus Gemcitabine and Capecitabine in 533 patients. This study was an open-label study in which both researchers and participants knew which treatment was being administered. Compared with Gemcitabine alone, treatment with the Gemcitabine/Capecitabine combination produced a significantly higher objective response rate (12.4% *vs.* 19.1%, respectively) and progression-free survival. (*Cunningham et al, 2009)*.

The results of a European phase III trial (ACCORD/PRODIGE) that compared the non-Gemcitabine regimen FOLFIRINOX (LV5-FU plus Oxaliplatin plus Irinotecan) to Gemcitabine were reported by *Conroy et al.* The median survival on the FOLFIRINOX arm was 11.1 months, versus 6.8 months for Gemcitabine alone. FOLFIRINOX proved more toxic with complications including febrile neutropenia despite the selection of patients with eastern cooperative oncology group (ECOG) performance status of 0-1 in this trial. It has still been recommended by the NCCN for treatment of patients with metastatic or locally advanced unresectable disease with good performance status.

The European study group for pancreatic cancer (ESPAC)-3 trial, an adjuvant therapy trial involving 1088 patients, showed no significant outcome of survival between the groups of Gemcitabine or folinic acid and 5 Fluorouracil. The median survival differed by a mere 0.6 months between the two arms of this trial with Gemcitabine only treated patients having less adverse affects, (*Neoptolomos et al., 2009*).

Phase III trials have also been done comparing Gemcitabine alone with Gemcitabine combined with Cisplatin (*Heinemann et al., 2006, 2008; Coluccci et al., 2002, 2009*), Capecitabine (*Cunningham et al., 2005, 2009; Herrmann et al., 2007*), Exatecan (*Abou-Alfa et al., 2005*), Irinotecan (*Rocha Lima et al,. 2004; Statopoulos et al,. 2006*), Oxaliplatin (Louvet et al., 2005; Poplin et al., 2009) and Permetrexed (*Oettle et al, 2005*), with a median survival ranging between 5 to 7.5 months on the whole. These therapies have failed to show any overall survival benefit but in some of these trials there was a marginal effect on progression free survival for some patients (*Anastasios et al, .2010*).

ESPAC-4 trial is currently underway. This trial is aimed at patients who have had total surgical resection of the tumour. It is looking at the efficacy of Gemcitabine and Capecitabine in this patient group administered within 10 weeks of surgical intervention with a two year follow up. (Liverpool Cancer Trial unit).

1.2.2.1.2 Neoadjuvant therapy

This is therapy that is given to shrink a tumour before the primary treatment such as surgery is performed. This is done in the hope that there is an increased chance of removal or the whole tumour during surgery and result in a better overall survival. Studies performed by Pisters and colleagues using preoperative chemoradiation, intraoperative radiation and a preoperative paclitaxel/ radiation combination in patients with resectable disease. They showed the median survival of patients to be up to 19 months compared to that of 12 months with surgery alone, (*Pisters et al., 2002*). There was, however, severe toxicity in these patients and currently insufficient data to support its use in the clinical setting.

In a review by Raut and colleagues, they deduced that there was an increase in the rate of R0 (complete resection with no residual microscopic tumour) resections and a reduction in recurrence and metastases in patients having neoadjuvant therapy compared to immediate surgery, (*Raut et al., 2004*). The benefit of neoadjuvant therapy is currently obscure as the evidence is based on retrospective and phase II studies (*Klautke et al, 2008*). Loehrer and colleagues performed a phase III study of Gemcitabine and radiotherapy vs. Gemcitabine alone for patients with locally advanced unresectable disease. Gemcitabine plus radiotherapy was shown to have added toxicity and the progression free survival was a mere 0.2 months longer than the Gemcitabine only group, (*Loehrer et al*, 2008). The multicentre phase III NEOPAC trial is underway to ellucidate the efficay of neoadjuvant Gemcitabine/Oxaloplatin and adjuvant Gemcitabine versus adjuvant Gemcitabine alone. It aims to provide data un overall survival in patients post pancreatic head surgery.

1.2.2.1.3 Targeted therapies

The identification of genetic changes that may occur in PDA and their effect on the signalling pathways involved in cell cycle regulation, DNA damage and repair, cell communication and development pathways have raised hope in identifying possible new target therapies. The phase III trials of Gemcitabine *vs.* combination therapy with either Tipifarnib (RAS family inhibitor), *Van Cutsem et al., 2004,* Marmisat (MMP inhibitor), *Bramhall et al*., *2001*, Bavacizumab (VEGF inhibitor) *Kindler et al* and Erlotinib (EGFR inhibitors), *Vervenne, W. et al.,2008,* have all failed to show an improved overall survival when compared to Gemcitabine alone. Bay 12-9566, a specific inhibitor of MMP-2, MMP-3, MMP-9 and MMP13 was shown to have an even worse overall survival when compared to Gemcitabine, (*Moore et al*., *2003*).

The more recent trials have been focused on new combinations such as Gemcitabine/Lemalidomide (MEK inhibitor), Gemcitabine/GDC-0449 (Anti smoothened), (*Von Hoff et al., 2011),* GEM/Nab- Paclitaxel vs. Gemcitabine and FOLFIRINOX (Fluorouracil, Leucovorin, Irinotecan, Oxaliplatin) -phase III. This last study showed a survival of 11.1 months compared with 6.8 months; a significant improvement thus far.

1.2.3 Pancreatic cancer and the stroma

It has been established that cancers are the product of several somatic mutations that have developed in the epithelial cell. Their behaviour, however, is heavily influenced by the surrounding tumour microenvironment or stroma. The stroma is believed to play a significant role in the tumourigenesis of pancreatic cancer, especially in PDAs where there is a particularly dense stromal reaction. This dense reaction is a hallmark sign of pancreatic cancer.

The complex stroma consists of a variety of cells including fibroblasts, pericytes, endothelial cells, smooth muscle cells, leucocytes, macrophages, mast cells and the extra-cellular matrix (ECM) as well as secreted growth factors and cytokines, (*Lorusso et al, 2008*). The vasculature of the tumour microenvironment, however, should not be ignored as its role is crucial in metastasis. Angiogenesis is supported by the secretion of endothelial growth factors e.g. vascular endothelial growth factor (VEGF) .Both tumour cells and stroma are sites of VEGF production (*Fukumura et al, 1998*). Targeted anti VEGF therapy, Bevacizumab in combination with chemotherapy has been approved as first line treatment in metastatic colorectal cancer, (Ferrara *et al., 2004*).

Within the tumour microenvironment stromal fibroblasts are largely responsible for the synthesis and deposition of the ECM. They also produce growth factors that act in an autocrine, (on the same cell), and paracrine, (on neighbouring cells), fashion to influence the growth of carcinoma cells. Although the exact role of the tumour stroma is not yet fully understood, there are a few who believe that the surrounding stroma is a host response to the invading cancer and acts to contain its growth, (*Hartel et al, 2004)*. The predominant view, however, is that of a 'Seed and Soil Hypothesis' of carcinogenesis, proposed over a century ago*, Paget, S., Lancet, 1889, supported by* (*Bhowmick et al, 2004), (Orimo et al, 2006) and* (*Hu et al, 2008),* which suggests that stroma constituents are recruited by the tumour and hence generate a microenvironment for cancer cells to proliferate.

The proof of this activation may be reflected in the modified extracellular matrix of the tumour stroma when compared to normal stroma, (*Ronnov-Jesse*n *et al* 1995). Growth factors such as transforming growth factor beta (TGFß), insulin-like growth factor (ILGF) I and II, granulocyte macrophage–colony stimulating factor (GM-CSF) and platelet derived growth factor (PDGF) are some of the factors responsible for stromal activation. TGFß has been shown to be one of the main factors involved in the induction of myofibroblast transdifferentiation and aggregation, (*Ronnov-Jessen et al, 1995; Lukas et al,* 2009; *Brenmoehl et al, 2009)* and PDGF promotes myofibroblast differentiation indirectly via TGFß activity on stromal cells.

The communication between tumour and stroma cells has been shown to lead to the activation of the TGF-b/SMAD, HGF/MMP, Wnt and Hedgehog signalling pathways. The communication is primarily through autocrine and paracrine signalling believed to be responsible for the development of the prolific microenvironment that promotes tumourigenesis, (*Mahadevan and Von Hoff, 2007),* and supports the survival of the tumour.

The dominant cell found in tumour stroma is the stellate CAF. It is said to represent almost 95% of the cell types found and is responsible for the dense desmoplastic reaction seen around the tumour *in vivo*. Apart from the histological differences seen in these CAFs on stromal activation, they proliferate and migrate more than their normal counterparts, (*Schol et al 1985, 1988)*. There is evidence that these cells may differ phenotypically from fibroblasts associated with normal epithelium and they promote tumourigenesis, (*Carpelan-Holmstrom, 2005*; *Direkze, et al, 2004*; *Dubernard, et al, 2008)*.

1.3 The Stellate Cancer-associated fibroblast

1.3.1 The Cancer-associated fibroblasts (CAF)

Desmoplasia is defined as fibrous connective tissue with an altered extracellular matrix. This change in the stroma is formed in response to an invasive epithelial carcinoma and is the hallmark of PDA. The mechanism behind this stromal change is yet to be fully defined.

Normal fibroblasts are embedded within the fibrillar extracellular matrix (ECM) of connective tissue, which consists largely of type I collagen and fibronectin and plays a role in wound healing. Fibroblasts interact with their surrounding microenvironment through an integrin network including α1 β1 integrin. They typically, appear as fusiform cells with a prominent actin cytoskeleton and vimentin intermediate filament (Figure1.2). Fibroblast-specific protein 1 (FSP1), which is a member of the family of S100 Ca 2+ binding proteins, is specific for fibroblasts in normal tissues.

Cancer-associated fibroblasts are activated fibroblasts within the desmoplasia. They are stellate cells that express α-smooth muscle actin, ECM proteins and growth factors that may act in an autocrine and paracrine fashion to potentiate and support the survival of a tumour and have also been referred to as myofibroblasts, tumour associated fibroblasts and stellate cells.

Fibroblasts that acquire an activated phenotype are associated with an increased proliferative activity and enhanced secretion of ECM proteins such as type I collagen and tenascin C. There is also an increased secretion of fibronectin that contains the extra domain, (EDA-fibronectin) and secreted protein acidic and rich in cysteine (SPARC) as shown in Figure1.2 below.

The CAFs produce cytokines and components of the ECM that affect cancer cell growth and invasiveness. They have been reported to have the ability to induce epithelial oncogenesis, (*Olumi et al 1999*, *Orimo et al 2006)*. Collagen types I and III and *de novo* expression of tenascin C induce an altered ECM, which potentially provides additional oncogenic signals such as stromal-cell-derived factor 1 (SDF1), Transforming growth factor- (TGF) and Hepatocyte growth factor (HGF) to resident epithelia, leading to cancer acceleration and invasion. Activated fibroblasts or CAFs, have been shown to be important promoters of tumour growth and progression. Despite this, however, the signals that mediate the transition from normal fibroblast to CAF are not fully understood and further studies are therefore required to determine whether CAFs do indeed have a unique fibroblast phenotype.

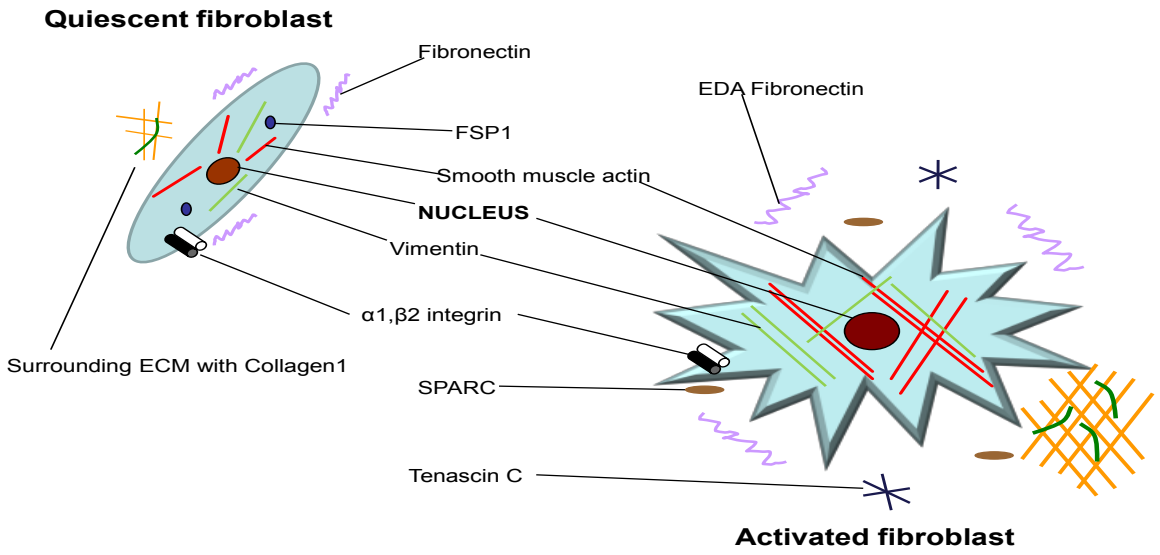


Figure 1.2 This figure shows the normal quiescent fibroblast with its fusiform shape. The extra cellular matrix (ECM) surrounding the fibroblast contains collagen 1. Within the cell the actin and vimentin fibres are seen and Fibroblast specific protein (FSP1).The figure on the right shows the stellate shaped activated fibroblast .There is increased extracellular matrix production as shown by secretion of Tenascin C and Collagen I, EDA-fibronectin and specific protein acidic rich in cysteine (SPARC). The vimentin and alpha smooth muscle actin fibres are more prominent in the activated fibroblast suggesting greater activity. This activation is attributed to the effect of growth factors, ECM proteins and chemokines.

1.3.2 Origins of the Cancer-associated fibroblast

Early assumptions concluded that the stellate CAF was merely an 'activated fibroblast' derived from the connective tissue around the tumour, since they are morphologically similar to their quiescent counterparts. The *in vitro* evidence for this originated from exogenous stimulation of fibroblasts with cytokines and TGFβ to induce expression of myofibroblast markers, (*Ronnov Jessen et al, 1995; Tomasek et al, 1995)*. It is now known that additional factors are also required for this activation, including myeloid precursors and bone marrow derived mesenchymal cells, (*Mishra et al,. 2008)*. Animal studies where the bone marrow has been transplanted with recombinantly tagged stem cells show a redistribution of these precursor cells within the tumour stroma bearing myofibroblast characteristics, (*Direkze et al, 2004; Sangai et al, 2005)*.

Intriguingly, human bone marrow-derived mesenchymal stem cells exposed to tumour-conditioned medium over a prolonged period of time assume a CAF-like myofibroblastic phenotype. These cells exhibit not only similar gene expression profiling but also functional properties of CAFs including sustained expression of SDF1, the ability to promote tumour cell growth both *in vitro* and in an *in vivo* co-implantation model and expression of myofibroblast markers, including αSMA and FSP, (*Franz et al, 2007).* Other studies also suggest that mesenchymal stem cells selectively home to tumours, where they contribute to the formation of tumour-associated stroma including CAFs ,(*Franz et al, 2007; Hall et al, 2007; Karnoub et al, 2007; Dubernard et al, 2008).*

Another accepted source of the CAF includes the epithelial layer of tumours . *In vitro* studies have shown that induced cultures of epithelial cells undergo epithelial to mesenchymal transition (EMT), (*Lee et al, 1999, Oldfield et al, 2001)*. EMT is now a recognised mechanism of forming fibroblasts. Myofibroblasts from breast cancers, (*Patterson et al, 2003*, *Monifar et al, 2000)*, as well as lung epithelia, were found to share genetic patterns with their respective epithelial compartments, (*Kim et al, 2006)*.

As previously mentioned, fibroblasts are spindle shaped polarised cells and can be activated from their quiescent state. It has been proposed that there are three types of EMT. Type 1, involved in embryonic development, type 2, in the formation of fibroblasts from epithelial cells and type 3, which is linked to cancer progression, (*Zeisburg et al, 2009*). Although the mechanism of type 3 is not fully elucidated, it is believed to be the means by which metastatic cells form. (*Kalluri et al., 2009, Zeisburg et al.,2009*). Zeisburg and his group went further to identify criteria both in vitro and in vivo that confirm the presence of EMT.

Further evidence to demonstrate that CAFs are derived from organ specific cells has been seen in pancreatic cancers. Studies have shown that the main cell type that contributes to stroma formation is the activated pancreatic stellate cell (PSC), (*Haber et al, 1999; Yen et al, 2002, Apte et al, 1998; Bachem et al, 2004)*. These cells are closely related to hepatic stellate cells, which are integral in the pathogenesis of liver fibrosis. Quiescent PSCs are found in the periacinar regions in

the pancreas and are characterised by the storage of fat droplets. They also express desmin and vimentin. In PDA, as well as in chronic pancreatitis, the PSCs become activated and develop features of myofibroblasts. Understanding the origins of CAF will help to highlight the genetic changes, if any, which may occur during its transformation.

1.3.3 Crosstalk between the CAF and tumour

Cancer-associated fibroblasts are activated by a variety of cytokines produced by tumour cells, including interleukins, fibroblast growth factors (FGFs), TGFβ and PDGF. In turn, CAFs are found to produce cytokines and components of the ECM that affects cancer cell invasiveness and growth. They include FGFs, VEGF, connective tissue growth factor (CTGF), matrix metalloproteinases (MMPs), collagens and fibronectin. They are also known to produce ILGF-1 and II, the actions of which appear to predominantly impart tumour growth by conveying survival signals, (*Hwang et al*, 2008).

Many *in vitro* studies of CAF activation have only focussed on individual cytokines. There is currently only one gene expression study examining the effects of activated CAF using co-culture experiments (*Orimo et al, 2006*). Research that used mouse models of genetically altered fibroblasts demonstrated a direct involvement of resident fibroblasts in the initiation of cancer (*Olive et al., 2009*). A further link between growth factors and stellate CAFs in tumour initiation was proposed by findings indicating that normal fibroblasts are required to maintain epithelial homeostasis, whereas CAFs probably initiate and promote tumorigenic alterations in epithelial cells, (*Kalluri et al, 2006*)

CAFs are also suspected to promote tumour progression through specific communications with cancer cells. They have been found to facilitate the invasiveness of otherwise non-invasive cancer when co-injected into mice but the details of this mechanism are still being investigated (*Hu et al, 2008*). Furthermore, animal models have been used to suggest that Sonic Hedgehog (SHH) signalling promotes the migration and invasion of human pancreatic myofibroblasts thereby increasing the desmoplastic and stromal reaction, (*Madhevan, Von Hoff et al 2007*).

Sonic Hedgehog (SHH) binds to the Patched-1 (PTCH1) receptor. In the absence of the SHH ligand, PTCH1 inhibits Smoothened (SMO), a downstream protein in the pathway. *(Taipale et al, 2002).* The binding of SHH relieves SMO inhibition, leading to activation of the GLI transcription factors Gli1 and Gli2 (activators) and the Gli3 (repressor). Activated Gli accumulates in the nucleus and controls the transcription of hedgehog target genes, Figure 1.4. The sequence of molecular events that connect Smoothened to the Gli transcription factors is poorly understood and requires further investigation as this pathway can prove a useful target in the management of pancreatic cancer. PTCH1 has recently been reported to repress transcription of hedgehog target genes through a mechanism independent of Smoothened suggesting the existence of a non-canonical pathway, *(Rahnama et al., 2006).*

The expression of Hh ligands and essential components of the pathway, including PTCH and SMO, have been reported in up to 70% of human pancreatic ductal adenocarcinoma specimens (*Thayer et al., 2003)*. In addition, several studies have proposed that Hh ligands produced by tumour cells activate Hh signalling and tumour cell growth in an autocrine/ juxtacrine manner *(Thayer et al., 2003, Pasca di Magliani et al., 2006)*.

Previously, research focused heavily on the presence of hedgehog signalling in the pancreatic epithelium. Research performed by a Cambridge group led by Olive and Tuveson found that the hedgehog pathway is in fact effected within the stromal compartment, (*Olive et al., 2009*). Sauvage and his group also reported that for hedgehog–expressing tumours lacking mutations in the pathway, hedgehog signalling was indeed occurring in the stroma and not the cancer epithelial cells. They demonstrated that the hedgehog ligand from the cancer cell was activating the adjacent stroma. This data was corroborated with evidence by Olive and Tuveson who showed, using mouse models, that a hedgehog inhibitor could deplete the stroma and re-vascularise poorly perfused tumours, giving evidence that the stroma can be targeted by hedgehog antagonists.

Part of the ability of tumour cells to evade programmed cell death is derived from survival signals supplied by the stromal compartment. Since there is increasing evidence that the tumour stroma may be crucial in determining the invasive and metastatic potential of many cancers, understanding the biology of the stellate

cancer associated fibroblast and its stroma has therapeutic potential. There may be benefit, for example, in reducing the cross-activation of the CAF and stromal cells by inhibitors of PDGF, VEGF and other mediators, many of which are becoming commercially available. Further therapeutic manipulations in the future may involve reversing the activation of CAF, which is an area that has not been studied. Thus far, the activated phenotype of CAF has been shown to be reversed by ligands of the peroxisome proliferator-activated receptor-gamma (PPARγ) pathway, as well as antioxidants, (*Haber et al, 1999; Cat B et al*, 2006).

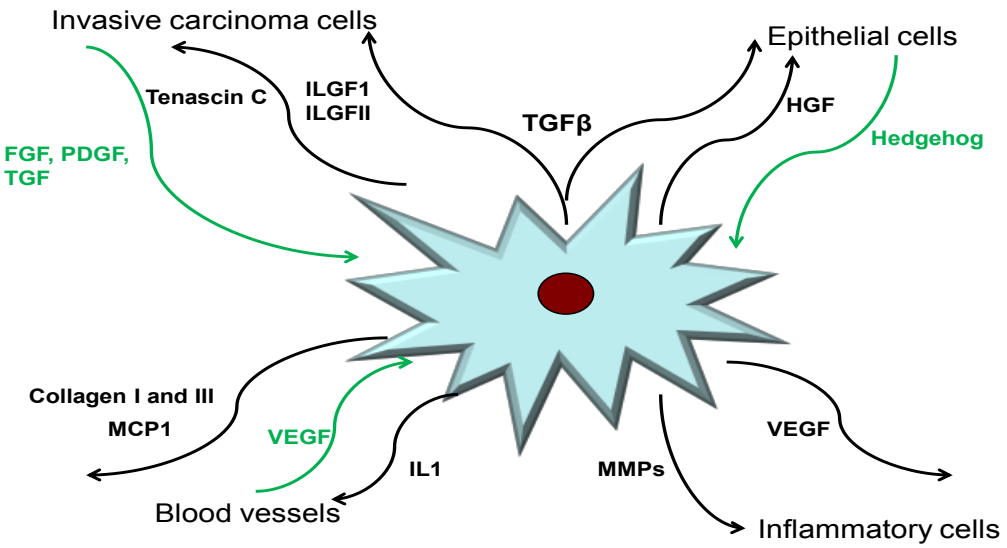


Figure1.3. Factors involved in crosstalk between the CAF and the surrounding stroma. TGFβ and HGF promote proliferation and transformation. The Interleukins and Collagen I and III are responsible for angiogenesis, the inflammatory response, invasion and metastasis. Matrix metalloproteins and VEGF promote angiogenesis (*Madhevan et al 2007*). FGF: fibroblast growth factor, PDGF: platelet derived growth factor, HGF: hepatocyte growth factor, IL1: interleukin 1, MMP: matrix metalloproteinases, VEGF: vascular endothelial growth factor, ILGF: Insulin like growth factor.

1.3.4 Genetic changes

Although the epithelial cancer cells of PDA have been studied extensively *(Hartel et al, 2004; Bhowmick et al, 2004; Hu et al, 2008),* relatively less is known about the stroma, and in particular the CAF surrounding the tumour. However, evidence is emerging to suggest that stromal elements may harbour cancer associated mutations or chromosomal changes in a variety of different cancers. Cancer-associated fibroblasts have been reported to carry a unique set of chromosomal aberrations, for example, the stromal cells of ovarian, breast and prostate cancers harbour loss of heterozygosity (LOH) and p53 mutations (*Olumi et al,1999, Orimo et al, 2006*).

Significant aberrations between the CAFs' LOH signature and both tumour grade and lymph node metastases have been reported in women diagnosed with sporadic breast tumours (*Fukhino et al, 2007*). Furthermore, in breast cancer, which has a very similar desmoplastic response to PDA, stellate CAFs are found to have defective p53/p21 pathways, reflecting neoplastic changes (*Liotta et al, 2001)* . Of clinical importance, genetic changes in the stroma correlated with tumour grade and nodal metastases more so than with epithelial genetic changes (*Paget S, 1889; Kalluri et al, 2006)*. In contradiction to this, other studies using Single Nucleotide Polymorphism (SNP) arrays show no genetic changes in the stroma of breast cancers *(Hanahan /Weinberg, 2000)*.

1.3.4.1 Somatic mutations

It has been proposed that the stellate CAF may have acquired somatic genetic alterations similar to that seen in malignant epithelium. This was based on the ability of stellate CAFs to be propagated in vitro for prolonged periods and yet maintain their cancer-promoting phenotype (*Olumi et al, 1999; Kuperwasswer et al, 2004*). Several studies have shown that the somatic mutations acquired by stellate CAFs are associated with tumourigenesis (*Patocs, et al, 2007; Weber et al, 2006; Weber /Zhang et al, 2007*). For example, frequent somatic mutations in tumour suppressor genes such as phosphatase and tensin homolog (PTEN) and P53 have been reported in fibroblasts associated with breast carcinomas (*Weber et al, 2006; Kurose et al, 2002*). The mutations were found to be distinct between cancer cells and stellate CAFs, ruling out the possibility of these mutations being due to contamination.

Not all studies support the theory of somatic alterations in CAFs. Allinen and colleagues undertook array CGH and SNP array analysis of carcinoma cells and myofibroblasts from ductal breast carcinoma. Numerous alterations were noted in the epithelial cells but the myofibroblasts and other non epithelial tumour associated cells were found to be normal (*Allinen et al, 2004*). There is therefore a debate as to the presence or absence of stellate CAF somatic mutations. Campbell and colleagues have suggested that studies reporting frequent somatic mutations may be flawed. This is partly because previous studies have accredited the enhanced ability of individual fibroblasts to promote tumourigenesis to these somatic mutations *(Campbell et al, 2009)*.These reports used limited numbers of cells derived from

micro-dissected formalin-fixed paraffin-embedded (FFPE) tissues and mutation assessment can be severely compromised when using the limited quantities of DNA, typical of FFPE tumours (*Farrand et al, 2002; Sieben et al, 2000; Kern et a, 2006*).

1.3.4.2 Loss of heterozygosity and SNPs

Currently there has only been one study on pancreatic cancer CAFs which showed no genomic changes using SNP arrays in cultured CAF or p53 mutations using immunohistochemistry (*Walter et al., 2008*). This study used cultured CAF from PDA resection specimens with an unknown proximity of the CAF to the tumour making the validity of the results questionable. In this study, fibroblasts were isolated from whole tumour biopsies rather than direct micro-dissection of tumour juxtaposed fibroblasts. The CAF alterations may therefore have been masked by the presence of normal fibroblasts. In light of the findings in other cancers, there is a need to study the possibility of chromosomal changes in PDA using more state-of-the-art technology, which would use both micro dissected stroma and CAF cell lines for validation.

Below is a table showing the studies of chromosomes and gene copy number alterations (CNA) reported in CAFs of different cancers including PDA.

Authors	Cancer Type	Tissue	Experiment methods	Significant results
Patocs	Breast	LCM	LOH/AI (386 markers)	19-25% LOH in stroma 7q, 10q, 15q, 16p, 17q associated with prognosis
Fukhino	Breast	LCM	LOH/AI (386 markers)	Chromosome changes associated with prognosis 1,2,5,11,18,20,22
Tuhkanen	Ovarian	LCM	LOH/AI (110 markers)	10.8 changes (6.6gains, 4.2losses) 6q, 7q, 11q, 12q, 16q
Ellsworth	Breast	LCM	LOH/AI (52 markers)	10% changes in stroma alone Chromosomes 10,11
Monifar	Breast	LCM	LOH/AI (12 markers)	20-75% changes Most frequent 11q, 16q, 17q
Paterson	Bladder	LCM	LOH/AI (3 markers)	78% changes 3p, 9q, 17p
Kurose	Breast	LCM	LOH/AI (13 markers)	17-61% changes 1,2,3,6,8,10,11,13,16,17,22
Qi	Breast/ Ovarian	LCM/ culture	SNP (250K)	1 LCM change Ch 22 1 cell line change Ch7, 10
Allinen	Breast	Cell sorting	SNP (250K)	No genetic changes
Walter	Pancreas	Culture	SNP (250K)	No genetic changes
Campbell	Breast	LCM/ culture	SNP (500K)	No genetic changes

Table1.1. Studies of chromosomes/gene copy number changes in CAFs**.** There has only been one study on pancreatic cancer CAFs. This study showed no genomic changes using SNP arrays in cultured CAF or in p53 mutations using immunohistochemistry**.**

1.3.4.3 Gene expression

To date our knowledge of the gene expression profile specific to pancreatic cancer is still scarce. The few studies that have been performed on the stroma from tumour blocks are proving to be controversial (*Sato et al, 2004; Pilarsky et al, 2008*). In one study using micro dissected PDA stroma, the expression of more than 200 genes was shown to be altered in the stroma of PDA as compared with chronic pancreatitis samples. However, in another similar study, no such alterations were observed but instead at least 100 common stromal gene expression profiles were seen in both PDA and chronic pancreatitis samples (*Binkley et al., 2004*). The latter study used subtraction of gene expression patterns to obtain their data, which is inherently less reliable. There is therefore a need to perform more detailed cross-platform studies of PDA stroma and stellate CAF, both using gene expression arrays and chromosomal analysis. Table 1.2 shows the results of gene expression arrays performed on CAFs.

Authors	Cancer	Tissue	Comparison	Microarray	Genes expressed in common
Pilarsky	Pancreas	Histology	CaS vs. CP	Affymetrix	COL10A1, COL11A1, MATN3, CXCL14, TNFSF4
Binkley	Pancreas	Histology*	CaS/CP vs. CaE	Affymetrix	
Sato	Pancreas	Cell lines	AcPSC vs. NonPSC	Affymetrix	MCP1, COX2, CXCL8, CXCL1, CXCL2
Iacobuzio	Pancreas	Cell lines	CaS vs. CaE	SAGE	
Buchholz	Pancreas	Cell lines	PSC(nonCAF) vs. NF	Operon	
Glass	Pancreas	Cell lines (rat)	AcPSC vs. NonPSC	Affymetrix	
Micke	Skin (BCC)	Histology	CAF vs. NF	Sanger	SPARC, MGP, CILP, COL5A2, MMP11, PDGFRL
Nagakawa	Colorectal (liver mets)	Cell lines	CAF vs. NF	Affymetrix	FGF1, MCP1, COX2, COL4A1, COL6A2, PDGFA, IGFBP7, IGFBP5, CTGF, VEGF, TGFB2
Mellick	Breast	Histology	CaS vs. CaE	Incyte,	
Singer	Breast	Cell lines	CAF vs. NF	Micromax	TGFB1
Finak	Breast	Histology	CAF vs. NF (prognosis)	Agilent	
Casey	Breast	Histology	CaS vs. NS	Affymetrix	COL10A1, COL11A1, TGFB1, FGF1, SPARC, MATN3, MGP, CILP, MMP7, MMP1, MMP13, TIMP3
Boersma	Breast	Histology	CAF vs. CAF (inflam)	Affymetrix	
Richardson	Prostate	Histology	CaS vs. NS	Affymetrix	
Allinen	Breast	Histology	CsS vs. CaE	SAGE	

Table1.2. Studies using gene expression microarrays on CAFs. Gene expression obtained by subtraction of signals between specimen, and other histology samples obtained by laser-capture micro dissection. X – Studies comparing Cancer-associated stroma/fibroblasts against non-cancer stroma/fibroblasts with genes which are up- or down regulated in at least two different studies, X – Genes which are in the same family (or similar) to others described in at least two different studies, CaS – cancer stroma, CP – chronic pancreatitis, CaE – cancer epithelium, NS – normal stroma, PSC – pancreatic stellate cells, AcPSC – activated/stimulated PSC, NonPSC - non-stimulated PSC, CAF – cancer stromal fibroblast, NF – normal fibroblast, CAF (inflam) – CAF from inflammatory breast cancer.

1.3.4.4 Pluripotency in the CAF

As mentioned previously, in section 1.3.3, the cancer-associated fibroblast is stimulated to its activated stellate phenotype from a quiescent state with the aid of cytokines from the tumour epithelial cells. As described, this happens in an autocrine and paracrine fashion along with the signalling pathways such as Wnt, Notch, Hedgehog and receptor tyrosine kinase. These pathways have been linked to cancer stem cell status and reprogramming mechanisms. They are also involved in the activation and stimulation of quiescent fibroblasts to their active state and support their proliferation.

The ability of the CAF to develop into or from different mature cells, based on environmental stimulants, is open for discussion. Kadera *et al* showed that primary CAFs were not derived from tumour epithelial cells with the use of KRAS sequencing and in situ immunofluorescence staining for epithelial and mesenchymal markers. These included SMA, pancytokeratin, Vimentin and GFAP, (*Kadera et al., 2013*). Their research also showed that co-injecting CAFs with tumour cells into genetically modified mice, enhanced tumour growth but no tumour was produced when CAFs were injected alone. This would suggest that these cells are unable to act as an autonomous clone and unable, on their own, to produce a separate lesion from the tumour.

With respect to the stem cell like qualities of the CAF, it has been demonstrated that the transcription factors Klf4 and Sox2, downstream of the microRNA-200 family promote a stem cell like, tumour initiating phenotype in pancreatic cancer, (*Li and Laterra, 2012*). Zinc finger E-box binding homeobox protein (ZEB1) inhibits the miR-

200 family, which induce epithelial cell differentiation. These transcription factors (Oct-3/4, Sox2, KLF4 and c-Myc) have been shown to induce an embryonic like pluripotent stem cell from fibroblasts cultured from mice, (*Takahashi et al.,2007*). However, the stem cell like behaviour in human pancreatic stellate cancer associated fibroblasts is yet to be elucidated. This data may provide further insight into the understanding of the aggressive nature of this disease.

1.4 Chemoresistance in pancreatic ductal adenocarcinomas

Chemo-resistance in pancreatic ductal adenocarcinoma has been a limiting factor to disease management. Many forms of the cancer develop resistance soon after a fleeting initial response to Gemcitabine but Gemcitabine as yet remains the gold standard of adjuvant therapy. This Chemo-resistance is multifactorial and has been attributed to several factors including poor drug accumulation, altered targets and increased repair of drug induced DNA damage, (*Sebens et al, 2011).* This is compounded by the paucity of a suitable screening tool or biomarkers to help identify the presence of the disease at an early and less aggressive stage.

Currently, patients tend to present at a locally advanced stage of disease. At this stage it is more difficult to achieve a satisfactory response to the current chemotherapeutic regimes used. The key factors at a molecular level include cancer cell genetic mutations, poor drug delivery to the tumour site, activated tumour-stromal cell interactions with promote tumourigenesis and cross-talk of signalling pathways within the stroma that promote tumour development and resistance. These are discussed in further detail below.

1.4.1 Genetic mutations

Pancreatic cancer is characterised by a unique molecular fingerprint with activating point mutations at codon 12 of the K-ras gene found in more than 90 % of cases, (*Moore et al., 2001*). The tumour suppressor gene p53 has been found to be inactivated in 60% and DPC4/Smad4 altered in 50%, of xenografted cancers, (*Hahn et al., 1996*)**.** These factors undoubtedly play a role in tumour development and the changes are believed to contribute toward chemoresistance. See table 1.3

Cell line	K-Ras	AKT2 19q	9p LOH	P16 HD	13q LOH	17P LOH	P53 Mut	MKK4 HD	18q LOH	DPC4 HD	DPC4 Mut
AsPc1	12 Asp	Ampl	LOH	2bp del	LOH	LOH	1bp del	HD	LOH	-----	100 Thr
BxPc3	-----	Poss Ampl	LOH	?	LOH	LOH	220 Cys	-----	LOH	HD	-----
MiaPaCa2	12 Cys	-----	LOH	HD	-----	LOH	248 Trp	-----	LOH	-----	-----
Panc1	12 Asp	Ampl	LOH	HD	LOH	LOH	273 His	-----	LOH	-----	-----
Su86.86	12 Asp	Ampl	LOH	HD	LOH	LOH	245 Ser	-----	LOH	-----	-----
HPAC	12 Asp						WT			-----	WT
Hs776T	61 His	-----	LOH	-----	-----	-----	R	----	LOH	HD	?
PL5											
PL45											

Table 1.3 The common genetic changes found in pancreatic cancer cell lines**. "-----"**refers to No genetic alteration; blank is undetermined; **HD** homozygous deletion, the gene is not present and mutations **Mut** cannot be assayed; **Del** intragenic deletions; **bp** base pairs; **R** rearrangement of one of the alleles of p53 and the other has a deletion resulting in inactivity of the p53 gene; WT wild type sequence. For K-ras, p53 and DPC4 the codon and amino acid change is shown. Blank spaces indicate no published data. These cell lines showed no MKK4 mutations or BRCA2 mutations, not shown in this table.

1.4.1.1 Micro RNA gene expression profiling

Recent interest has been on Micro RNAs and their role in cancer development and progression. These are a small class of non-coding RNAs between 19 to 25 nucleotides long, *(Bartel et al.,2004)*, believed to have important roles in uncontrolled cell division and poor cell differentiation. (*Ambros et al.,1984, Reinhart et al., 2000*). MicroRNAs have therefore been linked to cancer as this is the endpoint of poor cell differentiation. In human tissues micro RNAs are believed to inhibit tumour suppressor genes. They do this by targeting messenger RNA and are sometimes referred to as Oncomirs. They are believed to affect post-transcriptional gene expression by inhibiting the translational process. The mechanisms suggested include direct cleaving of the target messenger RNA and well as possibly reducing the rate of the initiation step in mRNA translation. A non cleaving pathway has also been postulated but the mechanism is not yet elucidated, *(Valencia –Sanchez et al.,2006).*

Bloomston and his colleagues used miRNA microarray to identify 30 upregulated and 4 downregulated miRNAs that were present in pancreatic cancer and of importance miR- 21 and 155 were uniquely expressed in pancreatic cancer. Granted there was some overlap, none of those overexpressed were found to be present simultaneously in either cancer, normal and acute pancreatitis tissue. They suggested miR-21, miR-155, miR-221 and miR-222 as key players, with miR-221 being particularly highly expressed in pancreatic cancer compared to the benign tissue groups but its role or mechanism is unclear, (*Bloomston et al.,2007*). See table 1.4.

Szafranzka *et al* used miRNA arrays to profile those miRNAs differentially expressed in PDAC compared to benign tissue. They identified 11 microRNAs that were strongly downregulated by up to 5 fold in PDAC and a further 11 that were upregulated. In their 8 PDAC samples, miRNA- 222 was again found to be upregulated as was seen by Bloomston *et al,* See table 1.4.

Xue and colleagues showed upregulation of miR-196 and downregulation of miR-148a and miR-217 in PDAC and its precursors compared to regular parenchyma. They reported a significant overexpression of miR-21 in PDAC and high expression of miR10b in its precursors, PaIN II and III, *(Xue et al., 2013).* Their findings have suggested that these Oncomirs may be markers to discern between normal tissue and cancer precursors. Du Rieu *et al* also showed its expression to increase in the early stages of PDA development, particularly in the low grade pre-malignant PanIN lesions, (*Du Rieu et al*.,2009).

Micro RNA-21 has been the focus of many recent publications in PDA and has shown to be more cancer cell specific than mRNA *(Lu et al., 2005).* Dillhoff and colleagues used Fluorescent in situ hybridization to show that miRNA-21 is highly overexpressed in pancreatic cancer tissues compared to benign tissue. They found no correlation with tumour size, node status, T-stage or differentiation but correlated strong expression with poor outcome in patients with node negative disease. (*Dillhoff et al., 2008*)

A Japanese group showed an increase in proliferation and resistance to Gemcitabine in cells infected with miR-21 precursor. The converse was seen when miR-21 was inhibited. They correlated the mRNA expression of MMP2, MMP9 and VEGF with miR-21 expression, linking miR-21 to cell proliferation and invasion, (*Moriyama et al., 2009*).

In 2013 Kadera and his group published their findings in which tumour associated fibroblasts were induced by epithelial tumour cells to express miR-21. They proved miRNA expression in these CAFs using Fluorescent in situ hybridization and inhibition of this miRNA in epithelial cells and CAFs gave an additive effect in reducing tumour invasion. (*Kadera et al., 2013*). This oncomir may soon become another key in the chemoresistant nature of PDA.

Author	Platform used	Tissue	Upregulated microRNAs in PDAC	Downregulated microRNAs in PDAC	Genes affected
Bloomston	Microarray 1100 miRNA probes		221, 222, 21, 155, 196a-2	375	KIT (stem cell factor) Predictor of survival
Szafranzka	Microarray 377 miRNA probes	cell lines	93, 196a, 196b, 203, 205, 210, 224 221, 222	29c, 30a, 3p, 96, 130b, 141, 148a, 216, 217, 375, 494, 148b,	CDKi (1b/1c)
Szafranzka		Primary neoplastic tissue	18a, 31, 93, 221, 205, 224 *	216, 217	
Xue		Primary neoplastic tissue	21, 196	148a, 217	

Table 1.4 MicroRNA changes in PDA. Highlighted are the MicroRNA and the significant genes found to be influenced by them

1.4.2 Chemoresistance due to alterations in gene products involved in Gemcitabine uptake

Genetic and epigenetic alterations found in the gene products involved in Gemcitabine transport and metabolisms have been associated with resistance. The nucleoside transporter hENT1 is important for cellular uptake of Gemcitabine. Genetic alterations leading to decreased levels of hENT-1 appear to be associated with Gemcitabine resistance, (*Giovannetti E et al*, 2006) The changes in the levels of gene products associated with Gemcitabine uptake also appear to play a significant role in resistance. Decreased levels of Deoxycytidine kinase (dCK), up-regulation of Deoxycytidine deaminase (CDA catalyses and deaminates GEM) and the up-regulation of ribonucleoside reductase M1 and M2, (*Duxbury et al, 2004)*, all appear to affect Gemcitabine resistance. Aberrant expression of genes associated with apoptosis and cell survival have also been implicated, specifically S100A4. Up-regulation of this S100 family gene may increase resistance to Gemcitabine by regulation of BNIP3**,** a hypoxia induced pro-apoptotic gene. (*Mahon et al, 2007; Erkan et al*, 2005).

1.4.3. Up-regulated survival pathways /down-regulated apoptosis and protein secretion

An alteration in survival pathways in combination with the downregulation of apoptosis is believed to play a significant role in chemoresistance as discussed by *Kim* and *Gallick*. Upregulation of the Phosphatidylinositol 3-kinase, protein kinase B (PI3 kinase/AKT) pathway has been shown in pancreatic cancers, (*Asano et al, 2004),* and this has been implicated in Gemcitabine resistance, (*Asano et al, 2004).* Decreased C-SRC and C-Met activation have also been shown to play a role in Gemcitabine resistance, (*Duxbury*[2] *et al*, 2004; *Bondar et al, 2002;* Ng *et al 2000; Ng SS, et al 2001)*. Increased HMGA1, which induces a stem cell like state has been implicated in Gemcitabine resistance, (*Liau SS et al, 2006)*. Activated MAPK/ERK, although dose dependent, (*Zhao et al*, 2006) and the activation of focal adhesion kinase, *(Duxbury et al, 2004);* have also been implicated in Gemcitabine resistance in pancreatic cancer. Finally, upregulation of Heat shock protein 27 (HSP27) in resistant pancreatic cell lines suggests an anti-apoptotic response thus conferring relative resistance to therapy (*Sayaka Mori-Iwamoto et al, 2008).*

Zavoral and colleagues have summarised the many oncogenes and tumour suppressor genes involved in the signalling pathways implicated in pancreatic cancer tumourigenesis and progression. The RAS, AKT and Wnt signalling pathways have all been implicated due to their roles in transcription and proliferation as well as the cell cycle regulators SMAD/DPC, CDKN2A/P16 and Tp53, which are all integral players in cell apoptosis. (*Zavoral et al, 2011*). These elements, although functional in tumour initiation and progression, due to the aggressive nature of pancreatic cancer, may be contributors to the resistant nature of the disease.

1.4.4 Pancreatic Stellate cells and chemoresistance

The stellate cell has been implicated in the chemoresistance of pancreatic cancer; however, the exact mechanism by which this occurs has not been fully identified. Hwang and associates showed that in the presence of human pancreatic stellate cells, cancer cells, in particular BXPC3 show no significant change in cell number when exposed to Gemcitabine or irradiation, (*Hwang et al*, 2008). They also found an increase in the anti apoptotic signalling pathway expression whereby the cancer cell lines responded to stellate conditioned media with a multiple fold increase in AKT and ERK expression after several minutes when co-cultured with human stellate cells. They showed that stellate cells were necessary for tumour initiation and growth and without them tumours failed to develop on their own. Co-injection of stellate with BxPc3 in orthotopic mice resulted in metastases in a dose dependent manner.

Stellate cancer associated fibroblasts themselves have already been implicated in the pro-genesis of several cancers including breast, pancreas, lung, (*Pageau et al*, 2011), cutaneous squamous cell carcinoma, (*Commandeur et al*, 2011), as well as the aggressiveness of others such as oral squamous cell carcinoma, (*Sobral et al, 2011),* making them viable targets when considering options for chemotherapy in the fight against pancreatic cancer.

1.4.5 The hedgehog signalling pathway

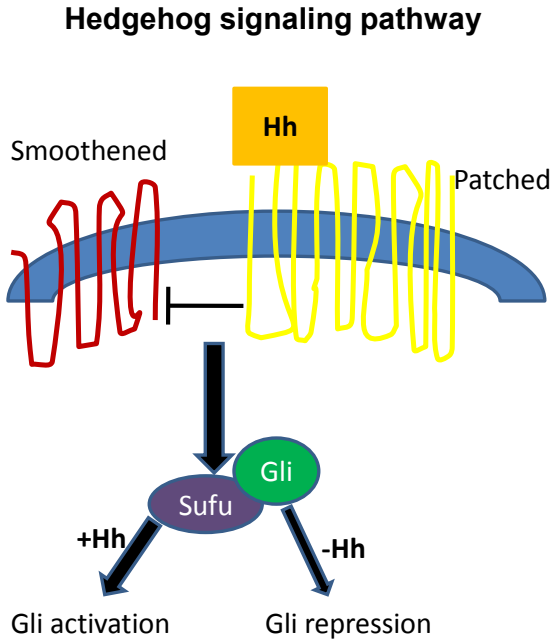


Figure 1.4 The Hedgehog signalling pathway

Patched, is a twelve-pass membrane protein that inhibits Smoothened, a seven-pass membrane protein, in the absence of hedgehog binding. In the presence of hedgehog binding, the inhibitory function of Patched on Smoothened is reversed and a Gli complex is formed which promotes the activation of Gli transcription factors. In the absence of the hedgehog ligand binding to patched, Gli acts as a repressor of protein transcription.

The hedgehog signalling pathway has proved to be a key player in the development and proliferation of PDA. This pathway was previously thought to stimulate the epithelial cells of tumours, resulting in tumour progression. It has since been shown that this pathway is activated in the activated stromal compartment (*Yauch et al, 2008*; *Olive/Tuveson et al, 2009)*. Hedgehog stimulates stromal proliferation via paracrine signalling and inhibition of this pathway has shown to have therapeutic potential.

Smoothened is a membrane protein in the hedgehog pathway. A smoothened inhibitor when used in combination with Gemcitabine to treat genetically modified mice was found to increase the median survival by more than 2 fold, (*Olive/Tuveson et al, 2009).* These KPC mice (KrasLSL.G12D/+; p53R172H/+; PdxCretg/+) have pancreas-specific *Kras*^{G12D} and *Trp53*^{R172H} mutations, *(Olive/Tuveson et al, 2009).*

Olive and colleagues have shown that the use of hedgehog inhibitors can alter communication between the tumour and stroma via the hedgehog pathway, interrupting the feedback loop necessary for stromal activation and development and resulting is stromal depletion. This depleted stroma becomes less of a barrier to chemotherapeutic intervention as drug delivery to the tumour is somewhat enhanced. Hedgehog signalling has also been shown to be directly responsible for tumour cell growth in other cancers such as prostate cancer, (*Domenech et al, 2012).*

1.4.6 Stromal density and chemoresistance

The density of stroma is also believed to be chemoprotective in that it hinders adequate drug delivery to an already resistant cancer. Notably PDA has a particularly prolific desmoplastic reaction making it comparable to breast cancer where greater than 90 percent of cells are pancreatic stellate cells. Studies have attempted to perforate this dense barrier in order to access the tumour thereby facilitating better drug delivery. They showed a 60% increase in Gemcitabine concentration in the tumours if preceded by a hedgehog inhibitor, and the combination of this inhibitor with Gemciabine more than doubled mouse survival compared with Gemcitabine alone, (*Olive/Tuveson et al, 2009*).

Several compounds have been identified as potential key players in the chemoresistant nature of pancreatic cancer. Fibroblast activating protein, which is seen in the activated fibroblast, is one of the factors implicated with the development of the stromal compartment and has recently been identified as a possible prognostic indicator for PDA, (*Min et al*, *2012*). It alters the extracellular matrix, making it a more favourable environment for tumour invasion. Disruption of this fibroblast activating protein effect has been found to hinder tumour invasion, (*Lee, Mullins et al, 2011*; *Santos et al, 2009),* making it a potentially useful chemotherapeutic target.

1.5 Aims

To rule out genetic changes in the stellate cancer associated fibroblast believed to be responsible for tumour development and progression.

To elucidate any changes and behaviour of the stellate cancer associated fibroblast that may play a role in tumour progression and chemoresistance.

To profile PDA cell lines and stellate cancer associated fibroblasts with the use of high throughput screening which will look at the drug response of these cells to known chemotherapeutic compounds and help identify potential targets or drug combinations that may be further examined

Chapter 2

Materials and Methods

2.1 Materials

2.1.1 General Materials

Dry ice,

Glass pipettes,

100% alcohol,

Multiwell plates

13mm cover slips

Water bath @ 37°C,

Vortex and Centrifuge,

0.22 and 0.45 µm filters,

Falcon tubes, 15 and 50ml,

PCR gel cast and equipment

5, 10 and 25ml plastic pipettes,

5, 10 and 15 ml Luer lock syringes,

Tissue culture flask (25cm²) 0.2µ vented blue seal cap,

Tissue culture flask (175cm²) with vented blue seal cap

Tissue culture flask (75cm²) with vented orange seal cap

50ml, 100ml and 1000ml beakers and measuring cylinders,

2.1.2 Materials for cell culture

Reagent	Recipe	Source	Store
DMEM	Dulbecco's modified Eagles medium 1X + Glucose 4.5g/	Invitrogen (Gibco) Cat#11960	4°C
Pen/Strep	Penicillin G sodium salt 5000 units. Streptomycin Sulphate in 0.85% saline 5000µg/ml	Invitrogen (Gibco)	-20ºC
FCS	Fetal Bovine Serum, 50ml aliquots	Invitrogen (Gibco) Lot 07F1753K	-20ºC
L-Glutamine	100X liquid 29.8mg/ml in .85% saline, 100ml	Invitrogen (Gibco) Cat#25030081	-20ºC
Trypsin 10X	Trypsin EDTA solution 100mls	Invitrogen (Gibco) Cat# 35400-27	-20ºC
Versene 1X	100 ml solution	Invitrogen (Gibco) Cat# 15040 Lot 3048582	-20ºC
Panc1	PANC1 cell line	ATCC number CRL-1469	Liquid Nitrogen
PBS	Phosphate buffered saline	Invitrogen (Gibco) Cat# 10010-023	RT
DMSO	Dimethy sulfoxide	Sigma D4540-100ml	RT

2.1.3 Materials for Immunohistochemistry

Reagent	Recipe	Source	Store
PBS pH 7.4	Phosphate buffered saline	Invitrogen (Gibco) Cat# 10010-023	RT
IFF	PBS+ 1%BSA +2% Fetal Calf Serum	Made up prior to use	4°C
BSA	Biotinylated secondary antibody	Sigma Aldrich	4°C
Alexa conjugate	2mls IFF+ 2µl mouse 488+ 2µl Rab555 for 1 in 1000 solution	Invitrogen Cat# A-21370	4°C
Vecta shield	No counter stain	Vector labs Cat# H-1000	4°C
Triton –X 100	Triton X100 in PBS	Sigma Aldrich CAT #: 9002-93-1	25°C
Clear nail varnish	As per protocol	Any retailer	RT
Primary antibody	Alpha SMA mouse 488 Vimentin goat IgG	R and D systems CAT #IC1420G CAT #AF2105	4°C
Paraformaldehyde	4% Paraformaldehyde	Sigma Aldrich Cat# P6148	RT

2.1.4 Materials for Protein gel analysis

Reagent	Recipe	Source	Store
15ml tube	Acetone resistant conical tube 17x120mm,	BD Cat# 352096	RT
50 ml tube	Acetone - resistant Falcon tubes	BD Cat#352098	RT
Filter Devices	Amicon-Ultra 4ml Centrifugal Filter devices 3KD	Amicon	RT
Tris- HCL	Tris hydroxymethyl methylamine 1M pH 7.60	Sigma #T-2788 Lot 072k8417	RT
Gradient Gel	Novex Tris-Glycine 4-20% gradient gel	Novex	4°C
Cyber safe DNA gel stain	10µl of 10000X concentrate in DMSO	Invitrogen Cat#S33102 Lot 489224	RT
RNase free DNase set	As per protocol	Qiagen Mat#1023460	RT

2.1.5 Materials for Laser capture micro-dissection

Reagent	Recipe	Source	Store
Adhesive cap	Adhesive cap 500 opaque	Carl Zeiss Cat#415101-4400-250 Lot 000732-09	RT
Picopure®	DNA extraction Kit	Life Technologies Arcturus Cat# Kit 0103. Lot 137842	RT
Zymo research	DNA clean and concentrate™-5 kit	Zymo research cat#d4013 Lot ZRC163134	RT
Ambion	Recover All Total Nucleic acid Isolation	Ambion Cat#AM1975 Lot 0905032	RT
Qiagen	QiAmp DNA mini Kit (50)	Qiagen Cat# 51304 Lot 133192112	RT
Sterile water	DNase-RNase free Sterile water	Sigma Lot 019k2374	RT
NaSCN	8.1g of NaSCN in 100ml nuclease free water	Sigma Aldrich Cat#251410	RT

2.1.6 Reagents for PicoGreen assay

Reagent	Recipe	Source	Store
Quant-iT™ PicoGreen® dsDNA Assay Kits	Pico green reagent TE Buffer-10 mM Tris-HCl, 1 mM EDTA, pH 7.5 Lambda DNA standard	Invitrogen	4°C RT 4°C

2.1.7 Reagents for Multiplex PCR

Reagent	Recipe	Source	Store
10X Buffer	Gene amp 10X pcr buffer	Qiagen Multiplex PCR Kit Cat# 206143	-20ºC
MgCl2	25mM $MgCl_2$	Qiagen Multiplex PCR Kit Cat# 206143	-20ºC
dNTP mix	10 mmol each	Qiagen Multiplex PCR Kit Cat# 206143	-20ºC
TAE Buffer	20mls TAE in 1L of H_20 1:50	Sigma Aldrich Cat# T9285	RT
Agarose	0.8g Agarose in 100mls of TAE 1:50	Sigma Aldrich Cat# G4510	-20ºC
Primer mix	1.25µM each	Qiagen Multiplex PCR Kit Cat# 206143	-20ºC
Taq	5U/µl	Qiagen Multiplex PCR Kit Cat# 206143	-20ºC
Female and male DNA	100ng each		4°C

2.1.8 Reagents for Array CGH

Reagent	Recipe	Source	Store
Bioprime labelling kit	Random primers Cy3, Cy5 Klenow	Invitrogen Cat#18095011	RT
dNTP stock	12µl dATP, dGTP, dTTP and 6µl of dCTP 100mM stocks in 1ml TE	Qiagen Kit C – 28004	-20ºC
Qiagen Mini Elute purification kit	Buffer PB- Binding buffer Buffer EB- Elution buffer Buffer PE	Qiagen Kit C – 28004 Lot 133206093 Lot 130161242 Lot 133203411	RT
SSC	Saline-sodium citrate	Breakthrough lab Code66 Batch 49	RT
SDS	Sodium dodecyl sulphate	USB Lot 115185	RT
Formamide	Deionised Formamide	MP Lot R26530	-20ºC
BSA	filter 1g of BSA dissolved in 49.5mls H_20	Sigma Lot 08/16291	RT
Yeast tRNA	As per protocol	Invitrogen Cat#15401-029	-20ºC

2.1.9 Reagents for Fluorescent in- Situ Hybridisation

Reagent	Recipe	Source	Store
NaOAc	Sodium Thiocyanate As per protocol	Sigma Aldrich	RT
Salmon sperm	As per protocol	Invitrogen Cat#15632-011	-20ºC
Colcemide	As per protocol	Invitrogen Cat#15210-040	4°C
Alcohol	70%, 90% and 100%	Sigma Aldrich	RT
PBS	Phosphate buffered saline	Invitrogen (Gibco) Cat# 10010-023	RT
Trypsin	Trypsin EDTA solution 100mls	Invitrogen (Gibco) Cat# 35400-27	-20ºC
Methanol	Mixed with acetate to form fixative solution	Sigma Aldrich	RT

2.1.11 Reagents for Cell titre-Glo Luminescence

Reagent	Recipe	Source	Store
384 well plates	As per protocol	Corning	RT
Cell titre-Glo one solution assay reagent	1:4 dilution with PBS	Promega Cat#G8461	-20ºC
PBS	Phosphate buffered saline	Invitrogen (Gibco) Cat# 10010-023	RT

2.1.12 Reagents for Plasmid DNA transfection

Reagent	Recipe	Source	Store
Trans-IT-2020 reagent	2.5mg/ml in 80% ethanol	Mirus Cat# MIR5410 Lot# KLN04315	-20°C
Opti-MEM reduced serum Medium	As per protocol	Invitrogen Cat# 11058-021	4°C
6 well plates	As per protocol	Cat#3335	RT

2.2 Methods

2.2.1 Ethics approval

Ethics approval was obtained from the research ethics committee via the tissue bank at the Hammersmith hospital prior to the acquisition of samples.

2.2.2 Tissue collection

For primary fibroblasts, fresh tissue samples of Pancreatic Ductal Adenocarcinoma (PDA) were collected, with informed patient consent, in collaboration with the hepatopancreatobiliary (HPB) unit at the Hammersmith Hospital. Tissue samples were immediately taken for primary culture under aseptic conditions.

2.2.3 Cell culture

Primary cultures of stromal fibroblasts were established from surgically resected pancreatic cancer specimens from patients with moderate to poorly differentiated PDAs. Immediately post resection, tissue from the tumour edge was removed under aseptic conditions. The fresh tissue was cut into 1mm³ fragments and mounted on a culture dish. The tissue was then cultured in DMEM (Dulbecco's Modified Eagles Medium) supplemented with 10% Fetal Calf Serum (FCS), L-Glutamine, Penicillin and Streptomycin. Once plated, the cells were allowed to adhere by incubation at 37˚C in a humidified atmosphere containing 5% CO_2. A successful culture was evident by an outgrowth and proliferation of a monolayer of spindle-shaped cells from the tissue blocks. This usually occurred after 10 days. The explants were observed every 2 days at which time they were fed with new media as necessary.

Fibroblasts were sub-cultured by trypsinisation into T25 flasks. Once confluent, the fibroblasts were subcultured into T75 flasks following which they were either frozen in liquid nitrogen in DMSO or passaged to a secondary culture. In order to remove cells from the primary explants, 1 ml of 1:4 Trypsin and Versene was introduced into the Petri dishes containing outgrown fibroblasts. This was then incubated at 37°C in 5% CO_2 for 5 minutes or until disaggregated. Gentle tapping was used to help detach the 'sticky' fibroblasts from the base of the Petri dish used. Once detached, the cells were suspended in culture medium (DMEM) and centrifuged at 1000rpm for 5 minutes at room temperature. The supernatant was removed and the remaining pellet re-suspended in fresh culture media and transferred into a filtered T25 flask. Isolation and growth of CAFs were performed using the outgrowth method. This involved 2 or 3 passages until a sufficient monolayer (a confluent T75 ≥70% coverage) was acquired. Secondary cultures were incubated under the same conditions as primary cultures as described above.

The pancreatic ductal cell lines were purchased from American Type Culture Collection, (ATCC). The pancreatic cancer lines purchased were PANC-1, AsPC-1, MiaPaCa-2, HPAC, HS776T, BxPc3, PL45 and SU86.86. Dr Claus Jorgensen of the Institute of Cancer Research donated PL5. These cell lines were expanded and cultured as described above in DMEM or RPMI according to ATCC instructions. See table 2.1.

Dr. Ralf Jesnowski of the University of Heidelberg, Germany kindly donated the immortalised stellate cell line. The cells were isolated by the outgrowth method and were immortalized by transfection with SV40 large T antigen and human telomerase (hTERT), (*Jesnowski et al, 2005*).

Cell line	Source	Cell type	Gender	Media used
AsPC-1	ATCC	Epithelial	Female	RPMI-1640
BxPc3-3	ATCC	Epithelial	Female	RPMI-1640
HPAC	ATCC	Epithelial	Female	DMEM
Hs776T	ATCC	Epithelial	Male	DMEM
MiaPaCa-2	ATCC	Epithelial	Male	DMEM
PANC-1	ATCC	Epithelial	Female	DMEM
PL5	Dr Claus Jorgensen	Epithelial	Male	DMEM
PL45	ATCC	Epithelial	Male	DMEM
SU86.86	ATCC	Epithelial	Female	RPMI-1640
RLT-PSC STELLATE CELLS	Dr Ralf Jesnowski	Stellate Fibroblasts	Unknown	DMEM

Table 2.1 Cell lines. According to ATCC, ASPC-1 was derived from the ascitic fluid of a female patient with a poorly differentiated pancreatic cancer. HPAC is a pancreatic adenocarcinoma epithelial cell line explanted from a female pancreas with a moderate to well differentiated pancreatic adenocarcinoma of ductal origin. Hs776T was originally derived from a lymph node metastasis of a male patient with an undefined differentiated pancreatic tumour. Panc-1 cells were originally derived from a female patient with a poorly differentiated pancreatic tumour. MiaPaCa-2 was explanted from a male patient with a poorly differentiated pancreatic cancer. Su86.86 cell line was derived from the liver metastases of a female patient with a moderate to poorly differentiated pancreatic lesion.

Passage was performed by firstly adding 1: 4 Trypsin and Versene solution to the monolayer and incubating for 5 minutes under usual culture atmospheric conditions. The cells were then washed in culture media (DMEM or RPMI containing FCS) in order to neutralise trypsin activity and this solution was centrifuged to obtain a cell pellet. The supernatant was removed and the pellet re-dissolved in fresh media before being transferred to a T75 or T150 flask or frozen in liquid nitrogen. Figure 2.1 below shows primary fibroblasts at different stages of passage.

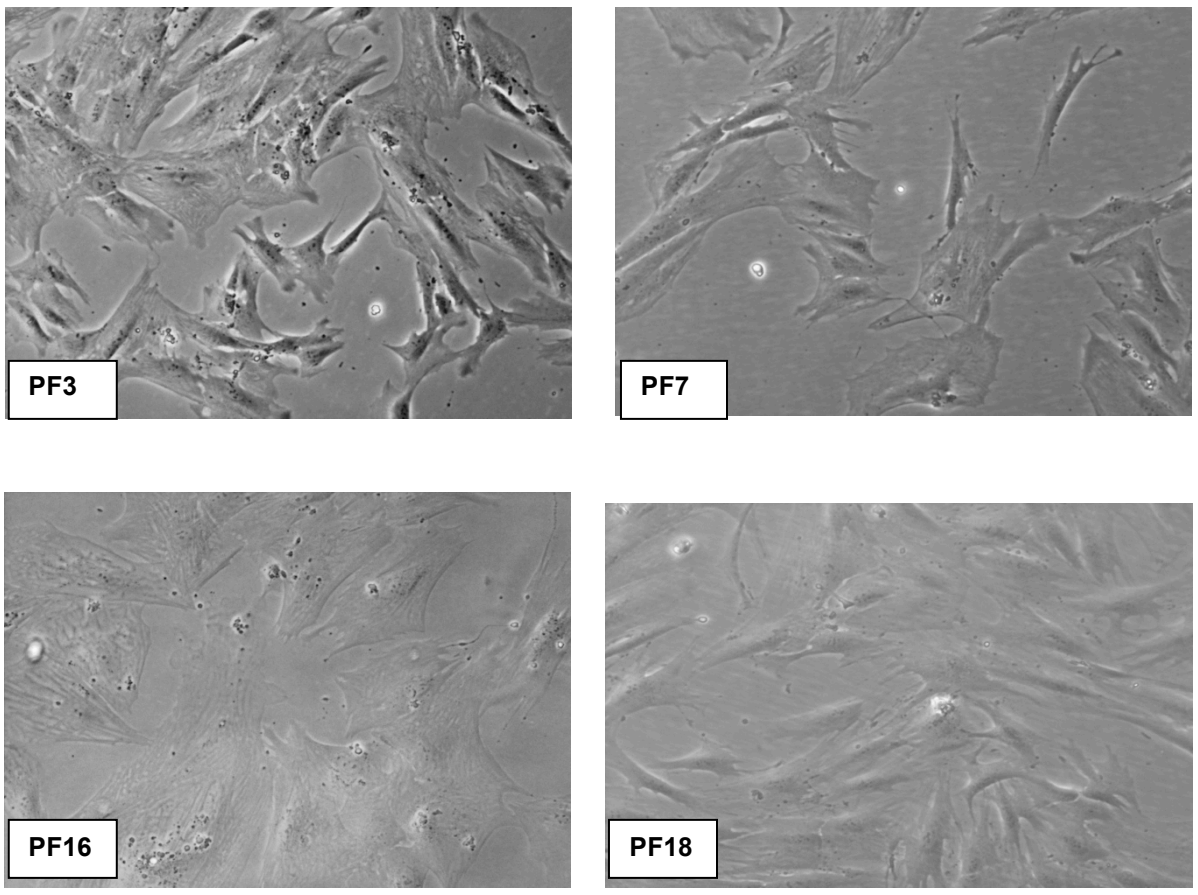


Figure 2.1 Electron microscopy of primary fibroblasts at x10 magnification, the cells appear spindle shaped. Pictures were taken at 60% confluence, a) PF3 fibroblasts at passage 5, b) PF7 fibroblasts at passage 7, c) PF16 at passage 1, d) PF18 at passage 4.

For the purpose of cell storage the pellets that were not passaged following trypsinisation, as described above, were re-suspended in a freezing solution of 10% Dimethylsulfoxide (DMSO) and 90% culture media before being placed into 1.8ml screw cap freezing tubes and kept in -80˚C for 24 hours. This was done to introduce slow freezing and prevent crystallisation prior to cryostorage in liquid nitrogen. To thaw frozen cells, the freezing tubes were warmed to 37°C and culture media was added. The suspension was centrifuged at 1000rpm for 5 minutes at room temperature and re-suspended in fresh culture media before being transferred to a culture flask T25 for incubation.

2.2.4 Immunoflourescent labelling of cells on cover slips

Cells were cultured on 13mm cover slips in multiwell plates and allowed to grow to 70% confluence. Once confluent the cells were fixed with 4% Paraformaldehyde in phosphate buffered saline (PBS) at pH 7.4 for 1 hour. This was rinsed in PBS and stored in 0.5mls of PBS at 4°C to prevent the fixed cells from desiccation. The PBS was then removed and the cells permealised with 0.5% TritonX-100 in PBS over 10 minutes. The cells were then rinsed in PBS twice followed by a protein carrier IFF. IFF was made up of PBS, 1% BSA and 2% FCS. The primary antibodies were appropriately diluted in IFF and the cells were incubated with this for 40 minutes on a shaking incubator. They were then washed in PBS three times at 5 minutes each and incubated with the Alexa conjuagte1 in 1000 in IFF for a further 40 minutes. They were then washed in PBS plus DAPI 1 in 10000 three times at 5 minutes each, rinsed in PBS and dipped in water. The cover slips with adhered cells were carefully drained and mounted in 4µl vectashield on slides. Excess vectashield was carefully

blotted and the cover slips sealed with nail varnish onto the slides. These were either stored at 4°C prior to viewing or stored for longer at 20°C.

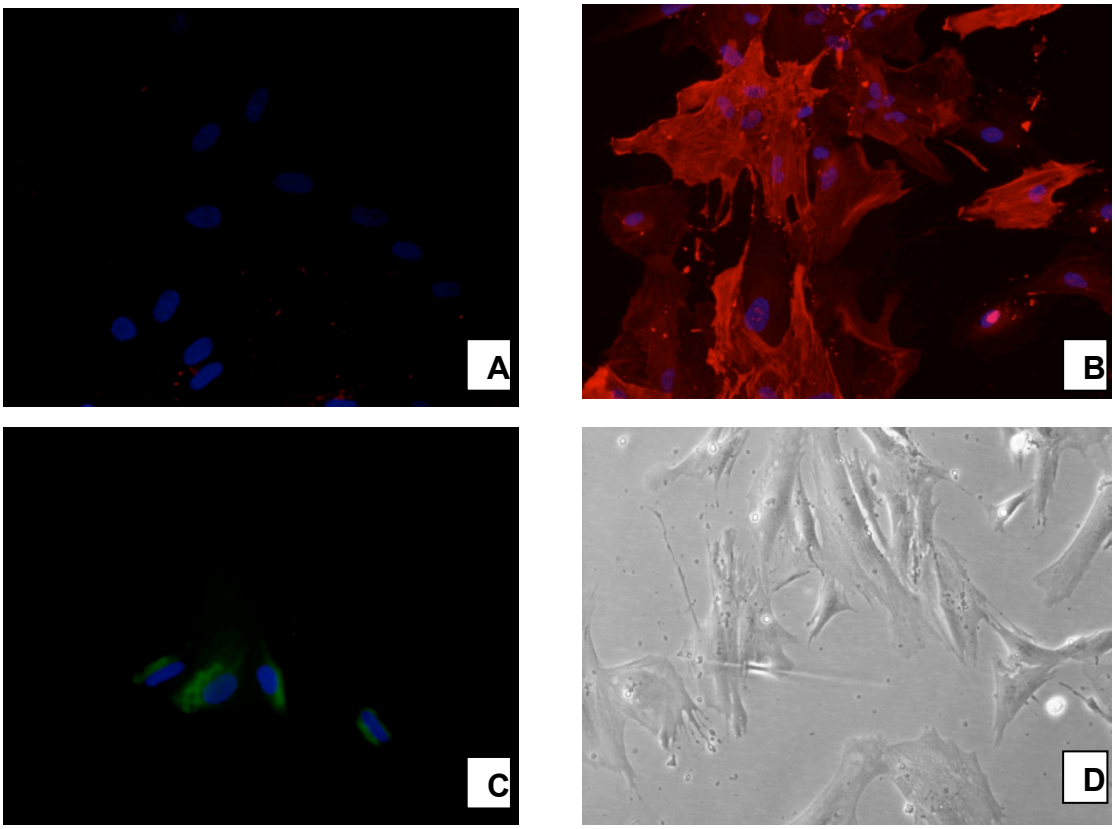


Figure 2.2. Immunohistochemistry of primary fibroblasts, A) Negative stain for αSMA (no red seen), B) Pancreatic CAFs immunostained for αSMA (red) and counterstained with DAPI (blue), C) FAP (Fibroblast activating protein, green stain), D) unstained fibroblasts as seen under a light microscope 10X magnification.

2.2.5 Laser-capture microdissection (LCM) of FFPE

Deciphering the cellular and molecular interactions that drive disease within the tissue microenvironment holds promise for discovering drug targets in the future. Laser-capture micro-dissection is a method used to procure pure sub-populations of tissue cells, such as stroma, under direct microscopic visualisation. LCM technology can harvest the cells of interest directly, to give a histologically pure enriched cell population.



Figure 2.3 Zeiss PALM Laser Capture Micro-dissection station. This photo shows the exact set up used to obtain micro-dissected tissues fro Formalin Fixed Paraffin embedded samples.

This system was initially developed for the analysis of solid tumours, in particular, prostate cancer. The system, based on an inverted bright-field light microscope, has been previously described by Emmert-Buck et al and has since been improved. In PALM systems, separation of the specimen occurs with a laser beam focused so precisely that a beam accuracy of less than 1µm can be achieved. The selected specimen is removed with a software controlled laser beam and catapulted by a laser pulse into a collection device. This procedure ensures that no unwanted elements reach the specimen. Because the laser is only directed at the sample for less than 1 nano second, it does not transfer any heat. The process is completely contamination free and guarantees the best possible preservation of the material.

Archived samples of formalin fixed paraffin embedded (FFPE) blocks of PDA were retrieved, including 1 block of chronic pancreatitis. Each slide was micro-dissected to isolate the tumour and stromal components using the PALM Microbeam micro dissection system (Carl Zeiss) according to published methods. In order to obtain sufficient quantities of DNA for downstream applications (≥ 1500ng), 12 slides of each block were required.

Ten-micrometre sections were cut from FFPE tissue blocks and placed onto glass membrane slides. One slide of each sample was stained with Haematoxylin and Eosin in order to correctly identify regions of stroma and glandular tissue and to guide the sections to be cut by LCM. A consultant Histopathologist identified suitable areas of stroma and glandular tissue. The same areas were identified and outlined on methylene green stained slides. This process consisted of immersion in Xylene (deparaffinisation step) for 5 minutes followed by hydration in graded alcohol concentrations, (100% and 70% alcohol respectively) and de-ionised water. The slides were then immersed in methyl green dye for a further 5 to 10 minutes to achieve a light stain. Twelve serial sections were cut out from the laser capture slides and catapulted into adhesive caps of 500µl tubes using the PALM Laser micro dissection system.

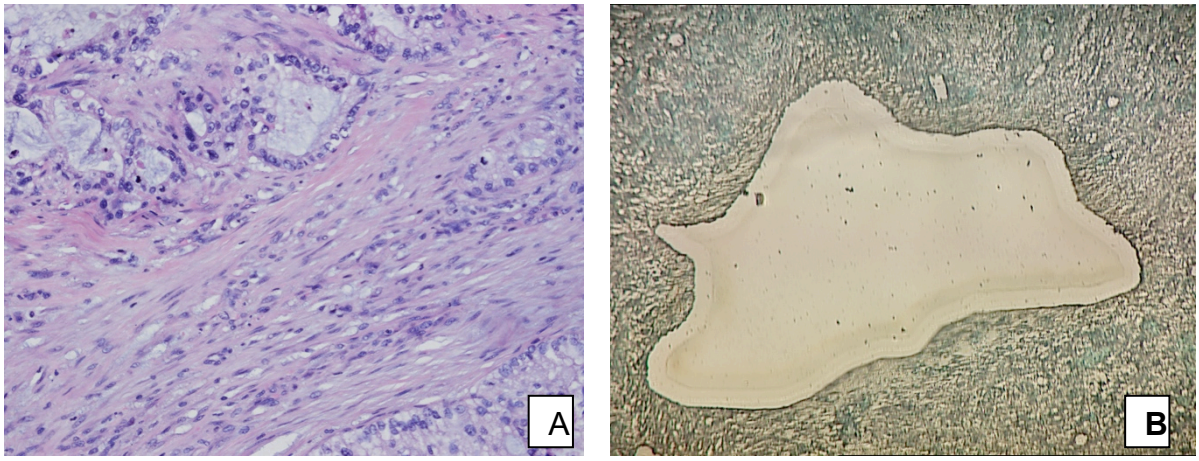


Figure 2.4 H and E stained and LCM methyl green cut sample of FFPE Haematoxylin and Eosin staining of FFPE samples and LCM of the area as seen on the P.A.L.M system. A) A magnified area of stromal fibroblasts with H and E staining, B) A methyl green stained slide with an area of micro-dissected stroma using the PALM laser system

DNA was isolated using the Arcturus – Pico Pure® DNA Extraction Kit- KIT0103. An initial fragmentation step was used with 1ml of 1M sodium thiocyanate (NASCN). For this step the tissue was transferred to a 1.5ml tube. The samples were incubated overnight at 38ºC then centrifuged at maximum 10,000g and the Sodium Thiocyanate (NASCN) removed. The samples were washed with sterile PBS 1ml and centrifuged for 5 minutes. This step was repeated and the PBS removed. A proteinase K solution was made up by adding 155µl of reconstruction buffer provided to a vial of proteinase K mix. This was placed on ice immediately. Samples were immersed in 50µl to 155µl of proteinase K solution dependent on volume in the tube and tubes were incubated overnight at 65˚C (minimum 16 hours) followed by a 10 minute incubation at 95˚C in order to inactivate the proteinase K. The samples were allowed to cool to room temperature.

The DNA obtained was then subjected to a clean and concentrate step using Zymo research DNA Clean and Concentrate ™-5. A DNA binding buffer double the volume of the current concentration in each microcentrifuge tube was added to each double stranded (ds) DNA sample, i.e. 100µl. The new mixture was loaded onto a Zymo spin column and this was mounted onto a 2ml collection tube. This was centrifuged at full speed (≥ 10,000g) for 30 seconds and the subsequent flow through was discarded. Two hundred microlitres of the wash buffer provided was then added to each Zymo column and centrifuged for 30 seconds at maximum sped of 10,000g and the flow-through discarded. This step was repeated in order to thoroughly wash the DNA. The Zymo spin column was then placed onto a new 1.5ml collection tube and 10-15µl of water added for DNA elution. This was centrifuged at maximum speed of 10,000g for 30 seconds. The DNA concentration was then quantitated using a Nanodrop® 1000 spectrophotometer.

Pico green Assay for double stranded DNA (dsDNA) quantification

PicoGreen is a fluorochrome that selectively binds dsDNA and has characteristics similar to that of SYBR-Green I. It has an excitation maximum at 480 nm and an emission peak at 520 nm. When bound to dsDNA, very little background interference occurs since the unbound dye does not fluorescence. Fluorescence enhancement of PicoGreen is greater than 1000 fold; Pico Green is 10,000-fold more sensitive than Ultra Violet (UV) absorbance methods and highly selective for dsDNA over single stranded (ss) DNA and RNA.

The samples to be assayed were processed in duplicate. Each sample was placed on a plate as a 'neat' and a, 1:10 dilution. The samples were diluted in 1 x hydroxymethylaminomethane (tris) and ethylenediaminetetraacetic acid (EDTA), (TE) buffer. The DNA standards were prepared based on a low range standard curve, (Table 2.1). Ninety nine microlitres of 1 x TE was added to all test sample wells and 100µl to the blank wells. A calculated volume of 1 x TE was added to the standard wells based on the low range standard curve. The standard DNA was added to the appropriate wells, followed by 100µl of PicoGreen to all wells excluding the empty ones. This was left at room temperature for 2-5 minutes and the samples were read on the Perkin Elber Victor™ X5 scanner using Perkin Elber 2030 Manager software.

50ng/ml control DNA stock (µl)	Volume of TE (µl)	Diluted PicoGreen reagent (µl)	Final DNA concentration	DNA in 200µl assay
100	0	100	25ng/ml	5ng
40	60	100	10ng/ml	2ng
10	90	100	2.5ng/ml	500pg
4	96	100	1ng/ml	200pg

Table 2.1 The low range standard curve used for Pico Green quantification. A low range curve was chosen as a predictor as the values that were expected should fall within these ranges. This was used as a scale to quantify the DNA concentrations.

2.2.6 Array CGH of primary cells and FFPE

Bacterial artificial chromosomes (BACs) are large insert genomic clones that have been widely used in aCGH studies (*Tan et al., 2007*). Bacterial artificial chromosome probes vary in length from 100 to 200 kb and the resolution (i.e. the distance between each DNA target represented on the array) of each BAC array is defined by the number of unique probes it contains. The probe content of genome-wide BAC arrays range from 2,400 to 32,000 unique elements, (the tiling path array). Tiling path arrays (i.e. arrays where each BAC overlaps with its contiguous BACs) provide a resolution of up to 50 kb, given that a genomic change can only be detected if it is sufficiently big to significantly change the hybridization intensity in one of the channels (i.e. change the red: green ratios). The ratio of fluorescent intensities (red and green) is proportional to the ratio of the copy numbers of the DNA sequences in the test and reference genomes.

Equal intensities of the fluorescent dyes on a probe are interpreted as this region of the genome having an equal quantity of DNA in the sample and reference DNA. If, however, there is an altered Cyanine3 (Cy3) to Cyanine 5(Cy5) ratio, this is interpreted as a loss or a gain of the sample DNA at that specific region on the genome, (*lee et al*, 2007). Any genomic imbalances found would be validated with metaphase fluorescent in situ hybridization. These platforms provide sufficiently intense signals for the detection of single-copy number alterations, accurately define the boundaries of genomic aberrations, and, importantly, can be applied to archival FFPE tissue as well (*Little et al, 2006; Johnson et al, 2006).*

DNA was purified from cell pellets using the Qiagen DNeasy Extraction Kit according to the manufacturers' protocol. Equal amounts of labelled genomic DNA from a test and a reference sample were co-hybridized to an area representative of the genome. Pooled DNA can be used as controls (*Shinawi et al*, 2008) and a pooled female DNA obtained from the Institute of cancer research was used in this methodology. Genomic DNA of the samples and the control were differentially labelled with dCTP-(Cy3) and (Cy5). Hybridization of repetitive sequences was blocked using human Cot-1 DNA. The slides were scanned into image files using an Axon 4000B scanner (Axon instruments, Burlington, CA, USA).

The spot intensities were measured and the gpr image files quantified using Genepix Pro6 image analysis software (Axon instruments). These gpr files were analysed to produce the copy number analysis. Smoothed Log2 ratio values less than 0.12 were categorised as losses, >0.12 as gains and in between as unchanged. Amplifications were defined as smoothed log2 ratios values greater than 0.4.

Figure 2.5 below is a schematic representation of the principle of array CGH. This figure shows the steps in BAC array CGH. (1) BAC clones are selected from a physical map of the genome, see figure 2.6. (2) DNA samples are extracted from selected BAC clones and their identity is confirmed by DNA fingerprinting or sequence analysis. (3) A multi-step amplification process generates sufficient material from each clone for array spotting. Each clone is spotted in replicate onto a solid support. Reference DNA and test DNA are differentially labelled with cyanine 3 and cyanine 5 respectively. (4) The two labelled products are combined and hybridized onto the spotted slide. (5) Images from hybridized slides are obtained by scanning in two channels. Signal intensity ratios from individual spots can be displayed as a simple plot (6) or by using more complex software such as SeeGH, which can display copy number alterations (CNA) throughout the whole genome.

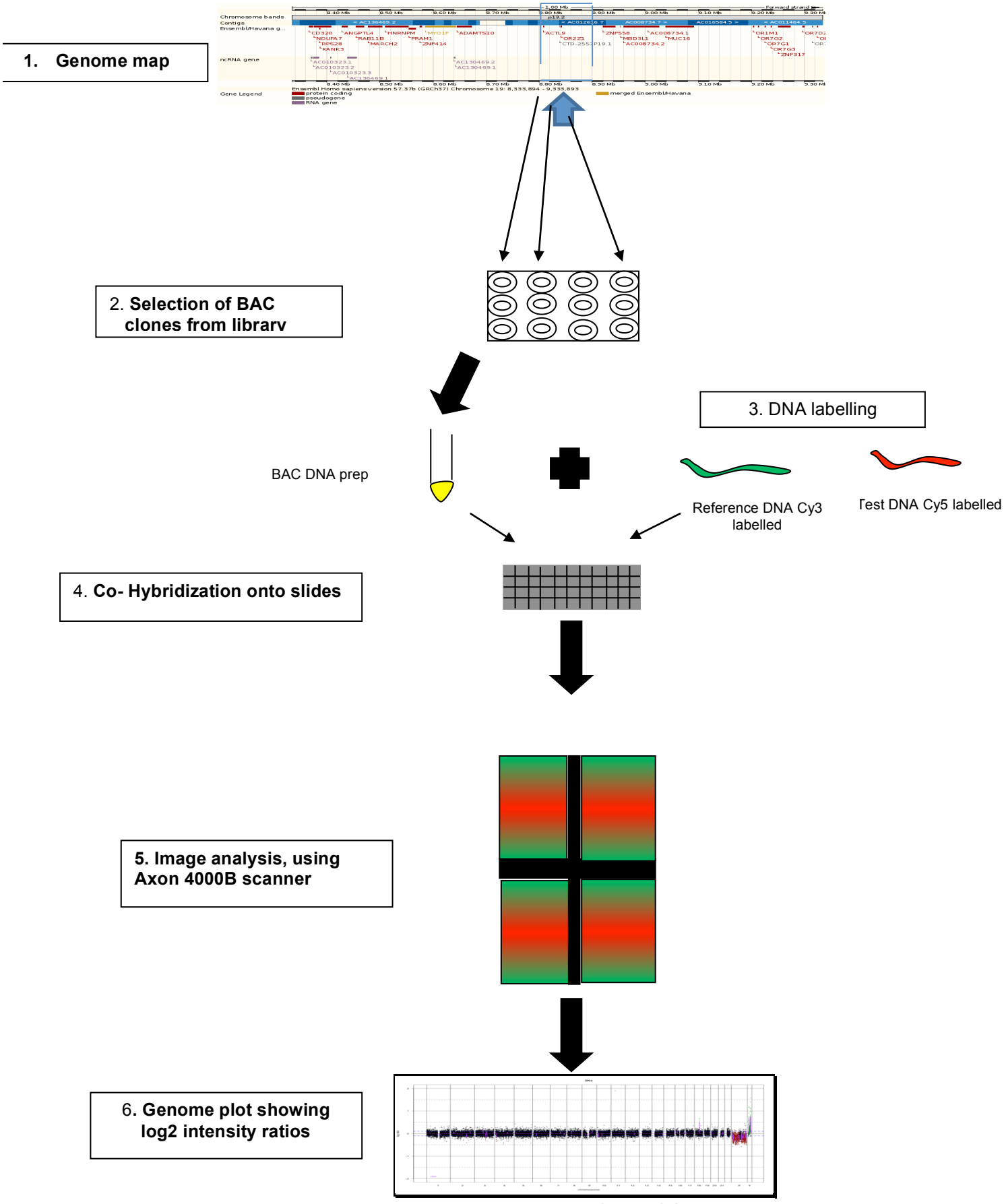


Figure 2.5 Principle of arrayCGH.

The array CGH platform used for this study was constructed at the Breakthrough Breast Cancer research centre and comprised about 32000 BAC clones tiled across the genome and spotted onto corning GAPS11 coated glass slides (Corning, NY, USA). Six hundred nanograms of the sample DNA and same sex, all Female DNA, (Breakthrough Breast Cancer research centre) were placed into a 0.5ml thin tube and appropriately labelled. The volumes required based on the starting concentration are represented in the Table 2.2. Ultra filtrated water was added to a total concentration of 21µl.

DNA Sample	Concentration needed	Volume	H20 added
PF3	80ng/µl	8µl	13µl
PF7	100ng/µl	6µl	15µl
PF9	100ng/µl	6µl	15µl
PF16	100ng/µl	6µl	15µl
Panc1	100ng/µl	6µl	15µl
Female DNA	75ng/µl	8µl	13µl

Table 2.2 DNA concentrations and volumes added for initial labelling step

A pooled Female DNA, from 24 individuals, was used as the control for all experiments. Twenty microlitres of random primers was added to each tube and denatured for 5 minutes at 95˚C. This was placed immediately on ice for 10 mins and 5µl of deoxribonucleotide triphosphate (dNTP) stock, 3µl of Cy3 or Cy5 and 1µl of Klenow was added to each tube and the mixture incubated overnight in the thermo cycler. The dNTP stock was made up of 12µl dATP, dGTP, dTTP and 6µl of dCTP at 100mM stock in I ml Tris/EDTA, (TE) buffer.

Purification of the labelling reaction (Qiagen MinElute Purification Kit)

For each sample, five volumes of binding buffer (PB) were added to each labelled material, vortexed and transferred to a mini elute column. This was centrifuged for 1 minute at 13,000 rpm and the flow through discarded. Subsequently 700µl of Wash Buffer was added and centrifuged at the above speed and the flow through discarded. To avoid any residue of ethanol in the samples they were centrifuged again at 13,000 rpm. Twelve microlitres of elution buffer (EB) was added to the middle of the filters within their columns and then centrifuged at 13,000 rpm for 1 minute.

Sample precipitation

Tumour and reference DNA were combined in a thick 0.5ml tube and 100µl (1µg/µl) of Cot-1 DNA, 2µl of NaOAc pH 7.0 and 300µl of ice-cold 100% ethanol was added to each sample. The mixed reagents were precipitated at 20°C for 1-2 hours and then centrifuged at 13,000 rpm for 30 minutes. The supernatant was removed and the samples air dried.

Slide preparation:

The pre- hybridization buffer was heated and filtered. Slide pre-Hybridisation buffer was made up of 49.5mls of UF water, 25mls of 20x SCC, 25mls of deionised formamide and 0.5mls of 20% SDS per 100 ml solution. The slides were placed into the pre-hybridisation blocking buffer (in a 50ml falcon tube) and incubated for a minimum of 45 minutes at 42˚C (optimally 2hrs). Following this the slides were rinsed in de-ionised water and spun at 2000rpm for 2 minutes to dry.

Hybridisation

Forty five microlitres of hybridization buffer was added to each of the sample pellets. Hybridisation buffer was made up with 250µl of Deionised formamide, 50mg of Dextran Sulphate, 50µl 20x SCC, 50µl of 20%SDS, 20 µl of 100µg/µl yeast tRNA and 130 µl of ultrafiltrated water per 500µl solution. The samples were left at room temperature in the dark for 30-45 minutes. They were then vortexed and centrifuged to ensure that the pellet reconstituted completely in the hybridisation buffer. They were denatured for 15 minutes at 70˚C and re-annealed for 30 minutes at 37˚C (using PCR machine). Each sample was applied to the cover slip (24x60mm) and the slide was carefully lowered onto the cover slip. The slides were then placed in a moist Hybridisation chamber and incubated at 42˚C overnight.

Wash solutions

Wash 1, 0.1% Sodium dodecyl sulphate (SDS), consisted of 10mls of 20x Saline-sodium citrate (SSC), 0.5mls of 20%SDS and 89.5mls of Ultra-filtrated water per 100 mls of solution. Wash 2, 50% formamide was made up of 10mls of 20x SCC, 50mls of formamide and 40mls of ultrafiltrated (UF) water per 100 mls of solution and wash 3 was made using 1ml of 20 times SCC and 99mls of UF.

Stringency wash

The slides were washed in Wash1 (20x SCC, 0.1% SDS) for 15 minutes at 45˚C and then the cover slip removed slowly by allowing it to gently slip off the slide. This was followed by wash 2 (20x SCC, 50% formamide, pH 7.0) for 15 minutes at 45˚C, Wash 1 (20x SCC, 0.1% SDS) for 30 minutes at 45˚C, Wash 3 (0.2x SCC) for 15 minutes at room temperature and finally Wash 3 (0.2x SCC) for 15 minutes at room temperature. They were then centrifuged at 2000rpm for 2 minutes. The slides were scanned using an Axon 4000B scanner (Axon instruments) and images were processed using Genepix Pro 5.1 image analysis software.

2.2.7 Fluorescent in Situ Hybridisation (FISH)

Fluorescent in Situ Hybridisation mapping was used to map the clones of any possible deletions. The cells were mounted onto slides and labelled with BAC clones representative of the areas suspected to have genomic changes. These clones were hybridized and a fluorescent probe added prior to inspection under microscopy. Cells were viewed in metaphase.

Mapping of BAC clones

Clones were chosen from an available 32K clone library at the Institute of cancer research. They were mapped based on the array CGH location of possible genomic changes as shown below. See figure 2.6.

Region overview of CH19p13.2

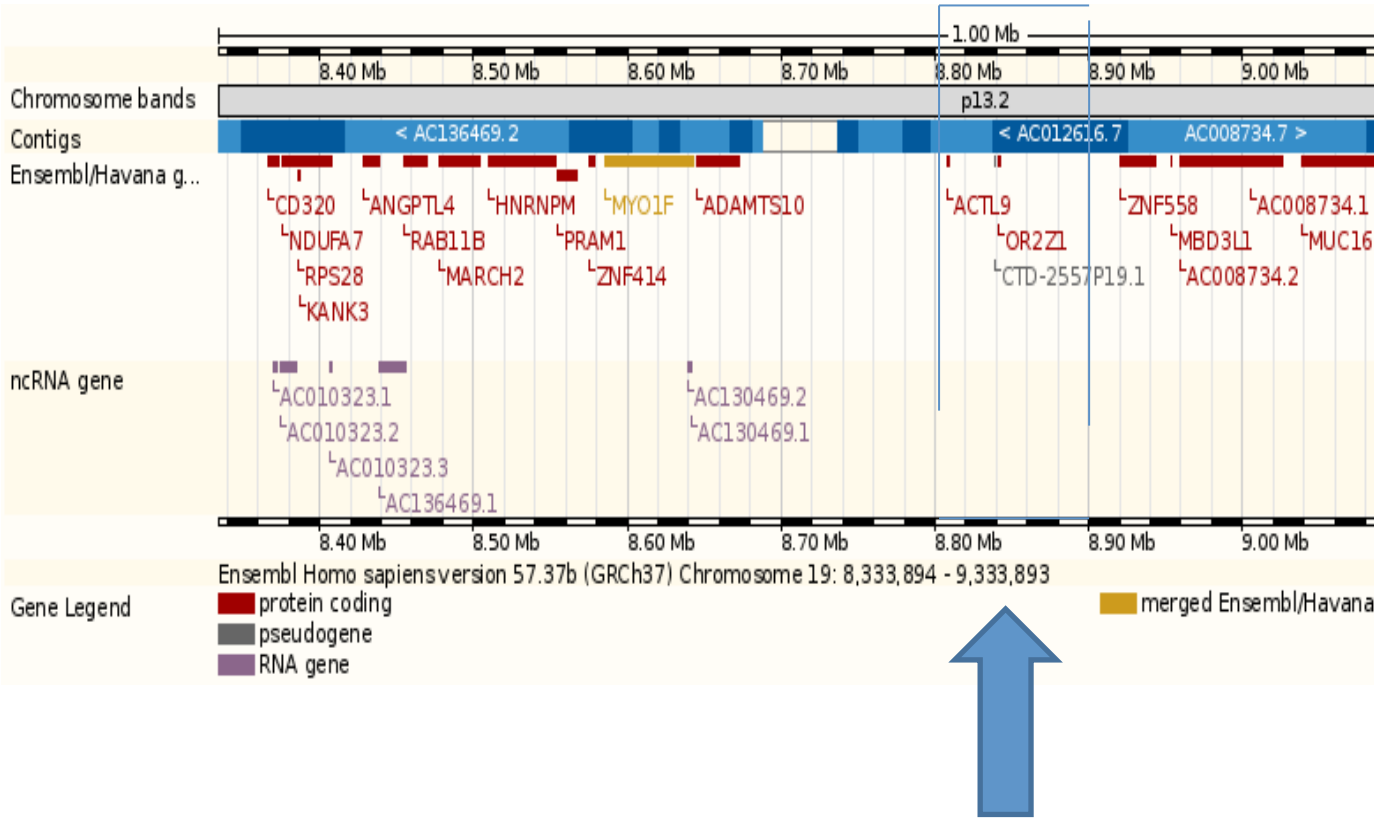


Figure 2.6 Region overview of Chromosome 19P 13.2 showing a possible gain

The clones used from the Library were as follows:

1) RP11- 743O10

2) RP11- 361O08

3) RP11- 282G19

4) RP11- 367L15

5) RP11- 598E05

6) RP11- 680A23

The DNA concentration of each BAC clone was measured via Nanodrop

BAC clone	DNA concentration	260/280	260/230
1	1393.1	1.58	1.81
2	813.5	1.71	2.01
3	1272.8	1.61	1.85
4	1050.1	1.65	1.88
5	1147.7	1.57	1.78
6	926.7	1.69	1.96

Table 2.3 DNA concentrations of the BAC clones chosen. Each sample was made up to 20µl in 200 µl. These were vortexed well and 5µl of the 1 in 10 diluted solutions was used for Biotin labelling.

Biotin Labelling

Bacterial artificial chromosomes DNA was labelled with Biotin in a 45µl reaction. 5µl of amplified BAC DNA diluted to 1 in 10 as described previously was mixed with 20µl of random primers and 23µl of H_2O. This mixture was denatured at 95ºC for 5 minutes and placed on ice immediately for 10 minutes. Five microlitres of dNTP and 1µl of Klenow DNA polymerase was added to this mixture. After quickly vortexing and spinning the solution was incubated for 3 hours at 37 ºC via PCR.

Purification

Preparation of G50 columns prior to purification

These columns are vortexed for one minute and the ends snapped off and placed into an empty 1.5ml eppindorf. This is spun at 48rpm for 1.5 minutes and the column transferred to a new tube.

Purification step

One hundred microlitres of amplified biotin labelled BAC DNA was added to each column and this was centrifuged. Each sample was then transferred to a 0.5ml thick tube.

Precipitation

To 44µl of each sample 50µl of H_2O, 60µl of COT1, 2µl of salmon sperm, 16.4µl of NaOAc and 360µl of 100% ethanol was added. After Vortexing the samples were precipitated at -80 ºC for 1 hour. Following precipitation the samples were centrifuged at 13.2K rpm, the supernatant discarded and the precipitate dried for 5 to 7 minutes at 37 ºC. This process of centrifugation and removal of supernatant was repeated and the samples dried again for 5 minutes at 45 ºC. Twelve microlitres of hybridization buffer was added to each dried pellet and incubated at 37 ºC for 10 minutes.

Slide preparation

The slides were placed in 70% acetic acid for 10 minutes followed by repeated washes in PBS. The slides were then dehydrated in 70%, 90% and 100% alcohol consecutively for 2 minutes each. The slides were dried on a warmer at 45 ºC for 1 minute then at room temperature for a further 10 minutes.

Generating a metaphase from growing cells

The cells were exposed to 2µl of Colcemide per ml of media and incubated for 2.5 hours in humidified air at 37°C and 5% CO_2. Following this, the culture media was removed and 7mls of trypsin was added to each T75 flask and cells were allowed to detach for 7 minutes under the same conditions. Once the cells were fully detached, 15mls of pre-warmed distilled water or KCL0.0075M was added and left to incubate for a further 15 minutes. Fixative solution, (200mls of 3:1 methanol to acetate) was then added to the cells and this was quickly vortexed and centrifuged at 1500rpm for 5 minutes. The resulting supernatant was poured out and the cells re-suspended in another 15mls of fixative solution. This was again centrifuged at 1500rpm for 5 minutes. The latter step was repeated and the cells were stored in 5mls of fixative solution at -20ºC. For use the cells were centrifuged for 5 minutes and resuspended in 1 ml of fixative solution prior to mounting onto slides. The pictures are taken of the probes in metaphase spread

2.2.8 Drug screening and Cell titre Glo (CTG) measurement

2.2.8.1 Cell titration for Gemcitabine curves

Prior to performing the Ashworth plate 10 compound library screen on the PDA cell lines, an initial simple cell titration was performed in order to ascertain the growth pattern of the pancreatic cancer cell lines obtained from ATCC. Cells were plated in a reducing number from 1x 10^4 cells per well to 7.8x10^{-2} cells per well on day 1, in 96 well plates and allowed to expand. Cell Titre Glo (CTG) read at Day 6 determined that 1000 cells per well was the suitable cell count to be used for further experiments. With this cell number plated there were 20,000 to 25,000 cells per well after a 72 hour period. These cells expanded suitably into a monolayer without overcrowding or cell death.

2.2.8.1.1 Gemcitabine resistance after 72 hours of treatment

Once the cell count to be used had been established, it was then necessary to review the response of these cells to Gemcitabine. A simple experiment to establish the response to Gemcitabine was performed. This was done firstly after 72 hours of exposure to a reducing dose of Gemcitabine. PDA cell lines PANC-1 and BxPc3 were plated on 96 well plates at 1x10^3, 2x 10^3, 3x10^3 and 4x10^3 cells per well. Twenty four hours post plating; the cells were fed with Gemcitabine ranging from -5M to-11M and a 0M control. As per protocol, CTG readings were done seventy two hours post treatment with Gemcitabine and the data analysed for cell survival.

The four concentrations of 1000, 2000, 3000 and 4000 cells per well were used to see if there wound be a difference in the pattern of sensitivity or resistance based on cell number.

2.2.8.1.2 Gemcitabine resistance after 6 days of treatment

After 4 days of exposure to Gemcitabine the cells were washed and fed with Gemcitabine free media. The CTG reading was performed after 72 hours as per protocol. The same experiment was repeated; however, on day 4 the media was changed to Gemcitabine free media and CTG readings done on day 6. This was to observe the true effect of the drug already taken up by the PDA cells. The results of these experiments are discussed in further detail in chapter 4.

2.2.8.2 Cell titre Glo (CTG) survival readings

The liquid from each plate was removed by tipping and the plates spun to dryness for a few seconds via centrifuge at 1000rpm. Cell titre Glo solution was made in a ratio of 1 in 4 with PBS. This bioluminescent marker quantifies the ATP in cells which is a representative of those that are metabolically active. Using the Multidrop Combi Reagent Dispenser 25 µl of CTG solution was applied to each well. This was incubated in darkness on a rotating platform for ten minutes before being read on a plate reader. The data collected was collated and analysed using R' and Cell HTS software programming in order to find compounds to which the pancreatic cancer cell lines were sensitive to. Graph pad Prism (version 5.0) was used to carry out statistical analysis.

2.2.8.3 High throughput screening

For the Ashworth plate 10 compound library drug screen, cells were cultured as previously described in order to obtain a greater than 70% confluent monolayer in a T75 flask. These cells were trypsinised and re-suspended in fresh media. A 10µl sample of cell suspension was mixed with 10µl of tryptan blue staining dye and read using the Countess® Automated Cell Counter. The number of live cells only, was used to calculate the volume of cell suspension required to give 1000 cells per well per 384 well plate. On average about 40,000 cells were necessary for each 384 well plate or $1.2x10^6$ for triplicate plates of each sample at a volume of 25µl per well. The cells were plated using the Multidrop Combi Reagent Dispenser from Thermo Scientific. These plates were incubated for 24 hours at 37ºC and 5% humidified CO_2. The cells were then exposed to the Plate 10 compound library by serial dilutions of a previously prepared plate of chemotherapeutic compounds. Each drug was administered in volumes that would represent four concentrations, 1µM, 10µM, 100 µM and 1000 µM respectively and these were administered using the Hamilton automated liquid handler robot. Following application of the drug library to each cell line, the triplicate samples were again incubated for 72 hours at 37ºC and 5% humidified CO_2. On day 4 the plates were read for cell viability.

2.2.9 Luciferase marking of PDA and stellate cell lines

Prior to coculture experiments, it is necessary to mark both PDA cell lines and stellate cells with distinct bioluminescent markers that can be differentiated when read using CTG.

2.2.9.1 Generating Renilla and Firefly luciferase plasmid

The vector chosen was pcDNA3 (Invitrogen, Life technologies) for Renilla and pIRESpuro3 for Firefly. The vector with the synthetic Renilla insert was pCMV5C/chRluc or chFluc respectively, see figure 2.7.

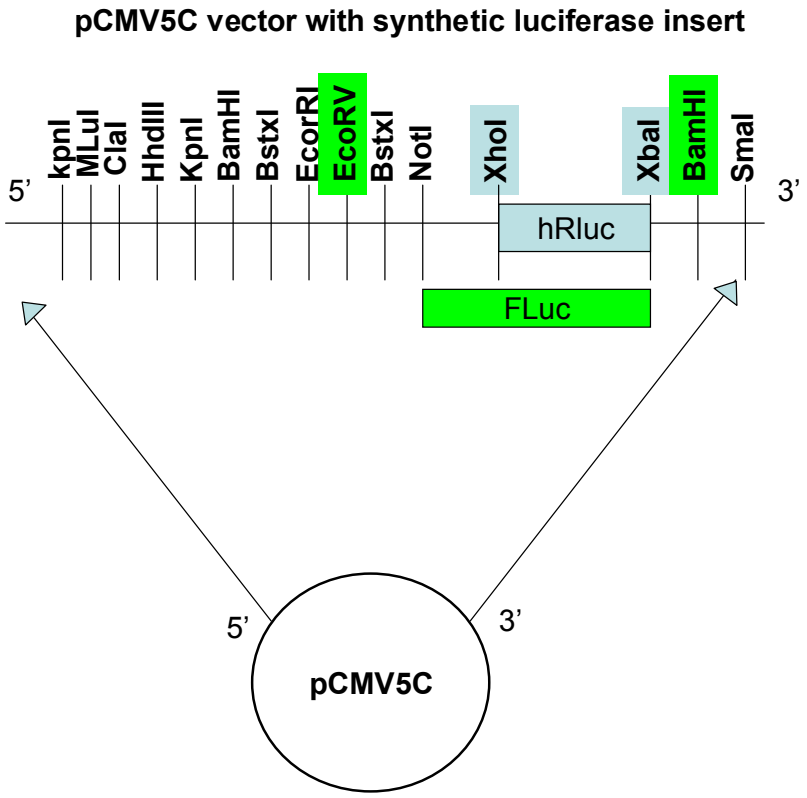


Figure 2.7 Luciferase plasmid containing the synthetic Renilla and Firefly insert. The vector is 5.4 kilo bases in length, resistant to ampicillin and containing the cloning site XhoI/XbaI for Renilla luciferase. In Firefly luciferase XhoI disappears from the cloning site but XbaI is still present. The ligation sites for each luciferase are shown in green for Firefly and blue for luciferase.

The steps to cloning involved firstly purification of the plasmid (using mini prep and nanodrop) followed by digestion and purification of the insert, ligation, transformation, amplification of he clones and finally, sequencing. The end result being that of a purified insert placed into a plasmid vector and cloned to be used in coculture.

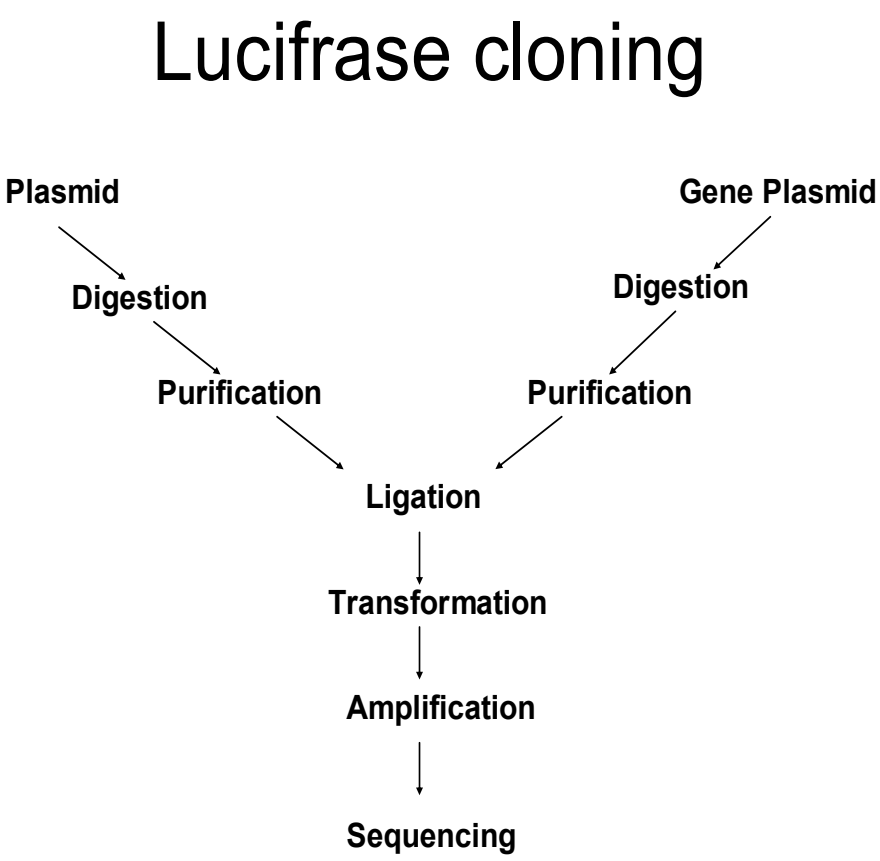


Figure 2.8 Steps in Luciferase cloning

2.2.9.2 Plasmid purification using Gen-Elute™ HP plasmid miniprep kit and protocol

Harvesting, lysis and preparation of the cleared lysate

Each sample was processed in duplicate. One millilitre of plasmid was pelleted at ≥ 12,000xg for one minute and the supernatant discarded. The plasmids were resuspended in 200µl of resuspension solution and pipetted up and down to mix. Two hundred microlitres of lysis buffer was added and the solution gently inverted 6 - 8 times to mix. This was allowed to clear for 3-5 to minutes. Three hundred and fifty millilitres of neutralizing or binding buffer was added and the mixture gently inverted 4 to 6 times. The debris was pelleted at ≥ 12,000xg for 10 minutes via centrifuge.

Column preparation

The miniprep binding column was inserted into a microcentrifuge tube and 500µl of column preparation solution was added to the column. This was centrifuged at ≥ 12,000xg for 30 seconds to one minute and the flow through was discarded.

Binding, washing and elution of Plasmid DNA

The cleared lysate obtained earlier was transferred to the prepared column and centrifuged at ≥ 12,000xg for 30 to 60 seconds to bind the DNA to the column. The flow through was discarded. To wash away contaminants, 500µl of wash solution1 was added to the column and centrifuged at ≥ 12,000xg for 30 to 60 seconds and the flow through discarded. This was followed by a second wash with 750µl of wash solution 2 which was centrifuged at the same speed for 30 o 60 seconds. This flow through was also discarded and the column was centrifuged for an additional 1 minute at ≥ 12,000xg to remove any excess ethanol. The binding column was then

transferred to a fresh collection tube and 100µl of elution solution added to the column. This was centrifuged at ≥ 12,000xg for 60 seconds. The concentration of each sample was quantified by nanodrop, see table 2.4 below.

Sample	DNA concentration ng / µl
Firefly 1	141.83 ng / µl
Firefly 2	176.25 ng / µl
Renilla 1	148.01 ng / µl
Renilla 2	161.42 ng / µl

Table 2.4 Nanodrop quantification of Plasmid DNA

2.2.9.3 Digestion

This step was necessary to digest the gene from the PCR product and the plasmid prior to insertion into pCDNA3 and pIRESpuro3. The enzymes needed, their respective buffers and plasmids are shown in table 2.5

Insert	Enzymes needed	Buffer	Plasmid
Firefly1	EcorV, BamH1	3	pIRESpuro3
Renilla 1	Xho1, Xba1	4	pcDNA3

Table 2.5 Enzymes and buffers needed for luciferase digestion

Each sample was made up with a mixture of enzyme, DNA, Buffer10X, BSA 10X and H_2O to a volume of 50 µl. The solutions were incubated for 1 hour at 37ºC and the enzymes inactivated by incubation at 80 ºC. To prevent re-ligation the samples were treated with phosphatase 10,000U/ml. for this, 0.5 µl of phosphatase was added and the mixture incubated for one hour at 37ºC then stored at -20 ºC.

Reagent	**Firefly1**	**Renilla 1**	**pcDNA3**	**pIRESpuro3**
Enzyme	0.5 +0.5	0.5 +0.5	0.5 +0.5	0.5 +0.5
DNA (1µg)	7µl	6.7µl	0.5µl	1.5µl
Buffer 10X	5µl	5µl	5µl	5µl
BSA 10X	5µl	5µl	5µl	5µl
H_2O	32µl	32.25µl	38.5µl	37.5µl

Table 2.6 Reagent mix for digestion step

2.2.9.4 Agarose gel purification and DNA extraction

A 1% agarose gel was made using 1.2g of agarose 120mls volume. Twelve microlitres (1X) of 10000X gel green nucleic acid was added and mixed to a yellow orange solution and the gel poured into the mould. Once the gel was set the Tae buffer was added to the mould. Gel loading dye was added at 10µl per sample making each sample a total of 50µl plus 10µl of dye. Thirty microlitres of each sample was loaded in duplicate along with a quick load 1kb ladder. The gel was run a 100V, 0.13 Amp for 1 to 1.25 hours. The gel in Figure 2.9 shows the ligated Renilla with very strong bands and a very weak Firefly bands. This may have been due to the need for longer ligation time, multiple ligation sites and the cut fragment (insert alone).

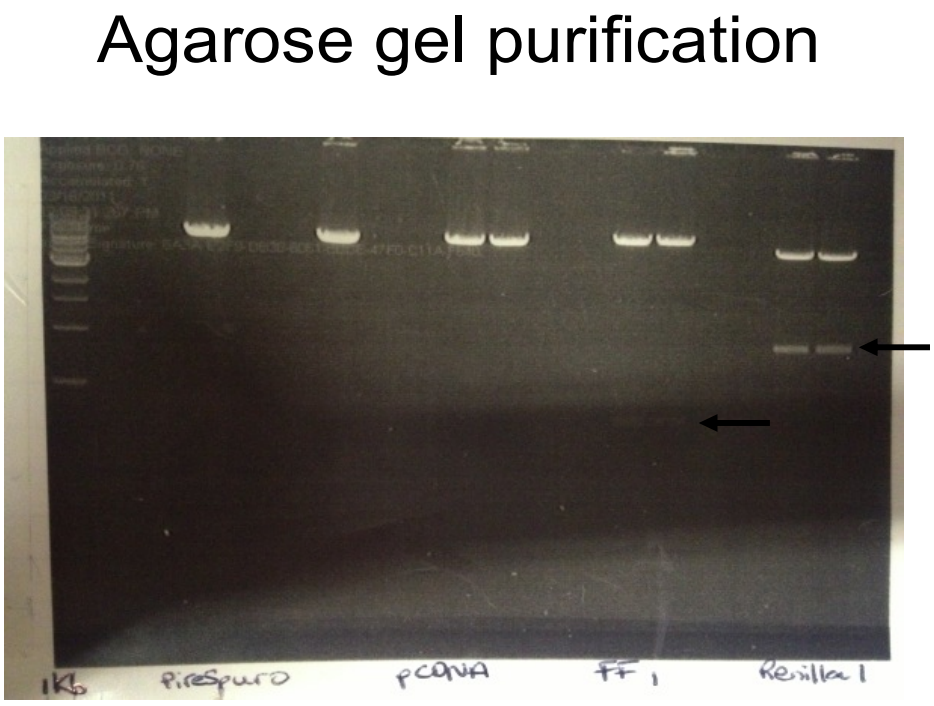


Figure 2.9 Agarose Gel purification and extraction of Renilla and Firefly luciferase

The bands from the gel in figure 2.9 were cut out with a clean sharp scalpel and their molecular weight measured as below prior to DNA extraction.

Sample	Weight of gel sample
pIRESpuro3	0.41g
pcDNA3	0.40g
Firefly luciferase	0.32g
Renilla luciferase	0.24 g

Table 2.7 Molecular weights of Gel bands

Using the QIAquick Gel extraction protocol (Qiagen) the DNA was extracted. Buffer GQ was added to the gel, in a 3:1 ratio (100mg to 100µl), to obtain a yellow colour indicating a pH of ≤7.5. This was incubated at 50ºC for 10 minutes to completely dissolve the gel. This was aided by vortex of the tube every 2 to 3 minutes during incubation. One hundred microlitres of isopropanol was added to the sample and mixed. Using a spin column within a collection tube each sample was applied to the column and centrifuged for one minute at 13000 rpm in order to bind the DNA to the column. The flow though was discarded. For DNA that was to be used for direct sequencing and in vitro transcription, 0.5mls of buffer GQ was added to the column and centrifuged for one minute at 13000 rpm. Following this, the column was washed with 0.75mls of buffer PE and centrifuged for one minute at 13000 rpm and the flow through discarded.

On completion of the washing steps the column was centrifuged in a 2ml collection tube for 1 minute at 13000 rpm. The DNA was eluted in a clean 1.5 ml microcentrifuge tube using 50 µl of buffer EB (10nM Tris-Cl, pH8.5). The DNA was quantified using nanodrop as shown in table 2.6.

Sample ID	DNA concentration	260/280	260/230
Firefly1	3.09	1.65	0.01
Firefly1	2.65	2.71	0.01
Renilla 1	3.73	2.73	0.01
Renilla 1	3.31	2.43	0.01
pcDNA3	7.82	2.33	0.02
pIRESpuro	11.74	1.82	0.04

Table 2.8 Nanodrop quantification of DNA extracted from the Agarose gel

2.2.9.5 Ligation of luciferase insert into vector

For the insertion of the luciferase marker into the vector the same procedure was used for both Renilla and Firefly luciferase. The ligation ration calculator used was a 3:1 ratio of 3 inserts to 1 bacterium. A 20µl reaction was made up of 2µl of 10X buffer, 1µl of Enzyme, 10µl of Vector, 5µl of insert (Renilla or Firefly) and 2µl of H_2O. This mixture was incubated at room temperature for 2 hours. The following is a description of the procedure using Renilla Luciferase.

2.2.9.6 Transformation of the DNA

The DNA was transformed into DH5α™ competent cells, (Invitrogen), onto an agar plate fed with penicillin. For the negative control no plasmid was used and the positive control was pUC19 control DNA (Invitrogen). One micro litre of ligated DNA (1-10ng) was added to the competent cells and 2.5µl to the control. This was mixed gently by hand and incubated on ice for 30 minutes. Without shaking, the cells were then heat shocked for 20 seconds in a 42ºC water bath and then placed on ice for 2 minutes. Five hundred micro litres of pre warmed medium was added to each sample and the tubes were incubated at 37ºC for 20 minutes at 225rpm. Twenty microlitres to 200µl of each transformation was spread onto pre-warmed agar plates ensuing well spaced colonies. For the positive control pUC19, 100µl was spread onto a plate containing 100µg/ml of Ampicillin. The agar plates wee incubated overnight at 37 ºC.

Transformation results

Twenty four hours later the results were as follows. There were no colony formations on the negative control, multiple colonies over the entire plate of the positive control and 5 colonies seen for Renilla luciferase.

2.2.9.7 Amplification of colonies

The 5 colonies were amplified in 1X Ampicillin and 2.5ml of LB media (broth). This was placed in a shaking incubator at 37 ºC overnight. The Amplified DNA was prepared using Gen-Elute™ HP plasmid miniprep kit and protocol as previously described. Each sample was prepared in duplicate and the results were tabulated below.

Colony	Concentration ng / µl	For 1ug of DNA
C1	166.80	5.9µl
C2	126.78	7.88µl
C3	172.96	5.78µl
C4	168.71	5.93µl
C5	141.97	7.04µl

Table 2.9 Average concentrations of colonies formed.

The DNA of the formed colonies was digested and run on a gel in order to ascertain the presence of the Renilla insert. A 50 µl mixture was made up of the reagents necessary for the digestion of the DNA. This consisted of 0.5µl of each enzyme Xho1 and Xba1, 5µl each of buffer 10X and BSA, 1 microgram of DNA and the rest made up with H_2O, table 2.10. The mixture was incubated for 15 minutes at 37ºC.

Reagent	C1	C2	C3	C4	C5	Negative
Enzyme	0.5 +0.5	0.5 +0.5	0.5 +0.5	0.5 +0.5	0.5 +0.5	0.5 +0.5
DNA	5.9 µl	7.88 µl	5.78 µl	5.93 µl	7.04 µl	0.5 µl
Buffer 10X	5µl	5µl	5µl	5µl	5µl	5µl
BSA	5µl	5µl	5µl	5µl	5µl	5µl
H_2O	33µl	31µl	31µl	33µl	33µl	32µl

Table 2.10 Reagent mix for digestion of colonised DNA and negative control. BSA was made from 100X BSA (Biolabs) by adding 10µl of BSA to 90µl of H_2O. The negative control used was pcDNA3.

Ten micro litres of 6X loading dye was added to each sample and they were loaded onto a gel. The results are displayed in figure 2.10. All 5 colonies showed the Renilla insert present and there was none present in the negative control.

Agarose Gel of Colonies containing Renilla luciferase insert

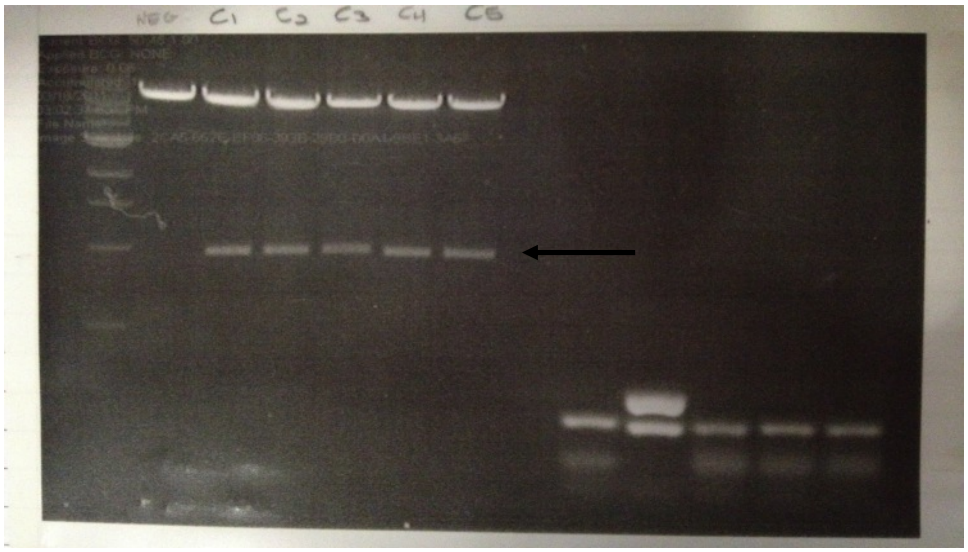


Figure 2.10 Agarose gel showing the 5 colonies with the Renilla insert.

Chapter 3

Array Comparative Genomic Hybridization of stellate cells (From cultured primary pancreatic specimens and formalin fixed paraffin embedded laser capture microdissected tissue stroma)

3.1 Introduction

Cancer associated fibroblasts are activated stellate cells believed to be integral to the communication between tumours and stroma thereby promoting tumourigenesis. It has not yet been elucidated whether their tumour promoting ability is due to crosstalk via secretory products from the tumour itself or its stroma or via genetic changes to activated fibroblasts. Normal fibroblasts are involved in the fibrotic reaction leading to scarring but they are also involved in the desmoplastic reaction surrounding the tumour.

Stellate cells display a change in morphology in their activated state and maintain this phenotype for prolonged periods whilst being propagated in culture. It has therefore been suggested that genetic changes are responsible for this behaviour, (*Orimo et al 1999*). Allinen and colleagues performed Array CGH and single nucleotide polymorphism array (SNP) analysis of myofibroblasts from ductal breast carcinoma. The myofibroblasts and other non epithelial tumour associated cells were found to be normal (*Allinen et al, 2004*).

Further studies have suggested that there are no genetic changes in these cells (*Walter K Omura et al 2008*). This study, the only one to date performed on pancreatic ductal adenocarcinoma, used a SNP array platform (250k) on cultured cells. It was then proposed that the absence of changes found was due to the possibility of normal fibroblasts being cultivated, (*Campbell et al., 2009).* There is therefore a debate as to the presence or absence of somatic mutations in stellate cells and a need to ensure that results obtained are indeed from tumour associated fibroblasts.

The following experiments aim to characterise these changes, using the array CGH platform, on cultured tumour juxtaposed cells as well as formalin fixed paraffin embedded tissue. This platform is sufficient to detect any copy number alterations that may be present, (*Kallioniemi, 2008*). Copy number alterations have been implicated in cancer initiation and progression. The loss or gain of function seen at specific gene loci tends to affect cellular pathways that control cell behaviour such as proliferation and apoptosis. These mechanisms are used by transformed cells to alter cell proliferation, growth and metastasis, (*Kallioniemi, 2008*).

3.2 Cell culture

Primary stellate cancer associated fibroblasts were cultured as described in Materials and Methods section 2.2.2. They were not immortalised. As previously explained these stellate cells originated from primary wedge resections obtained with consent via the histopathology department at the Hammersmith Hospital. Stellate fibroblast explants were labelled in order of their acquisition, e.g. PF1, was the first explant obtained, PF2, the second and PF 20 was the 20^{th} sample. These cells were cultured from tissue within 5mm from the tumour margin.

For the experiments described, cells were used at passage 3 or 4 to obtain a less differentiated group of cells and 70% confluence. Table 3.1 below, shows all samples obtained and those that were found to be suitable for array CGH and fluorescent in situ hybridisation. Suitability was determined by the histological appearance of pancreatic ductal adenocarcinomas and good cell expansion in culture. The cells that were used were found to be healthy and growing up to approximately passage 9 after which growth slowed dramatically.

Of the primary sections obtained 8 primary samples were successfully explanted, primary fibroblasts (PF), PF3, PF7, PF8, PF9, PF16, PF18 and PF20. Of these PF3, 8 and 9 were extremely slow growing and PF7, PF16, PF18 and PF20 were more successful in culture without immortalisation. Non stellate cells were excluded from further experiments; however, PF10 and PF11 were expanded and stored in liquid nitrogen as they showed good proliferation. Those cells with no growth or expansion were discarded, see Table 3.1.

Cell culture library from primary wedge resections

NAME	HISTOLOGY	CELL TYPE
PF1	Pancreatic Ductal Adenocarcinoma	Fibroblasts
PF2	Pancreatic Ductal Adenocarcinoma	No growth
PF3	Pancreatic Ductal Adenocarcinoma	Fibroblasts
PF4	Pancreatic Ductal Adenocarcinoma	No growth
PF5	Pancreatic Ductal Adenocarcinoma	No growth
PF6	Pancreatic Ductal Adenocarcinoma	No growth
PF7	Pancreatic Ductal Adenocarcinoma	Fibroblasts
PF8	Pancreatic Ductal Adenocarcinoma	Fibroblasts
PF9	Pancreatic Ductal Adenocarcinoma	Fibroblasts
PF10	Ampullary Carcinoma	Epithelial cells
PF11	Ampullary Carcinoma	Epithelial cells
PF12	Pancreatic Ductal Adenocarcinoma	Infected , No growth
PF13	Chronic Pancreatitis	No growth
PF14	Pancreatic Ductal Adenocarcinoma	No growth
PF15	Pancreatic Ductal Adenocarcinoma	No growth
PF16	Pancreatic Ductal Adenocarcinoma	Fibroblasts
PF17	Ampullary Carcinoma	Epithelial cells
PF18	Pancreatic Ductal Adenocarcinoma	Fibroblasts
PF19	Chronic Pancreatitis	No growth
PF20	Pancreatic Ductal Adenocarcinoma	Fibroblasts

Table 3.1 Primary explants cultured from pancreatic wedge resections, their histology and growth pattern. Primary fibroblasts PF3, PF7, PF8, PF9, PF16, PF18 and PF20 were successfully explanted.

3.3 DNA yield and quality

For the archived samples of FFPE tissue that were micro-dissected, DNA was extracted using Arcturus® Picopure DNA extraction kit KIT0103, Life Technologies, UK. Formalin Fixed Paraffin Embedded tissue is known to have poor DNA yields following micro-dissection and therefore only suitable samples with sufficient DNA, (600ngs), for array CGH were used from this archive. DNA concentrations were determined by nanodrop spectrophotometry from which only higher concentrations of DNA were used and a 260/280 reading of 1.7 and greater was considered good quality DNA, see table 3.2. Low DNA concentrations were not taken to the next step. These samples underwent the thiocyanate defragmentation step prior to Proteinase K dissolution which proved to acquire greater quantities of DNA on nanodrop spectrophotometry.

Archival FFPE specimens obtained for LCM Initial specimen blocks

Sample	No of LCM slides	Stromal DNA Concentration	260/ 280	260/230
A15	5	16.8ng/µl	1.24	0.64
	6	13.7ng/µl	1.26	0.82
C16	1	3.6ng/µl	2.08	1.67
	4	12.9ngµl	1.48	0.58
	6	33.7ng/µl	1.69	1.22
	6	11.2ng/µl	1.49	0.22
3J	4	11.0ng/µl	2.34	-0.70
	4	15.0ng/µl	1.39	0.65
C33	1	7.1ng/µl	1.41	0.58
	5	23.1ng/µl	1.95	1.75
	6	43.1ng/µl	1.83	1.93
A17	4	10.8ng/µl	1.47	0.74
	4	6.1ng/µl	1.79	2.56
	6	36.1ng/µl	1.54	1.03
A22	4	12.7ng/µl	1.43	0.78
	4	19.5ng/µl	1.30	0.87
	6	37.86ng/µl	1.93	1.33
	6	23.9ng/µl	1.86	1.28
	6	65.1ng/µl	1.88	1.87
8F	4	13.4ng/µl	1.33	0.63
	5	12.1ng/µl	1.74	2.03
F17	2	49.7ng/µl	1.76	1.77
10T	1	8.7ng/µl	1.98	0.73
	6	33.8ng/µl	1.55	1.24
EB4	4	11.8ng/µl	1.42	0.77
	6	58.3ng/µl	1.93	1.18
ROT4	3	12.9ng/µl	2.35	1.93
EB1	3	14.2ng/µl	1.99	1.05
3K	1	7.5ng/µl	1.47	0.51
	3	45.6ng/µl	1.96	1.61
	6	36.18ng/µl	1.87	0.72
	6	25.0ng/µl	1.79	1.55
76H	4	20.3ng/µl	1.19	0.64

Table 3.2 This table shows the full list of all the archival samples obtained and the nanodrop spectrophotometry of the DNA of the microdissected stromal tissue.

3.3.1 Pico Green assay of DNA from LCM samples

DNA from FFPE tissues may sometimes be contaminated with proteinaceous material and single stranded DNA which may give a falsely high reading of DNA concentration. Double stranded DNA is needed for arrayCGH and in order to establish the true concentration of dsDNA in these samples, Pico-green assay, specific for dsDNA, was performed.

Pico Green, as discussed in the methodology, selectively binds dsDNA. It has an excitation maximum at 480 nm and an emission peak at 520 nm. When bound to dsDNA, fluorescence enhancement of Pico Green is greater than 1000 fold. The background interference that is seen with nanodrop spectrophotometry is eliminated as unbound dye does not fluorescence. Pico Green is 10,000-fold more sensitive than Ultra Violet (UV) absorbance methods and highly selective for dsDNA over single stranded (ss) DNA and RNA.

In table 3.4 column 3 shows the true dsDNA concentration obtained via Pico Green assay. When expressed as a percentage, it was found that 10 to 20 percent of the DNA concentration obtained via nanodrop was true double stranded DNA.

Pico green quantification of double stranded DNA in LCM tissues

Sample	Nanodrop concentration	Pico Green ds DNA concentration	%of dsDNA Pico Greene vs. nanodrop
A22 stroma	65.1ng/µl	6.6ng/µl	10.2%
C33 stroma	141.08ng/µl	31.9ng/µl	22.6%
EB4 stroma	49.14ng/µl	4.5ng/µl	9.2%
3K stroma	96.29ng/µl	9.8ng/µl	10.2%

Table 3.3 This table shows that using Pico green assay, between 10 to >20% of the nanodrop concentration was dsDNA. These samples were freshly cut and the DNA extraction process was started on the same day.

3.4 Array CGH analysis results

Array CGH as described in methodology was performed on primary cells and FFPE DNA. The array CGH protocol has been described in chapter 2 section 2.2.6. The platform used for this study was constructed by the Breakthrough Microarray Laboratory and comprises a fluorescence in situ hybridization (FISH) mapped tiling path array set of 32,000 bacterial artificial chromosome (BAC) clones from Children's Hospital Oakland Research Institute (http://bacpac.chori.org/) spaced at approximately 50 kb intervals throughout the genome. All 32,000 BAC clones were spotted onto single Corning GAPSII-coated glass slides (Corning).

Six hundred nanograms of reference (normal DNA extracted from blood lymphocytes pooled from 24 females) and tumour DNA were labelled with Cy3- or Cy5-conjugated dCTP (Amersham Biosciences) using random primed BioPrime DNA labelling (Invitrogen Life Technologies) according to the manufacturer's protocol, modified to incorporate 1.0 mmol/L Cy dye, 0.6 mmol/L dCTP, and 1.2 mmol/L dATP, dGTP, and dTTP. After labelling at 37ºC for 18 hours, non-incorporated reaction constituents were removed by MinElute Reaction Cleanup (Qiagen Ltd). Labelled reference and tumour DNA were co-precipitated with 100mg human Cot-1 DNA (Invitrogen Life Technologies) at 20ºC for 1-2 hours followed by re-suspension in 50mls hybridization buffer (50% deionized formamide, 10% w/v dextran sulphate, 2x SSC, 2% SDS, 20 mg yeast tRNA).

Denaturation of labelled DNA was performed at 70°C for 15 minutes, followed by incubation at 37ºC for 30 minutes to allow blocking of repetitive sequences by human Cot-1 DNA. Denatured DNA samples were hybridized to the microarray at 37ºC overnight. Following hybridization, slides were washed in 2x SSC/0.1% SDS for 15 minutes at 45ºC to remove the coverslips, followed by 50% deionized formamide/2º SSC wash for 15 minutes at 45ºC. Finally, slides were washed in 2x SSC/ 1% SDS for 30 minutes at 45ºC and twice in 0.2x SSC for 15 minutes at room temperature. After post hybridization washing, slides were dried by centrifugation at 2,000 rpm for 2 minutes. Following hybridization and washes, slides were scanned using an Axon 4000B scanner (Axon Instruments) and images were processed using Genepix Pro 5.1 image analysis software (Axon Instruments).

Data were smoothed using a local polynomial adaptive weights smoothing (aws) procedure for regression problems with additive errors (*Hupe et al, 2004)*. The red, green fluorescent intensities represented on the array were analysed using R statistic software to generate a genome plot for each sample. A change in intensities represented as an unequal Cy3:Cy5 ratio is interpreted as a loss or gain in the DNA of that sample at that locus on the genome. The aws log2 ratio of each BAC clone is plotted on the y-axis and according to its genomic location on the x-axis. BAC clones that are gained (aws log2 ratio > 0.12) or amplified (aws log2 ratio > 0.4) are represented as green dots, clones with no change in copy number (aws log2 ratio 0.12 to -0.12) are represented by black dots and clones which are lost, (aws log2 ratio < - 0.12) are represented as red dots.

3.4.1 Genome plots for primary cultured fibroblast samples

Figure 3.1 below, displays the genome plot representation for the primary cancer associated fibroblasts of PF3, PF7, PF9 and PF16 respectively. The raw data shows a relatively clean signal with a low level of experimental noise, demonstrating the high quality of DNA.

3.4.2 Genome plots for FFPE samples

Laser capture micro-dissected tissue of FFPE stromal fibroblasts also showed consistent results when compared to the cultured primary cancer associated fibroblasts. The deletion seen on 19p was noted in the fibroblasts cultured from primary cells. This region examined, using the same R statistical software as for the cultured cells, showed expected normal variants as opposed to a new deletion, leading to the conclusion that these samples also show no copy number alterations in this region.

In Figure 3.2, both Laser capture micro-dissected samples show a flat line signal apart from the signal loss seen in chromosome 19p in sample C33 and the possible gain at chromosome 18 in sample 3KS. Notably the signal loss of chromosome 19 is not present in the latter.

Genome plots for primary cultured fibroblasts PF3, PF7, PF9 and PF16

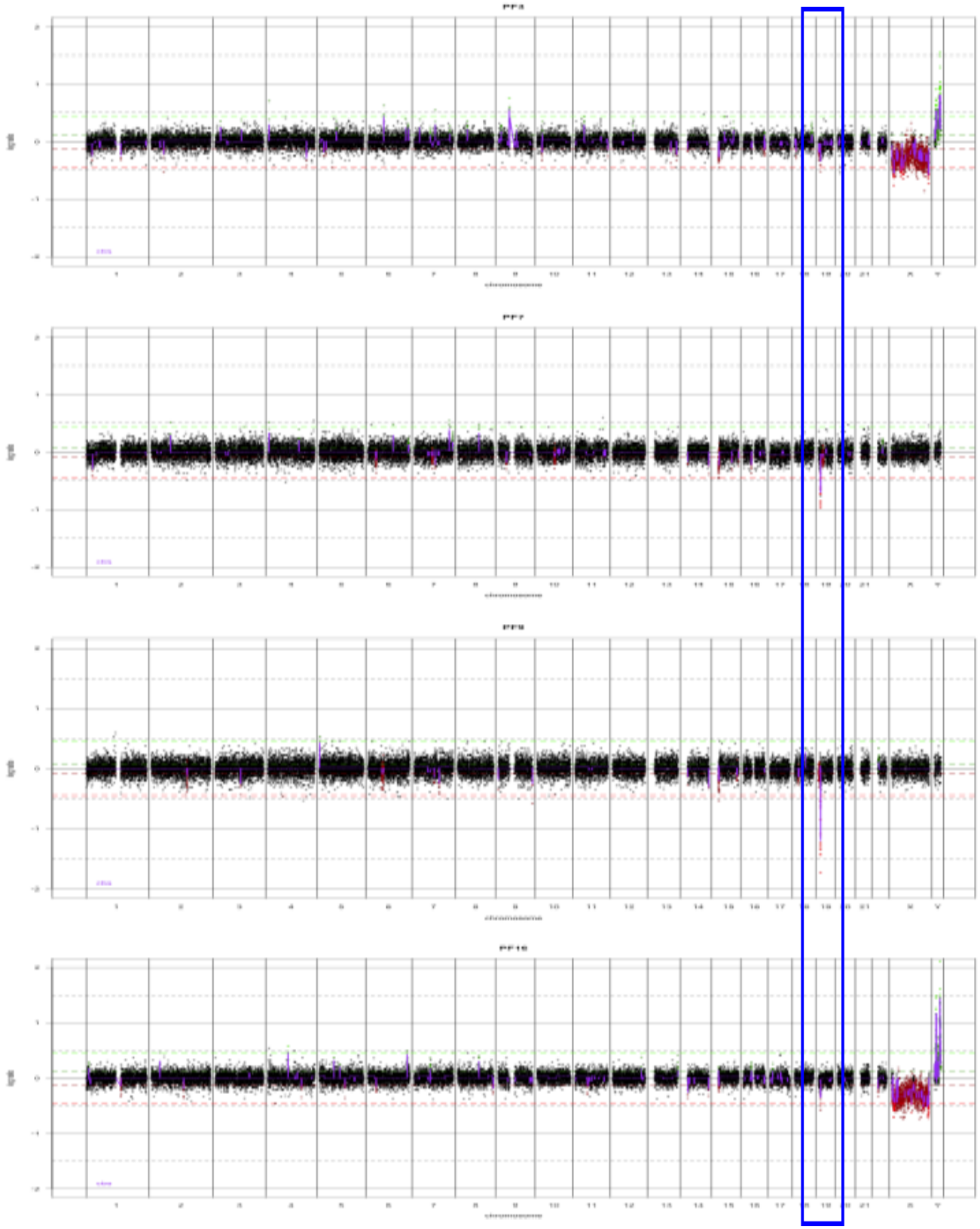


Figure 3.1 All four primary stellate fibroblasts show a deletion at chromosome 19p13.2.

Genome plot of Formalin Fixed Paraffin Embedded stroma C33 and 3KS

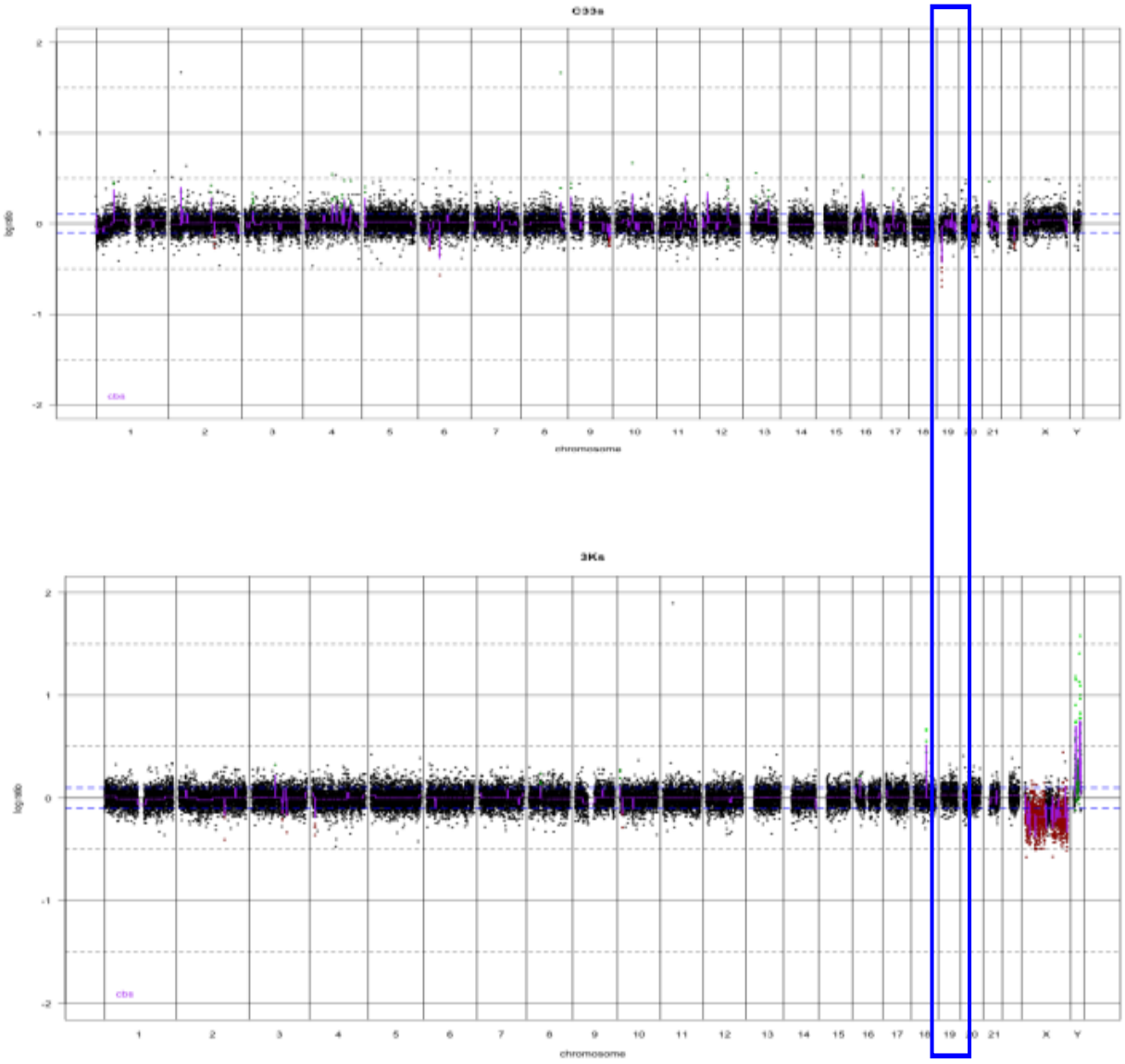


Figure 3.2 a. Genome plot of FFPE stroma C33 and 3KS. This genome plot of C33 displays no significant genomic gains or losses seen apart from a signal in the short arm of chromosome 19 below the threshold of -0.4. **b.** Genome plot of FFPE stroma 3KS. This figure shows a signal at chromosome 18 but none at chromosome 19 as seen in the previous samples.

All amplifications and deletions seen were reviewed in a database of genomic variants, (Http://projects.tcag.ca/variation/). This database contains the full chromosome list, their associated genes and the variations that have been found and documented at their loci. This includes normal variants. An MTable was generated from the array CGH spot diagram and from this the values seen at chromosome 19p13.2, corresponding to that of the deletion seen on the genome plots, were reviewed. The ranges obtained from the MTable for the common possible deletions found, not shown, were entered into genetic profile software to review the gene profile within the locus chr19:8665706-8955628, see table 3.4. This data was used to generate the region overview as below, see figure 3.3.

	Locus	Landmark	Variation ID	Variation Type	Cytoband	position Mb	Known genes in the locus
230	chr19:8665706-8955628	RP11-79F15	Variation_0220	CopyNumber	19p13.2	8.7	MBD3L1
		chr19:8,719,093..8,725,990	Variation_0508	CopyNumber	19p13.2	8.7	MUC16
		chr19:8,721,564..8,796,961	Variation_0509	CopyNumber	19p13.2	8.7	ZNF558
		RP11-367L15	Variation_0808	CopyNumber	19p13.2	8.7	OR2Z1
		chr19:8,677,224..8,680,932	Variation_102785	CopyNumber	19p13.2	8.7	ACTL9
		chr19:8,702,687..8,765,913	Variation_114724	CopyNumber	19p13.2	8.7	
		chr19:8,750,405..8,762,840	Variation_114725	CopyNumber	19p13.2	8.8	
		RP11-367L15	Variation_2239	CopyNumber	19p13.2	8.7	
		RP11-142H6	Variation_2240	CopyNumber	19p13.2	8.7	
		chr19:8,712,861..8,720,323	Variation_23574	CopyNumber	19p13.2	8.7	
		chr19:8,708,296..8,763,911	Variation_30888	CopyNumber	19p13.2	8.7	
		chr19:8,706,686..8,763,160	Variation_32229	CopyNumber	19p13.2	8.7	
		chr19:8,691,080..8,742,965	Variation_35691	CopyNumber	19p13.2	8.7	
		chr19:8,716,313..8,763,271	Variation_35692	CopyNumber	19p13.2	8.7	
		chr19:8,716,371..8,742,073	Variation_35693	CopyNumber	19p13.2	8.7	
		chr19:8,719,093..8,725,990	Variation_35694	CopyNumber	19p13.2	8.7	
		chr19:8,721,564..8,796,961	Variation_35695	CopyNumber	19p13.2	8.7	
		chr19:8,724,877..8,776,684	Variation_35696	CopyNumber	19p13.2	8.7	
		chr19:8,733,580..8,741,789	Variation_35697	CopyNumber	19p13.2	8.7	
		chr19:8,854,953..8,864,763	Variation_35698	CopyNumber	19p13.2	8.9	
		chr19:8,875,808..8,909,190	Variation_35699	CopyNumber	19p13.2	8.9	
		chr19:8,758,670..8,832,847	Variation_4067	CopyNumber	19p13.2	8.8	
		RP11-282G19	Variation_5079	CopyNumber	19p13.2	8.7	
		RP11-367L15	Variation_5080	CopyNumber	19p13.2	8.7	
		RP11-680A23	Variation_5081	CopyNumber	19p13.2	8.7	
		RP11-14H8	Variation_5082	CopyNumber	19p13.2	8.7	
		RP11-203K6	Variation_5083	CopyNumber	19p13.2	8.8	
		chr19:8,724,851..8,732,344	Variation_5933	CopyNumber	19p13.2	8.7	
		chr19:8,733,767..8,740,067	Variation_5934	CopyNumber	19p13.2	8.7	
		chr19:8,745,302..8,750,615	Variation_5935	CopyNumber	19p13.2	8.7	
		chr19:8,750,627..8,761,175	Variation_7225	CopyNumber	19p13.2	8.8	
		chr19:8,708,231..8,764,008	Variation_73310	CopyNumber	19p13.2	8.7	
		chr19:8,760,207..8,761,253	Variation_73311	CopyNumber	19p13.2	8.8	
		chr19:8,665,706..8,666,882	Variation_78066	CopyNumber	19p13.2	8.7	
		chr19:8,708,232..8,763,914	Variation_78067	CopyNumber	19p13.2	8.7	
		chr19:8,708,232..8,710,028	Variation_78068	CopyNumber	19p13.2	8.7	
		chr19:8,854,660..8,916,483	Variation_78071	CopyNumber	19p13.2	8.9	
		chr19:8,854,660..8,955,628	Variation_78072	CopyNumber	19p13.2	8.9	
		chr19:8,918,584..8,935,058	Variation_78073	CopyNumber	19p13.2	8.9	
		chr19:8,924,793..8,955,628	Variation_78074	CopyNumber	19p13.2	8.9	
		chr19:8,665,706..8,666,882	Variation_89065	CopyNumber	19p13.2	8.7	
		chr19:8,708,232..8,765,499	Variation_89067	CopyNumber	19p13.2	8.7	
		chr19:8,709,718..8,711,531	Variation_89070	CopyNumber	19p13.2	8.7	
		chr19:8,710,338..8,711,486	Variation_89071	CopyNumber	19p13.2	8.7	
		chr19:8,918,584..8,955,628	Variation_89074	CopyNumber	19p13.2	8.9	
		chr19:8,920,610..8,935,058	Variation_89075		19p13.2	8.9	

Table3.4. Variation locus showing the variation types found at 19p13.2 and the genes known in this locus, chr19:8665706-8955628.

Region overview of CH19p13.2

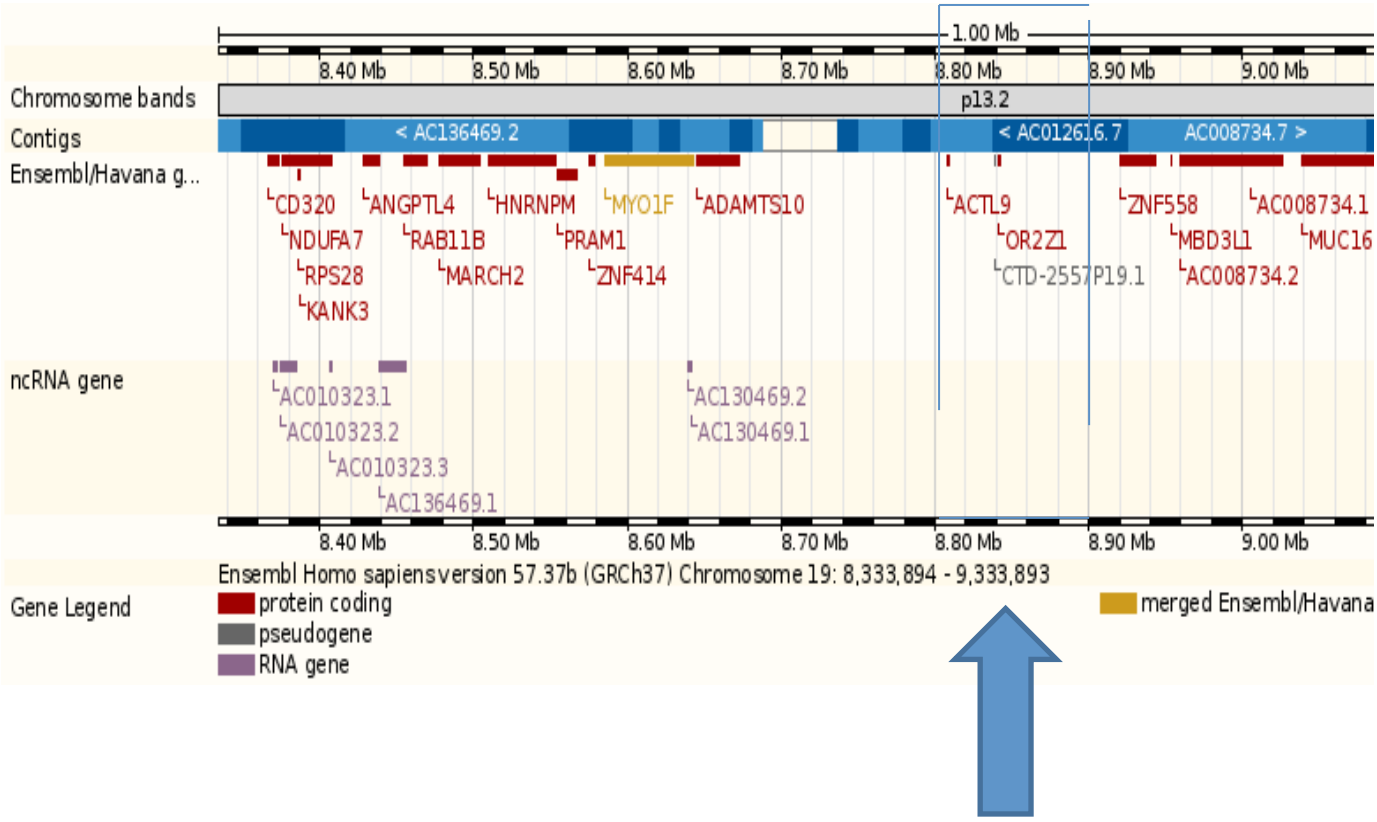


Figure 3.3 Region overview of Ch19p13.2. (www.ensembl.org). Above is the region overview of the short arm of chromosome 19p where a possible genomic deletion was noted in all four cultured primary stellate CAFs and FFPE tissue DNA. The genes highlighted, ACTL9 and OR2ZL were both common, normal variant, copy number alterations on the Http://projects.tcag.ca/variation/ database provided, suggesting that there are no true genomic changes in the above fibroblast cell lines.

3.5 Fluorescent in situ hybridisation (FISH) analysis of Copy Number alterations

In order to validate that the deletions seen on Array CGH were indeed normal variants and to rule out the presence of homozygous deletions or a true loss at chromosome 19, the tissues from the cultured cells were subject to fluorescent in situ hybridisation, (FISH). Bacterial Artificial Chromosome clones RP11- 282G19, RP11- 367L15, RP11-680A23 were mapped based on the location of genomic deletions seen on chromosome 19p13.2. The clones were chosen from a library provided by the Institute of Cancer Research. The clones were hybridized and a fluorescent probe was added. The cells with these probes were mounted onto slides and viewed in metaphase. A normal lymphocyte cell was used as a control to show the presence of the clones. Both alleles were seen on fluorescent microscopy of these cells in metaphase, see figure 3.4 below.

The same validation experiment was conducted on cultured primary fibroblasts PF3, PF7, PF9 and PF16 in order to confirm the findings of the array CGH on these fibroblasts. See figure 3.5. Clearly visible are the control probes in red as well as both alleles a chromosome 19p13.2 as both alleles are clearly demonstrated I suggests the absence of any homozygous deletions at this locus and therefore no true loss, see figure 3.5.

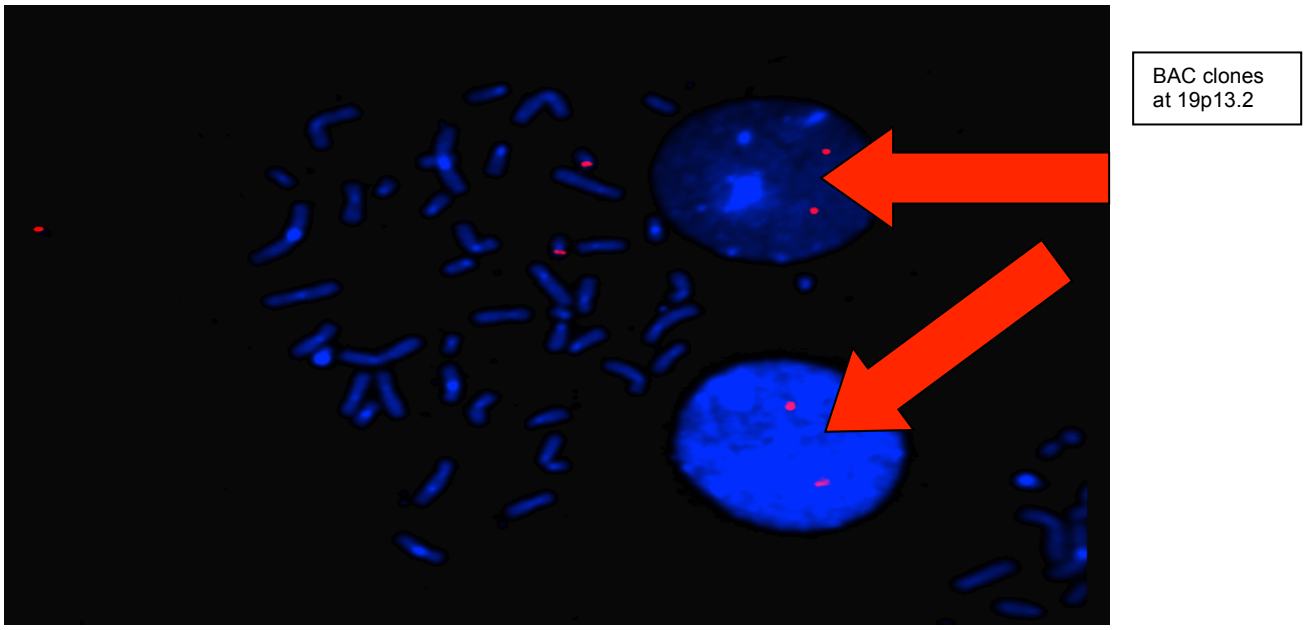


Figure 3.4 FISH analysis of Copy Number Variations in a normal lymphocyte cell as seen in metaphase showing presence of 19p13.2 BAC clones. This normal human metaphase spread shows the presence of both BAC clone alleles at 19p13.2 in an unaltered lymphocyte.

FISH Probes

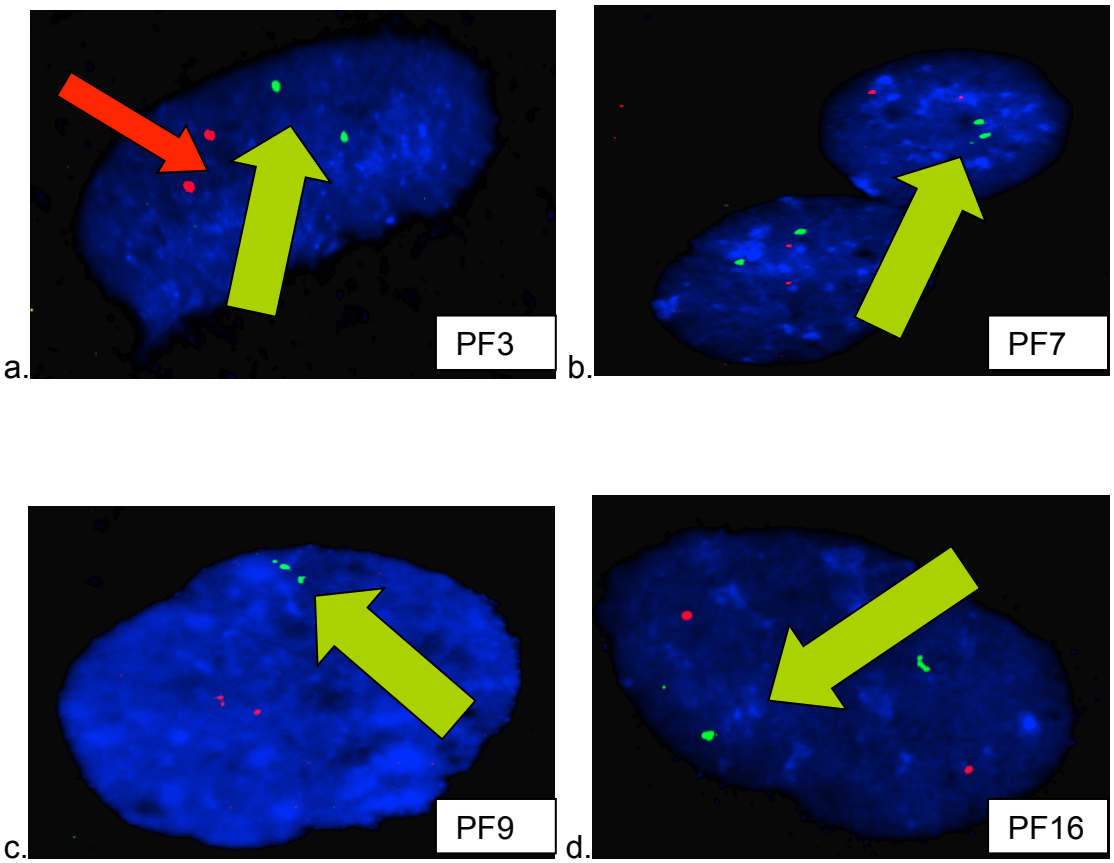


Figure3.5 This figure shows the metaphase spread of a nucleus of a PF3, PF7, PF9 and PF16 stellate CAFs. FISH probe analysis of the primary fibroblast shows the presence of both alleles at chromosome 19p13.2 labeled in green. The absence of homozygous deletions confirms no true loss at this locus.

3.6 Discussion

Cell cultures established from fresh tissue ensures that a pure sample is obtained and allows for control of the number of passages at which the cells are used. Cell lines were obtained from primary explants of PDA tissue. On average about 27 to 30 cases of surgery for Pancreatic cancer are performed each year at the Hammersmith hospital Hepatobiliary unit. This figure includes Whipple and other pancreatic procedures. All samples were taken with informed consent from patients admitted to this department.

As shown in the results, (Table 3.1), 8 cell lines were successfully explanted, Primary fibroblasts (PF), PF3, PF7, PF8, PF9, PF16, PF18 and PF20. Of these PF3, 8 and 9 were extremely slow growing and PF7, PF16, PF18 and PF20 were more successful in culture without immortalisation. These were the samples out of 20 initial specimens that produced a pure fibroblast culture, and did not become infected. In the initial stages of cell culture positive outgrowth was the limiting factor to the successful establishment of cell lines. Other limiting factors were the acquisition of the fresh samples and infection. Along with sterile conditions the growth media used was supplemented with antibiotics in order to discourage infection and the culture conditions were consistent throughout at 37°C and 5%CO_2.

The primary fibroblast cultures were tested for mycoplasma infection with each passage. ‘No outgrowth’ was determined after a minimum of one week and maximum of 10 days. The cell lines that were established were shown by immunohistochemistry to be free of epithelial cells. This analysis on PDA fibroblasts closely mimics these studies with the use of fibroblasts cultured from whole tumour biopsies. For this reason laser capture microdissection was performed to obtain a pure population of tumour-juxtaposed fibroblasts.

In this study we show that there are no homozygous copy number alterations seen in the either stromal cancer associated cultured fibroblasts or the FFPE stromal fibroblasts from PDA specimen. The recurrent deletion seen at the 19p13.2 locus harboring the ACTL9 and OR2ZL genes were found to be normal variants. The arrayCGH findings were supported by FISH, which confirmed that there were no homozygous deletions at this gene locus.

The evidence presented thus far has not been consistent and not all studies support the theory of somatic alterations in stellate cells. The scepticism arose where the quality of DNA was put into question as well as the type of fibroblast explanted, i.e., normal vs. tumour associated. For this reason it was necessary to use tumour juxtaposed, stellate cells for the experiments performed and ensure that sufficient and good quality DNA was obtained for array CGH studies and fluorescent in situ hybridisation.

Previous evidence has accredited the enhanced ability of individual fibroblasts to promote tumourigenesis to somatic mutations found in them, (*Patocs et al., 2007, Weber et al., 2006, 2007*). These studies used paraffin embedded tissue for their experiments. FFPE is known to produce a limited number of cells and therefore a low yield of DNA. Poor quantity, as seen with FFPE tissue, will reduce the likelihood of acquiring good quality of DNA. Therefore, the finding of frequent somatic mutations reported in these studies, may have been technically flawed. As seen from the results in PDA stromal tissue, (Table 3.4) only up to 20% of the DNA yield measured via nanodrop is indeed dsDNA. In order to eliminate doubt as to the validity of results obtained only dsDNA, as confirmed by Pico Green assay, was used for arrayCGH of the FFPE samples obtained.

In 2004, Allinen and colleagues found that non-epithelial tumour associated cells showed no copy number variations, (*Allinen et al, 2004)*. A further study, 4 years later, using SNP arrays on cultured stellate CAFs from PDA resection specimens also showed similar findings with no genomic changes in the stromal tissue, (*Omura et al June,* 2008). Of Importance, the latter study is unclear as to whether the fibroblasts used in were extracted from the immediate tumour juxtaposed region. Fibroblasts that are furthest from the tumour may be normal, and this has put the validity of the findings into question. All stromal tissue used in this study of PDA stromal cells were tumour juxtaposed to within 5mm from the tumour margin.

In keeping with recent publications in which no evidence was found for DNA aneuploidy, somatic genetic alterations or CNA in a set of 57 stromal cell fractions used, (*Corver et al, 2011),* this study using arrayCGH has also found a lack of CNA in the stromal tissue of pancreatic ductal adenocarcinoma. Corver and colleagues used flow cytometry and 6K SNP arrays to study DNA aneuploidy, percentage of S phase (synthesis phase of DNA) loss of heterozygosity and CNA in cervical cancer from both stromal cell fractions and FFPE samples. They showed that the stromal cell fractions from this cancer group was DNA diploid and was found to have the same genotype as those of the patient-matched normal tissue and are therefore genetically stable. The findings in this study using PDA are in agreement with the conclusion that these cells are genetically stable.

The presence of tumour stimulates a change in morphology of the stellate cells through crosstalk between the tumour cells and the stroma. This communication results in an activated phenotype of the stellate cells and they lose their quiescent elliptical shape. The smooth muscle actin and vimentin fibres become elongated and more prominent and there is increased extracellular matrix production as seen by the increased tenascin C, collagen I, EDA fibronectin and SPARC (specific protein acidic rich in cysteine).

This study has found no homozygous genetic changes in these activated stellate cells, It therefore puts even more emphasis on the theories that suggest the cytokine mediated activation and signalling pathways, upregulated during cancer progression and metastases, play a significant role in the tumour growth and development that occurs in the presence of stellate cells, (*Olive/Tuveson et al, 2009*). These findings have not ruled out the presence of heterogeneous or epigenetic changes in either group of fibroblasts and further investigations are warranted into these profiles in order to gain more insight into the genetic changes undergone in this cell group.

Chapter 4

Pancreatic cancer cells and chemoresistance

4.1 Introduction

4.1.1 Chemoresistance in pancreatic ductal adenocarcinoma (PDA) is a limiting factor to disease management

Chemoresistance in pancreatic ductal adenocarcinoma has been a limiting factor in disease management, resulting in the poor prognosis of 6.4 months median survival, despite multiple clinical trials involving combination drug therapy. Many forms of PDAC develop resistance soon after a fleeting initial response to Gemcitabine. However, Gemcitabine remains the gold standard of adjuvant and neo-adjuvant therapy in the absence of more efficient therapies. It is a cytotoxic pyrimidine deoxynucleoside analogue with fluorine for hydrogen atom substitutions on the number 2 carbon atom of deoxycytidine.

4.1.2 Chemoresistance is multifactorial

This chemoresistance is multifactorial. It has been attributed to several factors, including the paucity of a suitable screening tool or biomarkers. Because of this, patients tend to present at a locally advanced stage of disease and tumours may be metastatic and resistant to the chemotherapeutic regimes used at the time of presentation. The key factors that play a role in resistance, at a molecular level, include cancer cell mutations, poor drug delivery and activated tumour-stromal cell interactions and signalling pathways within the stroma.

4.1.2.1 Cancer cell mutations, poor drug delivery, anti apoptotic factors, activated tumour-stromal cell interactions and signalling pathways.

4.1.2.1.1 Cancer cell mutations

Cancer cell mutations found in pancreatic cancer cells include *K-RAS* proto-oncogene substitutions, *AKT2* 19q amplifications, Loss of heterozygosity at 9p, 13q, 17p and 18q gene loci, homozygous deletions at p16 and *DPC/Smad4* and p53 mutations, (http://pathology.jhu.edu/pancreas/geneticsweb/Profiles). Pancreatic cancer is characterized by a unique molecular fingerprint with activating point mutations at codon 12 of the *K-RAS* gene found in more than 90 to 95% of cases, (*Moore et al, 2001*). The tumour suppressor gene *p53* has been found to be inactivated in 60% and *DPC4/SMAD4* has been reported as altered in 50% of xenografted cancers, (*Hahn et al, 1996*). Although the mechanism of action is unclear, these factors undoubtedly play a role in tumour development and are also believed to contribute towards chemoresistance.

In a recent paper by Biankin and colleagues, they defined 16 significantly mutated genes, confirmed the known significant mutations seen in pancreatic cancer (*KRAS, TP53, CDKN2A, SMAD4, MLL3, TGFBR2, ARID1A and SF3B1*), uncovered novel mutated genes including additional genes involved in chromatin modification such as (*EPC1),* enhancer of polycomb homologue1 involved in histone acetylation and (*ARID2),* AT rich interactive domain containing protein 2, needed in chromatin modification as well as genes involved in DNA damage repair (*ATM)*-ataxia telangiectasia mutated.(*Biankin et al., 2012*).

They identified novel genes involved in other mechanisms (*ZIM2, MAP2K4, NALCN, SLC16A4* and *MAGEA6*). Zinc finger imprinted 2 (ZIM2) is involved in regulation of transcription, Dual specificity mitogen activated protein kinase 4 (MAP2K4) is a toll like receptor signalling pathway, Sodium leak channel non-selective protein (NALCN) has a specific role in sodium channel activity, Solute carrier family 16 member 4 (SLC16A4) is a monocarboxylate transporter and Melanoma-assisted antigen 6(MAGEA6) is involved in protein binding.

Axon guidance pathway genes, recently implicated in cancer cell growth, survival, invasion and angiogenesis, (*Mehlen et al., 2011*), are regulators of neuronal migration and positioning during embryonic development. Biankin and his group also identified recurrent mutations and copy number variations in these genes in their cohort of samples. They found CNV losses in *ROBO1* and *SLIT2* in 5% of their patients suggesting aberrant signalling in this pathway as a common feature of PDAC, (*Biankin et al, .2012*).

4.1.2.1.2 Drug delivery: Gemcitabine transport, uptake and metabolism

4.1.2.1.2.1 Gemcitabine transport and uptake

Genetic and epigenetic alterations in the gene products involved in Gemcitabine transport and metabolism have been shown to affect resistance to chemotherapy in pancreatic cancer, (*Giovannetti et al, 2006)*. The human equilibrative nucleoside transporter-1 (hENT-1) transports Gemcitabine into cells, (*Mackey et al, 1998).* Those cells with low levels or lacking hENT-1 are highly resistant to Gemcitabine, (*Spratlin et al, 2004; Mackey et al, 1998*). The study, led by Mackey, suggested that passive uptake of Gemcitabine into cells was a minor component of Gemcitabine

uptake and in some cell lines used, the lack of mediated uptake, via hENT-1, conferred resistance to the anti proliferative activity of Gemcitabine by greater than 1000 fold.

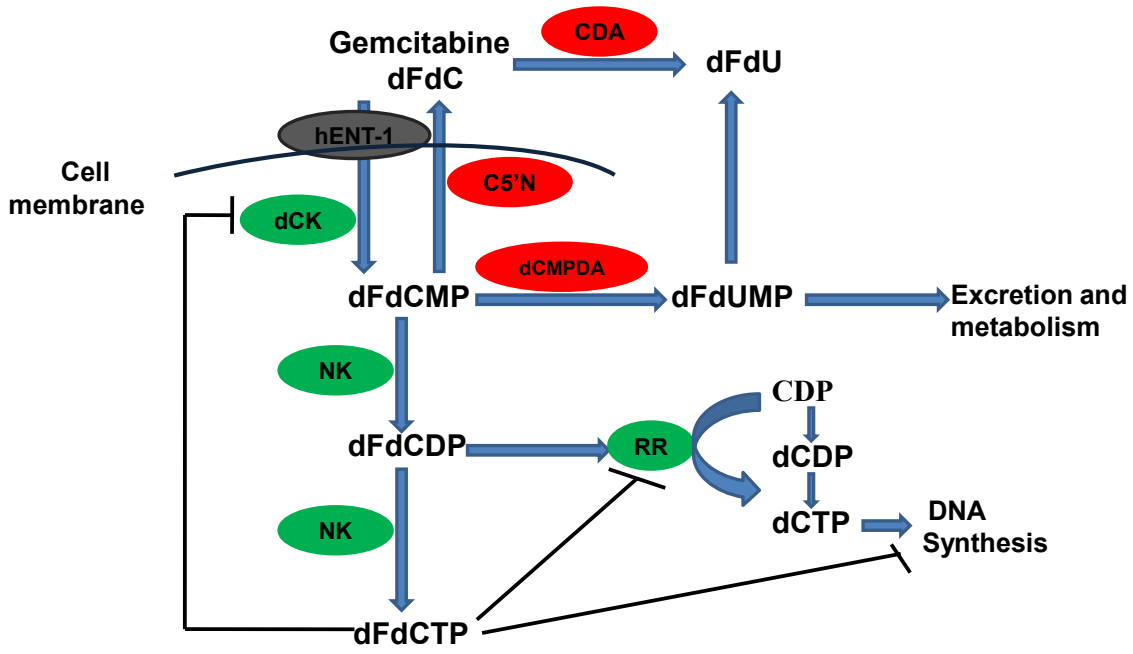
4.1.2.1.2.2 Gemcitabine Metabolism

The changes in the levels of gene products associated with Gemcitabine metabolism also play a significant role in resistance. Gemcitabine, 2'2'-Difluoro-2'deoxycytidine, must first be phosphorylated, to the active diphosphates and triphosphates which inhibit ribonucleotide reductase (RR). This inhibition reduces the deoxynucleoside triphosphate production that is required for DNA repair and synthesis, figure 4.1. The active metabolite also inhibits DNA polymerase which catalyses DNA synthesis.

Deoxycytidine kinase (dCK) is a rate limiting enzyme in the biotransformation of nucleoside analogues. It activates Gemcitabine and an increase in its activity has been shown to improve the efficacy of Gemcitabine, *(Blackstock et al, 2001; Kroep et al, 2002*). This effect was best seen in pancreatic cancer cell lines when used in combination with an inhibitor of Deoxycytidine deaminase (CDA). Deoxycytidine deaminase, catalyses and deaminates Gemcitabine to its inactive metabolite, figure 4.1. Increased levels of this enzyme would confer a degree of resistance to the cells involved, (*Neff et al, 1996*).

Duxbury and colleagues used small interfering RNA (siRNA) to show that the suppression of the ribonucleoside reductase M2 (RRM2) subunits enhanced Gemcitabine induced cytotoxicity in vitro. Gemcitabine together with RRM2 inhibition

was seen to significantly reduce tumour growth, increase tumour apoptosis and inhibit metastases in mouse xenograft models, (*Duxbury et al, 2004*).



Gemcitabine metabolism, activation and excretion

Figure 4.1 Human equilibrative nucleoside transporter-1 (hENT-1) transports Gemcitabine across the cell membrane into the cytoplasm. Deoxycytidine kinase (dCK) catalyses the phosphorylation of Gemcitabine (2'2'-Difluoro-2'deoxycytidine) to difluorodeoxycytidine monophosphate, (dFdCMP). Nucleoside kinases (NK) convert the monophosphate form to difluorodeoxycytidine 5'diphosphate (dFdCDP), and difluorodeoxycytidine 5'triphosphate (dFdCTP). Ribonucleoside reductase (RR) reduces Cytidine Diphosphate (CDP) to deoxycytidine Triphosphate (dCTP). The enzyme dCMP deaminase (dCMPDA) converts the monophosphate to an inactive metabolite, difluorodeoxyuridine monophosphate (dFdUMP), which is excreted. Cytoplasmic 5' nucleotidase (C5'N) reverses the action of dCK. Gemcitabine is deactivated by Deoxycytidine deaminase (CDA).

4.1.2.1.3 Acquired chemoresistance due to downregulation of proapoptotic genes and upregulation of antiapoptotic genes

An alteration in survival pathways is believed to play a significant role in chemoresistance as discussed by Kim and Gallick, (*Kim et al, 2008*). The abnormal expression of genes associated with apoptosis and cell survival has been implicated in chemoresistance, specifically *S100A4*. This S100 family gene enhances chemoresistance in pancreatic cancer by suppression of apoptosis, (*Mahon et al., 2007*).

Up-regulation of S100A4 is suspected to increase resistance to Gemcitabine by modulating BNIP3**,** a hypoxia induced pro-apoptotic gene in the Bcl-2 family of apoptosis-regulating molecules. BNIP3 activity normally induces a necrotic like cell death. It's silencing through the upregulation of S100A4 results in chemoresistance and correlates with poor survival in patients with pancreatic cancer. (*Mahon et al., 2007; Erkan et al., 2005)*.

Heat shock protein 27(HSP27), which is responsible for mediating the cells response to injury, was found to be expressed to a greater degree in resistant pancreatic cell lines. It acts as an anti-apoptotic factor and thereby confers a relative resistance to cells, (*Mori-Iwamoto et al., 2008).*

4.1.2.1.4 Activated tumour-stromal cell interactions and signalling pathways

Upregulation of the PI3 kinase/ AKT pathway has been shown in pancreatic cancers and this has been implicated in Gemcitabine resistance, (*Asano et al, 2004*). PI3 kinase phosphorylates the serine/threonine kinase PKB/AKT which then regulates the transcription of genes involved in cell survival within the nucleus, (*Ng SS et al., 2000*). It has been reported that PKB/AKT can phosphorylate and inactivate BAD, a proapoptotic member of the Bcl-2 family, (*Dragovich et al., 1998*). This suppression of apoptosis reduces the sensitivity of cells to the apoptotic effects of Gemcitabine.

Increased *SRC* kinase activity has been linked with inherent Gemcitabine resistance in pancreatic adenocarcinoma cells. Duxbury and colleagues used small interfering RNA to inhibit SRC tyrosine kinase. They found that the inhibition of *C-SRC* led to an increase Gemcitabine cytotoxicity via caspase mediated apoptosis, (*Duxbury et al, 2004).* This same group has linked the activation of focal adhesion kinase to Gemcitabine resistance in pancreatic cancer.

Increased *HMGA1* induces a stem cell like state. It is activated by the *MAPK/ERK* pathway in a dose dependent fashion, (*Zhao et al.*, 2006). In a study by Liau and colleagues they showed that a decrease in the *HMGA1* expression in xenograft mouse models resulted in an increase in apoptosis and promoted sensitivity to Gemcitabine in vitro, (*Liau et al., 2006*). Shah and colleagues have implicated *C-MET* as a factor that may contribute to Gemcitabine resistance. They found that *C-MET,* a tyrosine kinase believed to have a role in EMT transition, was upregulated in cells resistant to Gemcitabine, (*Shah et al, .2007*).

4.2 Compound library High throughput screening (HTS) of PDA cell lines

It seems reasonable to suggest that one approach to improving the PDAC response to chemotherapy is to take a combination strategy, as proven in other cancer types. As a first step towards identifying evidence based combination approaches for PDAC, I generated drug sensitivity profiles for a panel of commonly-used PDAC tumour cell models. These profiles were generated using a high-throughput screening platform in which cells can be exposed to a large panel of chemotherapeutics and targeted agents.

4.2.1 Ashworth plate 10 compound library

The Ashworth plate 10 compound library consists of 80 compounds. These include approved agents currently in clinical use as well as agents in early and late stages of development in the treatment of pancreatic cancer, see table 4.1.For the Ashworth plate 10 compound library drug screen, shown in figure 4.3, cells were cultured as previously described in order to obtain a greater than 70% confluent monolayer in a T75 flask, **(A)**. These cells were trypsinised and re-suspended in fresh media. A 10µl sample of cell suspension was mixed with 10µl of tryptan blue staining dye and live cell numbers estimated using the Countess® Automated Cell Counter, Invitrogen, and **(B)**. The number of live cells only, was used to calculate the volume of cell suspension required to give 1000 cells per well per 384 well plate. On average about 40,000 cells were necessary for each 384 well plate or $1.2x10^6$ for triplicate plates of each sample at a volume of 25µl per well. The cells were plated using the Multidrop Combi Reagent Dispenser, Thermo Scientific, **(C)**. These plates were incubated for 24 hours at 37ºC and 5% humidified CO_2. The cells were then exposed to the Plate 10 compound library by serial dilutions of a previously prepared

plate of chemotherapeutic compounds. Each drug was administered in volumes that would represent four concentrations, 1nM, 10nM, 100nM and 1000nM respectively and these were administered using the Hamilton automated liquid handler robot, **(D)**. Following application of the drug library to each cell line, the triplicate samples were again incubated for 72 hours at 37ºC and 5% humidified CO_2, **(E)**. On day 4 the plates were read for cell viability using Cell titre Glo bioluminescent marker as described below, **(F)**.

4.2.1.1 Map of the sample layout for HTS

Figure 4.2 below shows the layout of the 384 well plates into which the compounds were administered. The wells in column 2 labelled **N** were negative controls which contained DMSO only and the wells labelled **P** were the positive controls in which cells were treated with cytotoxic puromycin. Each quadrant of wells, for example, A3, B3, A4 and B4 was filled with one of four concentrations, 1nM, 10nM, 100nM and 1000nM respectively, of the compound being administered to the cells. All wells contained an equal volume at the end of drug administration.

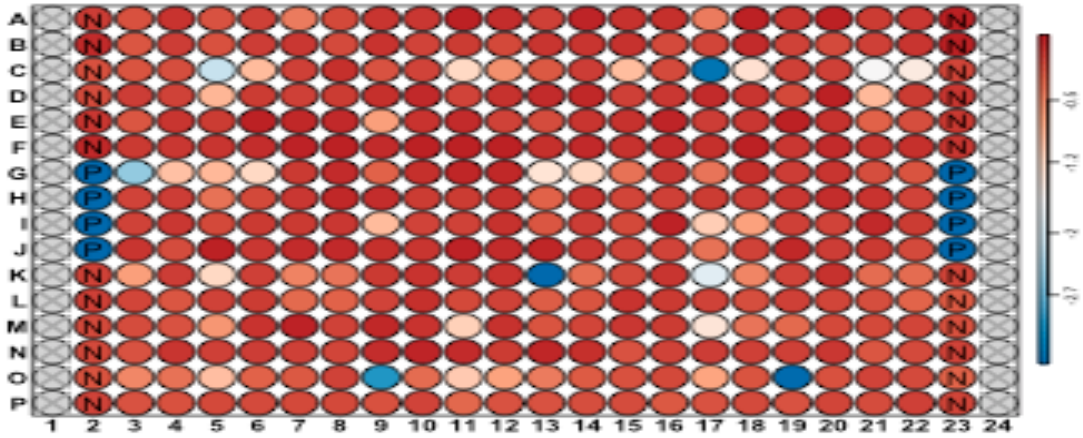


Figure4.2 Heat map of the 384 well High Throughput Screen. This heat map shows the plate 10 compound configuration of all 384 wells. The wells marked N (A2 to F2, K2 to P2, A23 to F23 and K23 to P23) are negative controls containing only DMSO. The cells marked P (2G to 2J and 23G to 23J) are positive controls of Puromycin. All other wells contained test samples to be treated.

Ashworth plate 10 compound library of agents

S)(1000nM)-+- camptothecin (TOPOIpoison)	Lapatinib (1000nM)(Her2i)
17-AAG (HSP90i)	Lestaurtinib (1mM)-(JAK2/FLT3/TrkAi)
2-methoxyestradiol (anti-angiogenesis)	MDV-3100 (CRPCi)
4-OH-tamoxifen (Eri)	MK-1175 (WEE1i)
5-FU (anti-metabolite)	MK-2512 (PARPi)
6-thioguanine (anti-metabolite)	MK-4827 (PARPi)
ABT-737 (Bcl2i)	Nilotinib (BCR-ABLi)
AG-14699 (PfizerPARPi)	Nutlin3 (MDM2i)
AZ4547 (FGFRi)	Olaparib (PARP1/2i)
BEZ-235 (PI3K/mTORi)	OL-PIX-A17A (LeadTh, PARPi)
BI-2536 (PLKi)	OL-PIX-F3-B (LeadTh, PARPi)
BIBW2992 (EGFR/HER2i)	**Paclitaxel (microtubule poison)**
Bleomycinsulfate (DNA breaks)	PBS-1086 (NfkBi)
BSI-201 (SanofiPARPi)	PBS-1169 (NfkBi)
Canertinib (pan-ErbBi)	PD-0332991 (CDK4/6i)
Carboplatin (DNA alkylation)	PD173074 (FGFRi)
Celecoxib (COX2i)	PD-184352 (Mbeki)
CT241533 (CHK2i)	PF-00299804 (pan-ErbBi)
Curcumin (NSAID)	PF-00477736 (CHK1i)
CyclophosphamideH20 (DNAalkylation)	PF-02341066 (MET/ALKi)
149Indomethacin (BCR-ABL/Srci)	PF-03758309 (PAKi)
Decitabine (DNAmeth)	PF-03814735 (Aurora)
DMX50-1281 (IKKEi)	PF-04691502 (PI3K/mTORi)
DMX501331-2 (IKKEi)	PF-04929113 (HSP90i)
DMX50-1338-2 (IKKEi)	PF-332991 (CDK4/6i)
DoxorubicinHCl (DNAintercalator)	Piroxicam (NSAID)
EB-47 (25mM)(1000nM) PARPi	PLX-4720 (Braid)
Erlotinib (EGFRi)	PRIMA1 (mut-p53activator)
Etoposide (TOPOIIi)	Resveratrol (NSAID)
Everolimus (mTORi)	Salinomycin (microtubule poison)
Flavopiridol (CDKi)	Sapacitabine (CNDAC)
GDC-0449 (SMOi)	SAR-20106 (CHK1, Sutton)
Gefitinib (EGFRi)	Sorafenib (inhibits RAF, PDGF, VEGF1&2)
Gemcitabine HCL (DNArepinhib)	Sunitinib (VEGFR1-3i, PDGFRi, Kiti, CSF1Ri)
GSK1904529A (IGFRi)	Sutent (Pfizer=sunitinib)
GSK2194069A (Faso)	Temozolomide (DNAalkylation)
GSK-2334470A (PDKi)	Vinorelbine (anti-mitotic)
Imatinibmesylate (Bcr-ABLi)	Voronostat (classI&IIHDACi)
Indomethacin (NSAID)	XAV-939 (TNKSi/Wnti)
KU0057788 (DNA-Pki)	
KU-59652 (ATMi)	

Table 4.1 Ashworth plate 10 compound library. This library consists of currently used chemotherapeutic agents such as Gemcitabine, 5-FU, Doxorubicin, and Oxaliplatin, agents in late stages of development such as Paclitaxel, pathway inhibitors such as GDC-0449, Pi3K/mTOR inhibitors and other compounds such as Non steroidal anti-inflammatory drugs which have been shown to have an anti-cancer effect.

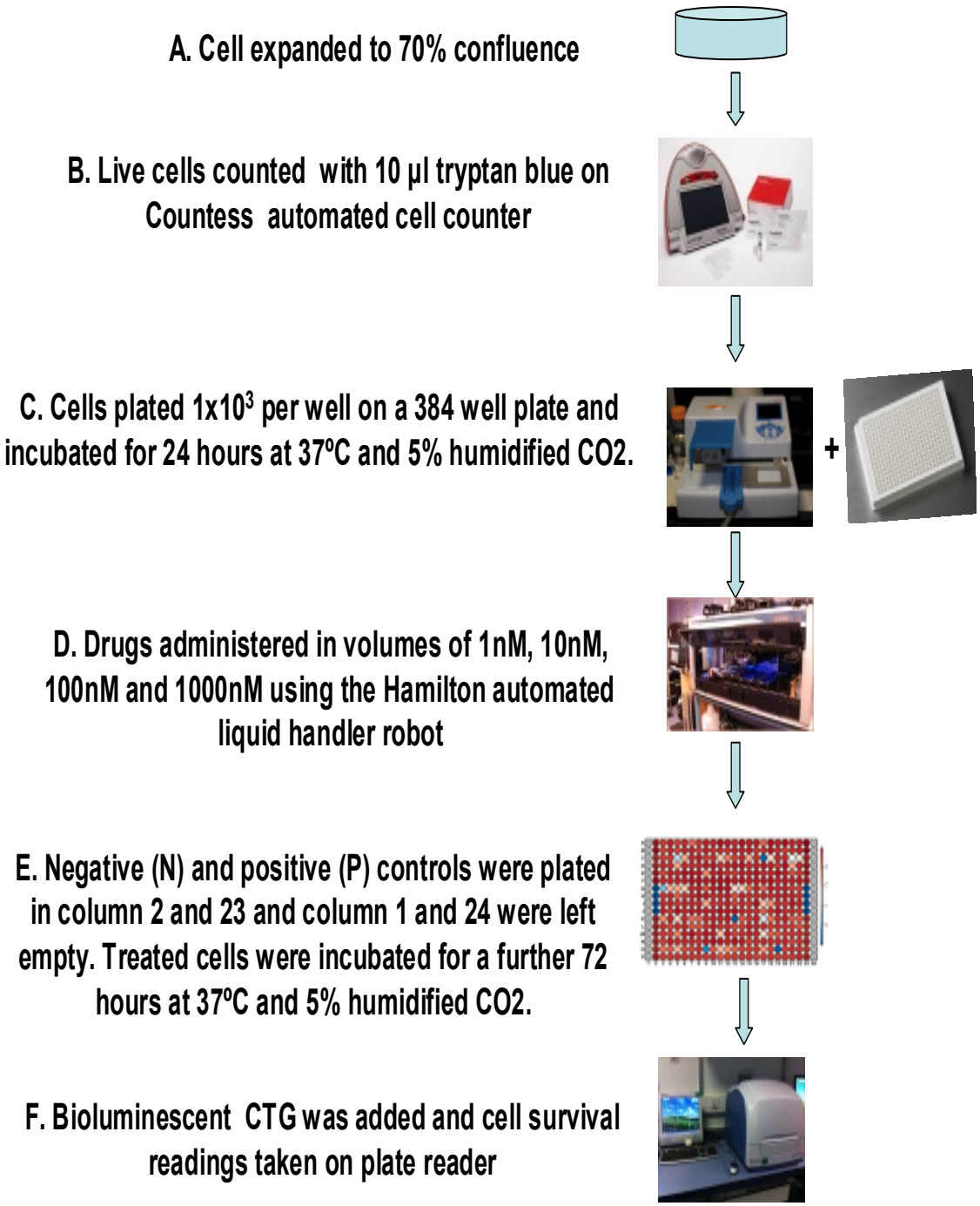


Figure 4.3 Schematic of High throughput screening

4.2.1.2 Cell titre Glo (CTG) survival readings

The liquid from each plate was removed by tipping and the plates were spun to dryness for a few seconds via centrifuge at 1000rpm. Cell titre Glo solution was made in a ratio of 1 in 4 with PBS. This bioluminescent marker quantifies the ATP in cells, which is a representative of those that are metabolically active. Using the Multidrop Combi Reagent Dispenser, 25µl of CTG solution was applied to each well. This was incubated in darkness on a rotating platform for ten minutes before being read on a plate reader at 550nM wavelength. The data collected was collated and analysed using R' and Cell HTS software programming in order to identify compounds to which the pancreatic cancer cell lines were sensitive. Graph pad Prism (version 5.0) was used to carry out statistical analysis. Cell survival was represented as a fraction of 1 in which 1 was equivalent to no cell death and 0.5 is the equivalent of 50 percent cell death.

4.2.6 Cell titration for PDA cell lines

Prior to screening the PDA cell lines, an initial simple cell titration was performed in order to ascertain the growth pattern of the pancreatic cancer cell lines. On day one of the experiment, cells were plated in a reducing number from $1x10^5$ to $7.8x10^{-2}$ per well in 96 well plates and allowed to expand. Cell titre Glo cell viability readings were taken at Day 6 and it was determined that $1x10^3$ cells per well were the suitable cell count to be used for further experiments. These cells expanded suitably into a monolayer without overcrowding or cell death, in the time period needed for the duration of the experiment.

In figure 4.4, cells plated at 1K per well were found to be in the linear phase of the curve. In order to avoid plateau of the CTG signal, it was necessary to do experiments with cell numbers that lie in the linear range of the curve in which the cells are in the growth phase.

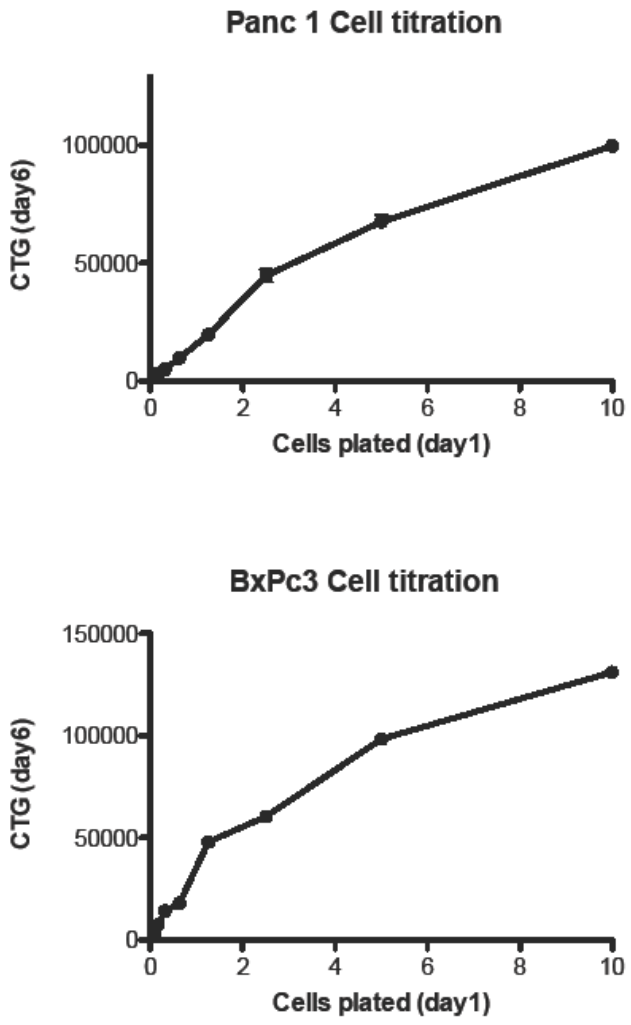


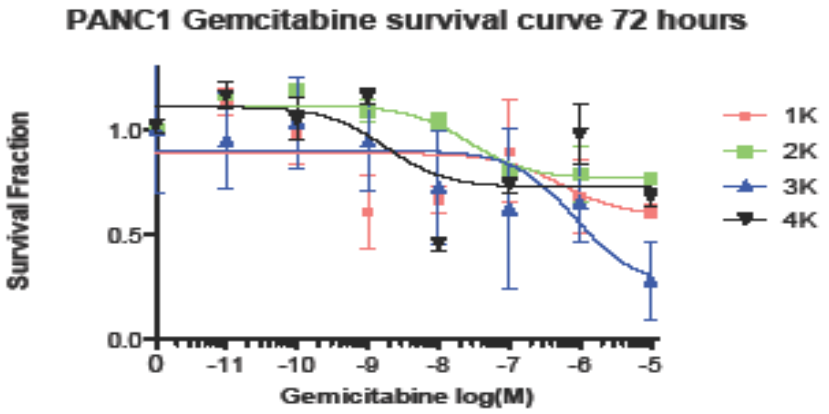
Figure4.4 Simple cell titration of epithelial cell lines. The X axis shows the number of cells, plated on day one, in thousands. This figure shows the duplication rate of the pancreatic cancer cell lines used. $1x10^3$ cells per well or 1K showed a suitable doubling time for these cell lines and was used as the plating number of choice for further experiments.

4.2.3 Baseline Gemcitabine resistance curves for PDA cell lines

Once the cell count to be used, $1x10^3$ cells per well, had been established, it was then necessary to review the response of these PDA cell lines to Gemcitabine. Prior to high throughput screening, a simple experiment to establish the response to Gemcitabine was performed.

4.2.3.1 Gemcitabine resistance after 72 hours of treatment

Pancreatic ductal adenocarcinoma cell lines PANC-1 and BxPc3 were plated on 96 well plates. Cells were plated at $1x10^3$, $2x10^3$, $3x10^3$ and $4x10^3$ cells per well for comparison of the patterns of sensitivity or resistance based on cell number, see figure 4.5. The cells were allowed to adhere for 24 hours post plating. They were fed with differing doses of Gemcitabine ranging from $1x10^{-5}$M (10μM) to $1x10^{-11}$M (0.01nM) and a 0M control was included. Seventy two hours post treatment with Gemcitabine, Cell titre Glo readings were done and the data analysed for cell survival. Initial resistance appeared higher in the cell lines that were plated in larger numbers on day one, (2K to 4K). This may be due to cell load.



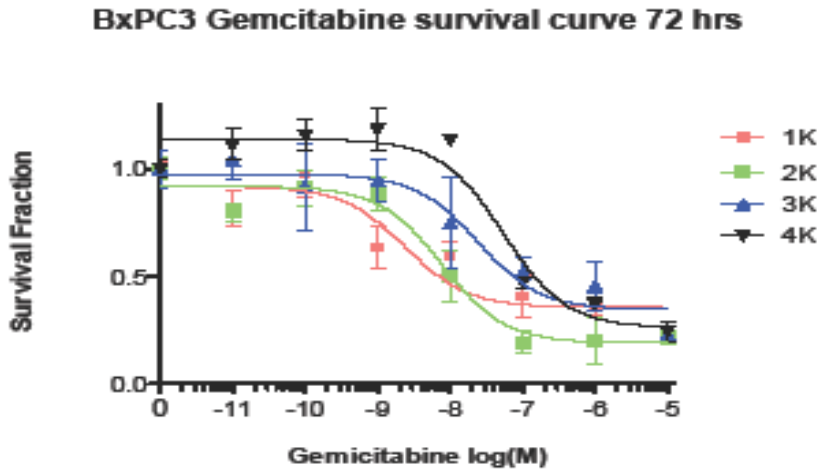
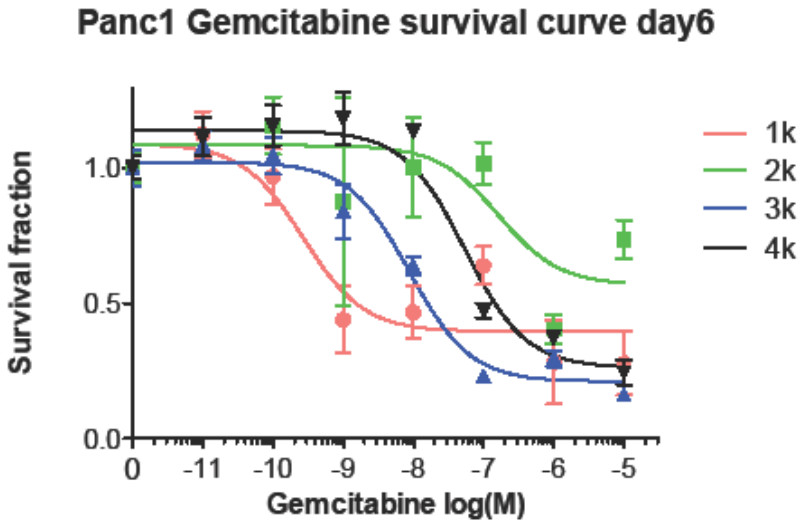


Figure 4.5 Gemcitabine survival curves 72 hours. On day one of this experiment, cells were plated at $1x10^3$(1K), $2x10^3$ (2K), $3x10^3$ (3K), and $4x10^3$(4K). The Gemcitabine concentrations used are represented on the X axis. These values represent times 10 increments of Gemcitabine from 0.01nM ($1x10^{-11}$) to 10μM ($1x10^{-5}$).

4.2.3.2 Gemcitabine resistance after 6 days of treatment

The same experiment was repeated; however, on day 4 the media was changed to Gemcitabine free media and CTG readings done on day 6. Figure 4.5 shows the resistance curves after this length of exposure. The survival curves obtained after 6 days were more pronounced than after 72 hours of exposure to Gemcitabine. Again, the greatest sensitivity was noted in the 1K ($1x10^3$) cells per well group at $1x10^{-9}$M (1nM) and $1x10^{-8}$ (10nM) concentration of Gemcitabine. There was only 50% cell survival in this group compared to almost no response in the 2K to 4K group at this low dose. At 10nM ($1x10^{-8}$) there was only 40% cell survival in the 1K group.

Figure 4.5 shows sensitivity to Gemcitabine to occur between $1x10^{-8}$M (10nM) and $1x10^{-9}$M (1nM) of Gemcitabine. All cell lines displayed a survival fraction less than 0.20 at ($1x10^{-7}$M) 100nM and ($1x10^{-6}$M) 1000nM. BxPc3 appeared more sensitive when compared to PANC-1. Asorza and colleagues performed similar experiments in which they looked at the resistance to Gemcitabine with and without CHk point silencing in the pancreatic cell lines. In their CHk point silenced cells there was an increase in sensitivity to Gemcitabine as seen by a shift in the curve. In their non silenced group however, both BxPc3 and MiaPaCa2 PDA cell lines showed sensitivity at log-8 (10nM) of Gemcitabine, (*Asorza et al, 2009*).



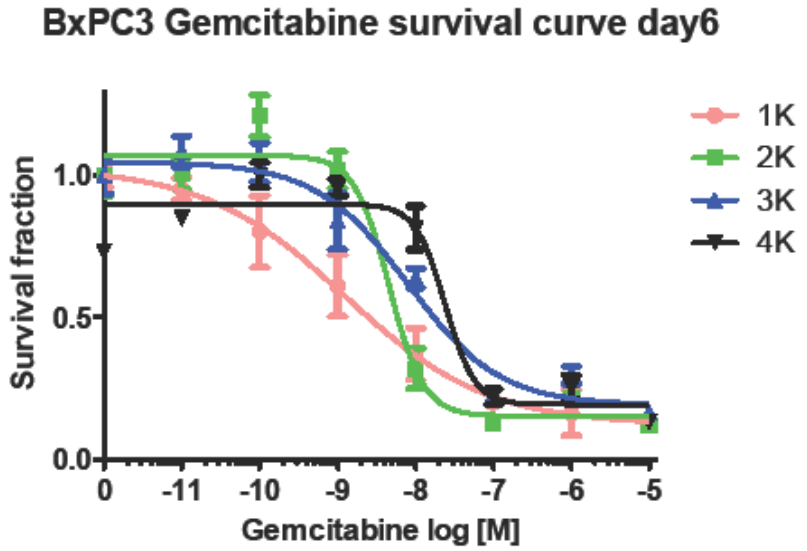


Figure 4.6 Gemcitabine survival curves day 6. The X axis shows the log values of Gemcitabine concentration. The value, log-9, represents $1x10^{-9}$(1nM) and log-6 represent $1x10^{-6}$(1000nM) concentrations of Gemcitabine. Each curve is representative of a triplicate experiment. Cell number was assessed and data normalised to the negative control and results plotted.

4.2.4 HTS Screen results of all PDA models

Having established the response of the cell lines to one of the plate 10 compounds, the screen was then expanded to profile all the PDA cell lines performed and include the full Ashworth library of chemotherapeutic agents. The results obtained were represented as heat maps, bar graphs and histograms which confirmed quality control of the HTS screens. Below are the results of the screens for each pancreatic cell line

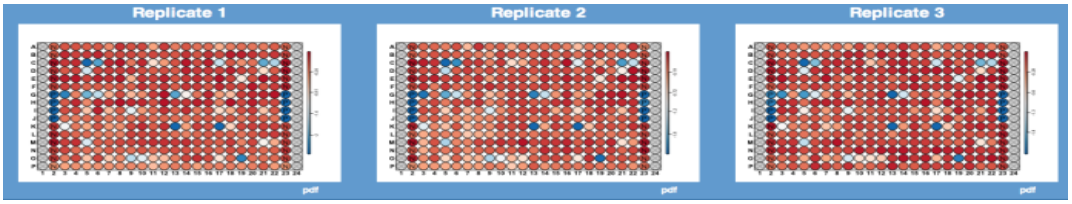
For quality control, the z prime factor is an indication of the signal to noise ratio of the CTG reading (assay output quantification) between the untreated cells (DMSO only, 0.2% volume to volume ratio (v/v)) and the cell death control. The z prime factor for all screens ranged form 0.5 to 0.78. It is essentially the ratio between the blue dots (positive control) and red dots as seen on the histograms). A screen with a value of >0.5 or higher was considered an excellent quality. The spearman rank correlation is another indication of the quality control of the screen. A value of greater than 0.5 is considered an acceptable screen. See appendix 1.

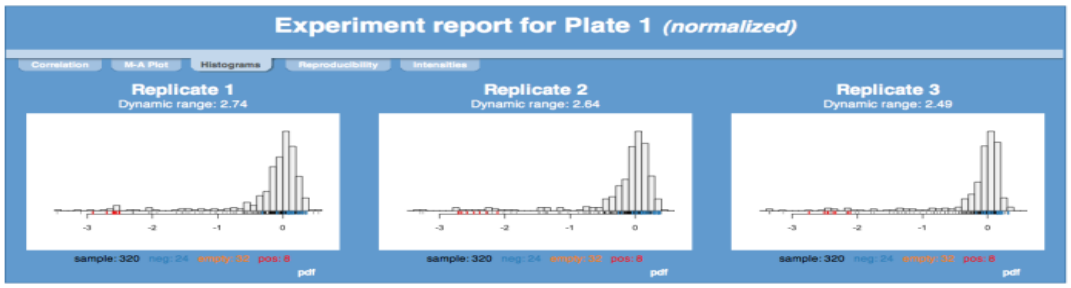
4.2.4.1 Cell Survival HTS results for AsPC-1

A.

ASPC QC:OK

Plate	Replicate	Channel	Filename	Status	Replicate dynamic range	Average dynamic range	Repeatability standard deviation	Spearman rank correlation (min - max)
1	1	1	ASPC-1.txt	✓	2.74	2.62	0.11	0.62 - 0.75
1	2	1	ASPC-2.txt	✓	2.64	2.62	0.11	0.62 - 0.75
1	3	1	ASPC-3.txt	✓	2.49	2.62	0.11	0.62 - 0.75





B.

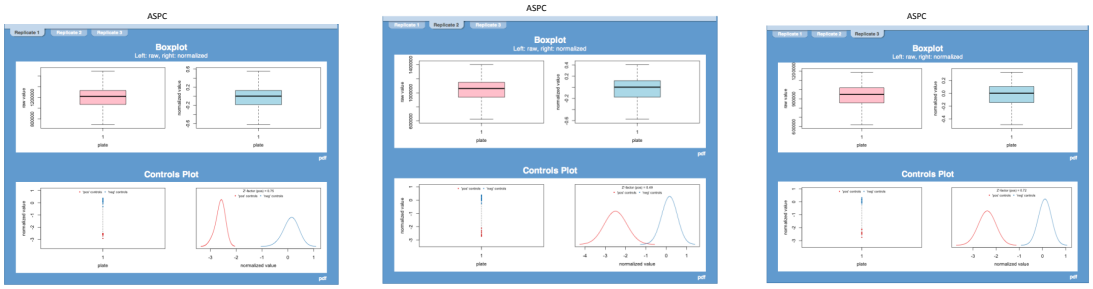


Figure4.7. Quality control for AsPC-1. A) AsPC-1 cell line screen results plate configuration and histograms with good quality control and output of the screen for this cell line. In b, the bar graphs have a normal distribution for positive and negative controls indicating a successful screen throughout replicates 1, 2 and 3.

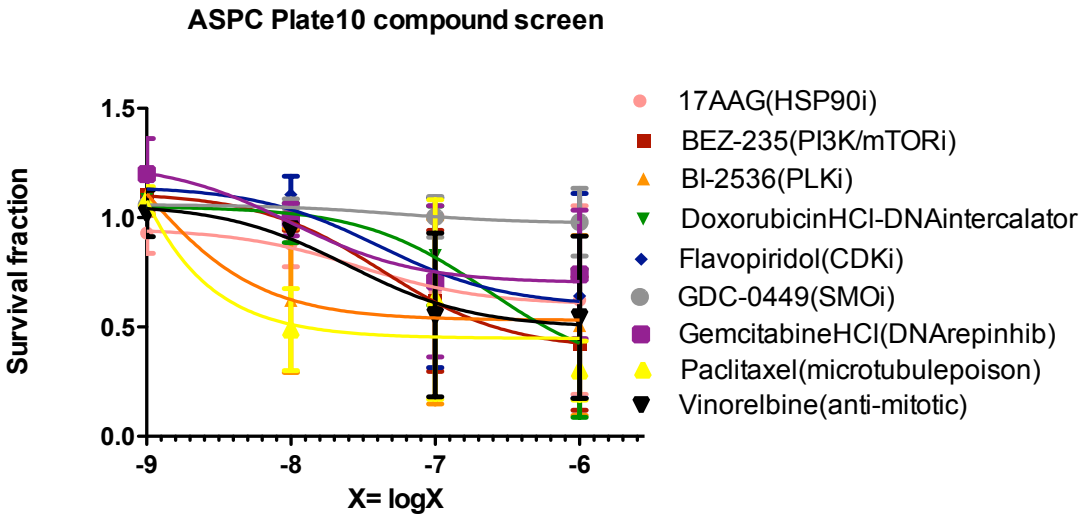


Figure4.8. This survival curve shows the screening results for compounds to which there was some sensitivity. The X axis shows the drug concentration used as a log value, where (-6) represents $1x10^{-6}$ or the equivalent of 1000nM, -7 (100nM), -8 (10nM) and -9 (1nM) respectively. Compounds that produced a cell death of 50% (survival ≤ 0.5) or more were considered to produce significant cell death.

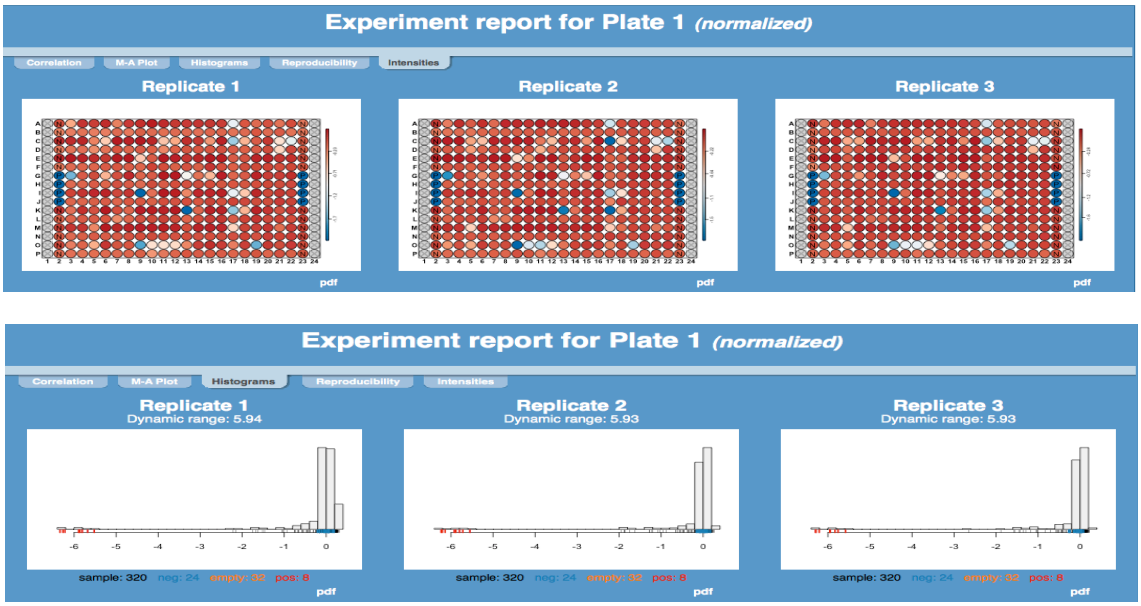
This survival curve shows a survival fraction of less than 0.5 in AsPC-1 cells in response to Paclitaxel and Bi-2536 (PLK) inhibitor at (-8)10nM concentrations of either drug. At (-7) 100nM, compounds that induced cell survival fraction of 0.7 or less includes Vinorelbine (anti-mitotic), BEZ-235 (PI3K/mTOR inhibitor), and 17 AAG (HSP90 inhibitor). Of note, there was no response to the smoothened inhibitor GDC-0449 in this epithelial cell line and the response to Gemcitabine was at the higher 100nM concentration where the survival fraction was still a high 0.7.

4.2.4.2 Cell Survival HTS results for HPAC

HPAC QC:OK

Plate	Replicate	Channel	Filename	Status	Replicate dynamic range	Average dynamic range	Repeatability standard deviation	Spearman rank correlation (min - max)
1	1	1	HPAC_1.txt	✓	5.94	5.93	0.06	0.86 - 0.9
1	2	1	HPAC_2.txt	✓	5.93	5.93	0.06	0.86 - 0.9
1	3	1	HPAC_3.txt	✓	5.93	5.93	0.06	0.86 - 0.9

A.



B.

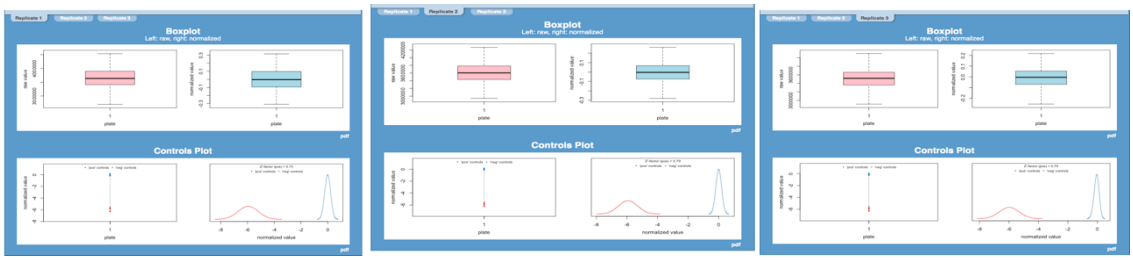


Figure 4.9 Quality control for HPAC. This z prime factor for this screen is 0.75 and spearment rank is within 0.86 to 0.9, indicating a successful screen.

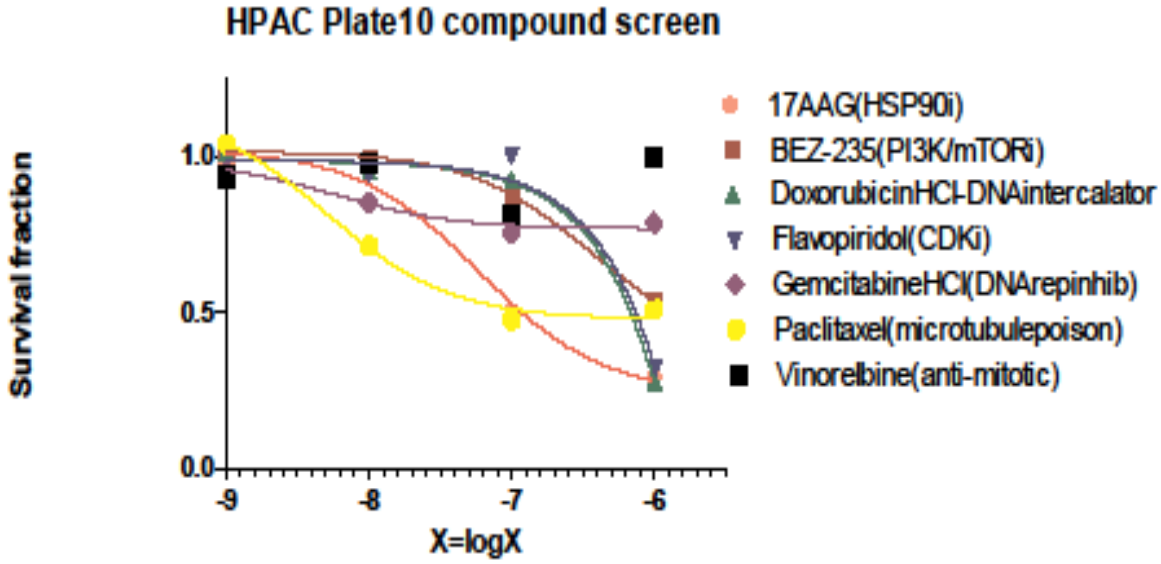


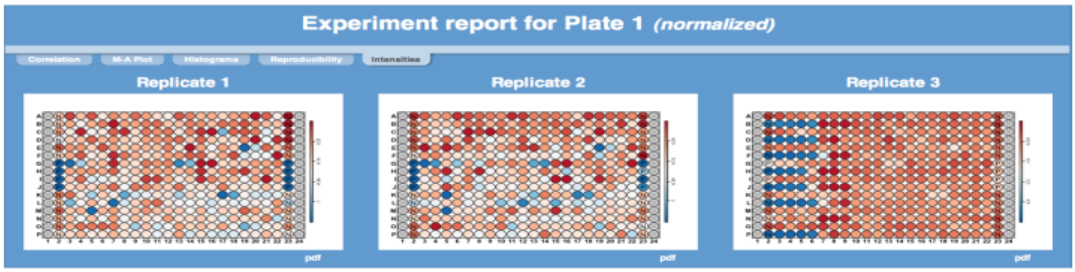
Figure4.10 Cell Survival High Throughput Screen results for HPAC. This survival curve shows the screening results for compounds to which there was some sensitivity including those that produced a cell death of 50% or more on HPAC cells. Compounds that produced a cell death of 50% (survival ≤ 0.5) or more were considered as having a significant effect

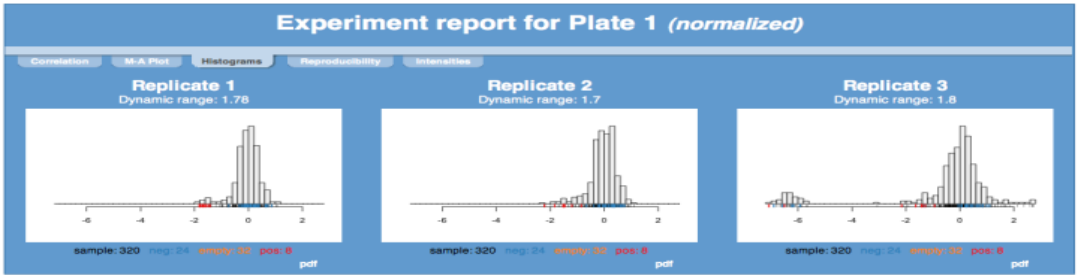
HPAC cells have shown significant sensitivity to Paclitaxel and HSP90 inhibitor compound BEZ-235 at 100nM of either compound with a survival fraction of 0.5. There was a limited response to Gemcitabine with a survival fraction of 0.8 at the highest concentration of 1000nM and no response to the smoothened inhibitor GDC-0449, (result not plotted).

4.2.4.3 Cell Survival HTS results for Hs776T

HS776T QC

Plate	Replicate	Channel	Filename	Status	Replicate dynamic range	Average dynamic range	Repeatability standard deviation	Spearman rank correlation (min - max)
1	1	1	HS776T-1.txt	✓	1.78	1.76	1.11	0.29 - 0.43
1	2	1	HS776T-2.txt	✓	1.7	1.76	1.11	0.29 - 0.43
1	3	1	HS776T-3.txt	✓	1.8	1.76	1.11	0.29 - 0.43





A.

B.

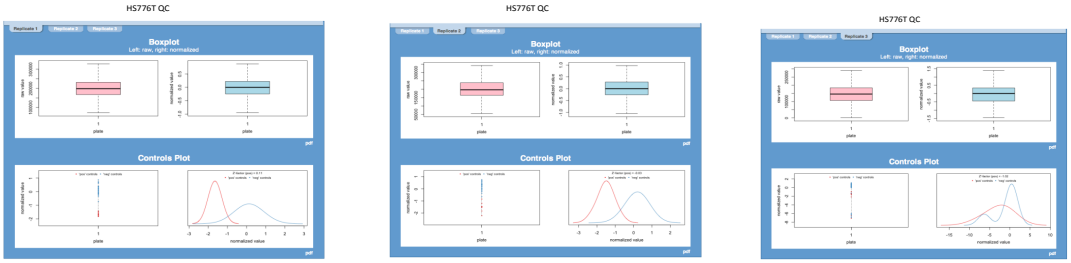


Figure 4.11 Quality control heat map, bar graph and box plot for Hs776T. A shows Hs776T cell line screen results plate configuration and histograms with quality control and output of the screen for this cell line. In B the bar graphs distribution accounts for errors in plating which were normalized during data analysis.

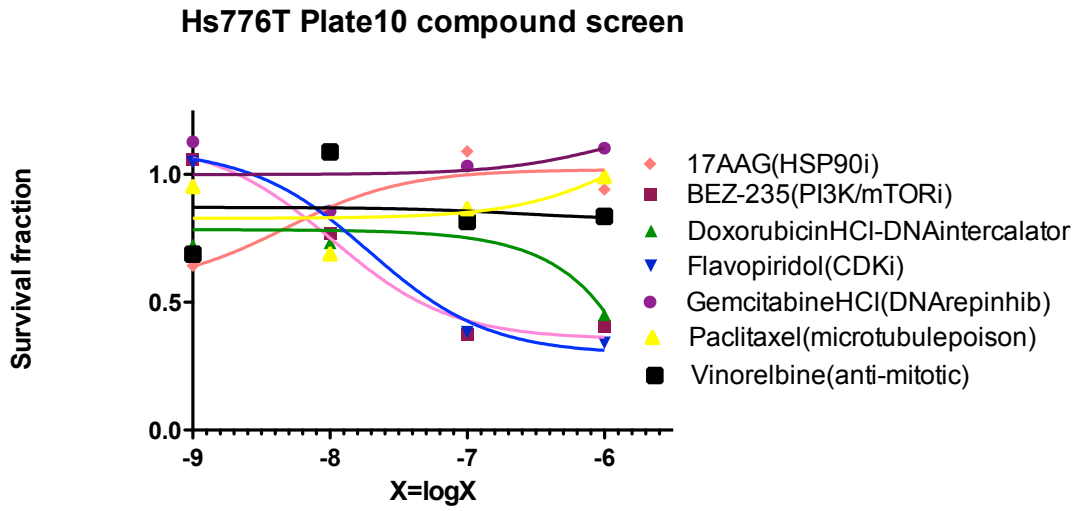


Figure4.12 Cell Survival HTS results for Hs776T.

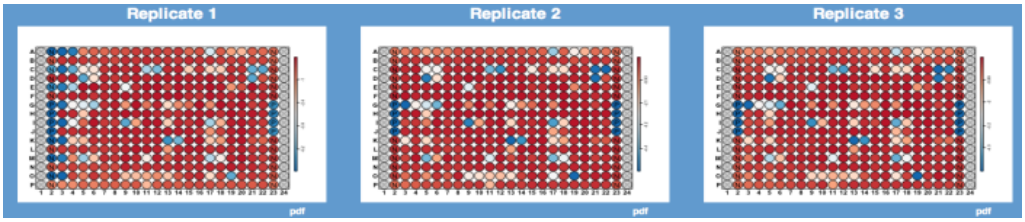
Hs776T appears to be resistant to most of the common drugs including Gemcitabine and Paclitaxel. A survival fraction of < 0.5 is seen at 100nM of Flavopiridol (a cyclin dependent kinase inhibitor) and HSP90 inhibitors. In a similar fashion to that of the other cell lines thus far, Hs776T showed no response to GDC-0449 smoothened inhibitor.

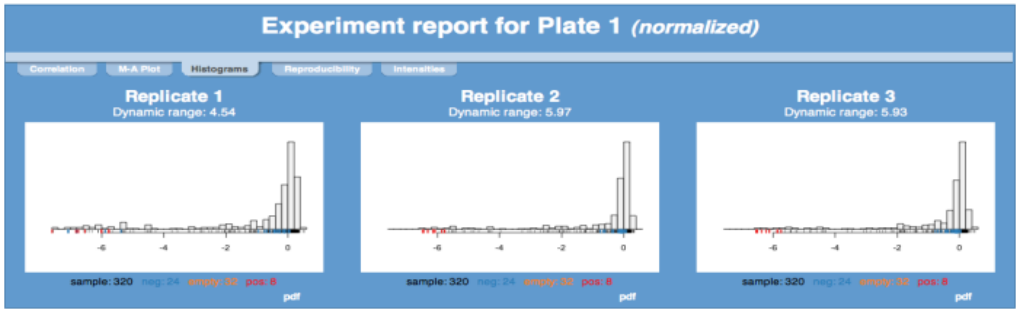
4.2.4.4 Cell Survival HTS results for PANC-1

A.

PANC-1 QC: OK

Plate	Replicate	Channel	Filename	Status	Replicate dynamic range	Average dynamic range	Repeatability standard deviation	Spearman rank correlation (min - max)
1	1	1	Panc1-1.txt	✓	4.54	5.48	0.61	0.85 - 0.9
1	2	1	Panc1-2.txt	✓	5.97	5.48	0.61	0.85 - 0.9
1	3	1	Panc1-3.txt	✓	5.93	5.48	0.61	0.85 - 0.9





B.

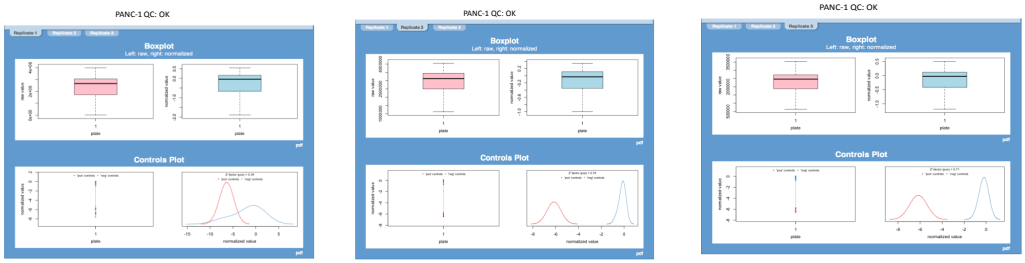


Figure 4.13 Quality control heat map, bar graph and box plot for PANC-1. Figure A shows PANC-1 cell line screen results plate configuration and histograms with good quality control and output of the screen for this cell line. In B, the bar graphs have a normal distribution for positive and negative controls indicating a successful screen throughout replicates 1, 2 and 3.

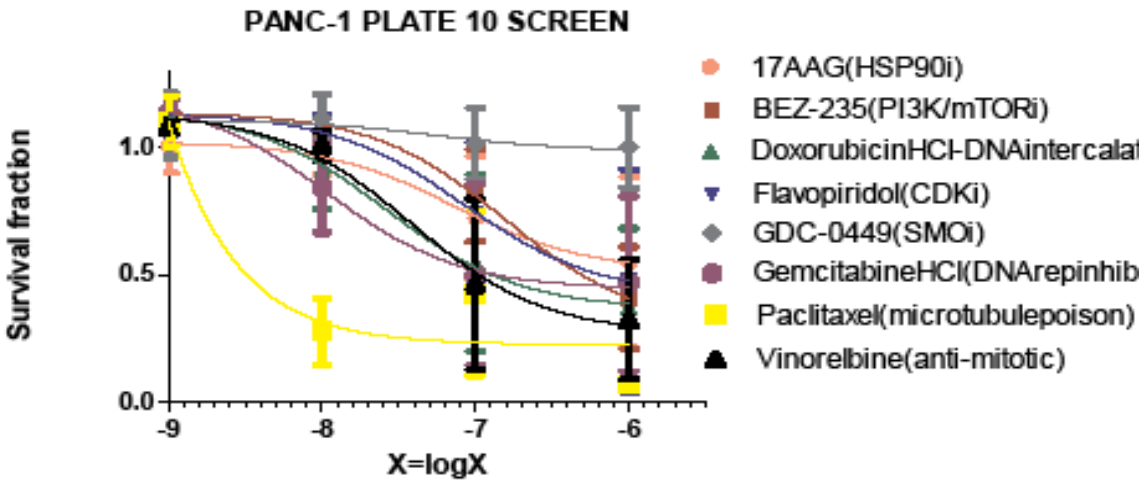


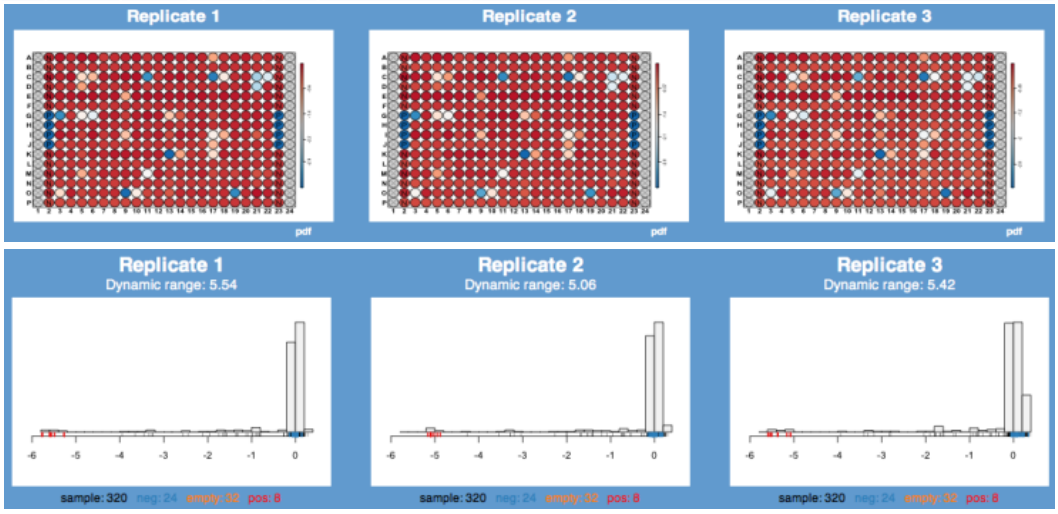
Figure4.14 Cell Survival HTS results for PANC-1.

PANC-1 cells displayed a marked response to Paclitaxel with a survival fraction of only 0.25 at 10nM concentrations of the drug. Treatment with 100nM of Gemcitabine, Vinorelbine and Doxorubicin produced a survival fraction of 0.5 in these cells. Of note there is no response to the smoothened inhibitor GDC-0449 in this PDA cell line as demonstrated in the survival curve, with 100 percent survival in cells that were exposed to this compound at all concentrations of the drug used. The response to BEZ-235 (PI3K/mTOR inhibitor), 17 AAG (HSP90 inhibitor) and Flavopiridol was moderate with a cell survival of 0.7 at 100nM concentrations and little or no response was seen at 10nM concentrations of these compounds.

4.2.4.5 Cell Survival HTS results for PL5

QC : PL5 OK

Plate	Replicate	Channel	Filename	Status	Replicate dynamic range	Average dynamic range	Repeatability standard deviation	Spearman rank correlation (min - max)
1	1	1	PL5-1.txt	✓	5.54	5.34	0.07	0.85 - 0.91
1	2	1	PL5-2.txt	✓	5.06	5.34	0.07	0.85 - 0.91
1	3	1	PL5-3.txt	✓	5.42	5.34	0.07	0.85 - 0.91



A.

B.

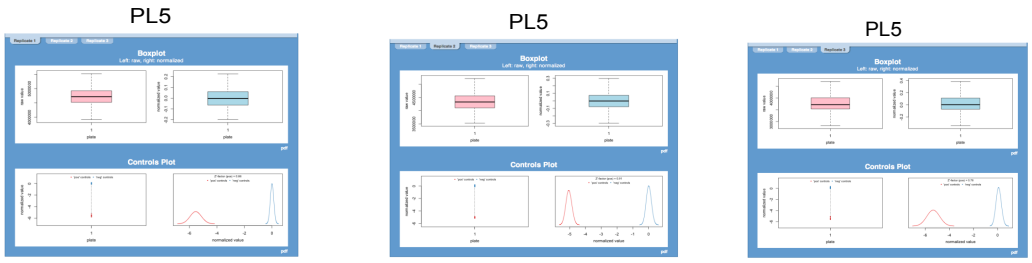


Figure4.15 Quality control heat map, bar graph and box plot for PL5. Figure A shows PL5 cell line screen results plate configuration and histograms with good quality control and output of the screen for this cell line. In B, the bar graphs have a normal distribution for positive and negative controls indicating a successful screen throughout replicates 1, 2 and 3.

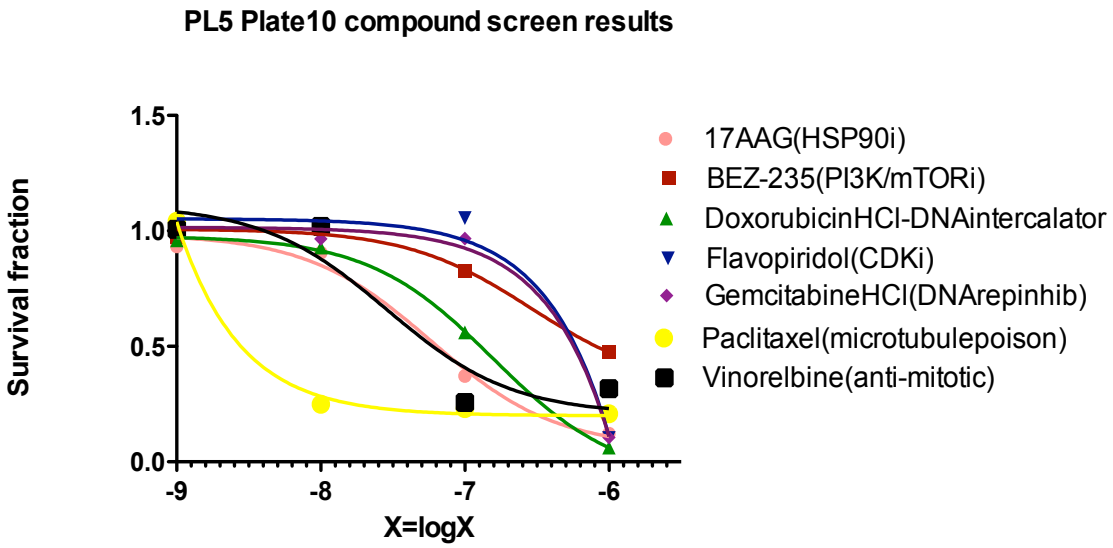


Figure4.16 Cell Survival HTS results for PL5.

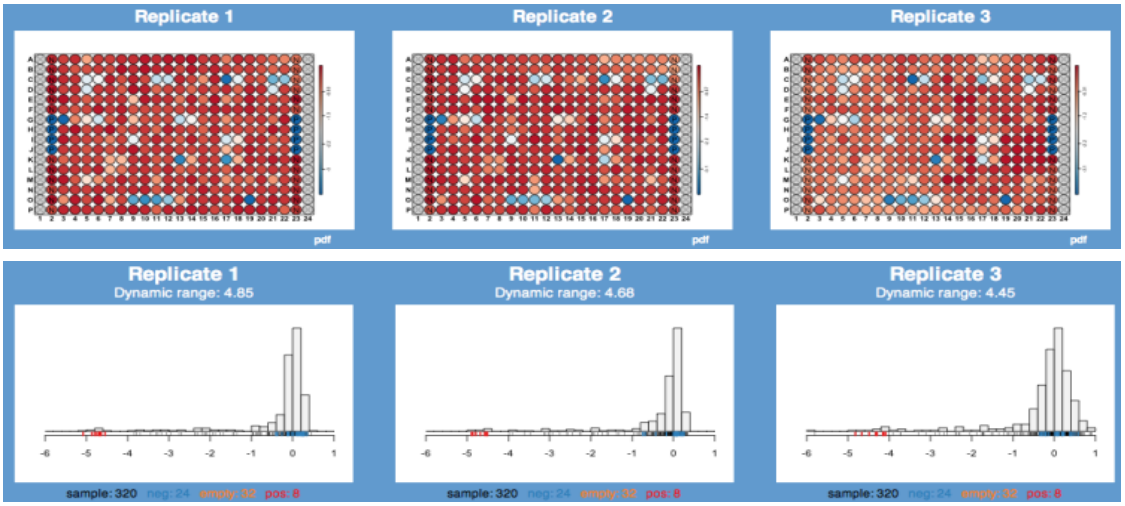
PL5 cells responded significantly to Paclitaxel with a mere 0.25 survival after exposure to the 10nM. There was some sensitivity seen with (-7M) 100nM concentrations of Vinorelbine, 17 AAG (HSP90 inhibitor) in which cell survival was ≤ 0.5. A moderate response was seen to the DNA intercalator, Doxorubicin, at this same concentration of 100nM. There was no response to Gemcitabine at lower concentrations and there was no response to GDC-0449 smoothened inhibitor, (not shown).

4.2.4.6 Cell Survival HTS results for PL45

QC:PL45 OK

Plate	Replicate	Channel	Filename	Status	Replicate dynamic range	Average dynamic range	Repeatability standard deviation	Spearman rank correlation (min - max)
1	1	1	PL45-1.txt	✓	4.85	4.66	0.24	0.35 - 0.5
1	2	1	PL45-2.txt	✓	4.68	4.66	0.24	0.35 - 0.5
1	3	1	PL45-3.txt	✓	4.45	4.66	0.24	0.35 - 0.5

A.



B.

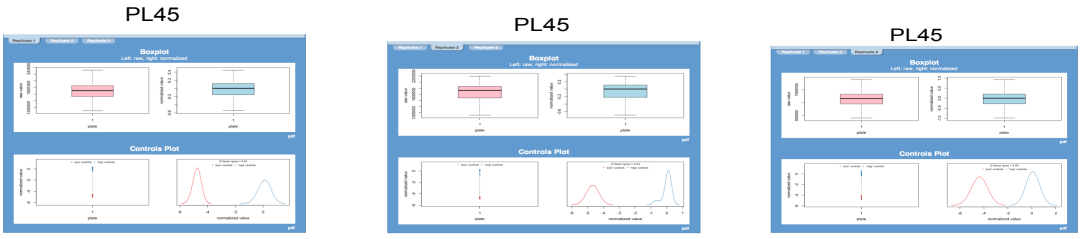


Figure4.17 Quality control heat map, bar graph and box plot for PL45. Figure a shows PL45 cell line screen results plate configuration and histograms with good quality control and output of the screen for this cell line. In b, the bar graphs have a normal distribution for positive and negative controls indicating a successful screen throughout replicates 1, 2 and 3.

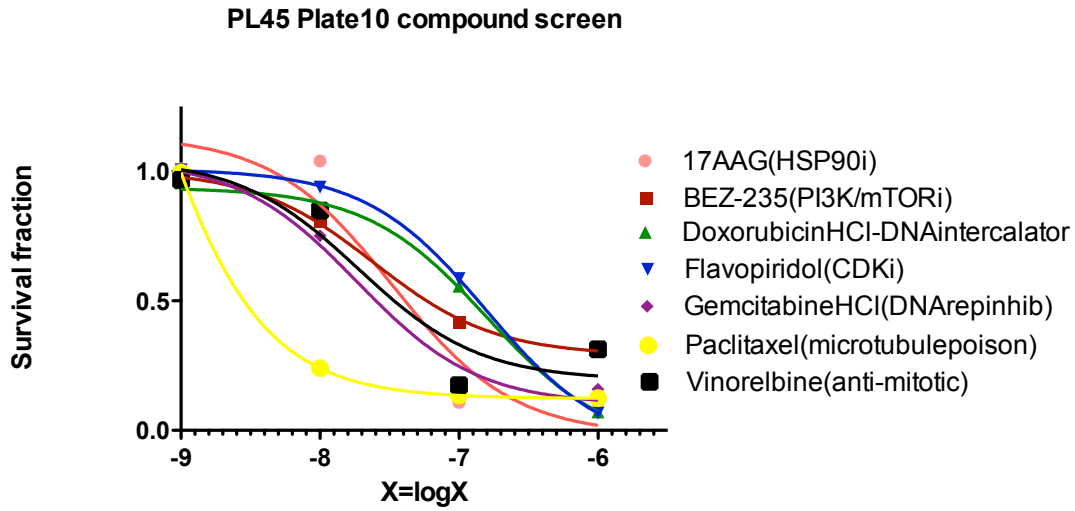
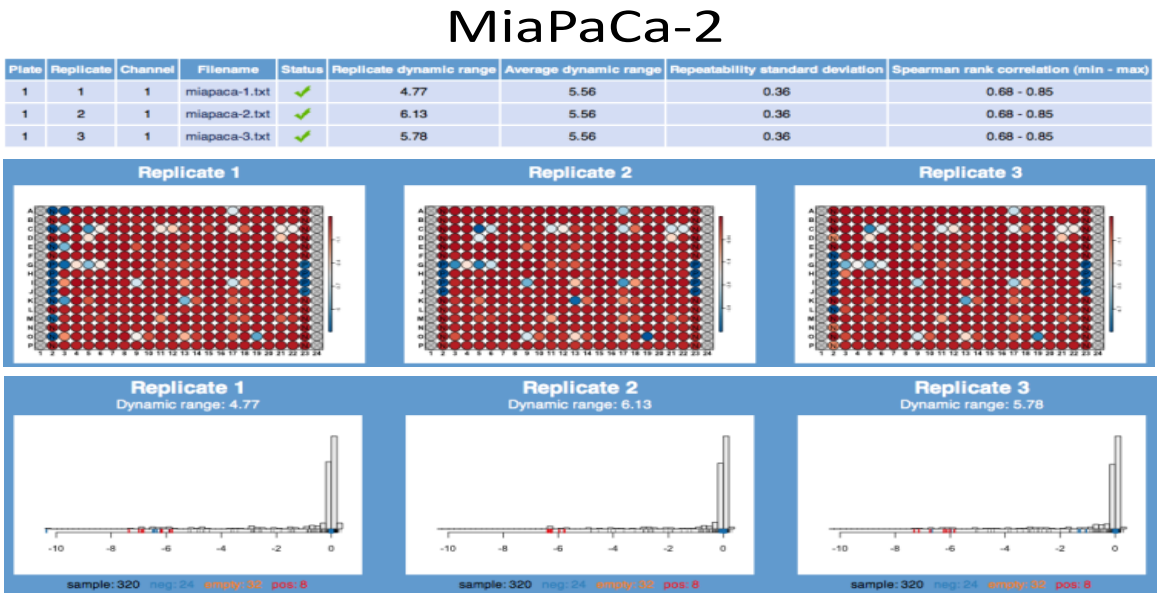


Figure4.18 Cell Survival HTS results for PL45.

Similar to what was seen in previous cell lines, PL45 showed a significant response to Paclitaxel with only a 0.25 survival fraction following treatment with as low as 10nM concentrations of the drug**.** There was also a significant cell death seen at 100nM concentrations of Vinorelbine, 17 AAG (HSP90 inhibitor) and BEZ-235 PI3K/mTOR inhibitor with a cell survival < 0.5. Flavopiridol and Doxorubicin had a moderate response in this PDA cell line with survival as high as 0.7. There was however, a good response to Gemcitabine with cell survival being a mere 0.25 at 100nM concentrations.

4.2.4.7 Cell Survival HTS results for MiaPaCa-2



A.

B.

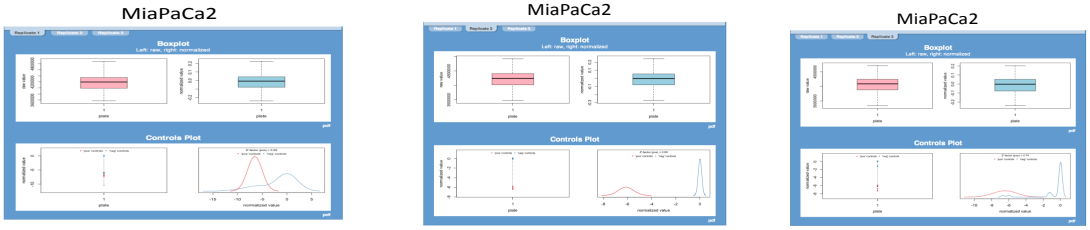


Figure4.19 Quality control heat map, bar graph and box plot for MiaPaca2. Figure A shows MiaPaCa2 cell line screen results plate configuration and histograms with good quality control and output of the screen for this cell line. In B, the bar graphs have a normal distribution for positive and negative controls indicating a successful screen throughout replicates 1, 2 and 3.

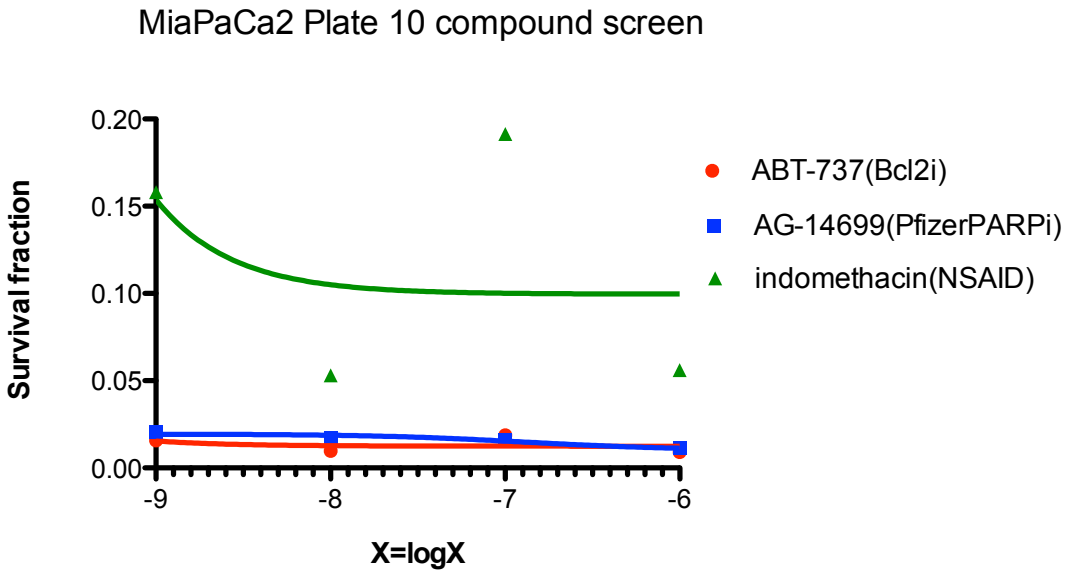
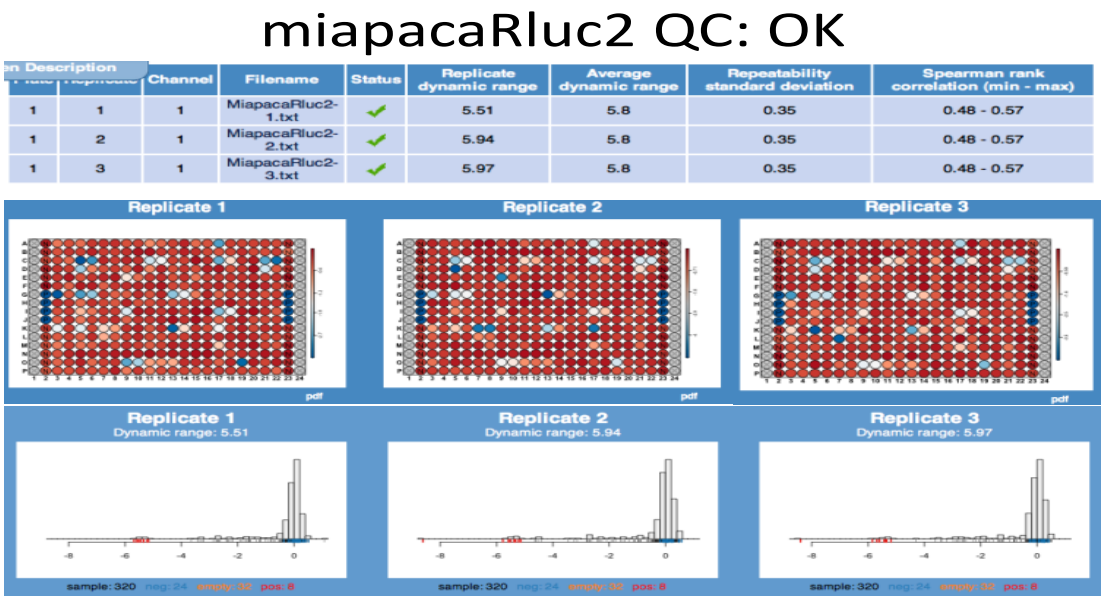


Figure4.20 Cell Survival HTS results for MiaPaca2.

MiaPaCa-2 cells showed a significant response to three compounds, a Bcl2 inhibitor, a PARP inhibitor and a non steroidal anti inflammatory drug (NSAID). The survival fraction of this cell line after exposure to these compounds was less than 0.15 even at low concentrations of 1nM. These cells were particularly sensitive to the PARP inhibitor and Bcl2 inhibitor with a less than 0.02 survival fraction. These cells showed no sensitivity to Gemcitabine, Paclitaxel or HSP inhibitors as seen by the previous PDA cell lines.

4.2.4.7.1 Cell Survival HTS results for clone 2 of luciferase marked MiaPaCa-2

A.



Channel	Filename	Status	Replicate dynamic range	Average dynamic range	Repeatability standard deviation	Spearman rank correlation (min - max)
1	MiapacaRluc2-1.txt	✔	5.51	5.8	0.35	0.48 - 0.57
2	MiapacaRluc2-2.txt	✔	5.94	5.8	0.35	0.48 - 0.57
3	MiapacaRluc2-3.txt	✔	5.97	5.8	0.35	0.48 - 0.57

B.

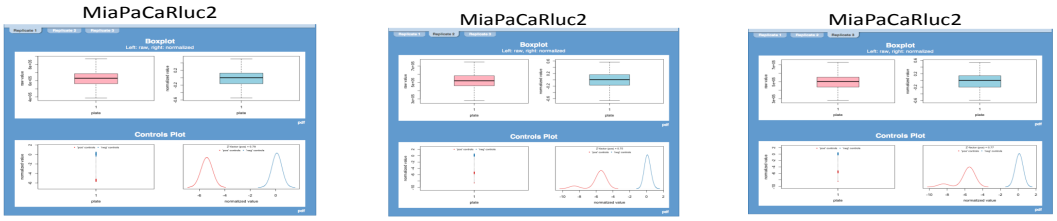


Figure4.21 Quality control heat map, bar graph and box plot for clone 2 of luciferase marked MiaPaca2.

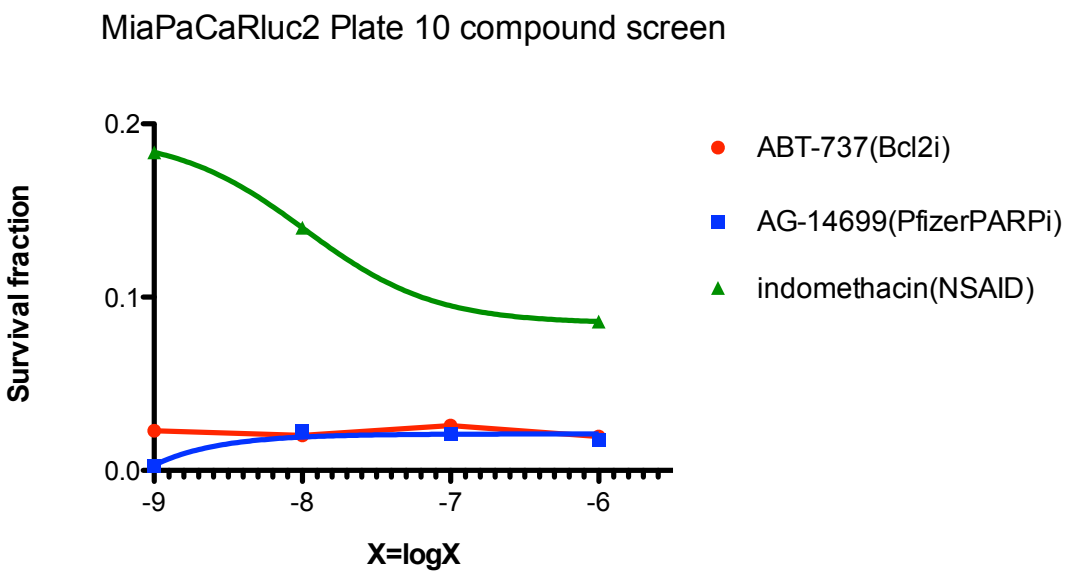
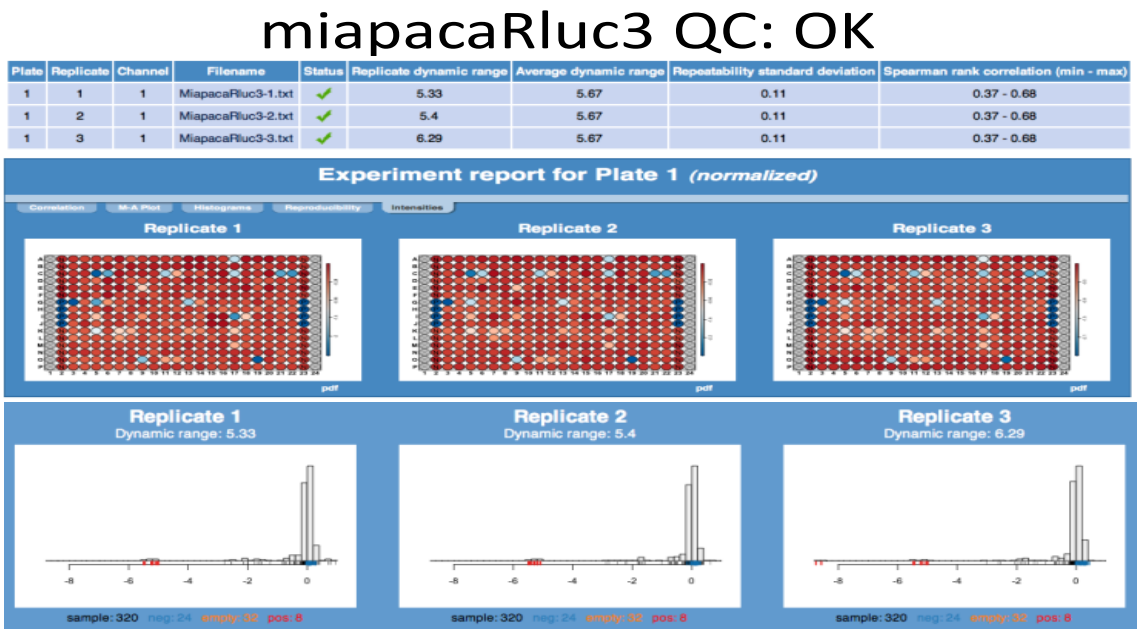


Figure4.22 Cell Survival HTS results for clone 2 of luciferase marked MiaPaca2.

This is a clone of a luciferase marked MiaPaCa-2 cell line. Cell survival was seen as less than 0.2 for all concentrations used suggesting significant cell death and sensitivity to these compounds.

4.2.4.7.2 Cell Survival HTS results for clone 3 of luciferase marked MiaPaCa-2

A.



B.

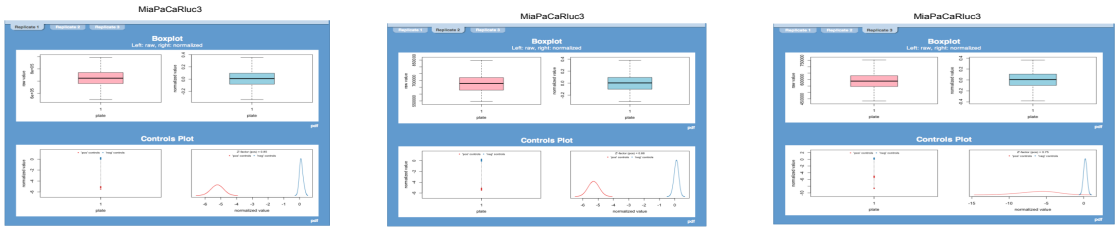


Figure4.23 Quality control heat map, bar graph and box plot for clone 3 of Renilla luciferase marked MiaPaca2

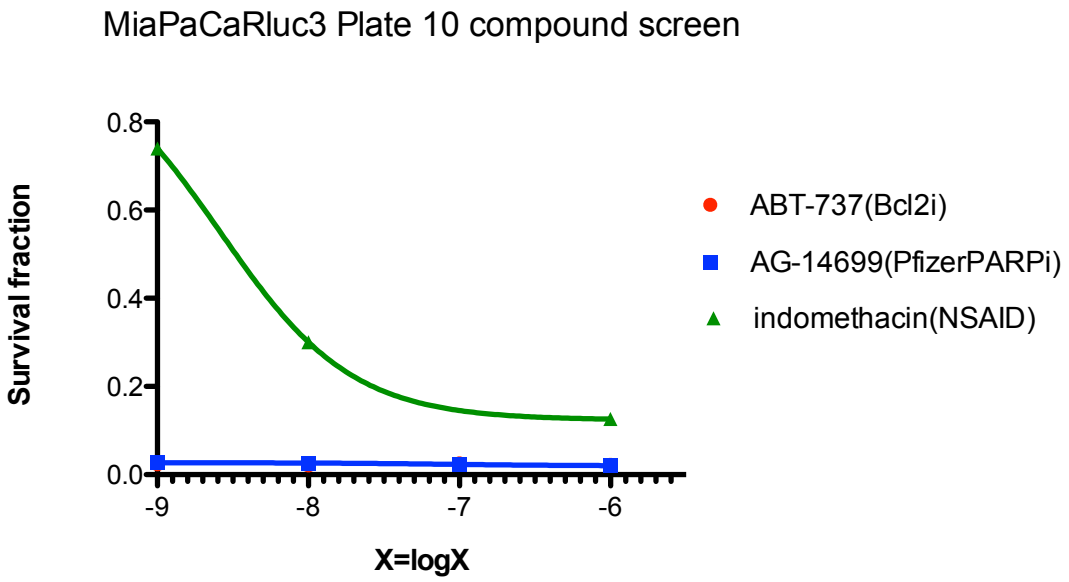


Figure4.24 Cell Survival HTS results for clone 3 of Renilla luciferase marked MiaPaca2.

This clone of a Renilla luciferase marked MiaPaCa-2 cell line showed the similar pattern of sensitivity to the parent cell line in which there was significant sensitivity to three compounds ABT-737 (Bcl-2 inhibitor), AG-14699 (PARP inhibitor) and Indomethacin (NSAID). The survival fraction of was less than 0.8 across all concentrations of these drugs with almost 100 cell death after treatment with the Bcl-2 and PARP inhibitors.

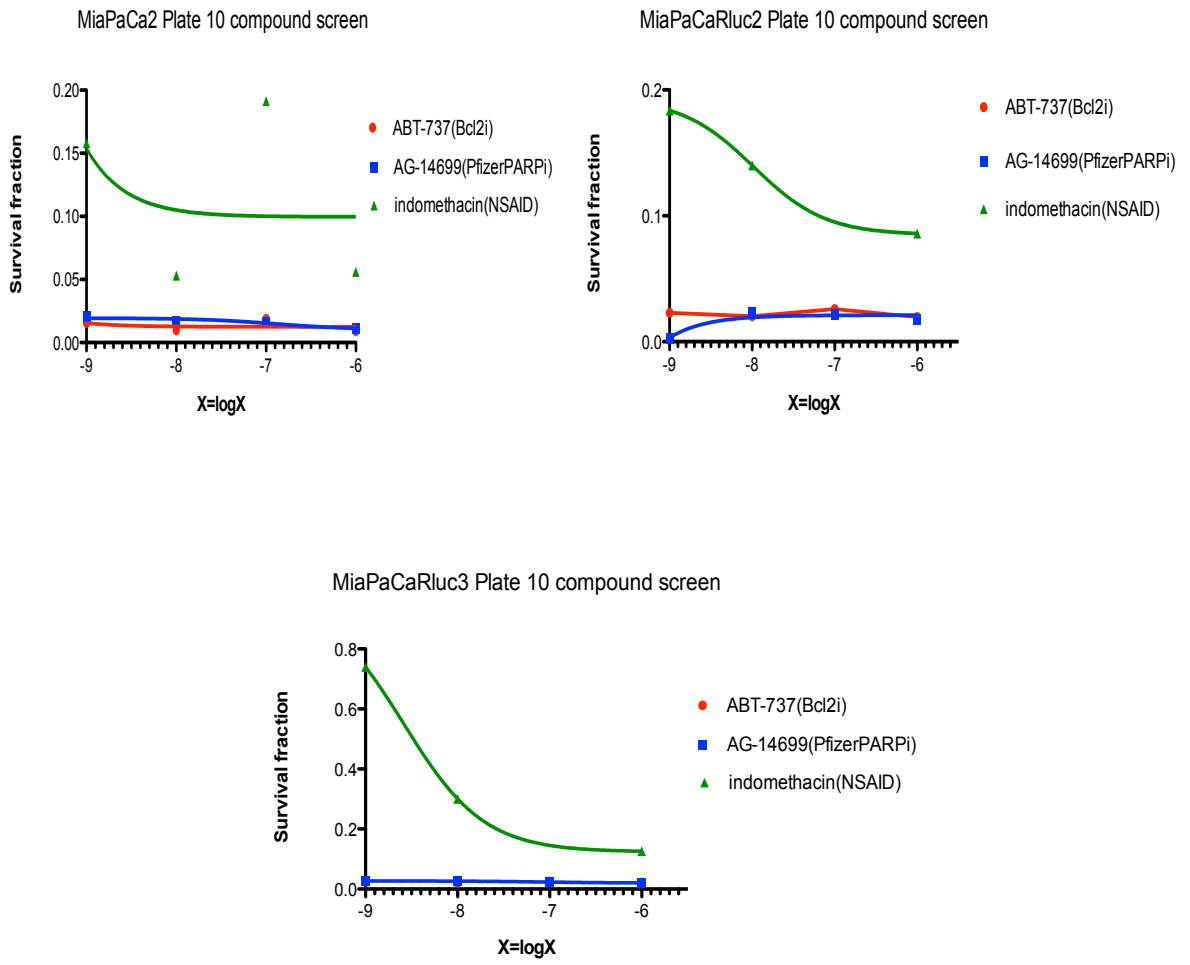
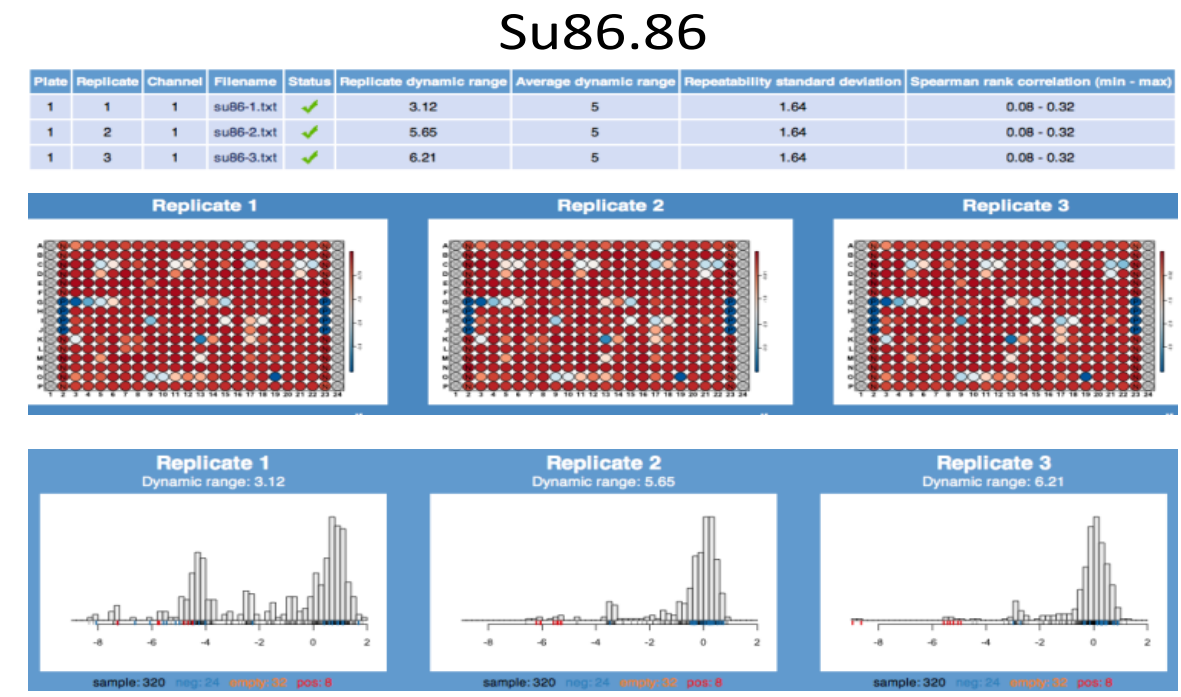


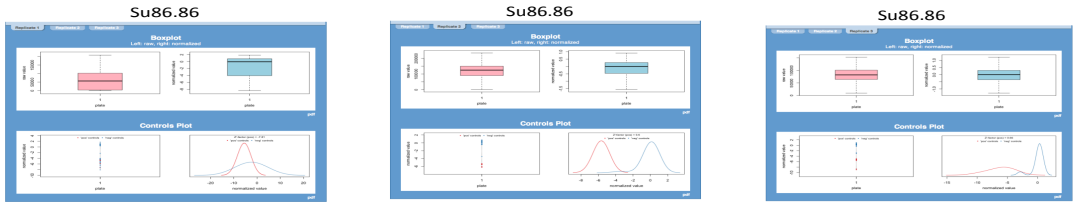
Figure4.25 Cell Survival HTS results for clone MiaPaca2 and its luciferase marked clones

Both clones and parent cell line responded in a similar fashion as discussed above. There was a significant response to three compounds, a Bcl2 inhibitor, Ag-14699 (a PARP inhibitor from Pfizer) and an NSAID, Indomethacin. Although clone 3 of the luciferase marked cells appeared most sensitive, both clones responded in a similar pattern to the parent cell line with almost total cell death from both the PARP inhibitor and the NSAID.

4.2.4.8 Cell Survival HTS results for Su86.86



A.



B.

Figure4.26 Quality control heat map, bar graph and box plot for Su86.86. Figure A shows Su86.86 cell line screen results plate configuration and histograms with good quality control and output of the screen for this cell line. In B, the bar graphs have a normal distribution for positive and negative controls indicating a successful screen throughout replicates 1, 2 and 3.

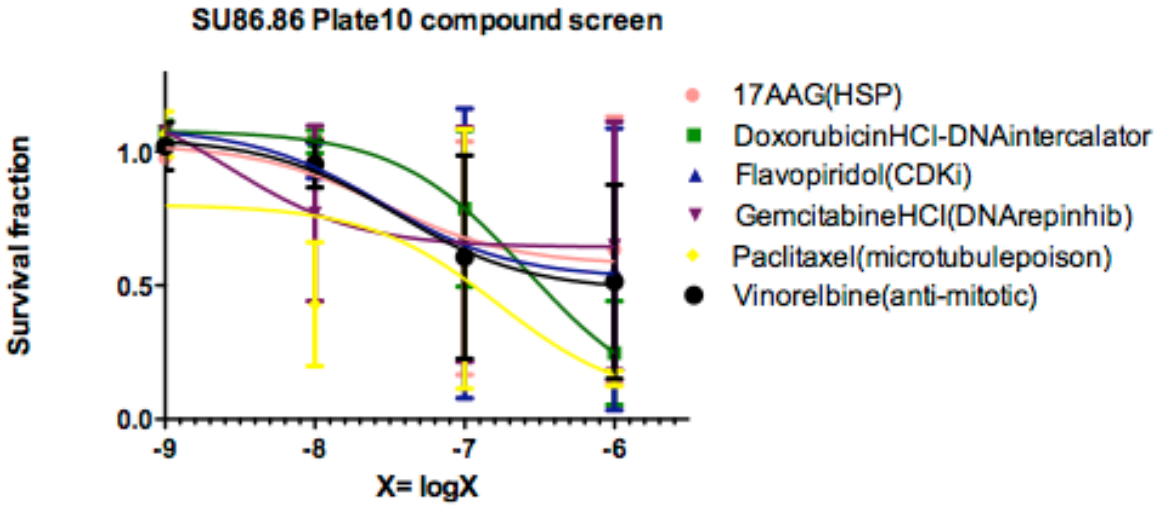


Figure4.27 Cell Survival HTS results for Su86.86.

The survival fraction of SU86.86 was 0.7 on exposure to Gemcitabine and Paclitaxel at 10nM concentrations. There was little response to any of the other compounds at this concentration. At the higher concentration of 100nM, survival fraction was 0.7 in response to Gemcitabine, Vinorelbine, Flavopiridol and HSP inhibitors. The greatest sensitivity was seen with Paclitaxel, with a survival fraction of 0.5 at 100nM of the compound.

4.2.5 Comparison of cell survival at low concentrations 10nM

Table 4.2 below, shows a list of the survival fractions of each cell line and the compounds to which they have shown sensitivity. A score of 1 indicates no cell death and 100% survival. A cell survival reading from 0.6 to 0.8 was considered a moderate response and 0.5 or less was considered a significant response to the drug. All cell lines with the exception of MiaPaCa-2 responded to Paclitaxel at this low concentration, with PL5, PL45 and PANC-1 having the greatest response to Paclitaxel with a survival fraction of 0.3 and ASPC-1 having a survival fraction of 0.5. HPAC, Hs766T and Su86.86 appeared more resistant to Paclitaxel. There was a poor response to Gemcitabine across all 8 cell lines with Aspc-1, HPAC, Hs766T, PL5 and MiaPaCa-2 having limited or no response at all and PANC-1, PL45 and Su86.86 having only a mild response with high survival fractions of 0.8 . None of the cell lines responded to the smoothened inhibitor GDC-0449 and there was a limited or no response to all of the other compounds at 10nM.

Cell survival for common hits seen from Ashworth HTS compound library screen at 10nM concentrations

Plate 10 compound hits	AsPC-1	HPAC	Hs776T	Panc-1	PL45	PL5	MiaPaCa-2	Su86.86
17 AAG HSP inhibitor	0.7	0.9	1	1	1	1	1	1
BEZ-235 PI3K/mTOR Inhibitors	1	1	1	1	0.8	1	1	1
BI-2536 PLKi	0.9	1	1	1	1	1	1	1
Doxorubicin DNA Intercalator	1	1	0.8	0.9	0.9	1	1	1
Flavopiridol] CDKi	1	1	0.8	1	1	1	1	1
Gemcitabine DNA repair inhibitor	1	0.9	1	0.8	0.8	1	1	0.8
Paclitaxel Microtubule suppressor	0.5	0.7	0.8	0.3	0.3	0.3	1	0.8
Vinorelbine Anti mitotic	1	1	0.9	1	0.8	1	1	1
GDC-0449 Smoothened inhibitor	1	1	1	1	1	1	1	1

Table 4.2 Cell Survival for PDA cell lines at ($1x10^{-8}$)10nM concentrations .

This table compares cell survival fractions following treatment with 10nM concentrations of each compound via high throughput screening. No colour = no response, = very significant response, , = significant response, = minimal response, = moderate response

4.2.6 Comparison of cell survival at higher concentration 100nM

As seen from table 4.3 b**elow**, 6 out of 8 PDA cell lines displayed a response to the microtubule suppressor Paclitaxel, particularly PL45, PL5 and PANC-1 (highlighted in red) which showed the lowest cell survival after treatment. ASPC-1, HPAC and SU86.86 displayed a 50% cell survival and Hs776T and MiaPaCa-2 had limited and no sensitivity to this compound. At this concentration there was also limited or no response to Gemcitabine from PDA cell lines HPAC, Hs776T, PL5 and MiaPaCa-2. PL45 and PANC-1 appeared more sensitive with very low cell survival fractions, PL45 being the most sensitive with a survival fraction of 0.3. None of the PDA cell lines showed any response to the smoothened inhibitor GDC-0449.

Cell survival for common hits seen from Ashworth HTS compound library screen at ($1x10^{-7}$)100nM concentrations

Plate 10 compound hits	AsPC-1	HPAC	Hs776T	Panc-1	PL45	PL5	MiaPaCa-2	Su86.86
17 AAG HSP inhibitor	0.7	0.5	1	0.7	0.3	0.4	1	0.7
BEZ-235 PI3K/mTOR inhibitors	0.6	0.9	0.4	0.7	0.5	0.9	1	1
BI-2536 PLKi	0.6	1	1	1	1	1	1	1
Doxorubicin DNA Intercalator	0.8	1	0.8	0.5	0.7	0.6	1	0.8
Flavopiridol CDKi	0.7	1	0.4	0.7	0.7	1	1	0.7
Gemcitabine DNA repair inhibitor	0.7	0.9	1	0.5	0.3	1	1	0.7
Paclitaxel Microtubule suppressor	0.5	0.5	0.9	0.3	0.2	0.3	1	0.5
Vinorelbine Anti mitotic	0.6	1	0.9	0.5	0.4	0.4	1	0.6
GDC-0449 Smoothened inhibitor	1	1	1	1	1	1	1	1

Table 4.3 Cell survivals for PDA cell lines at ($1x10^{-7}$)100nM concentrations. This table compares cell survival fractions following exposure to 100nM concentrations of each compound via high throughput screening. A score of 1 indicates no cell death and 100% survival. A low score indicated a better sensitivity to the drug, indicated in red.

4.3 Discussion

Several methods have been used to predict *in vitro* chemosensitivity of tumour cells to cytotoxic agents and different assays; clonogenic, which first expand tumour cells prior to treatment with cytotoxic agents and non-clonogenic assays in which primary tumour cells are exposed to chemotherapeutic drugs, have been employed. Chemosensitivity profiles have been reported for breast, stomach and liver cell lines (*Nakatsu et al,.2005*). This study reviewed genes that determine the chemosensitivity of these pancreatic ductal adenocarcinoma cell lines to a library of anti-cancer drugs.

For pancreatic cancer, studies have profiled the expression of individual genes implicated in chemoresistance, such as *BNIP3*, (*Erkan et al, 2005*), as well as those involved in Gemcitabine uptake and metabolism, (*Nakahira et al*, 2007; *Nakano et al*, 2007). Michalski and colleagues used the ATP-based tumour chemosensitivity assay (ATP-TCA) on primary resected pancreatic cells and used real time PCR to determine the RNA expression of specific genes associated with chemoresistance, (*Michalski et al. , 2008*). Sanger and broad have performed genomic and gene expression analyses, (www.cancerrxgene.org). They correlated the sensitivity patterns of their large library of cell lines with genomic and expression data in order to identify features that may predict sensitivity.

High throughput screening is a method that allows large volume screening of several compounds in the hope of new drug delivery. It is a drug screen compared to the genetic screens described above. From the compounds screened in this library, those that produced at least 50% cell death or a cell survival fraction of 0.5 or less included heat shock protein inhibitors, Pi3K/mTOR inhibitors, DNA intercalators, microtubule suppressors, anti-mitotics and cyclin dependent kinase inhibitors. Of the 8 PDA cell lines screened, none of these responded to treatment with the smoothened inhibitor GDC-0449, even at the highest concentration of 1μM.

The PDA cell lines above appear to be resistant to Gemcitabine at lower concentrations of the drug (10nM), and only PANC-1 and PL45 have displayed a 50% cell death or less than 0.5 cell survival fractions when exposed to higher concentrations of Gemcitabine. All the cell lines appeared resistant even at 1μM of Gemcitabine with the exception of PANC-1, PL5 and PL45. These PDA cell lines all had a low cell survival count at this concentration whilst all other cell lines showed minimal or no response.

With the exception of MiaPaCa-2 and Hs776T, all the other epithelial cell lines showed sensitivity to the lower 10μM concentration of Paclitaxel. PL45, PL5 and AsPC-1 had survival fractions ≤ 0.5, equivalent to 50% or more cell death. A similar pattern was seen at higher concentrations. Of note, MiaPaCa2 was resistant to Gemcitabine and Paclitaxel and showed no response to smoothened inhibitor compound GDC-0449. Although this is not appreciated at 10nM, the more sensitive cell lines in this group PANC-1, PL5 and PL45 also showed significant response (survival fraction ≤ 0.5) to the anti-mitotic, Vinorelbine and the heat shock protein inhibitor compound 17 AAG at 100nM concentrations of these compounds.

As mentioned before Sanger and Broad have compiled a database, from several sources, that correlated drug response with genetic alterations that may affect sensitivity of the cancer cell lines screened. They have screened over 1000 genetically characterised human cancer cell lines with a wide range of anti-cancer drugs, (www.cancerrxgene.org). The Sanger and Broad drug library did not include some of the hits obtained from drugs in the Ashworth compound library such as BEZ-235 the Pi3K/mTOR inhibitor and Flavopiridol and therefore these could not be compared. They did however have data on 17-AAG (HSP inhibitor), Doxorubicin, Dasantinib, Gemcitabine, Paclitaxel and Vinorelbine. Of their collection of PDAC cell lines, only ASPC-1 and MiaPaCa-2 were included.

The known genetic mutations in PDAC include mutations of *KRAS, AKT2, CDKN2A* (p16), *DPC/SMAD4* and *P53*. The number of mutations in these genes and their effect on sensitivity were correlated in the Sanger and Broad database. From their data, the gene mutation having any effect on sensitivity of pancreatic cell lines was *CDKN2A (p16).* Its effect on sensitivity was however limited with a maximum 55 fold increase in sensitivity to 17 AAG and minimum of 16 fold increase in sensitivity to Paclitaxel. There was a 100 fold increase in resistance to Doxorubicin with this genetic mutation. The other mutations commonly seen in PDAC were not found to have any notable effect on sensitivity or resistance. There were no genetic correlations found that affect sensitivity of PDAC lines to Vinorelbine and the genetic changes seen in *CDKN2A* and *SMAD4* had little correlation or affect on sensitivity of the PDAC cell lines to GDC-0449.

AsPC-1, HPAC, PANC-1, PL5, PL45 and Su86.86 appear to be the more sensitive cell lines when compared to MiaPaCa2 and Hs776T, with PL5, PL45 and PANC-1 displaying a comparatively larger amount of cell death on high throughput screening. Although there are no specific similarities in these two apparently resistant cell lines, the amplification in *AKT2*/ch 19q is absent in both MiaPaCa-2 and Hs776T and neither of them have the LOH at 13q, seen in the other cell lines. Based on the data from Sanger and broad neither AKT2 nor 13q LOH confer any degree of sensitivity or resistance in the cell lines screened. Of the two cell lines with the least response to drugs, only MiaPaCa2 has a homozygous deletion at *CDKN2A* (p16). Hs776T has no genetic alteration in this gene and p16 homozygous deletions can also be found in ASPC-1, PANC-1 and SU86.86.

Currently in the clinical setting, the drugs that have been used include Gemcitabine, Oxaliplatin, Capecitabine, Cisplatin and Irinotecan, with varying and limited outcomes, Gemcitabine being the gold standard of treatment. The results of the High throughput screen showed little cell death in response to Gemcitabine at lower concentrations (10nM) and a response in only 2 cell lines (PANC-1 and PL45) at the higher concentration of 100nM. Combination therapy has included some of the other compounds in the screen including, Gemcitabine/GDC-0449(Anti smoothened) and Gemcitabine/Nab- Paclitaxel. None of the PDAC models used in this study responded to the smoothened inhibitor however, there was significant cell death, up to 70%, in response to the microtubule suppressor Paclitaxel even at lower concentrations of the compound (10nM).

Chapter 5

Pancreatic stellate cells and chemoresistance

5.1 Introduction

The pancreatic stellate cell has been shown to be necessary for the development of tumours in KPC mouse xenograft models (*Olive/Tuveson et al., 2009).* Stellate cancer associated fibroblasts themselves have already been implicated in the aggressiveness of others cancers such as oral squamous cell carcinoma, (*Sobral et al., 2011).* This suggests a role for pancreatic stellate cell in tumour development and progression.

Due to the dense desmoplastic reaction particular to pancreatic cancer and the majority of cells in these tumours being pancreatic stellate cells, these cells may be intimately involved in the chemoresistant nature of these tumours*,* making them viable targets when considering options for chemotherapy in the fight against pancreatic cancer

Hwang and associates showed that in the presence of human pancreatic stellate cells, cancer cells, in particular BxPc3, show no significant change in cell number when exposed to Gemcitabine or irradiation, (*Hwang et al*, 2008). They also found an increase in the anti apoptotic signalling pathway expression whereby the cancer cell lines responded to stellate conditioned media with a multiple fold increase in AKT and ERK expression after several minutes when co-cultured with human stellate cells.

They showed that stellate cells were necessary for tumour initiation and growth and without them tumours failed to develop on their own. Co-injection of stellate with BxPc3 in orthotopic mice resulted in metastases in a dose dependent manner. (*Hwang et al., 2008*). The mechanism of this effect has not yet been elucidated but may be multi-factorial. These factors may include crosstalk between the stellate cells and the tumour and the related feedback mechanisms. Other contributing factors are that of increased signalling pathways involved in tumour development such as the hedgehog signalling pathway and the dense stroma which may act as a physical barrier to drug delivery, (*Olive et al., 2009*).

5.1.1 Crosstalk and chemoresistance

Pancreatic stellate cells are activated by a variety of cytokines produced by tumour cells, including interleukins, fibroblast growth factors (FGFs), TGFβ and PDGF. In turn, pancreatic stellate cells are found to produce cytokines and components of the ECM that affect cancer cell invasiveness and growth. They include FGFs, VEGF, connective tissue growth factor (CTGF), matrix metalloproteinases (MMPs), collagens and fibronectin. They are also known to produce insulin like growth factor IGF-1 and II, the actions of which appear to predominantly impart tumour growth by conveying survival signals, (*Hwang et al.*, 2008). Ueda and colleagues reported IGF-1 receptor (IGF1R) and epidermal growth factor receptor (EGFR) overexpression in the pancreatic ductal specimen resected, (*Ueda et al., 2006*). Their data suggests that EGFR family member signalling through IGF1R is important in signalling in cancer growth and survival.

Part of the ability of tumour cells to evade programmed cell death is derived from survival signals supplied by the stromal compartment. Since there is increasing evidence that the tumour stroma may be crucial in determining the invasive and metastatic potential of many cancers, understanding the biology of the activated stellate cell and its stroma has therapeutic potential. There may be benefit, for example, in reducing the cross-activation of the stellate cells and stromal cells by inhibitors of PDGF, VEGF and other mediators, many of which are becoming commercially available. Animal models have been used to suggest that Sonic Hedgehog (SHH) signalling promotes the migration and invasion of human pancreatic myofibroblasts thereby increasing the desmoplastic and stromal reaction, (*Madhevan, Von Hoff et al 2007*).

Other compounds have been identified as potential key players in the chemoresistant nature of pancreatic cancer. Fibroblast activating protein, which is seen in the activated stellate cell, is one of the factors implicated with the development of the stromal compartment and has recently been identified as a possible prognostic indicator for PDA, (*Min et al*, *2012*). It alters the extracellular matrix, making it a more favourable environment for tumour invasion. Disruption of this fibroblast activating protein effect has been found to hinder tumour invasion, (*Lee, Mullins et al, 2011*; *Santos et al, 2009),* making it a potentially useful chemotherapeutic target.

5.1.2 Hedgehog (Hh) signaling and chemoresistance

The hedgehog signalling pathway has proved to be a key player in the development and proliferation of PDA. This pathway was previously thought to stimulate the epithelial cells of tumours, resulting in tumour progression. It has since been shown that this pathway is activated in the stromal compartment (*Yauch et al, 2008)*. Hedgehog stimulates stromal proliferation via paracrine signalling and inhibition of this pathway has shown to have therapeutic potential.

The expression of Hh ligands and essential components of the pathway, including PTCH and SMO, have been reported in up to 70% of human pancreatic ductal adenocarcinoma specimens (*Thayer et al., 2003)*. In addition, several studies have proposed that Hh ligands produced by tumour cells activate Hh signalling and tumour cell growth in an autocrine/ juxtacrine manner *(Thayer et al., 2003, Pasca di Magliani et al., 2006)*. Previously, research focused heavily on the presence of hedgehog signalling in the pancreatic epithelium but research performed by a Cambridge group led by Olive and Tuveson found that the hedgehog pathway is in fact effected within the stromal compartment, (*Olive et al., 2009*).

Sonic Hedgehog (SHH) binds to the Patched-1 (PTCH1) receptor. In the absence of the SHH ligand, PTCH1 inhibits Smoothened (SMO), a downstream protein in the pathway. *(Taipale et al, 2002).* The binding of SHH relieves SMO inhibition, leading to activation of the GLI transcription factors Gli1 and Gli2 (activators) and the Gli3 (repressor). Activated Gli accumulates in the nucleus and controls the transcription of hedgehog target genes. PTCH1 has recently been reported to repress transcription of hedgehog target genes through a mechanism independent of Smoothened suggesting the existence of a non-canonical pathway, *(Rahnama et al., 2006).*

Yauch and his group reported that for hedgehog–expressing tumours lacking mutations in the pathway, hedgehog signalling was indeed occurring in the stroma and not the cancer epithelial cells, (*Yauch et al., 2008*). They demonstrated that the hedgehog ligand from the cancer cell was activating the adjacent stroma. This data was corroborated with evidence by Olive and Tuveson who showed, using mouse models, that a hedgehog inhibitor could deplete the stroma and re-vascularise poorly perfused tumours, giving evidence that the stroma can be targeted by hedgehog antagonists. A smoothened inhibitor when used in combination with Gemcitabine to treat genetically modified mice was found to increase the median survival by more than 2 fold, (*Olive/Tuveson et al, 2009).* These KPC mice (KrasLSL.G12D/+; p53R172H/+; PdxCretg/+) had pancreas-specific *Kras*^{G12D} and *Trp53*^{R172H} mutations, *(Olive/Tuveson et al, 2009).*

The sequence of molecular events that connect Smoothened to the Gli transcription factors is poorly understood and requires further investigation as this pathway can prove a useful target in the management of pancreatic cancer. Further therapeutic manipulations in the future may involve reversing the activation of stellate which is an area that has not been studied. Thus far, the activated phenotype of stellate cells has been shown to be reversed by ligands of the peroxisome proliferator-activated receptor-gamma (PPARγ) pathway, as well as antioxidants, (*Haber et al, 1999; Cat B et al*, 2006).

5.1.3 Stromal density and chemoresistance

The density of stroma is also believed to be chemoprotective in that it hinders adequate drug delivery to an already resistant cancer. Notably, PDA has a particularly prolific desmoplastic reaction making it comparable to breast cancer where greater than 90 percent of cells in the stroma are pancreatic stellate cells. Studies have attempted to perforate this dense barrier in order to access the tumour thereby facilitating better drug delivery. They showed a 60% increase in Gemcitabine concentration in the tumours if preceded by a hedgehog inhibitor, and the combination of this inhibitor with Gemcitabine more than doubled mouse survival compared with Gemcitabine alone, (*Olive/Tuveson et al, 2009*).

Olive and colleagues have shown that the use of hedgehog inhibitors can alter communication between the tumour and stroma via the hedgehog pathway, interrupting the feedback loop necessary for stromal activation and development and resulting is stromal depletion. This depleted stroma becomes less of a barrier to chemotherapeutic intervention as drug delivery to the tumour is somewhat enhanced.

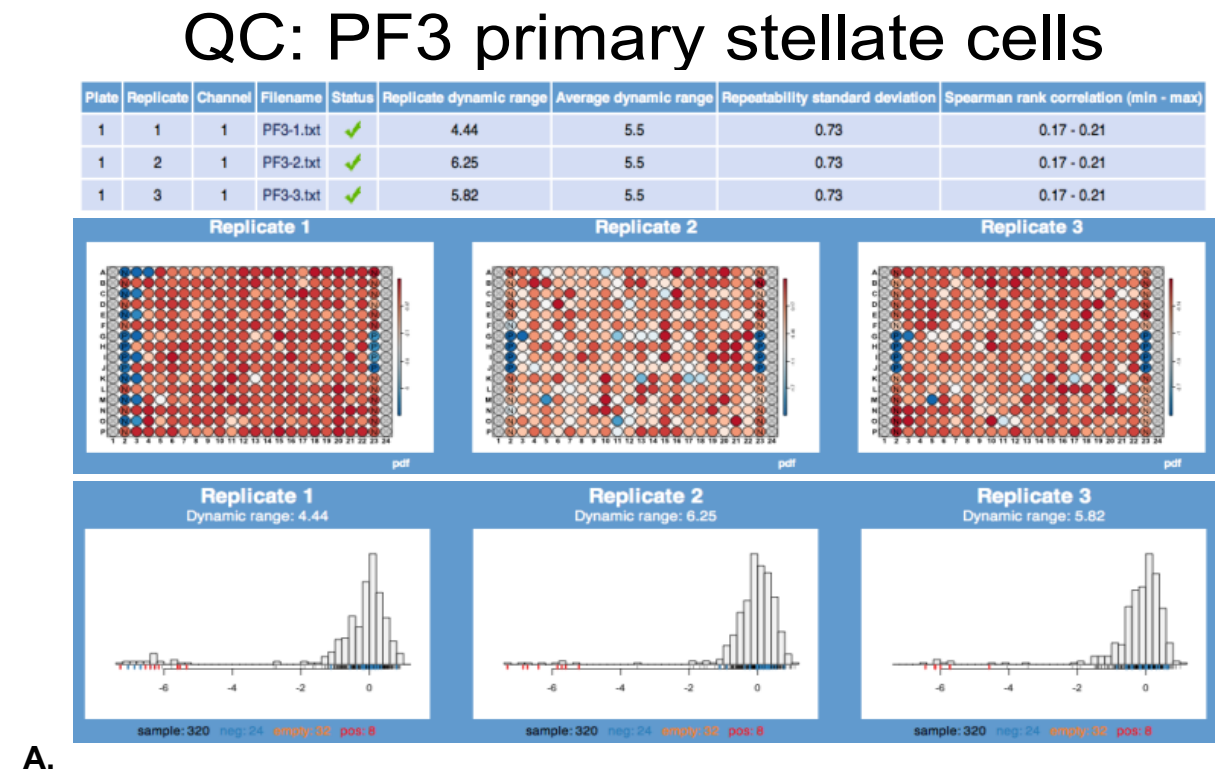
5.2 High throughput screen results of stellate cancer associated fibroblasts

There is currently very little data on the chemosensitivity of stellate cancer associated fibroblasts. Previous work has implicated stellate CAFs and their secretions in cancer progression when cultured with tumour cells. (*Vonlaufen et al, .2008*). Other studies have identified a role of extracellular matrix proteins in the acquired resistance to anticancer drugs. This study used in vitro models to show that resistance to cytotoxic drugs was dependent on these proteins. (*Miyamoto et al, 2004*). The actual mechanism was not identified. Further work is therefore needed to profile the role of these stellate cells in the chemoresistant nature of PDAC.

Primary non-immortalised stellate cells were cultured from wedge resections of PDA, described in Materials and Methods, and then screened under the same conditions as the PDA epithelial cell lines. These explants were cultured from samples taken within 5mm from the tumour edge (figure 2.1) and verified as a pure fibroblast culture using immunohistochemistry as shown in figure 2.2. They were expanded to an early passage 3 or 4 and to 70% confluence prior to storage in liquid nitrogen for future use. These cells were profiled using array CGH and displayed no copy number variations thereby confirming their genetic stability. The immortalised pancreatic stellate cell line displayed the same immunohistochemistry as that of the non-immortalised group. Both models were screened as described below.

The full Ashworth library of chemotherapeutic agents were used for the primary and immortalised stellate cells in the same manner as for the PDA cell lines. The results obtained were represented as heat maps, bar graphs and histograms which confirmed quality control of the HTS screens. Below are the results of the screens for each pancreatic stellate cell line. For quality control, the z prime factor is an indication of the signal to noise ratio of the CTG reading (assay output quantification) between the untreated cells (DMSO only, 0.2% volume to volume ratio (v/v)) and the cell death control. The z prime factor for all screens ranged form 0.5 to 0.78. It is essentially the ratio between the blue dots (positive control) and red dots as seen on the histograms). A screen with a value of 0.5 or higher was considered an excellent quality. The spearman rank correlation is another indication of the quality control of the screen.

5.2.1 Cell survival HTS results for PF3



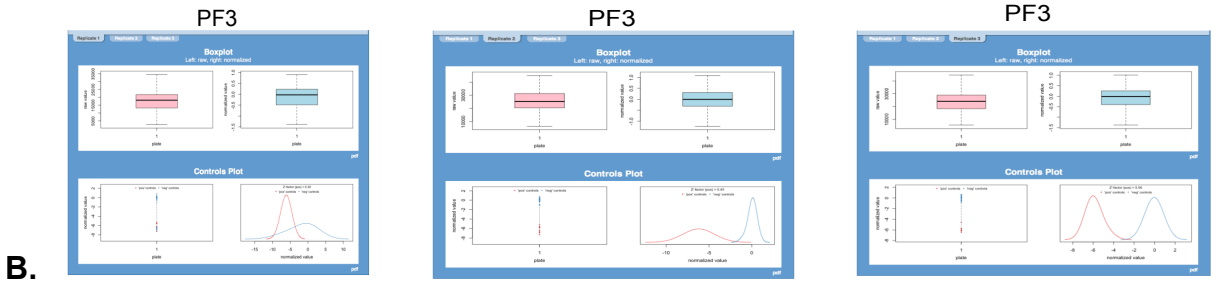


Figure 5.1 Quality control heat map, bar graph and box plot for PF3. Figure a shows PF3 cell line screen results plate configuration and histograms with good quality control and output of the screen for this cell line. In B, the bar graphs have a normal distribution for positive and negative controls indicating a successful screen throughout replicates 1, 2 and 3.

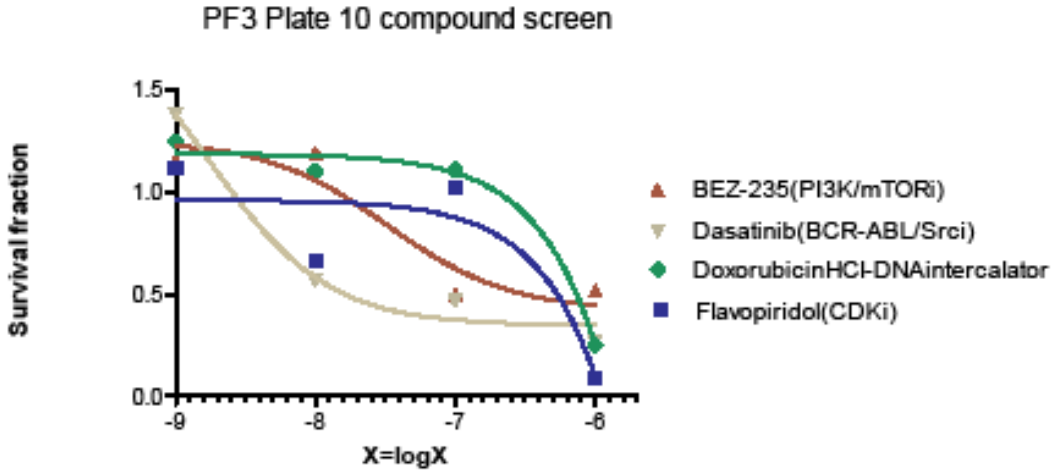


Figure 5.2 Cell Survival HTS results for primary stellate cell line PF3.

The cell survival curve for the primary fibroblast explant PF3 has shown sensitivity to Dasantinib at low concentrations of 10nM (-8) with a cell survival of 0.5. Results showed that there was no sensitivity to Gemcitabine or Paclitaxel. At 100nM (-7) concentrations of the Pi3K/mTOR inhibitor, BEZ-235, there was a moderate response with cell survival of 0.6.

5.2.2 Cell survival HTS results for PF18

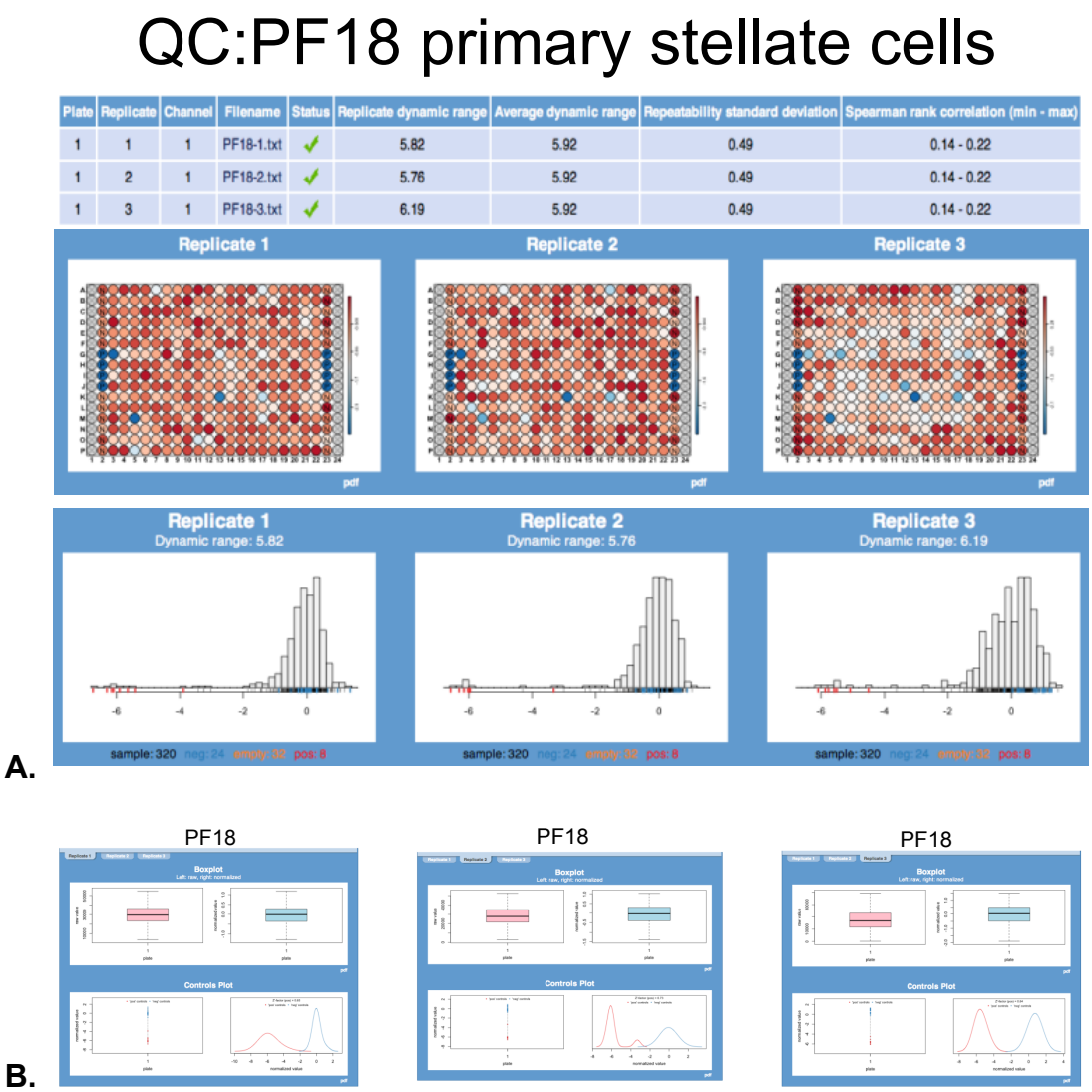


Figure 5.3 Quality control heat map, bar graph and box plot for PF18. Figure a shows PF18 cell line screen results plate configuration and histograms with good quality control and output of the screen for this cell line. In b, the bar graphs have a normal distribution for positive and negative controls indicating a successful screen throughout replicates 1, 2 and 3.

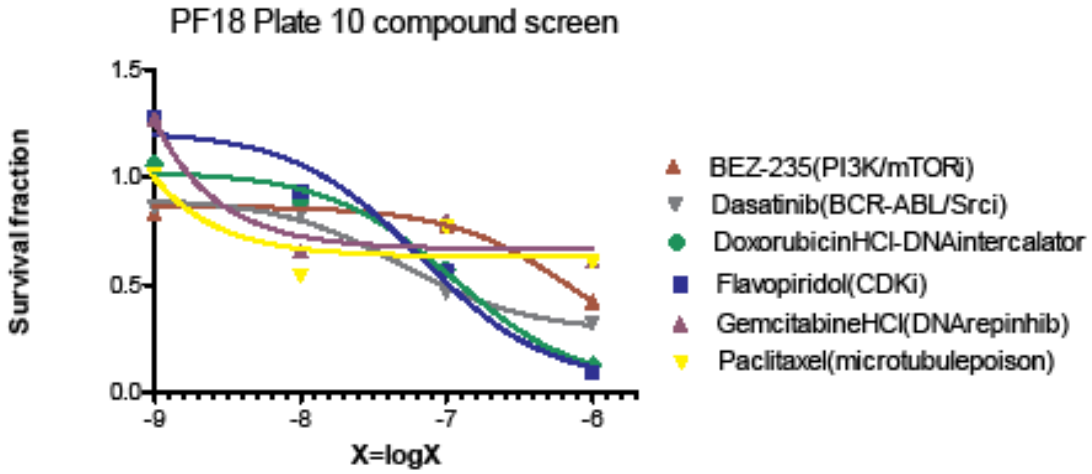


Figure 5.4 Cell Survival HTS results for primary stellate cell line PF18.

PF18 was sensitive to Dasantinib, Flavopiridol and Doxorubicin at 100nM. The cell survival fraction was 0.5 in response to each drug. Results showed that there was some sensitivity to Gemcitabine and Paclitaxel at the lower concentrations but this response plateaud at higher concentrations up to and including 1000nM.

5.2.3 Cell survival HTS results for PF20

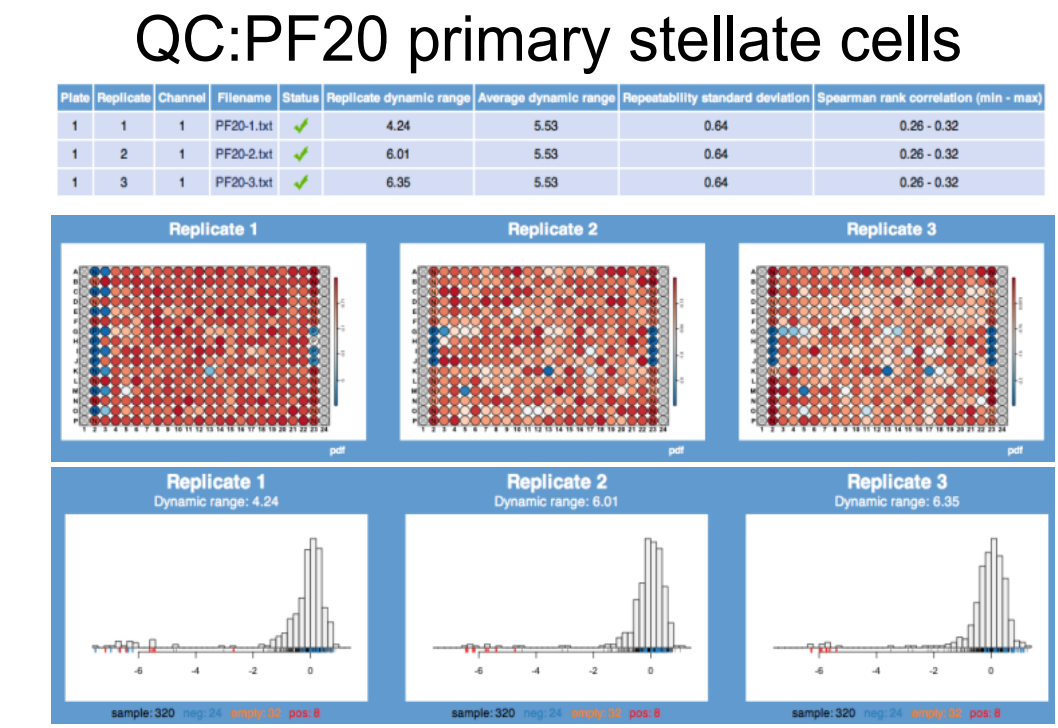


Figure 5.5 Quality control heat map, bar graph and box plot for PF18. A) PF18 cell line screen results plate configuration and histograms with good quality control and output of the screen for this cell line. B), the bar graphs have a normal distribution for positive and negative controls indicating a successful screen throughout replicates 1, 2 and 3.

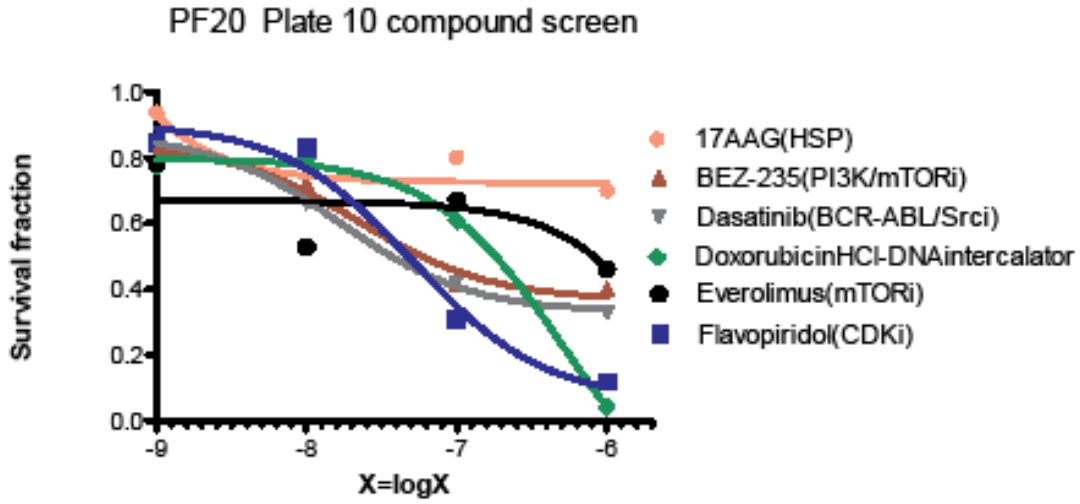


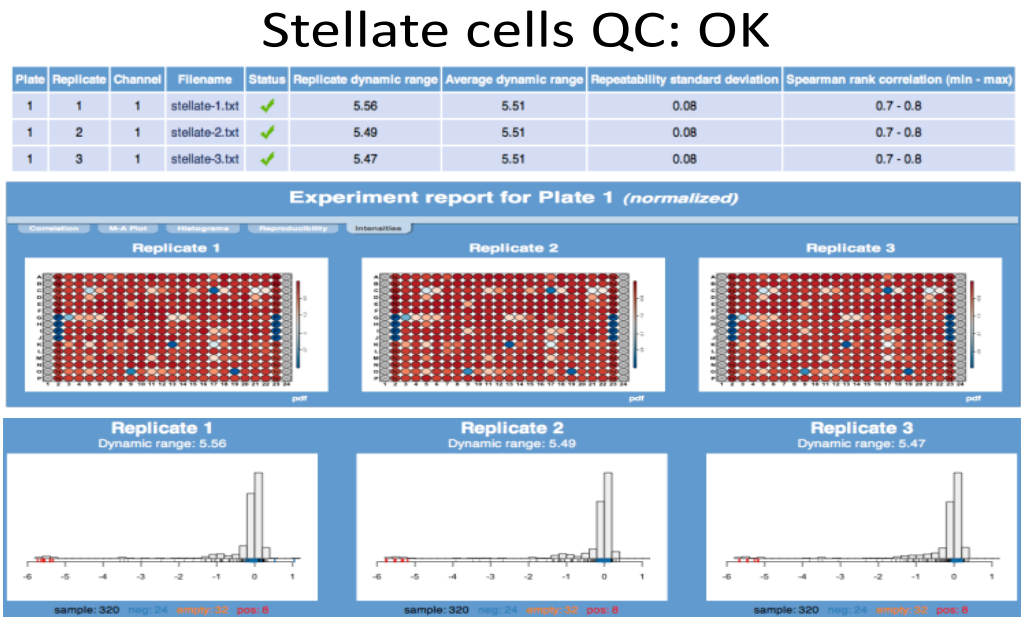
Figure 5.6 Cell Survival HTS results for primary stellate cell line PF20.

This primary non- immortalised stellate cell culture has shown a response to Dasantinib, BEZ-235 and Flavopiridol with survival fractions all < 0.5 only a 30% cell survival in cells exposed to Flavopiridol. These cells appeared to have some response to the heat shock protein inhibitors although limited.

5.2.4 Cell survival HTS results for Immortalised human pancreatic Stellate cells

Quality Control

A.



B.

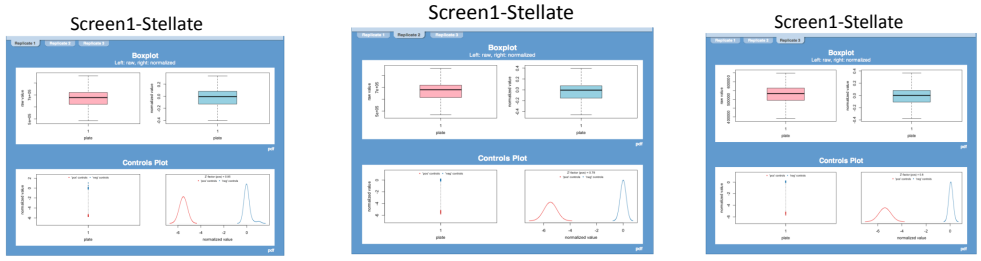


Figure 5.7 Quality control heat map, bar graph and box plot for Immortalised Human pancreatic stellate cells. Figure A shows Human pancreatic stellate cell line (HPSC) screen results plate configuration and histograms with good quality control and output of the screen for this cell line. In B, the bar graphs have a normal distribution for positive and negative controls indicating a successful screen throughout replicates 1, 2 and 3.

5.2.5 Repeat cell survival HTS results for Immortalised human pancreatic stellate cells

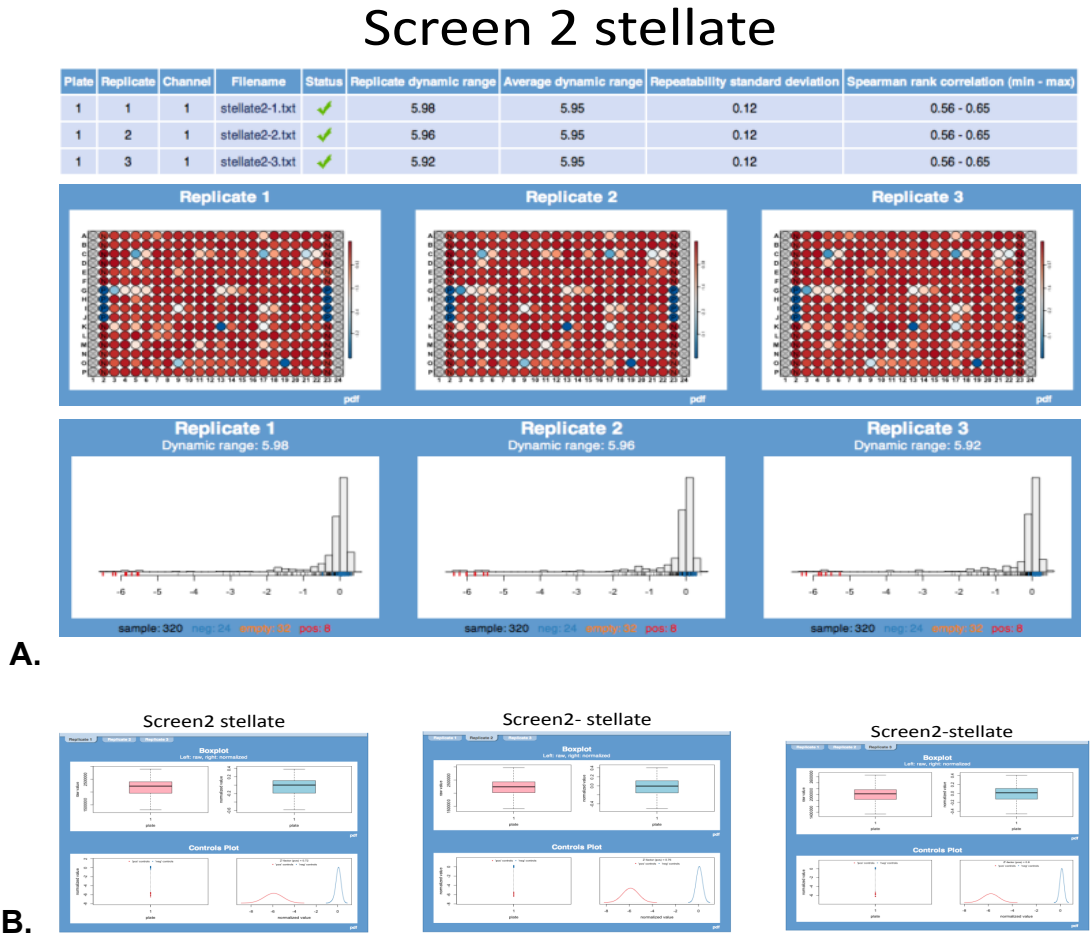


Figure 5.8 Quality control heat map, bar graph and box plot for Immortalised Human pancreatic stellate cells screen 2. Figure A shows HPSC cell line screen results plate configuration and histograms with good quality control and output of the screen for this cell line. In B, the bar graphs have a normal distribution for positive and negative controls indicating a successful screen throughout replicates 1, 2 and 3.

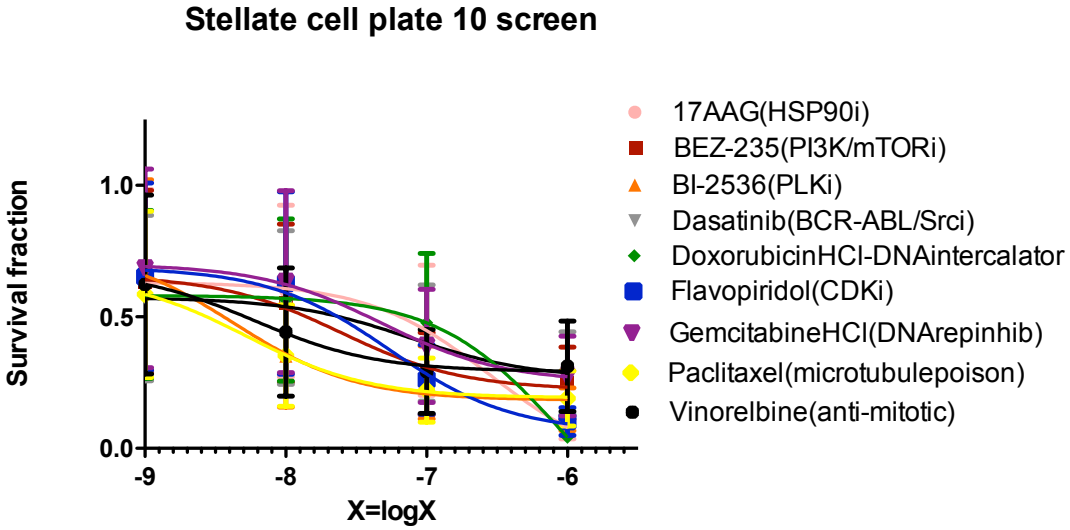


Figure 5.9 Cell Survival HTS results for Immortalized Human pancreatic stellate cells.

The immortalised stellate cells responded well to all of the main chemotherapeutic compounds with cell survival being less than 50% with Vinorelbine, 17 AAG heat shock protein inhibitors and Paclitaxel at the very low 10μM concentration of each drug. There is still a noted 40% cell death will all the drugs listed at the lowest concentration of 1nM. These cells seem more sensitive than their PDA counterparts.

5.2.6 Comparison of cell survival at low concentration of 10nM

Table 5.1 below shows cell survival following exposure to 10nM concentrations of each compound via high throughput screening. At 10nM the primary non-immortalised cell lines were resistant to most of these compounds. There was some response in all three primary cell lines to the PI3K/mTOR inhibitor compound (BEZ-235) and the BCR-ABL/SRC inhibitor (Dasantinib) even at this low concentration. The immortalised stellate cells we sensitive to all the common hits, even at this low concentration, with the exception of the smoothened inhibitor GDC-0449, to which there was no response. The greatest response was seen on exposure to the heat shock protein inhibitor (17 AAG) and the microtubule suppressor, (Paclitaxel). Both the immortalised and non-immortalised groups of stellate cells were resistant to the smoothened inhibitor, (GDC-0449).

Cell survival for common hits seen from the Ashworth High Throughput Screen compound library (10nM concentrations)

Plate 10 compound hits	PF3	PF18	PF20	Immortalised stellate cells
17AAG HSP inhibitor	1	1	0.8	0.4
BEZ-235 PI3K/mTOR inhibitors	0.6	0.8	0.7	0.5
BI-2536 PLKi	1	1	1	0.6
Dasantinib BCR-ABL/Src inhibitor	0.6	0.8	0.7	0.6
Doxorubicin DNA Intercalator	1	1	0.8	0.6
Flavopiridol] CDKi	1	1	1	0.6
Gemcitabine DNA repair inhibitor	1	0.7	1	0.6
Paclitaxel Microtubule suppressor	1	0.6	1	0.4
Everolimus mTOR inhibitor	1	1	0.7	0.5
GDC-0449 Smoothened inhibitor	1	1	1	1

Table 5.1 Cell survival z scores at 10nM concentrations of each compound. This table shows the z scores for the primary and immortalised stellate cells. Scores of 1 indicates no cell death and values less than 0.5 show a more than 50% cell death.

5.2.7 Comparison of cell survival at higher concentration of 100nM

Table 5.2 compares the cell survival of the primary stellate cells and the immortalised stellate cells at 100nM concentrations of the common hits. Both the immortalised and non-immortalised groups of stellate cells were resistant to the GDC-0449 smoothened inhibitor. All cells were sensitive to Dasantanib (BCR-ABL/Src inhibitor) with cell survival ≤ 0.5. Even at this higher concentration the primary non immortalised stellate cells showed limited or no response to Gemcitabine.

Cell survival for common hits seen from the Ashworth High Throughput Screen compound library (100nM concentrations)

Plate 10 compound hits	PF3	PF18	PF20	Immortalized stellate cells
17AAG HSP inhibitor	1	1	0.8	0.5
BEZ-235 PI3K/mTOR inhibitors	0.6	0.8	0.5	0.3
BI-2536 PLKi	1	1	1	0.2
Dasantinib BCR-ABL/Src inhibitor	0.4	0.5	0.4	0.4
Doxorubicin DNA Intercalator	1	0.5	0.7	0.5
Flavopiridol] CDKi	0.9	0.5	0.3	0.3
Gemcitabine DNA repair inhibitor	1	0.7	1	0.4
Paclitaxel Microtubule suppressor	1	0.6	1	0.2
Everolimus mTOR inhibitor	1	1	0.7	0.4
GDC-0449 Smoothened inhibitor	1	1	1	1

Table 5.2 This table shows cell survival z scores following exposure to 100nM concentrations of each compound via high throughput screening. Scores of 1 indicates no cell death and values less than 0.5 show a more than 50% cell death.

5.3 Discussion

Direct and indirect interactions between tumour cells and their microenvironment have been identified as potential molecular targets to overcome chemoresistance. For example, cancer-associated fibroblasts have been shown to protect MCF-7 cells against apoptosis by the topoisomerase inhibitor, Doxorubicin and the PARP-1 inhibitor, ABT-888. These oestrogen receptor positive (MCF-7) cells, when exposed to these drugs, in co-culture with fibroblasts, showed no affect on cell viability. This is believed to be due to the increase in mitochondrial activity, induced by the caveolin-1 depleted fibroblasts, which protects these cells from apoptosis. When cultured on their own MCF-7 cells displayed an 11.6 fold reduction in viability with Doxorubicin and a 6.8 fold reduction in viability with ABT-888. This is an example of the active role of stellate cells in chemoresistance, (*Martinez-Outschoorn et al., 2011*).

In the high throughput drug screens performed, the primary and immortalised stellate cell lines here both displayed sensitivity to the BCR-ABL/Src inhibitor (Dasantinib) and PI3kinase/mTOR inhibitor compound BEZ-235. There was a significant response to Dasantinib, across all the cell lines at the higher concentration of 100nM. The immortalized stellate cell line however, responded also to Gemcitabine, the microtubule poison Paclitaxel, the heat shock protein inhibitor compound 17 AAG and PI3kinase/mTOR inhibitor compound BEZ-235 at the lower 10nM concentrations of each compound.

As previously described, hedgehog produced by the epithelial cancer cells binds to smoothened receptors in the stroma. This paracrine activity leads to the disinhibition of Patched and a canonical production of Gli transcription proteins. These transcription factors are believed to be involved in stromal proliferation, tumour development and progression. Of note, neither the primary, nor immortalized stellate cell lines responded to the smoothened inhibitor when treated individually. This may be due to the presence of a non-canonical pathway involving Gli transcription factors that is independent of smoothened activation.

Overall the immortalised stellate cell line appeared less resistant to chemotherapeutic compounds in this drug library in comparison to the primary non-immortalized group. These cells were derived from chronic pancreatitis specimens and not pancreatic cancer and this may be a contributing factor. The cells however have the same phenotype when immunostained. The primary non-immortalised cells, which were indeed cancer associated, within 5mm of the tumour margin, were not found to have any homozygous genetic changes and therefore this would not be a contributing factor in the difference in sensitivity. The presence and role of heterozygous and epigenetic changes is yet to be elucidated.

Chapter 6 - Conclusion

The focus of this study was to elucidate any changes and behaviour of the stellate cancer associated fibroblast that may play a role in tumour progression and chemoresistance. It has been shown by several studies that pancreatic stellate cells play an integral role in tumour growth and development as tumours that are seeded with these stellate cells show 100 percent more growth *in vivo*, as opposed to when they were seeded on their own.

On stimulation, the tumour microenvironment undergoes changes during which, the more active extracellular matrix becomes an oasis for the tumour and supports its cell proliferation, invasion and angiogenesis. There are multiple pathways through which this may occur but the exact mechanisms are not yet fully understood. Apart from their physical presence in the activated state, factors derived from stellate cells also play a role in tumour growth and angiogenesis, (*Orimo[2] et al, 2005*). These factors may also oppose the action of chemotherapeutic drugs and the biology of the stellate cancer associated fibroblast to date makes them a plausible target in order to obtain a better response to chemotherapy**.**

Despite the duality in findings previously reported, this study has found no homozygous genetic changes in the stellate CAFs of pancreatic ductal adenocarcinoma. However, the presence of heterozygous and/or epigenetic changes is yet to be fully excluded in this group and their effects if any, identified. The arrayCGH platform used showed no change in genotype in these tumour-

juxtaposed cells in neither the explanted cells (5mm from the tumour margin), nor the intermingled fibroblasts obtained by laser captured microdissection. It therefore offers support to the suggestion that the mechanism by which these cells contribute to the aggressive nature of the disease may lie in the cross talk that occurs between these activated fibroblasts and the PDA epithelial cell as well as the signalling pathways involved.

Having found that the stellate cancer associated fibroblast does not acquire homozygous genetic mutations in the similar fashion to its epithelial counterpart; its genetic stability may make them more sensitive to chemotherapeutic agents. Multiple targets have been suggested as proposed therapies to different aspects of stellate cell differentiation and interaction, (*Gonda et al*, 2009); however, their efficacy has not been validated. As yet very little drug sensitivity data exists for PDA models and none for the stellate cells at all.

High Throughput Screening has never been done on PDA cell lines and pancreatic stellate cells and this is the first attempt to profile this group of cells using a large drug library with the common chemotherapeutic agents currently being used. Among the compounds identified in this screen were, heat shock protein inhibitors, Pi3 kinase inhibitors**,** BCR-ABL/Src inhibitors, DNA intercalators, CDK inhibitors, DNA repair inhibitors, microtubule suppressors, and mTOR inhibitors.

The stellate cells appeared more responsive to the drugs in the compound library compared to the PDA cell lines. This may be due to the fact that they have no genetic homozygous changes that may convey the degree of resistance seen in their PDA counterparts. They may have heterozygous or epigenetic changes but their behaviour in the drug library suggest that thus far these cells are responsive. This sensitivity may favour them as potential targets for therapeutic management of this disease.

Although it is not yet possible to make definitive statements about a particular drug being a good candidate for treatment, the findings from the HTS screens performed can highlight new possible drugs such as Dasantinib, which may be useful in combination with Gemcitabine and Paclitaxel in the management of pancreatic cancer. This data serves as a starting point to dissect drug sensitivity in this very hard to treat subtype of cancer.

The findings of this drug screen have identified compounds to that lead to a 50% or more cell death as well as those to which there is no response. This panel of cell lines have displayed a limited cell death to some of the more commonly used chemotherapeutic agents in pancreatic cancer such as Gemcitabine. This may indeed be linked to the genetic changes in the PDAC models however there is currently insufficient data to corroborate this. There were, however, varying degrees of sensitivity in these cell lines, which may suggest that PDAC may not necessarily be inherently chemoresistant.

Chapter 7 - Future work

A) Drug screen of co-cultured stellate and epithelial cells

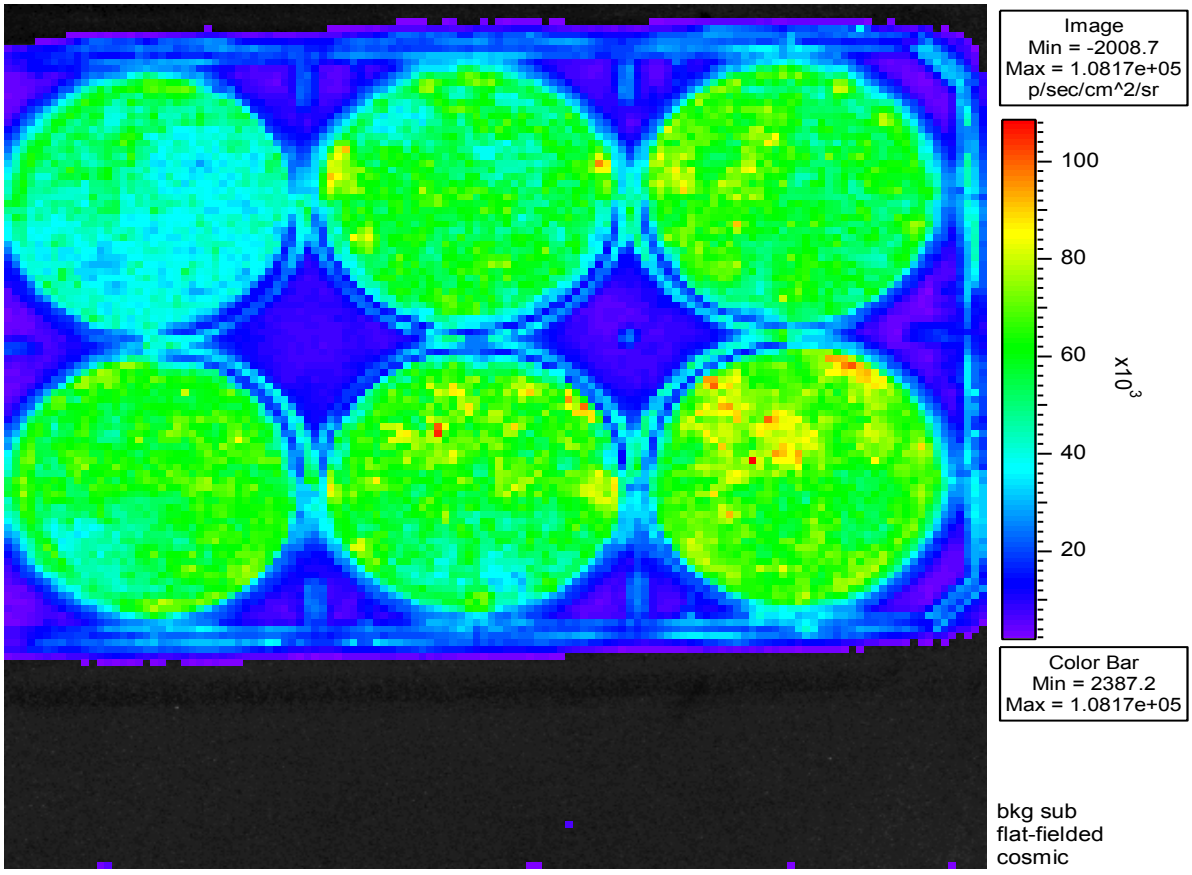
This is currently underway pending successful co-transfection of both epithelial and stellate lines with the appropriate bioluminescent markers. It is believed that co-cultures can be used to study cancer cell interactions with the stromal environment to help elucidate the role of stromal variation in tumour types. I believe this can be extrapolated to include the role that these stromal fibroblast play in conferring chemoresistance to these cancer cells and to what degree.

Development of bioluminescent markers for PDA cell lines and stellate cells

As described in chapter 2. The bioluminescent marker Renilla and firefly luciferase were constructed prior to transfection of the cell lines. The PDA cell line MiaPaCa-2 was the only cell line to successfully be transfected with the bioluminescent markers and it has been shown that the cells perform in a same manner as the parent cell line. In order to successfully complete this procedure however, a more successful, less cumbersome method of developing a marker is underway in order to transfect all lines involved. Dr Claus Jorgensen and his team at ICR are undertaking this.

Plasmid Transfection

Plasmid transfection was done using the TransIT®-2020 Transfection Reagent and Protocol. The cell lines were cultured 24 hours prior to transfection in 6 well plates. Cells were plated at $6x10^5$ in a volume of 2.5ml per well and incubated overnight at 37ºC and 5% humidified CO_2. Immediately prior to transfection the TransIT-2020 Reagent: DNA complex was prepared. For the 6 well plate used, 250 µl of Opti-MEM I Reduced-Serum Medium, 2.5µg of Plasmid DNA (Firefly luciferase) and 7.5µl of TransIT-2020 Reagent was mixed to a 2.5ml volume per well. The serum free media and plasmid DNA stock were mixed together by gentle pipetting. *Trans*IT-2020 Reagent was added to this mixture and mixed. This was left to form complexes for 15 to 30 minutes. The complex was added drop wise to each well and gentle rocking was used for even distribution. The cells were incubated for 72 hours and assayed for successful transfection.



Click # HK20111019154301
19 Oct 2011 15:43:13
Bin:HS (8), FOV12, f1, 10m
Filter: Open
Camera: IVIS 143, DW434

Series: Firefly Luc
Experiment:
Label: 48 hours post TransIT
Comment:
Analysis Comment:

The picture above shows the plasmid transfection with Firefly luciferase. Successful transfection of more than 80% of the epithelial cell line was seen. Based on the colour bar and above, the presence of green or above indicates good transfection.

Co-culture of epithelial and stellate cells

The identical plate 10 screen will be performed on bioluminescent marked stellate and epithelial cell lines as described above. Cells will be marked with either Firefly or Renilla luciferase and co-cultured in a 1:1 ratio of PDA to stellate cell onto the 384 well plate, maintaining the total cell count to 1000 cells per well. After 24 hours these cells were subjected to plate 10 screening as previously described and data analysed accordingly.

In vivo experiments

Orthotopic mouse models of carcinoma progression are well suited to the rapid preclinical testing of potential therapies. A xenograft model of PDA and stellate cell cells will be set up in nude mice, (BALB/$c^{nu/nu}$). Twenty four nude mice will be injected with different ratios of cancer to stellate cells. Each limb of 6 nude mice injected with a stellate cell: tumour cell ratio of 0:1, 1:1, 2:1 and 4:1 respectively with total cell count of $1X10^6$ cells per mouse. The samples will be injected in 50µl of PBS and checked twice weekly and tumours weighed and reviewed three times a week. The tumours will be excised at 12 to 15mm and sent for staining. Following the initial pilot study, this experiment will be used to observe the pattern of tumour progression with varying ratios of stellate cell present *in vivo*.

Combination drug screens

The efficacy of anticancer drugs needs to be evaluated in the context of their ability to target stellate CAFs and metabolically uncouple fibroblasts from epithelial cancer cells. This may involve combination drug screens with drug that have shown a significant response in both cancer and stellate cell including Oxaliplatin which has been included in several drug trials but was absent from the Ashworth drug library.

B) Identification of epigenetic and heterogeneous variations in CAFs that lead to its role in tumourigenesis or chemoresistance

SNP Arrays

Single nucleotide polymorphism or SNP is a DNA sequence variation in which a single nucleotide in the genome differs between paired chromosomes in an individual and usually two alleles are involved. As mentioned previously, this study thus far shows no CNV, i.e., no homozygous deletions. This does not rule out epigenetic changes or a heterogeneous population of cells. Normal tumours have a 50% decrease in one of the alleles due to a possible contaminated normal. Using SNP 6 Arrays we can look for a pure population of active fibroblasts and review regions with loss of heterozygosity or aberrations that do not necessarily result in copy number variations but may have aetiological significance in carcinogenesis or chemosensitivity. SNP will allow the review of that which is copy neutral and homozygous neutral. i.e. the silent deletion of one allele and its replacement with a duplicate copy of its neighbouring allele.

Micro RNA

MicroRNA has a role in gene activation. This will need to be performed on prospective samples for fresh frozen tissue including miRNAs such as Mir-21.

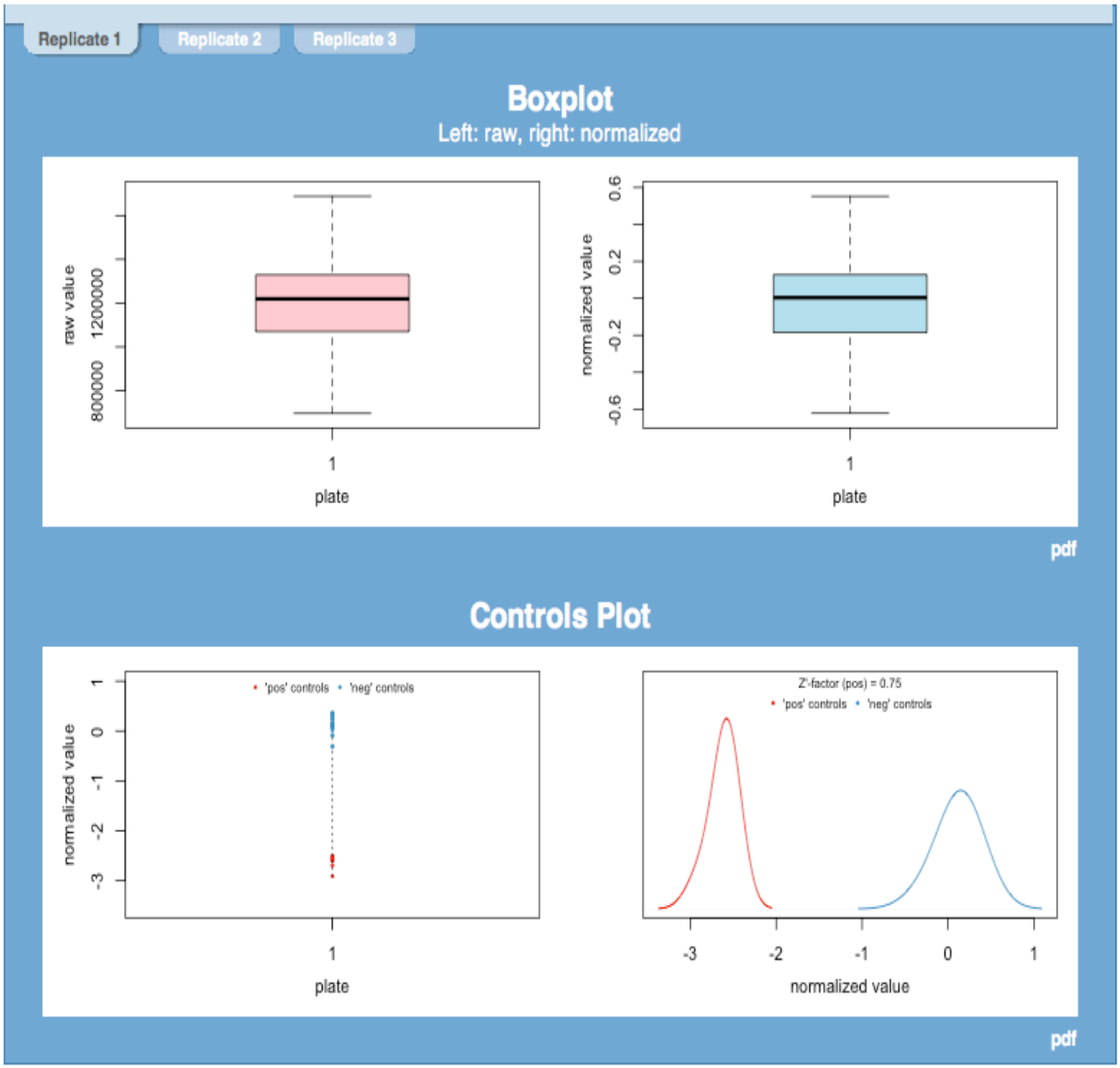
The integrity of the stromal reaction and its ability to effect a response

The question can be answered with the use of in vivo mouse experiments. They already grow in vitro and the immortalised stellate multiply rapidly in vitro. This data will be compared to studies that suggest that CAFs are unable to clone

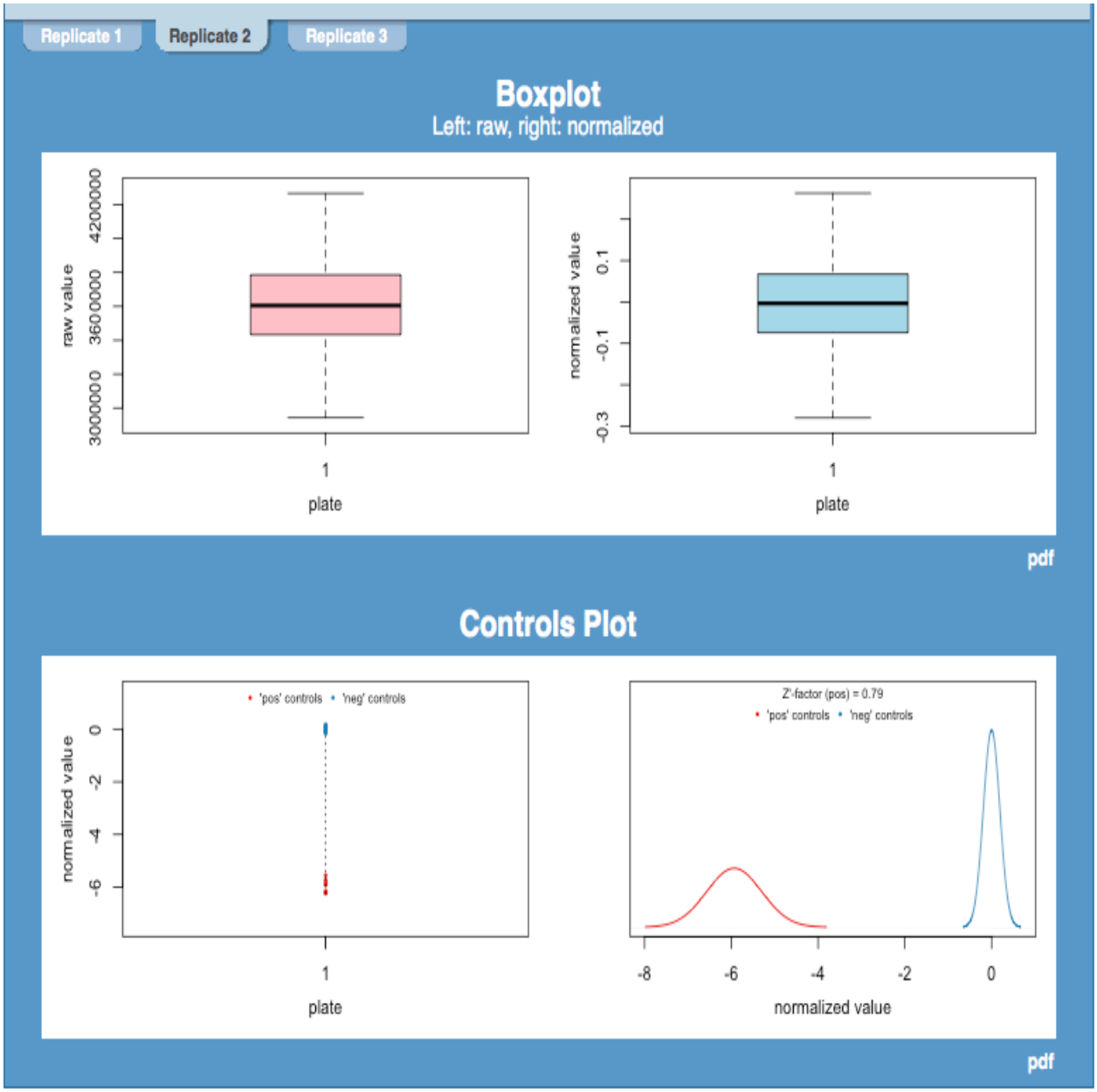
Appendix 1

Quality control z factor scores for cell lines

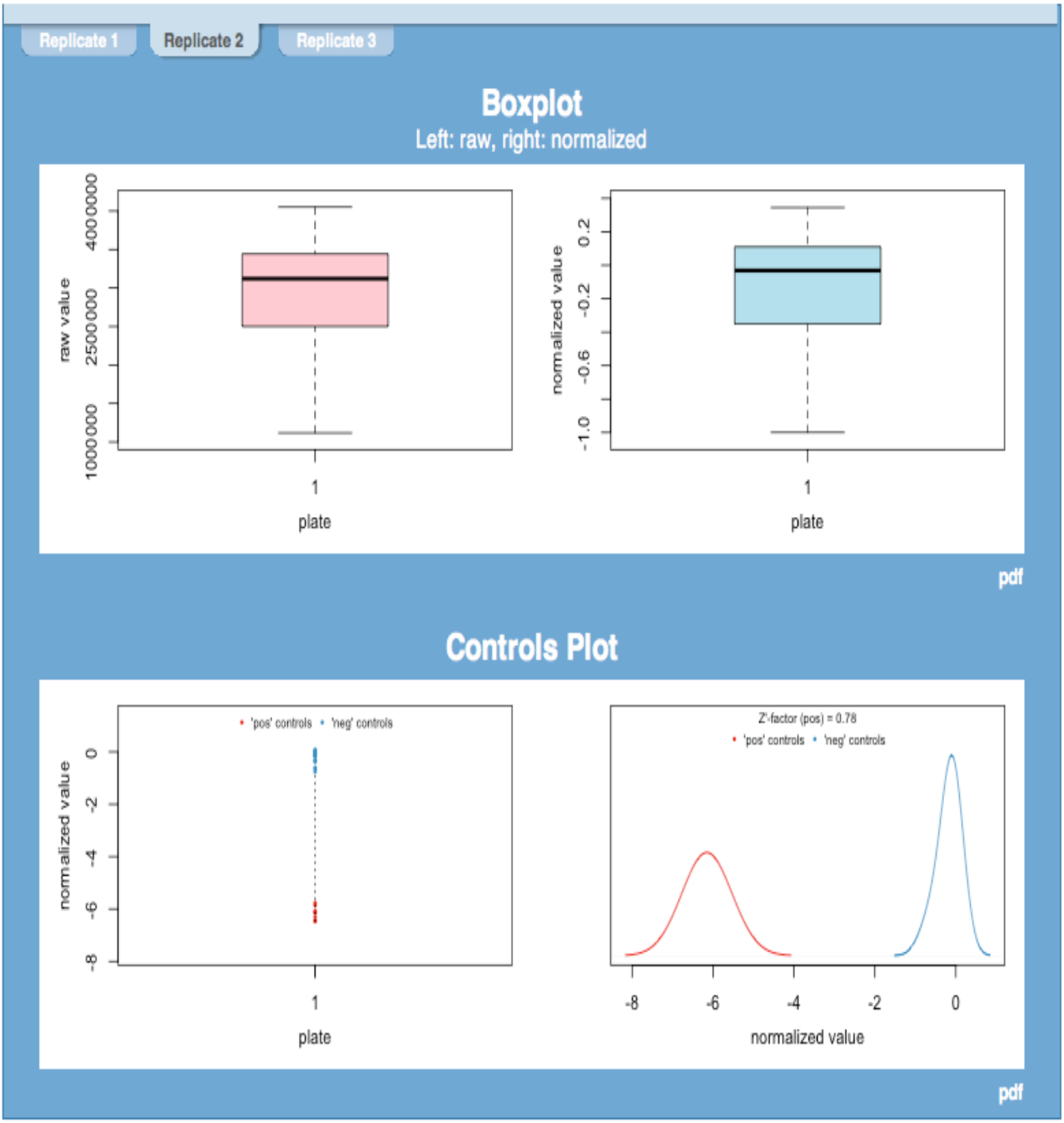
ASPC1 z factor score: 0.75



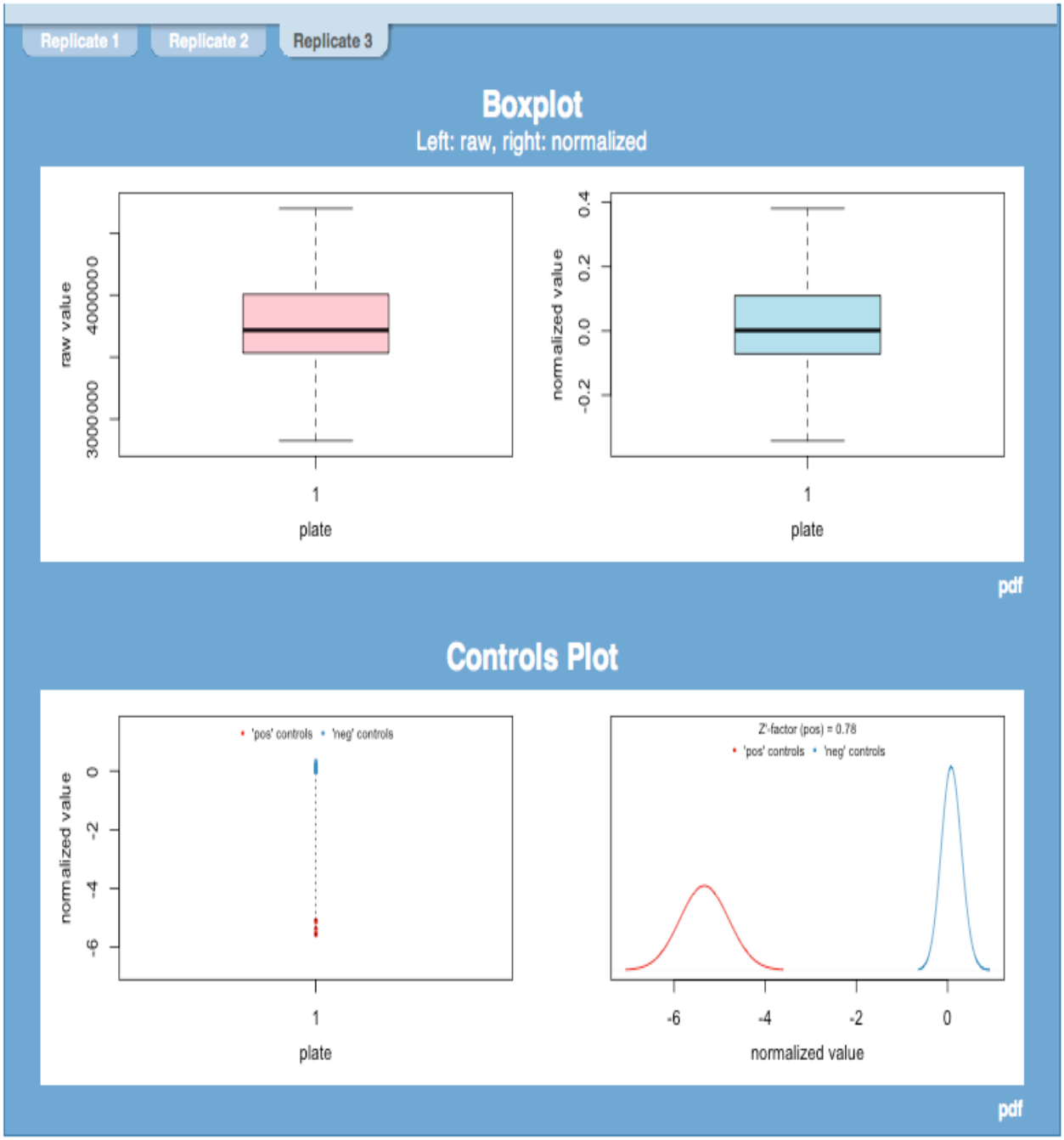
HPAC z factor score: 0.79



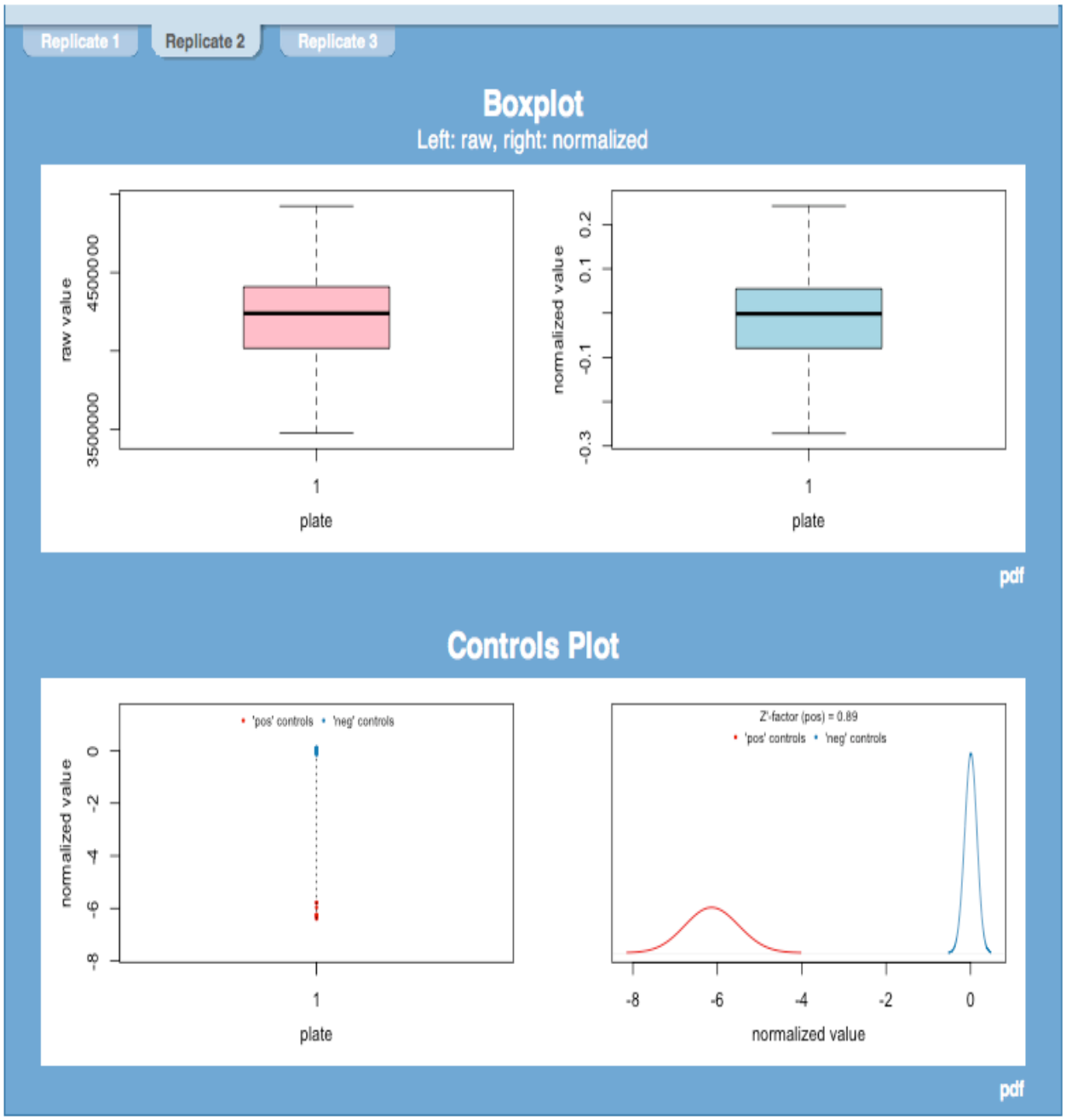
PANC1 z factor score: 0.78



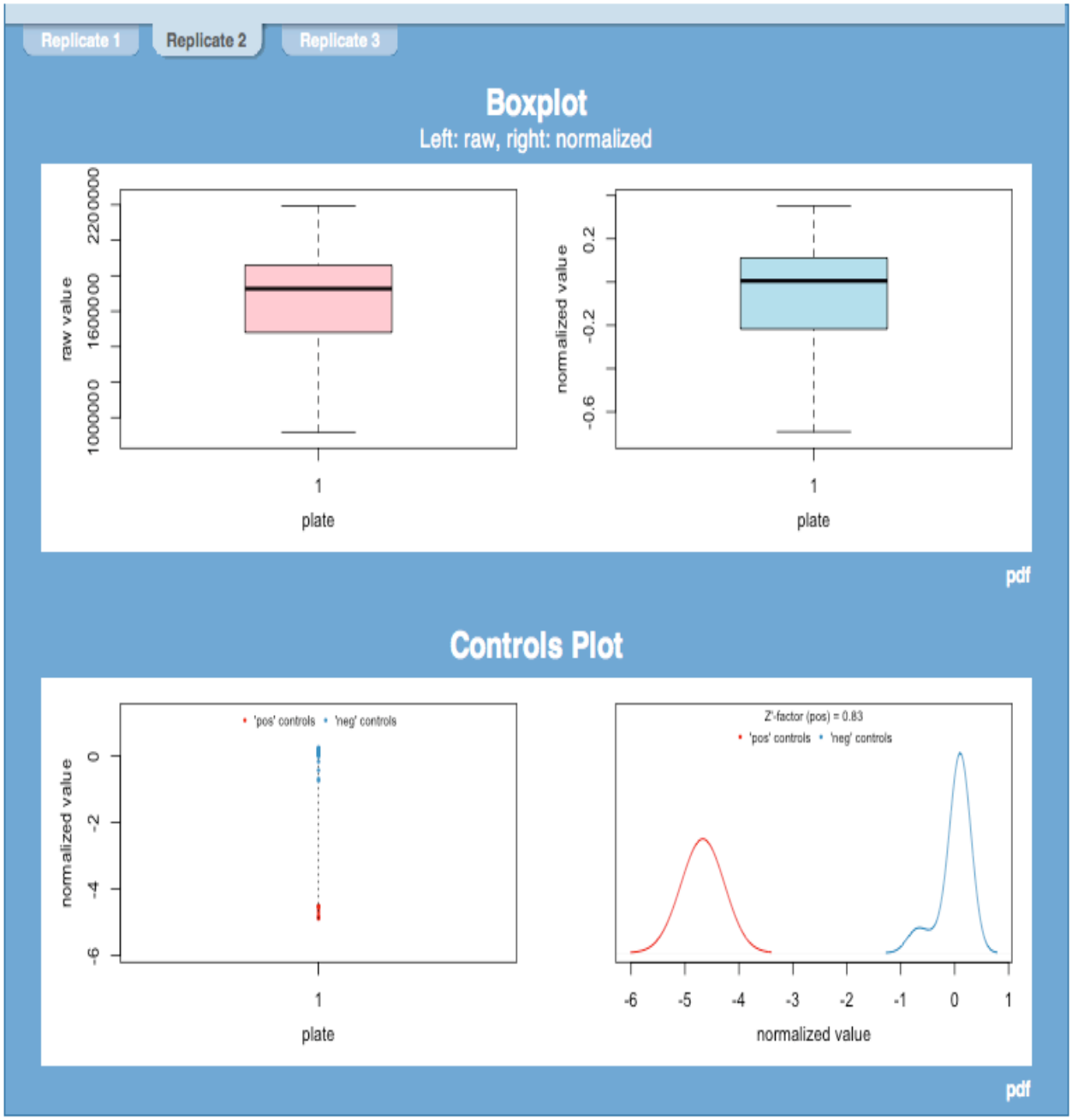
PL5 z factor score= 0.78



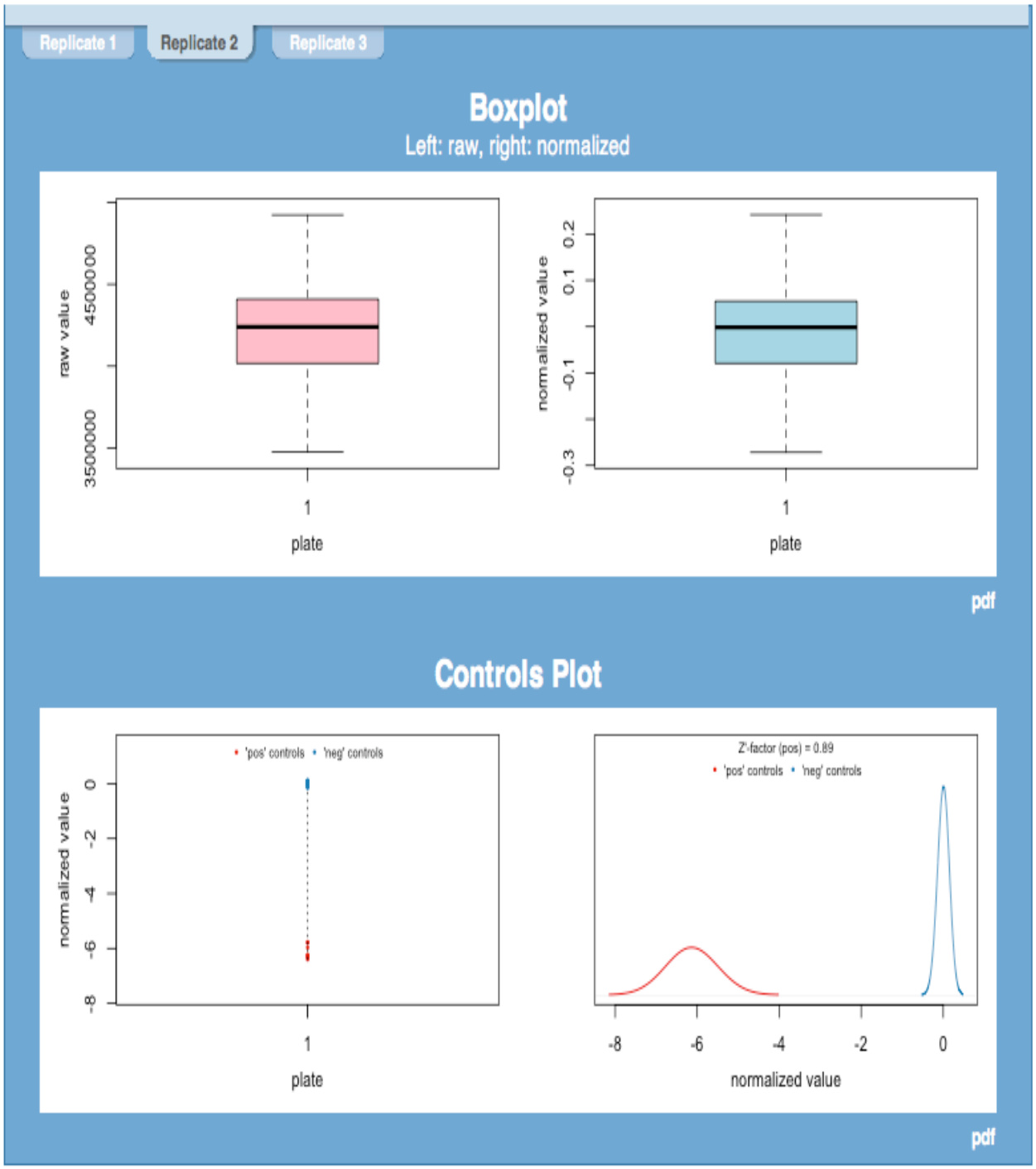
MiaPaCa2 z factor score =0.89



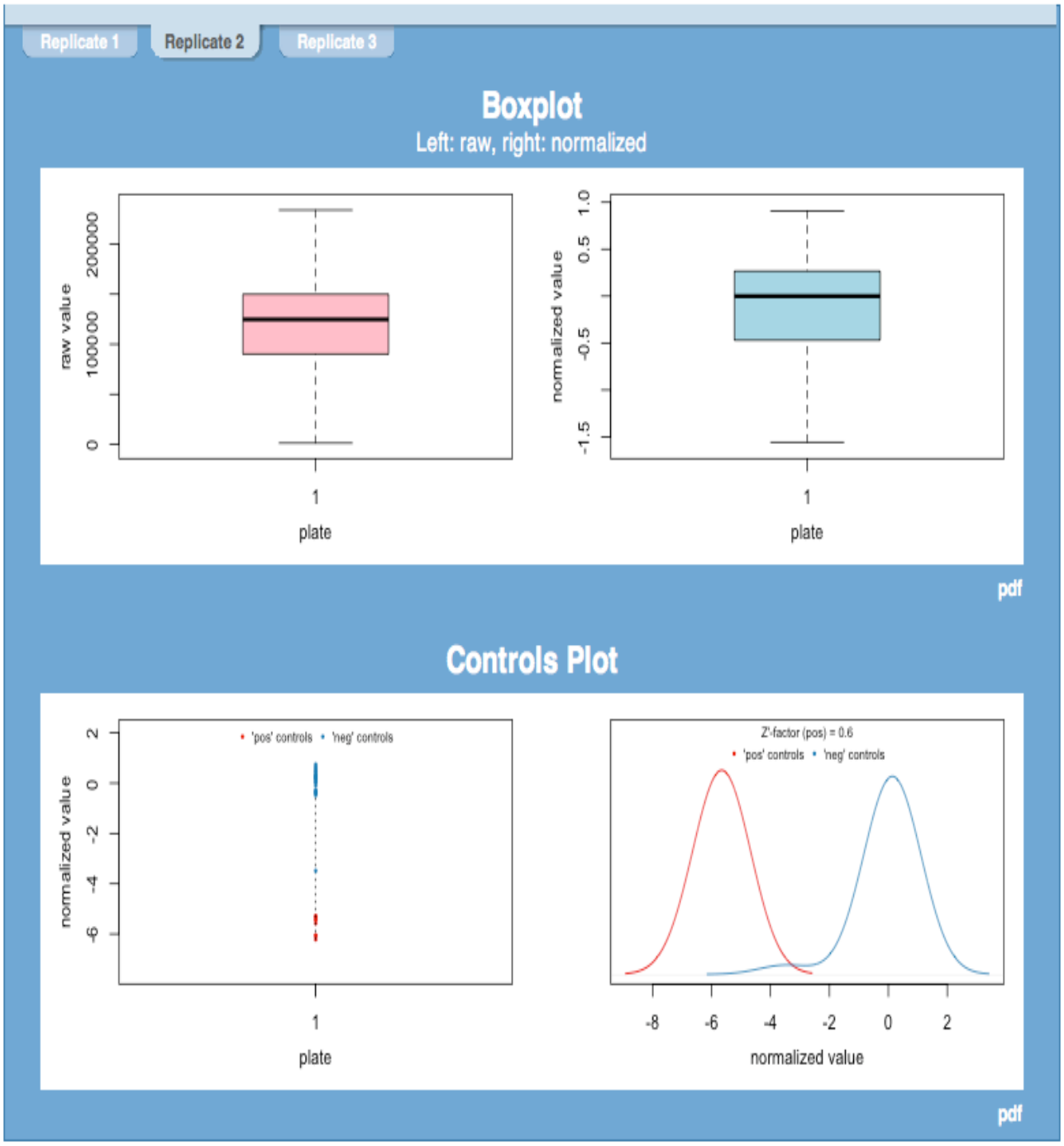
PL45 z factor score= 0.83



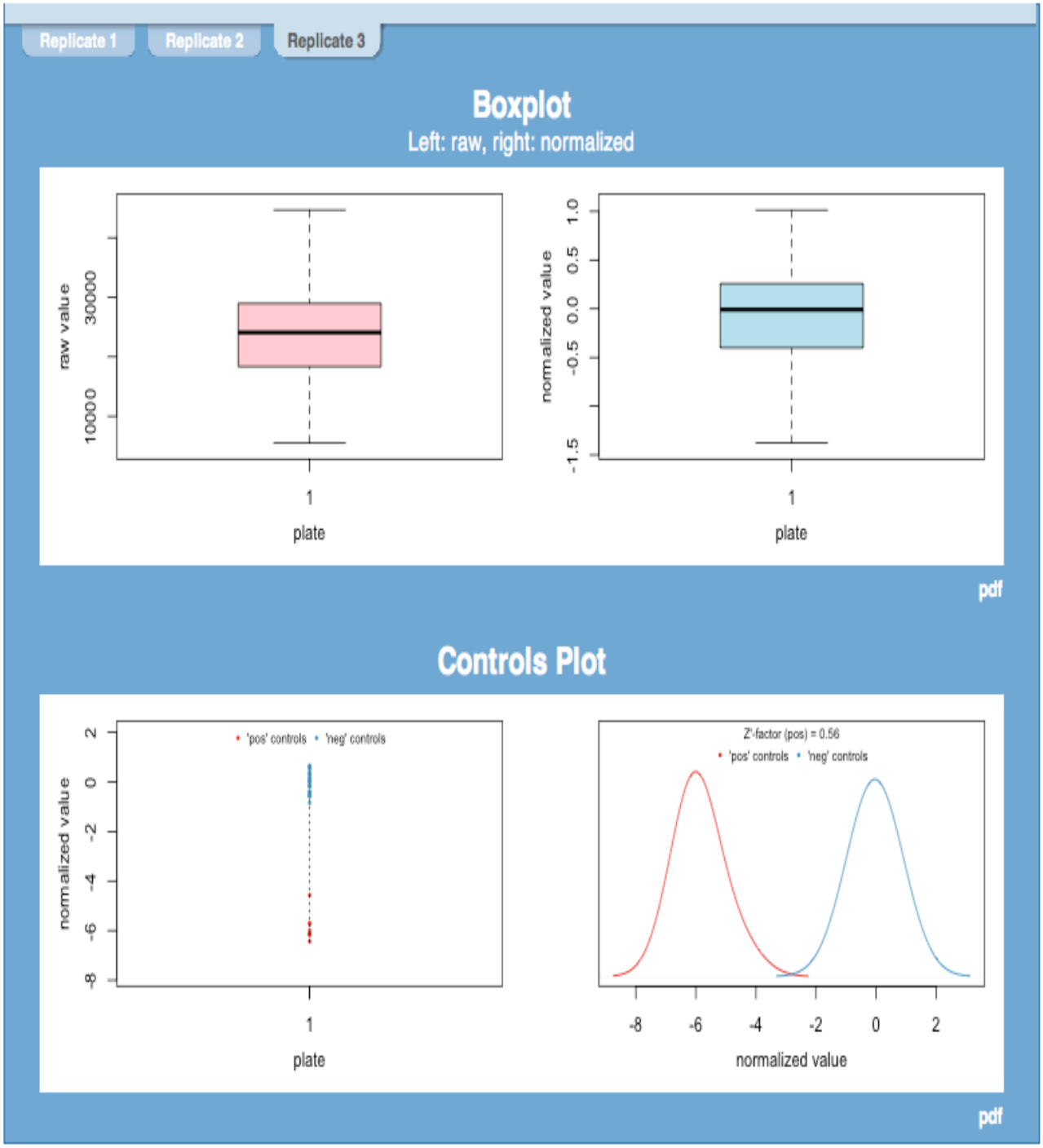
MiaPaCa2 z factor score = 0.89



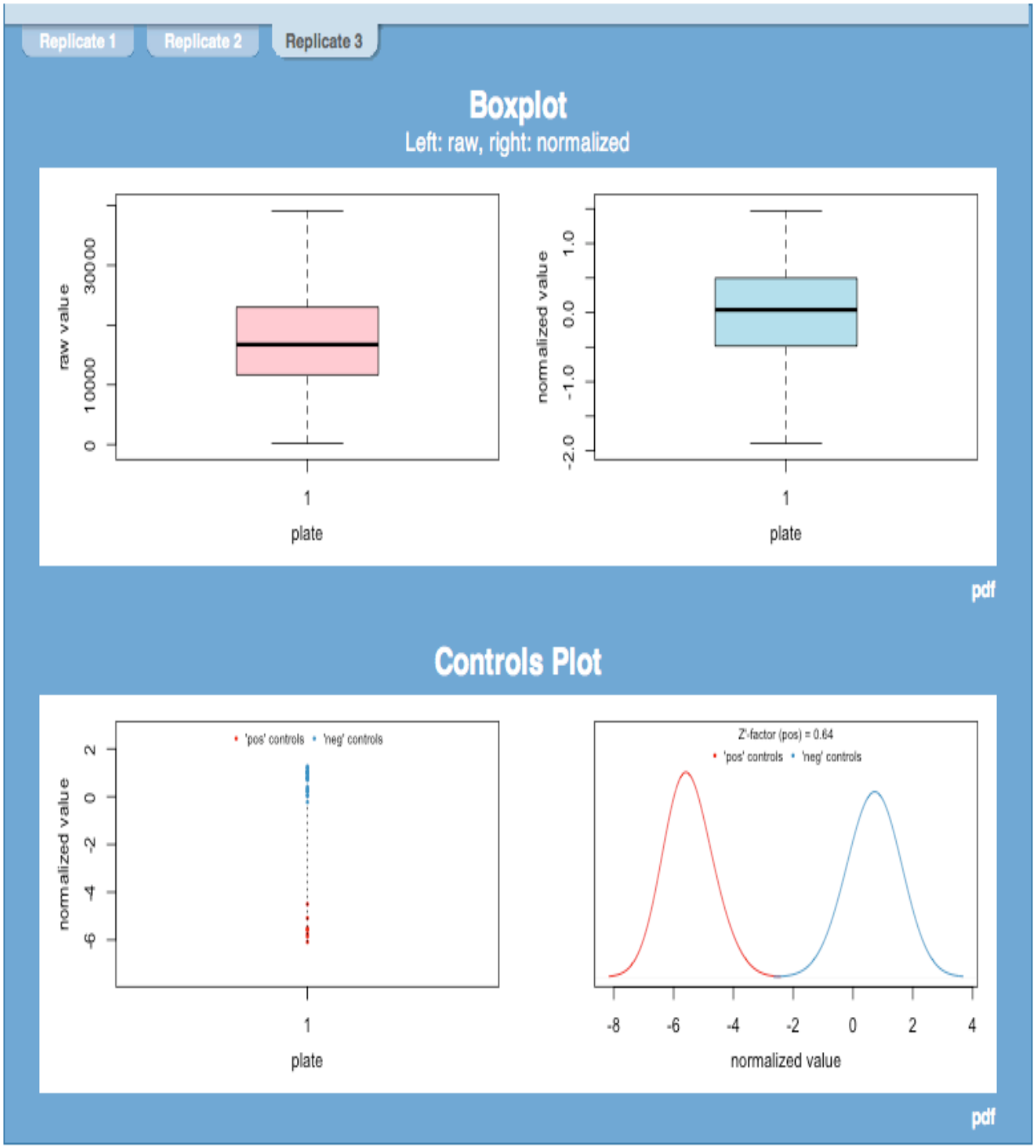
MiaPaCa2RLuc z factor score = 0.60



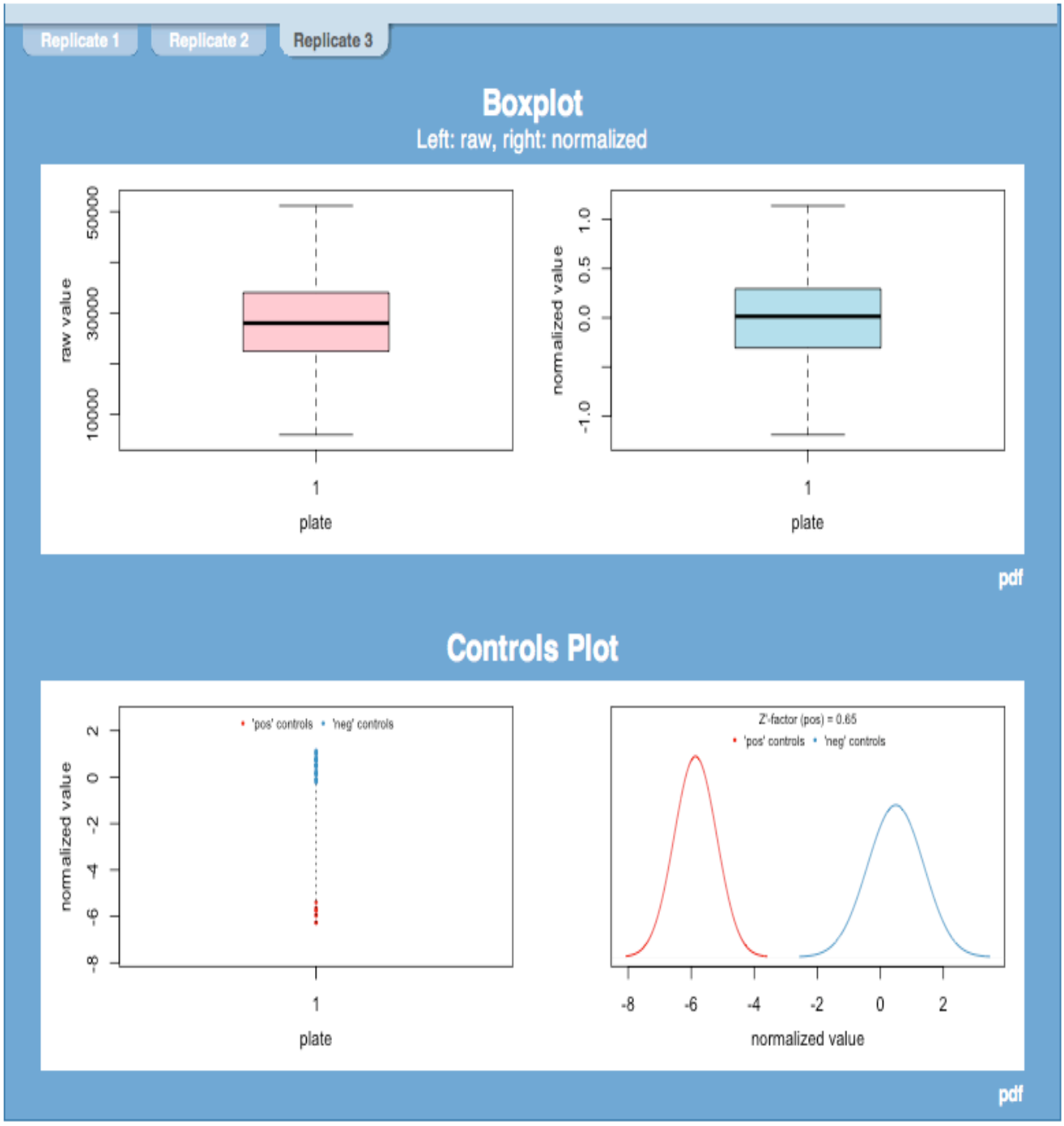
PF3 z factor score: 0.56



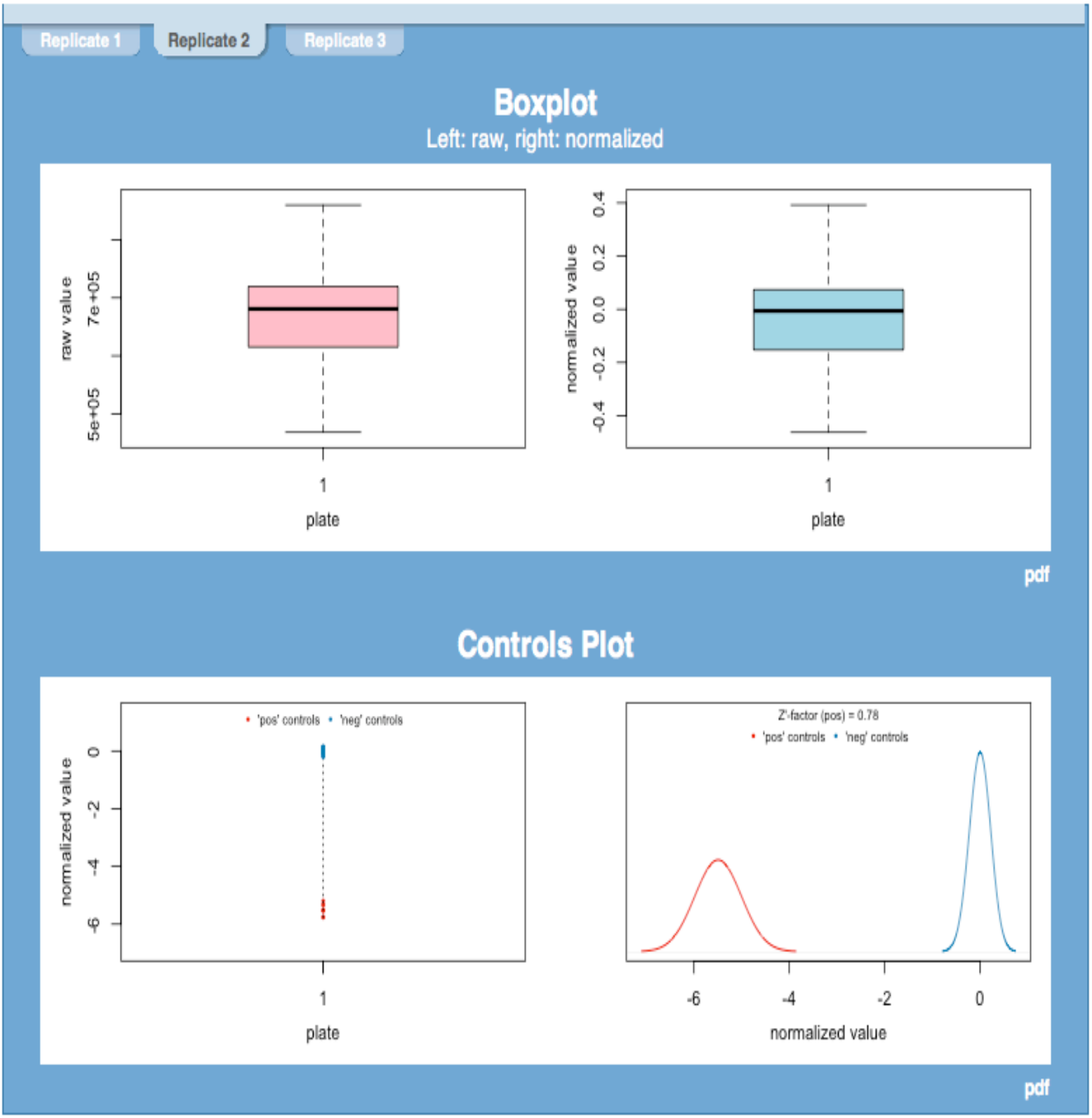
PF18 z factor score: 0.64



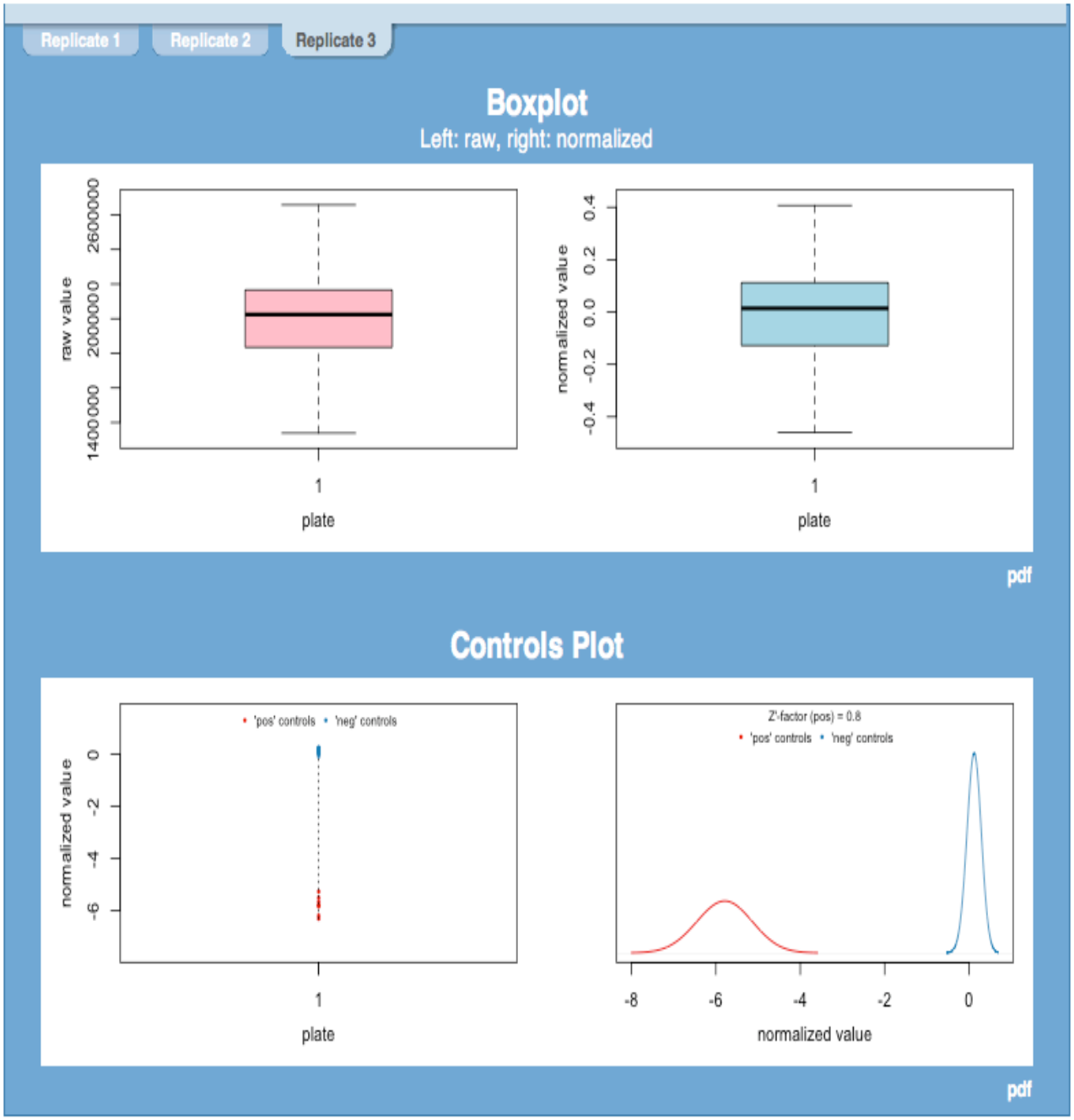
PF20 z factor score = 0.65



Stellate screen 1: z factor score = 0.78



Stellate screen 2: z factor = 0.8



References

1. Abou-Alfa GK, Letourneau R, Harker G, Modiano M, Hurwitz H, Tchekmedyian NS, Feit K, Ackerman J, De Jager RL, Eckhardt SG, O'Reilly EM. Randomized phase III study of exatecan and gemcitabine compared with gemcitabine alone in untreated advanced pancreatic cancer. J Clin Oncol. 2006 Sep 20; 24(27):4441-7.

2. Allinen M, Beroukhim R, Cai L, Brennan C, Lahti-Domenici J, Huang H, et al. Molecular characterization of the tumour microenvironment in breast cancer. Cancer Cell 2004 Jul; 6(1):17-32.

3. Allison DC, Bose KK, Hruban RH, Piantadosi S, Dooley WC, Boitnott JK, Cameron JL. Pancreatic cancer cell DNA content correlates with long-term survival after pancreatoduodenectomy. Ann Surg. 1991 Dec; 214(6):648-56.

4. Ambros, V. & Horvitz, H. R. Heterochronic mutants of the nematode Caenorhabditis elegans. Science 226, 409–-416 (1984).

5. Anderson KE, Mack T, Silverman D. Cancer of the pancreas. In: Schottenfeld D, Fraumeni JF Jr. *Cancer Epidemiology and Prevention*. 3rd Ed. New York: Oxford University Press; 2006.

6. Apte, M.V., P.S. Haber, T.L. Applegate, I.D. Norton, G.W. McCaughan, M.A. Korsten, R.C. Pirola, and J.S. Wilson, Periacinar stellate shaped cells in rat pancreas: identification, isolation, and culture. Gut, 1998. **43**(1): p. 128-33.

7. Armstrong T, Packham G, Murphy LB, Bateman AC, Conti JA, Fine DR, et al. Type I collagen promotes the malignant phenotype of pancreatic ductal adenocarcinoma. Clin Cancer Res 2004 Nov 1; 10(21):7427-37.

8. AsanoT, YaoY, ZhuJ, LiD, AbbruzzeseJL, Reddy SA. The PI 3-kinase/Akt signaling pathway is activated due to aberrant Pten expression and targets transcription factors NF-nB and c-Myc in pancreatic cancer cells. Oncogene 2004; 23:8571^80.

9. Azorsa DO, Gonzales IM, Basu GD, Choudhary A, Arora S, Bisanz KM, Kiefer JA, Henderson MC, Trent JM, Von Hoff DD, Mousses S. Synthetic lethal RNAi screening identifies sensitizing targets for gemcitabine therapy in pancreatic cancer. JTransl Med. 2009 Jun 11;7:43

10. Bachem, M.G., E. Schneider, H. Gross, H. Weidenbach, R.M. Schmid, A. Menke, M. Siech, H. Beger, A. Grunert, and G. Adler, Identification, culture, and characterization of pancreatic stellate cells in rats and humans. Gastroenterology, 1998. **115**(2): p. 421-32.

11. Bailey JM, Swanson BJ, Hamada T, Eggers JP, Singh PK, Caffery T, OuelletteM, Hollingsworth.MA.Sonic hedgehog promotes desmoplasia in pan creatic cancer. Clinical Cancer Res. 2008 Oct 1; 14(19):5995-6004.

12. Bartel DP. MicroRNAs: genomics, biogenesis, mechanism, and function. *Cell*. 2004;116:281-297.

13. Al B. Benson III, MD, Robert J. Myerson, MD, PHD, and Aaron R. Sasson, MD Pancreatic, Neuroendocrine GI, and Adrenal Cancers , cancer management 14th edition, 28 October 2011

14. Berlin JD, Catalano P, Thomas JP, Kugler JW, Haller DG, Benson AB 3rd. Phase III study of gemcitabine in combination with fluorouracil versus Gemcitabine alone in patients with advanced pancreatic carcinoma: Eastern Cooperative Oncology Group Trial E2297. J Clin Oncol. 2002 Aug 1; 20(15):3270-5.

15. [Best Evidence] Bernhard J, Dietrich D, Scheithauer W, Gerber D, Bodoky G, Ruhstaller T, et al. Clinical benefit and quality of life in patients with advanced pancreatic cancer receiving Gemcitabine plus Capecitabine versus Gemcitabine alone: a randomized multicenter phase III clinical trial--SAKK 44/00-CECOG/PAN.1.3.001. *J Clin Oncol*. Aug 1 2008; 26(22):3695-701.

16. Bhowmick NA, Neilson EG, Moses HL, Stromal fibroblasts in cancer initiation and progression. Nature 2004; 432:332-7

17. Bhowmick[2] NA, Chytil A, Plieth D, Gorska AE, Dumont N, Shappell S, Washington MK, Neilson EG, Moses HL (2004) TGF-beta signaling in fibroblasts modulates the oncogenic potential of adjacent epithelia. Science 303:848–851

18. Biankin AV, Waddell N, Kassahn KS, Gingras MC, Muthuswamy LB, Johns AL, Miller, DK, Wilson PJ, Patch AM, Wu J, Chang DK, Cowley MJ, Gardiner BB, Song S, Harliwong I, Idrisoglu S, Nourse C, Nourbakhsh E, Manning S, Wani S, Gongora M, Pajic M, Scarlett CJ, Gill AJ, Pinho AV, Rooman I, Anderson M, Holmes O, Leonard C, Taylor D, Wood S, Xu Q, Nones K, Fink JL, Christ A, Bruxner T, Cloonan N, Kolle G, Newell F, Pinese M, Mead RS, Humphris JL, Kaplan W, Jones MD, Colvin EK, Nagrial AM, Humphrey ES, Chou A, Chin VT, Chantrill LA, Mawson A, Samra JS, Kench JG, Lovell JA, Daly RJ, Merrett ND,

Toon C, Epari K, Nguyen NQ, Barbour A, Zeps N; Australian Pancreatic Cancer Genome Initiative, Kakkar N, Zhao F, Wu YQ, Wang M, Muzny DM, Fisher WE, Brunicardi FC, Hodges SE, Reid JG, Drummond J, Chang K, Han Y, Lewis LR, Dinh H, Buhay CJ, Beck T, Timms L, Sam M, Begley K, Brown A, Pai D, Panchal A, Buchner N, De Borja R, Denroche RE, Yung CK, Serra S, Onetto N, Mukhopadhyay D, Tsao MS, Shaw PA, Petersen GM, Gallinger S, Hruban RH, Maitra A, Iacobuzio-Donahue CA, Schulick RD, Wolfgang CL, Morgan RA, Lawlor RT, Capelli P, Corbo V, Scardoni M, Tortora G, Tempero MA, Mann KM, Jenkins NA, Perez-Mancera PA, Adams DJ, Largaespada DA, Wessels LF, Rust AG, Stein LD, Tuveson DA, Copeland NG, Musgrove EA, Scarpa A, Eshleman JR, Hudson TJ, Sutherland RL, Wheeler DA,Pearson JV, McPherson JD, Gibbs RA, Grimmond SM. Pancreatic cancer genomes reveal aberrations in axon guidance pathway genes. Nature. 2012 Nov 15; 491(7424):399-405.

19. Binkley CE, Zhang L, Greenson JK, Giordano TJ, Kuick R, Misek D, et al. The molecular basis of pancreatic fibrosis: common stromal gene expression in chronic pancreatitis and pancreatic adenocarcinoma.1. Pancreas 2004 Nov; 29(4):254-63.

20. Blackstock AW, Lightfoot H, Case LD, Tepper JE, Mukherji SK, Mitchell BS, Swarts SG, Hess SM. Tumour uptake and elimination of 2',2'-difluoro-2'-deoxycytidine (gemcitabine) after deoxycytidine kinase gene transfer: correlation with in vivo tumour response. Clin Cancer Res. 2001 Oct; 7(10):3263-8.

21. Bloomston M, Frankel WL, Petrocca F, Volinia S, Alder H, Hagan JP, Liu CG,Bhatt D, Taccioli C, Croce CM. MicroRNA expression patterns to differentiate pancreatic adenocarcinoma from normal pancreas and chronic pancreatitis. JAMA. 2007 May 2;297(17):1901-8

22. Boersma, B.J., M. Reimers, M. Yi, J.A. Ludwig, B.T. Luke, R.M. Stephens, H.G. Yfantis, D.H. Lee, J.N. Weinstein, and S. Ambs, A stromal gene signature associated with inflammatory breast cancer. Int J Cancer, 2008. 122(6): p. 1324-32.

23. Bondar VM, Sweeney-Gotsch B, Andreeff M, Mills GB, McConkey DJ. Inhibition of the phosphatidylinositol 3¶-kinase-AKT pathway induces apoptosis in pancreatic carcinoma cells in vitro and in vivo. Mol CancerTher 2002; 1:989^97.

24. Bramhall, S. R., Rosemurgy, A., Brown, P. D., Bowry, C. & Buckles, J. A. Marimastat as firstline therapy for patients with unresectable pancreatic cancer: A randomized trial. *J. Clin. Oncol*. 19, 3447–3455 (2001).

25. Brentnall TA, Lai LA, Coleman J, Bronner MP, Pan S, Chen R, Arousal of cancer-associated stroma: overexpression of palladin activates fibroblasts to promote tumour invasion. PLoS One. 2012; 7(1):e30219. Epub 2012 Jan 23.

26. British Society of Gastroenterology (2012), Guidelines for the management of gastroenteropancreatic neuroendocrine (including carcinoid) tumours (NETs),

27. Bronisz A, Godlewski J, Wallace JA, Merchant AS, Nowicki MO, Mathsyaraja H, Srinivasan R, Trimboli AJ, Martin CK, Li F, Yu L, Fernandez SA, Pecot T, Rosol TJ, Cory S, Hallett M, Park M, Piper MG, Marsh CB, Yee LD, Jimenez RE, Nuovo G, Lawler SE, Chiocca EA, Leone G, Ostrowski MC (2011)

Reprogramming of the tumour microenvironment by stromal PTEN-regulated miR- 320. Nat Cell Biol 14:159–167

28. Buchholz, M., H.A. Kestler, K. Holzmann, V. Ellenrieder, W. Schneiderhan, M. Siech, G. Adler, M.G. Bachem, and T.M. Gress, Transcriptome analysis of human hepatic and pancreatic stellate cells: organ-specific variations of a common transcriptional phenotype. J Mol Med, 2005. **83**(10): p. 795-805.

29. Buettner R, Mora LB, Jove R. Activated STAT signaling in human tumours provides novel molecular targets for therapeutic intervention. Clin Cancer Res. 2002; 8:945–954.

30. Burris HA 3rd, Moore MJ, Andersen J, Green MR, Rothenberg ML, Modiano MR, Cripps MC, Portenoy RK, Storniolo AM, Tarassoff P, Nelson R, Dorr FA, Stephens CD, Von Hoff DD. Improvements in survival and clinical benefit with gemcitabine as first-line therapy for patients with advanced pancreas cancer: a randomized trial. J Clin Oncol. 1997 Jun;15(6):2403-13

31. Campbell I, Polyak, K, HAviv, I. Clonal mutations in the Cancer-Associated Fibroblast: The Case against Genetic Coevolution .Cancer Res 2009; 69 (17).Sept 1 2009

32. Cat B, Stuhlmann D, Steinbrenner H, Alili L, Holtkotter O, Sies H, et al. Enhancement of tumour invasion depends on transdifferentiation of skin fibroblasts mediated by reactive oxygen species. J Cell Sci 2006 Jul 1; 119(Pt 13):2727-38.

33. Carpelan-Holmstrom M, Nordling S, Pukkala E, Sankila R, Luttges J, Kloppel G, et al. Does anyone survive pancreatic ductal adenocarcinoma? A nationwide

study re-evaluating the data of the Finnish cancer registry 4. Gut 2005 Mar; 54(3):385-7.

34. Casbas-Hernandez P Gene expression analysis of in vitro cocultures to study interactions between breast epithelium and stroma.

35. Casey, T., J. Bond, S. Tighe, T. Hunter, L. Lintault, O. Patel, J. Eneman, A. Crocker, J. White, J. Tessitore, M. Stanley, S. Harlow, D. Weaver, H. Muss, and K. Plaut, Molecular signatures suggest a major role for stromal cells in development of invasive breast cancer.

36. Colucci, G. *et al.* A randomized trial of gemcitabine (G) versus G plus cisplatin in chemotherapynaive advanced pancreati c adenocarcinoma: The GIP1 *(Gruppo Italiano Pancreas— GOIM/GISCAD/GOIRC)* study. *J. Clin. Oncol*. 27 (Suppl. 15), a4504 (2009).

37. Conroy T, Desseigne F, Ychou M, et al. FOLFIRINOX versus Gemcitabine for metastatic pancreatic cancer. *N Engl J Med*. May 12 2011;364(19):1817-25

38. Suzan Commandeur, Suet Huy Ho, Frank R. de Gruijl, Rein Willemze, Cornelis P. Tensen, Abdoelwaheb El Ghalbzouri, Functional characterization of cancer-associated fibroblasts of human cutaneous squamous cell carcinoma. *Experimental Dermatology Volume 20, Issue 9,* pages 737–742, September 2011

39. Corver WE, Ter Haar NT, Fleuren GJ, Oosting J. Cervical carcinoma-associated fibroblasts are DNA diploid and do not show evidence for somatic genetic alterations; Cell Oncol (Dordr). 2011 Dec;34(6):553-63

40. Cunningham, D. *et al.* Phase III randomized comparison of gemcitabine (GEM) versus gemcitabine plus capecitabine (GEMCA P) in patients with advanced pancreatic cancer [abstract]. *Eur. J. Cancer* 3 (Suppl. 3), a12 (2005).

41. Cunningham D, Chau I, Stocken DD, Valle JW, Smith D, Steward W, et al. Phase III randomized comparison of Gemcitabine versus Gemcitabine plus capecitabine in patients with advanced pancreatic cancer. *J Clin Oncol*. Nov 20 2009; 27(33):5513-8.

42. Dalgleish A. G., J. B. Bartlett, C. Galustian, R. A. Fryer; Molecular mechanisms underlying Gemcitabine resistance in pancreatic cancer and restoration of sensitivity using lenalidomide St. George's University of London, London, United Kingdom; Celgene Corporation, Summit, NJ J Clin Oncol 28, 2010 (suppl; abstr e13630)

43. Dangi-Garimella, S., Krantz, S. B., Barron, M. R., Shields, M. A., Heiferman, M. J., Grippo, P. J., Bentrem, D. J. and Munshi, H. G. (2011) Three-dimensional collagen I promotes gemcitabine resistance in pancreatic cancer through MT1-MMP-mediated expression of HMGA2. Cancer Res. **71**, 1019–1028

44. Dillhoff M, Liu J, Frankel W, Croce C, Bloomston M. MicroRNA-21 is overexpressed in pancreatic cancer and a potential predictor of survival. JGastrointest Surg. 2008 Dec;12(12):2171-6.

45. Direkze, N.C., K. Hodivala-Dilke, R. Jeffery, T. Hunt, R. Poulsom, D. Oukrif, M.R. Alison, and N.A. Wright, Bone marrow contribution to tumour-associated myofibroblasts and fibroblasts. Cancer Res, 2004. **64**(23): p. 8492-5.

46. Dubernard, G., S. Aractingi, M. Oster, R. Rouzier, M.C. Mathieu, S. Uzan, and K. Khosrotehrani, Breast cancer stroma frequently recruits fetal derived cells during pregnancy. Breast Cancer Res, 2008. **10**(1): p. R14.

47. Du Rieu MC, Torrisani J, Selves J, Al Saati T, Souque A, Dufresne M, Tsongalis GJ, Suriawinata AA, Carrère N, Buscail L, Cordelier P. MicroRNA-21 is induced early in pancreatic ductal adenocarcinoma precursor lesions. Clin Chem. 2010 Apr;56(4):603-12.

48. Duxbury MS, Ito H, Zinner MJ, Ashley SW, Whang EE. Focal adhesion kinase gene silencing promotes anoikis and suppresses metastasis of human pancreatic adenocarcinoma cells. Surgery 2004; 135:555^62.

49. Duxbury MS, Ito H, Zinner MJ, Ashley SW, Whang EE. SiRNA directed against c-Src enhances pancreatic adenocarcinoma cell Gemcitabine chemo-sensitivity. JAmColl Surg 2004; 198:953^9.

50. Duxbury MS, Ito H, Zinner MJ, Ashley SW, Whang EE. Inhibition of SRC tyrosine kinase impairs inherent and acquired Gemcitabine resistance in human pancreatic adenocarcinoma cells. Clin Cancer Res 2004; 10:2307 ^ 18.

51. Dragovich T., Rudin C. M., Thompson C. B. Signal transduction pathways that regulate cell survival and cell death. Oncogene, 17: 3207-3213, 1998

52. Dragovich , T, Erickson, R A, Pancreatic cancer, Medscape 2012

53. Erkan M, Kleeff J, Esposito I, et al. Loss of BNIP3 expression is a late event in pancreatic cancer contributing to chemo-resistance and worsened prognosis. Oncogene 2005; 24:4421^ 32.

54. Ellsworth, D.L., R.E. Ellsworth, B. Love, B. Deyarmin, S.M. Lubert, V. Mittal, and C.D. Shriver, Genomic patterns of allelic imbalance in disease free tissue adjacent to primary breast carcinomas. Breast Cancer Res Treat, 2004. **88**(2): p. 131-9.

55. Eric S. Calhoun, Jessa B. Jones, Raheela Ashfaq, Volkan Adsay, Suzanne J. Baker, Virginia Valentine,Paula M. Hempen,Werner Hilgers, Charles J. Yeo, Ralph H. Hruban, and Scott E. Kern, BRAF and FBXW7 (CDC4, FBW7, AGO, SEL10) Mutations in Distinct Subsets of Pancreatic Cancer Potential Therapeutic Targets Am J Pathol. 2003 October; 163(4): 1255–1260.

56. Farrand K, Jovanovic L, Delahunt B, et al. Loss of heterozygosity studies revisited: prior quantification of the amplifiable DNA content of archival samples improves efficiency and reliability. J Mol Diagn 2002; 4:150–8.

57. Ferrara N, Hillan KJ, Gerber HP, Novotny W. Discovery and development of bevacizumab, an anti-VEGF antibody for treating cancer**, Nat** Rev Drug Discov. 2004 May; 3(5):391-400.

58. Finak, G., N. Bertos, F. Pepin, S. Sadekova, M. Souleimanova, H. Zhao, H. Chen, G. Omeroglu, S. Meterissian, A. Omeroglu, M. Hallett, and M. Park, Stromal gene expression predicts clinical outcome in breast cancer. Nat Med, 2008. 14(5): p. 518-27.

59. Franz, M., P. Richter, C. Geyer, T. Hansen, L.D. Acuna, P. Hyckel, F.D. Bohmer, H. Kosmehl, and A. Berndt, Mesenchymal cells contribute to the synthesis and deposition of the laminin-5 gamma2 chain in the invasive front of oral squamous cell carcinoma. J Mol Histol, 2007. **38**(3): p. 183-90.

60. Fukino K, Shen L, Patocs A, Mutter GL, Eng C. Genomic instability within tumour stroma and clinicopathological characteristics of sporadic primary invasive breast carcinoma. JAMA 2007 May 16; 297(19):2103-11.

61. D. Fukumura, R. Xavier, T. Sugiura, Y. Chen, E.C. Park, N. Lu, M. Selig, G. Nielsen, T. Taksir, R.K. Jain, B. Seed, Tumour 334 N. Ferrara et al. / Biochemical and Biophysical Research Communications 333 (2005) 328–335 induction of VEGF promoter activity in stromal cells, Cell 94 (1998) 715–725.

62. Funamizu N, Okamoto A, Kamata Y, Misawa T, Uwagawa T, Gocho T, Yanaga K, Manome Y. Is the resistance of gemcitabine for pancreatic cancer settled only by overexpression of deoxycytidine kinase? Oncol Rep. 2010 Feb; 23(2):471-5.

63. Garcia-Manteiga J, Molina-Arcas M, Casado FJ, Mazo A and Pastor-Anglada M: Nucleoside transporter profiles in human pancreatic cancer cells: role of hCNT1 in 2',2,-difluorodeoxycytidine- induced cytotoxicity. Clin Cancer Res 9: 5000-5008, 2003.

64. Giovannetti E, Del Tacca M, MeyV, et al. Transcription analysis of human equilibrative nucleoside transporter- 1predicts survival in pancreas cancer patients treated with Gemcitabine. Cancer Res 2006; 66:3928^35.

65. Giovannetti E, Funel N, Peters GJ, Del Chiaro M, Erozenci LA, Vasile E, LeonLG, Pollina LE, Groen A, Falcone A, Danesi R, Campani D, Verheul HM, Boggi U. MicroRNA-21 in pancreatic cancer: correlation with clinical outcome andpharmacologic aspects underlying its role in the modulation of gemcitabineactivity. Cancer Res. 2010 Jun 1;70(11):4528-38

66. Glass, A., G. Kundt, P. Brock, R. Jaster, S. Liebe, J. Emmrich, and G. Sparmann, Delayed response toward activation stimuli in pancreatic stellate cells. Pancreas, 2006. **33**(3): p. 293-300.

67. Goetz JG, Minguet S, Navarro-Lérida I, Lazcano JJ, Samaniego R, Calvo E, Tello M, Osteso-Ibáñez T, Pellinen T, Echarri A, Cerezo A, Klein-Szanto AJ, Garcia R, Keely PJ, Sánchez-Mateos P, Cukierman E, Del Pozo MA. Biomechanical remodeling of the microenvironment by stromal caveolin-1 favours tumour invasion and metastasis. Cell. 2011 Jul 8; 146(1):148-63.

68. Gonda TA, Varro A, Wang TC, Tycko B. Molecular biology of cancer-associated fibroblasts: can these cells be targeted in anti-cancer therapy?; Semin Cell Dev Biol. 2009 Oct 16.

69. Guidelines for the management of gastroenteropancreatic neuroendocrine (including carcinoid) tumours (NETs), British Society of Gastroenterology (2012)

70. Haber, P.S., G.W. Keogh, M.V. Apte, C.S. Moran, N.L. Stewart, D.H. Crawford, R.C. Pirola, G.W. McCaughan, G.A. Ramm, and J.S. Wilson, Activation of pancreatic stellate cells in human and experimental pancreatic fibrosis. Am J Pathol, 1999. **155**(4): p. 1087-95.

71. Hahn SA, Kern SE. Molecular genetics of exocrine pancreatic neoplasms. *Surg Clin North Am*. Oct 1995;75(5):857-69

72. Hahn SA, Schutte M, Hoque AT, Moskaluk CA, da Costa LT, Rozenblum E, Weinstein CL, Fischer A, Yeo CJ, Hruban RH, Kern SE (1996) DPC4, a

candidate tumour suppressor gene at human chromosome 18q21.1. Science 271:350–353

73. Halfdanarson TR, Rubin J, Farnell MB, et al; Pancreatic endocrine neoplasms: epidemiology and prognosis of pancreatic endocrine tumours. Endocr Relat Cancer. 2008 Jun; 15(2):409-27.

74. Hall, B., M. Andreeff, and F. Marini, The participation of mesenchymal stem cells in tumour stroma formation and their application as targeted-gene delivery vehicles. Handb Exp Pharmacol, 2007(180): p. 263-83.

75. Hall, B., J. Dembinski, A.K. Sasser, M. Studeny, M. Andreeff, and F. Marini, Mesenchymal stem cells in cancer: tumour-associated fibroblasts and cell-based delivery vehicles. Int J Hematol, 2007. 86(1): p. 8-16.

76. Hanahan, D. and R.A. Weinberg, The hallmarks of cancer. Cell 2000. 100(1): p. 57-70

77. Hanley AB, Burch R. Re: The role of STAT-3 in the induction of apoptosis in pancreatic cancer cells by benzyl isothiocyanate. J Natl Cancer Inst. 2009; 101:893; author reply 893–894.

78. Hartel, M., F.F. Di Mola, A. Gardini, A. Zimmermann, P. Di Sebastiano, A. Guweidhi, P.Innocenti, T. Giese, N. Giese, M.W. Buchler, and H. Friess, Desmoplastic reaction influences pancreatic cancer growth behaviour. World J Surg, 2004. **28**(8): p. 818-25.

79. Heinemann V, Quietzsch D, Gieseler F, Gonnermann M, Schönekäs H, Rost A, Neuhaus H, Haag C, Clemens M, Heinrich B, Vehling-Kaiser U, Fuchs M,

Fleckenstein D, Gesierich W, Uthgenannt D, Einsele H, Holstege A, Hinke A, Schalhorn A, Wilkowski R. Randomized phase III trial of gemcitabine plus cisplatin compared with gemcitabine alone in advanced pancreatic cancer. J Clin Oncol. 2006 Aug 20;24(24):3946-52

80. Heinemann, V., Boeck, S., Hinke, A., Labianca, R. & Louvet, C. Meta analysis of randomized trials: Evaluation of benefit from Gemcitabine based combination chemotherapy applied in advanced pancreatic cancer. *BMC Cancer* 8, 82 (2008).

81. Herrmann, R. *et al.* Gemcitabine plus capecitabine compared with gemcitabine alone in advanced pancreatic cancer: a randomized, multicenter, phase III trial of the Swiss Group for Clinical Cancer Research and the Central European Cooperative Oncology Group. *J. Clin. Oncol.* 25, 2212–2217 (2007).

82. Hu M, Polyak K, Microenvironmental regulation of cancer development. Curr Opin Genet Dev 2008; 18:27-34

83. Hwang RF, Moore T, Arumugam T, Ramachandran V, Amos KD, Rivera A, Ji B, Evans DB, Lodgson CD, Cancer associated stromal fibroblasts promote pancreatic tumour progression. Cancer Res 2008; 68 :(3). February 1, 2008

84. Iacobuzio-Donahue, C.A., B. Ryu, R.H. Hruban, and S.E. Kern, Exploring the host desmoplastic response to pancreatic carcinoma: gene expression of stromal and neoplastic cells at the site of primary invasion. Am J Pathol, 2002. 160(1): p. 91-9.

85. Ijichi H, Chytil A, Gorska AE, Aakre ME, Bierie B, Tada M, Mohri D, Miyabayashi K, Asaoka Y, Maeda S, Ikenoue T, Tateishi K, Wright CV, Koike K, Omata M, Moses HL. Inhibiting Cxcr2 disrupts tumour-stromal interactions and improves survival in a mouse model of pancreatic ductal adenocarcinoma. J Clin Invest. 2011 Oct; 121(10):4106-17.

86. Jesnowski R, Fürst D, Ringel J, Chen Y, Schrödel A, Kleeff J, Kolb A, Schareck WD, Löhr M. Immortalization of pancreatic stellate cells as an in vitro model of pancreatic fibrosis: deactivation is induced by matrigel and N-acetylcysteine. Lab Invest. 2005 Oct;85(10):1276-91

87. Julia Brenmoehl, Sandra Nicole Miller, Claudia Hofmann, Daniela Vogl, Werner Falk, Jürgen Schölmerich, Gerhard Rogler, Transforming growth factor-β1 induces intestinal myofibroblast differentiation and modulates their migratio**n;** World J Gastroenterol 2009 March 28; 15(12): 1431-1442.

88. Johnson NA, Hamada RA, Chimera K, et al. Application of array CGH on archival formalin-fixed paraffin-embedded tissues including small numbers of micro dissected cells. Lab Invest 2006; 86:968–978.

89. Jotzu C, Alt E, Welte G, Li J, Hennessy BT, Devarajan E, Krishnappa S, Pinilla S, Droll L, Song YH. Adipose tissue-derived stem cells differentiate into carcinoma-associated fibroblast-like cells under the influence of tumour-derived factors. Anal Cell Pathol (Amst). 2010;33(2):61-79.

90. Kadera BE, Li L, Toste PA, Wu N, Adams C, Dawson DW, Donahue TR. MicroRNA-21 in pancreatic ductal adenocarcinoma tumor-associated fibroblasts promotes metastasis. PLoS One. 2013 Aug 22;8(8)

91. Karnoub, A.E., A.B. Dash, A.P. Vo, A. Sullivan, M.W. Brooks, G.W. Bell, A.L. Richardson, K. Polyak, R. Tubo, and R.A. Weinberg, Mesenchymal stem cells within tumour stroma promote breast cancer metastasis. Nature, 2007. 449(7162): p. 557-63.

92. Kalluri, R., and Neilson, E.G. 2003. Epithelial- mesenchymal transition and its implications for fibrosis. *J. Clin. Invest.* **112**:1776–1784.

93. Kalluri R, Zeisberg M. Fibroblasts in cancer. Nat Rev Cancer 2006 May; 6(5):392-401.

94. Zeisberg, M., and Neilson, E.G. 2009. Biomark- ers for epithelial-mesenchymal transitions. *J. Clin. Invest.* **119**:1429–1437.

95. Kern SE, Winter JM. Elegance, silence and nonsense in the mutations literature for solid tumours. Cancer Biol Ther 2006; 5:349–59.

96. Kim, K.K., M.C. Kugler, P.J. Wolters, L. Robillard, M.G. Galvez, A.N. Brumwell, D. Sheppard, and H.A. Chapman, Alveolar epithelial cell mesenchymal transition develops in vivo during pulmonary fibrosis and is regulated by the extracellular matrix. Proc Natl Acad Sci U S A, 2006. **103**(35): p. 13180-5.

97. Kim MP, Gallick GE. Gemcitabine resistance in pancreatic cancer: picking the key players. Clin Cancer Res. 2008 Mar 1; 14(5):1284-5.

98. Kindler, H. L. *et al.* Phase II trial of bevacizumab plus Gemcitabine in patients with advanced pancreatic cancer. *J. Clin. Oncol.* 23, 8033–8040 (2005).

99. Kindler, H. L. *et al.* A doubleblind, placebo controlled, randomized phase III trial of Gemcitabine (G) plus bevacizumab (B) versus Gemcitabine (G) plus placebo (P) in patients with advanced pancreatic cancer (PC). A preliminary analysis of cancer and Leukemia Group B (CALGB) 80303 [abstract]. *J. Clin. Oncol*. 25 (Suppl.), a4508 (2007).

100. Klautke Gunther , Brunner Thomas B, Radiotherapy in Pancreatic Cancer PurposeStrahlenther Onkol 2008;184:557–64

101. Kornmann M, Beger HG, Link KH. Chemosensitivity testing and test-directed chemotherapy in human pancreatic cancer. Recent Results Cancer Res. 2003;161:180–195.

102. Kulke MH, Blaszkowsky LS, Ryan DP, Clark JW, Meyerhardt JA, Zhu AX, et al. Capecitabine plus erlotinib in Gemcitabine-refractory advanced pancreatic cancer. *J Clin Oncol*. Oct 20 2007;25(30):4787-92

103. Kurose K, Gilley K, Matsumoto S, Watson PH, Zhou XP, Eng C. Frequent somatic mutations in PTEN and P53 are mutually exclusive in the stroma of Breast carcinomas.

104. Kurose, K., S. Hoshaw-Woodard, A. Adeyinka, S. Lemeshow, P.H. Watson, and C. Eng, Genetic model of multi-step breast carcinogenesis involving the epithelium and stroma: clues to tumour-microenvironment interactions. Hum Mol Genet, 2001. **10**(18): p. 1907-13.

105. Kroep JR, Loves WJ, van der Wilt CL, *et al*: Pretreatment deoxycytidine kinase levels predict in vivo gemcitabine sensitivity. Mol Cancer Ther 1: 371-376, 2002.

106. Lee C, Iafrate AJ, Brothman AR, Copy number variations and clinical cytogenetic diagnosis of constitutional disorders. Nat Genet. 2007 Jul; 39(7 Suppl):S48-54.

107. Lee, E.H. and C.K. Joo, Role of transforming growth factor-beta in transdifferentiation and fibrosis of lens epithelial cells. Invest Ophthalmol Vis Sci, 1999. **40**(9): p. 2025-32.

108. Lee HO, Mullins SR, Franco-Barraza J, Valianou M, Cukierman E, Cheng JD FAP-overexpressing fibroblasts produce an extracellular matrix that enhances invasive velocity and directionality of pancreatic cancer cells. BMC Cancer. 2011 Jun 13; 11:245.

109. Levy L, Hill CS. Smad4 dependency defines two classes of transforming growth factor {beta} (TGF-{beta}) target genes and distinguishes TGF-{beta}-induced epithelial-mesenchymal transition from its antiproliferative and migratory responses. *Mol Cell Biol* 2005; **25**: 8108-8125

110. Li Y, Laterra J. Cancer stem cells: distinct entities or dynamically regulatedphenotypes? Cancer Res. 2012 Feb 1;72(3):576-80.

111. Liau SS, Ashley SW, Whang EE. Lentivirus-mediated RNA interference of HMGA1 promotes chemosensitivity to Gemcitabine in pancreatic adenocarcinoma. JGastrointest Surg 2006; 10:1254^ 62.

112. Liotta, L.A. and E.C. Kohn, The microenvironment of the tumour-host interface. Nature, 2001.**411**(6835): p. 375-9

113. Little SE, Vuononvirta R, Reis-Filho JS, et al. Array CGH using whole genome amplification of fresh-frozen and formalin-fixed, paraffin embedded tumour DNA. Genomics 2006; 87:298–306.

114. Loehrer P, Powell M, Cardenes H. A randomized phase III study of Gemcitabine in combination with radiation therapy versus Gemcitabine alone in patients with localized, unresectable pancreatic cancer: E4201. *J Clin Oncol*. 2008; 26(15S):214(abstract 4506).

115. Lorusso Girieca · Rüegg Curzio The tumour microenvironment and its contribution to tumour evolution toward metastasis. Histochem Cell Biol (2008) 130:1091–1103.

116. Louvet C, Labianca R, Hammel P, Lledo G, Zampino MG, André T, Zaniboni A, Ducreux M, Aitini E, Taïeb J, Faroux R, Lepere C, de Gramont A; GERCOR; GISCAD. Gemcitabine in combination with oxaliplatin compared with gemcitabine alone in locally advanced or metastatic pancreatic cancer: results of a GERCOR and GISCAD phase III trial. J Clin Oncol. 2005 May 20; 23(15):3509-16.

117. Lowenfels AB, Maisonneuve P, Cavallini G, Ammann RW, Lankisch PG, Anderson JR et al. Pancreatitis and the risk of pancreatic cancer. International Pancreatitis Study Group. N Engl J Med. May 20 1993; 328(20):1433-7.

118. Lu J, Getz G, Miska EA, Alvarez-Saavedra E, Lamb J, Peck D, Sweet-Cordero A, Ebert BL, Mak RH, Ferrando AA, Downing JR, Jacks T, Horvitz HR, Golub TR. MicroRNA expression profiles classify human cancers. Nature. 2005 Jun 9;435(7043):834-8

119. Lukas J. A. C. Hawinkels,1 Hein W. Verspaget,1 Johan J. van der Reijden,1 Johanna M. van der Zon,Jan H. Verheijen,2 Daniel W. Hommes,1 Cornelis B. H. W. Lamers1 and Cornelis F. M. Sier1, /Online publication February 17, 2009.

120. Mackey JR, Mani RS, Selner M, Mowles D, Young JD, Belt JA, Crawford CR, Cass CE. Functional nucleoside transporters are required for gemcitabine influx and manifestation of toxicity in cancer cell lines. Cancer Res. 1998 Oct 1;58(19):4349-57

121. Mahadevan, D. & Von Hoff, D. D. Tumour–stroma interactions in pancreatic ductal adenocarcinoma. *Mol. Cancer Ther.* 6, 1186–1197 (2007).

122. Mahon PC, Baril P, Bhakta V, et al. S100A4 contributes to the suppression of BNIP3 expression, chemo-resistance, and inhibition of apoptosis in pancreatic cancer. Cancer Res 2007;67:6786^95

123. Maitra A, Hruban RH. A new mouse model of pancreatic cancer: PTEN gets its Akt together. Cancer Cell. 2005;8:171–172

124. Martinez-Outschoorn UE, Goldberg A, Lin Z, Ko YH, Flomenberg N, Wang C, Pavlides S, Pestell RG, Howell A, Sotgia F, Lisanti MP. Anti-estrogen resistance in breast cancer is induced by the tumour microenvironment and can be overcome by inhibiting mitochondrial function in epithelial cancer cells. Cancer Biol Ther. 2011 Nov 15; 12(10):924-38. Epub 2011 Nov 15.

125. Mehlen et al. Novel roles for slits and neutrins: Nature Cancer 11, 188-197(2011)

126. Merika EE, Syrigos KN, Saif MW. Desmoplasia in pancreatic cancer. Can we fight it? Gastroenterol Res Pract. 2012; 2012:781765.

127. Mellick, A.S., C.J. Day, S.R. Weinstein, L.R. Griffiths, and N.A. Morrison, Differential gene expression in breast cancer cell lines and stroma-tumour differences in microdissected breast cancer biopsies revealed by display array analysis. Int J Cancer, 2002. **100**(2): p. 172-80.

128. Michalski CW, Erkan M, Sauliunaite D, Giese T, Stratmann R, Sartori C, GieseNA, Friess H, Kleeff J. Ex vivo chemosensitivity testing and gene expressionprofiling predict response towards adjuvant gemcitabine treatment in pancreatic cancer. Br J Cancer. 2008 Sep 2; 99(5):760-7. 10.1038/sj.bjc.6604528

129. Micke, P., K. Kappert, M. Ohshima, C. Sundquist, S. Scheidl, P. Lindahl, C.H. Heldin, J. Botling, F. Ponten, and A. Ostman, In situ identification of genes regulated specifically in fibroblasts of human basal cell carcinoma. J Invest Dermatol, 2007. **127**(6): p. 1516-23.

130. Min Shi, Dang-Hui Yu, Ying Chen, Chen-Yan Zhao, Jing Zhang, Qing-Hua Liu, Can-Rong Ni, and Ming-Hua Zhu, Expression of fibroblast activation protein in human pancreatic adenocarcinoma and its clinicopathological significance; World J Gastroenterol. 2012 February 28; 18(8): 840–846

131. Mishra, P.J., R. Humeniuk, D.J. Medina, G. Alexe, J.P. Mesirov, S. Ganesan, J.W. Glod, and D. Banerjee, Carcinoma-associated fibroblast-like differentiation of human mesenchymal stem cells. Cancer Res, 2008. **68**(11): p. 4331-9.

132. Moinfar, F., Y.G. Man, L. Arnould, G.L. Bratthauer, M. Ratschek, and F.A. Tavassoli, Concurrent and independent genetic alterations in the stromal and epithelial cells of mammary carcinoma: implications for tumourigenesis. Cancer Res, 2000. **60**(9): p. 2562-6.

133. Mori-Iwamoto S, Kuramitsu Y, Ryozawa S, Taba K, Fujimoto M, Okita K, Nakamura K, Sakaida I. A proteomic profiling of gemcitabine resistance in pancreatic cancer cell lines. Mol Med Report. 2008 May-Jun; 1(3):429-34.

134. Moriyama T, Ohuchida K, Mizumoto K, Yu J, Sato N, Nabae T, Takahata S, Toma H, Nagai E, Tanaka M. MicroRNA-21 modulates biological functions of pancreatic cancer cells including their proliferation, invasion, and chemoresistance. Mol Cancer Ther. 2009 May;8(5):1067-74

135. Moore, M. J. *et al.* Comparison of Gemcitabine versus the matrix metalloproteinase inhibitor BAY12–9566 in patients with advanced or metastatic adenocarcinoma of the pancreas: a phase III trial of the National Cancer Institute of Canada Clinical Trials Group. *J. Clin. Oncol*. 21, 3296–3302 (2003).

136. Nakagawa, H., S. Liyanarachchi, R.V. Davuluri, H. Auer, E.W. Martin, Jr., A. de la Chapelle, and W.L. Frankel, Role of cancer-associated stromal fibroblasts in metastatic colon cancer to the liver and their expression profiles. Oncogene, 2004. **23**(44): p. 7366-77.

137. Nakahira S, Nakamori S, Tsujie M, Takahashi Y, Okami J, Yoshioka S, Yamasaki M, Marubashi S, Takemasa I, Miyamoto A, Takeda Y, Nagano H, Dono K, Umeshita K, Sakon M, Monden M. Involvement of ribonucleotide

reductase M1 subunit overexpression in gemcitabine resistance of human pancreatic cancer. Int J Cancer. 2007; 120:1355–1363.

138. NakanoY, Tanno S, Koizumi K, et al. Gemcitabine chemoresistance and molecular markers associated with Gemcitabine transport and metabolism in human pancreatic cancer cells. BrJCancer 2007; 96:457^63.

139. Nakatsu N, Yoshida Y, Yamazaki K, Nakamura T, Dan S, Fukui Y, Yamori T. Chemosensitivity profile of cancer cell lines and identification of genesdetermining chemosensitivity by an integrated bioinformatical approach using cDNA arrays. Mol Cancer Ther. 2005 Mar; 4(3):399-412.

140. Naotake Funamizu , Aikou Okamoto, Yuko Kamata , Takeyuki Misawa , Tadashi Uwagawa , Takeshi Gocho , Katsuhiko Yanaga , Yoshinobu Manome, Is the resistance of Gemcitabine for pancreatic cancer settled only by over expression of deoxycytidine kinase? Oncol Reports 2010 Feb; 23(2):471-5.

141. National Comprehensive Cancer Network. NCCN Clinical Practice Guidelines in Oncology. Pancreatic Adenocarcinoma, v.2.2011. Available at http://www.nccn.org/professionals/physician_gls/pdf/pancreatic.pdf

142. Neff T and Blau CA: Forced expression of cytidine deaminase confers resistance to cytosine arabinoside and gemcitabine. Exp Hematol 24: 1340-1346, 1996.

143. Ng SS, Tsao MS, Chow S, Hedley DW. Inhibition of phosphatidylinositide 3-kinase enhances Gemcitabine- induced apoptosis in human pancreatic cancer cells. Cancer Res 2000; 60:5451^ 5.

144. Ng SS, Tsao MS, NickleeT, Hedley DW.Wortmannin inhibits pkb/akt phosphorylation and promotes Gemcitabine antitumour activity in orthotopic human pancreatic cancer xenografts in immunodeficient mice. Clin Cancer Res 2001; 7:3269^75.

145. Oettle H, Richards D, Ramanathan RK, van Laethem JL, Peeters M, Fuchs M, Zimmermann A, John W, Von Hoff D, Arning M, Kindler HL. A phase III trial of pemetrexed plus gemcitabine versus gemcitabine in patients with unresectable or metastatic pancreatic cancer. Ann Oncol. 2005 Oct; 16(10):1639-45. Epub 2005 Aug 8. Erratum in: Ann Oncol. 2006 Mar; 17(3):535.

146. Oldfield, M.D., L.A. Bach, J.M. Forbes, D. Nikolic-Paterson, A. McRobert, V. Thallas, R.C. Atkins, T. Osicka, G. Jerums, and M.E. Cooper, Advanced glycation end products cause epithelial-myofibroblast transdifferentiation via the receptor for advanced glycation end products (RAGE). J Clin Invest, 2001. 108(12): p. 1853-63.

147. Olive KP, Jacobetz MA, Davidson CJ, Gopinathan A, McIntyre D, Honess D, Madhu B, Goldgraben MA, Caldwell ME, Allard D, Frese KK, Denicola G, Feig C, Combs C, Winter SP, Ireland-Zecchini H, Reichelt S, Howat WJ, Chang A, Dhara M, Wang L, Rückert F, Grützmann R, Pilarsky C, Izeradjene K, Hingorani SR, Huang P, Davies SE, Plunkett W, Egorin M, Hruban RH, Whitebread N, McGovern K, Adams J, Iacobuzio-Donahue C, Griffiths J, Tuveson DA, Inhibition of hedgehog signalling enhances delivery of chemotherapy in a mouse model of pancreatic cancer. Science 12 June 2009: 1457-1461.

148. Olumi AF, et al. Carcinoma-associated fibroblasts direct tumour progression of initiated human prostatic epithelium. *Cancer Res.* 1999; 59:5002–11.

149. Orimo A, Weinberg RA. Stromal fibroblasts in cancer: a novel tumour promoting cell type. Cell Cycle 2006; 5:1597-601.

150. A. Orimo[2], P.B. Gupta, D.C. Sgroi *et al.* Stromal fibroblasts present in invasive human breast carcinomas promote tumour growth and angiogenesis through elevated SDF-1/CXCL12 secretion; Cell, 121 (3) (2005), pp. 335–348

151. P.Innocenti, T. Giese, N. Giese, M.W. Buchler, and H. Friess, Desmoplastic reaction influences pancreatic cancer growth behaviour. World J Surg, 2004. **28**(8): p. 818-25.

152. P. Kim and Gary E. Gallick, Gemcitabine Resistance in Pancreatic Cancer: Picking the Key Players, Michael *Clin Cancer Res 2008; 14:1284-1285. Published online March 3, 2008.*

153. Pageau SC, Sazonova OV, Wong JY, Soto AM, Sonnenschein C**,** The effect of stromal components on the modulation of the phenotype of human bronchial epithelial cells in 3D culture. Biomaterials. 2011 Oct; 32(29):7169-80. Epub 2011 Jul 2.

154. Paget, S., Lancet, 1889. **1**: p. 571-573.

155. Paterson, R.F., T.M. Ulbright, G.T. MacLennan, S. Zhang, C.X. Pan, C.J. Sweeney, C.R. Moore, R.S. Foster, M.O. Koch, J.N. Eble, and L. Cheng, Molecular genetic alterations in the laser-capture-microdissected stroma adjacent to bladder carcinoma. Cancer, 2003. **98**(9): p. 1830-6.

156. Patocs A, Zhang L, Xu Y, Weber F, Caldes T, Mutter GL, et al. Breast-cancer stromal cells with TP53 mutations and nodal metastases. N Engl J Med 2007 Dec 20; 357(25):2543-51

157. Patrick S. Moore , Bence Sipos , Simonetta Orlandini ,Claudio Sorio , Francisco X. Real, Nicholas R. Lemoine, Thomas Gress, Claudio Bassi, Günter Klöppel, Holger Kalthoff, Hendrik Ungefroren, Matthias Löhr, Aldo Scarpa, Virchows Genetic profile of 22 pancreatic carcinoma cell lines. Analysis of K-ras, p53, p16 and DPC4/Smad4, Arch (2001) 439:798–802

158. Pelzer, U. *et al.* A randomized trial in patients with Gemcitabine refractory pancreatic cancer. Final results of the CONKO 003 study [abstract]. *J. Clin. Oncol.* 26 (Suppl.), a4508 (2008).

159. Petersen, O.W., H.L. Nielsen, T. Gudjonsson, R. Villadsen, F. Rank, E. Niebuhr, M.J. Bissell, and L. Ronnov-Jessen, Epithelial to mesenchymal transition in human breast cancer can provide a non-malignant stroma. Am J Pathol, 2003 **162**(2): p. 391-402.

160. Pickard A, Cichon AC, Barry A, Kieran D, Patel D, Hamilton P, Salto-Tellez M, James J, McCance DJ, Inactivation of Rb in stromal fibroblasts promotes epithelial cell invasion; EMBO J. 2012 May 29.

161. Pilarsky C, Ammerpohl O, Sipos B, Dahl E, Hartmann A, Wellmann A, et al. Activation of Wnt signalling in stroma from pancreatic cancer identified by gene expression profiling10. J Cell Mol Med 2008 Dec; 12(6B):2823-35.

162. Pisters PW, Abbruzzese JL, Janjan NA, Cleary KR, Charnsangavej C, Goswitz MS. Rapid-fractionation preoperative chemoradiation,

pancreaticoduodenectomy, and intraoperative radiation therapy for resectable pancreatic adenocarcinoma. *J Clin Oncol*. Dec 1998; 16(12):3843-50.

163. Pisters PW, Wolff RA, Janjan NA, Cleary KR, Charnsangavej C, Crane CN. Preoperative paclitaxel and concurrent rapid-fractionation radiation for resectable pancreatic adenocarcinoma: toxicities, histologic response rates, and event-free outcome. *J Clin Oncol*. May 15 2002; 20(10):2537-44.

164. Poplin E, Feng Y, Berlin J, Rothenberg ML, Hochster H, Mitchell E, Alberts S, O'Dwyer P, Haller D, Catalano P, Cella D, Benson AB 3rd. Phase III, randomized study of gemcitabine and oxaliplatin versus gemcitabine (fixed-dose rate infusion) compared with gemcitabine (30-minute infusion) in patients with pancreatic carcinoma E6201: a trial of the Eastern Cooperative Oncology Group. J Clin Oncol. 2009 Aug 10; 27(23):3778-85.

165. Qiu, W., M. Hu, A. Sridhar, K. Opeskin, S. Fox, M. Shipitsin, M. Trivett, E.R. Thompson, M. Ramakrishna, K.L. Gorringe, K. Polyak, I. Haviv, and I.G. Campbell, No evidence of clonal somatic genetic alterations in cancer-associated fibroblasts from human breast and ovarian carcinomas. Nat Genet, 2008. **40**(5): p. 650-5

166. Rahnama F, Shimokawa T, Lauth M, Finta C, Kogerman P, Teglund S, Toftgard R and Zaphiropoulos PG (2006). "Inhibition of GLI1 gene activation by Patched1"]. Biochem *J* **394** (Pt 1): 19–26.

167. Raimondi S, Maisonneuve P, Lowenfels AB. Epidemiology of pancreatic cancer: an overview. Nat Rev Gastroenterol Hepatol. Dec 2009;6(12):699-708

168. Raut CP, Evans DB, Crane CH, et al. Neoadjuvant therapy for resectable pancreatic cancer. Surg Oncol Clin N Am 2004; 13:639–61, ix.

169. Reinhart, B. J. et al. The 21-nucleotide let-7 RNA regulates developmental timing in Caenorhabditiselegans.Nature403,901–-906(2000).

170. Riess, H. *et al.* A randomised, prospective, multicenter, phase III trial of gemcitabine, 5fluorouracil (5FU), folinic acid vs. Gemcitabine alone in patients with advanced pancreatic cancer [abstract]. *J. Clin. Oncol.* 23 (Suppl. 16), a4009 (2005).

171. Rocha Lima CM, Green MR, Rotche R, Miller WH Jr, Jeffrey GM, Cisar LA, Morganti A, Orlando N, Gruia G, Miller LL. Irinotecan plus gemcitabine results in no survival advantage compared with gemcitabine monotherapy in patients with locally advanced or metastatic pancreatic cancer despite increased tumour response rate. J Clin Oncol. 2004 Sep 15; 22(18):3776-83. PubMed PMID: 15365074.

172. Ronnov-Jessen, L., O.W. Petersen, V.E. Koteliansky, and M.J. Bissell, The origin of the myofibroblasts in breast cancer. Recapitulation of tumour environment in culture unravels diversity and implicates converted fibroblasts and recruited smooth muscle cells. J Clin Invest, 1995. **95**(2): p. 859-73.

173. Rulifson IC, Karnik SK, Heiser PW, ten Berge D, Chen H, Gu X, Taketo MM, Nusse R, Hebrok M, Kim SK. Wnt signaling regulates pancreatic beta cell proliferation. Proc Natl Acad Sci USA. 2007; 104:6247–6252.

174. Sebens S, Schäfer H. The Tumour Stroma as Mediator of Drug Resistance - A Potential Target to Improve Cancer Therapy? Curr Pharm Biotechnol. 2011 May 24

175. Sangai, T., G. Ishii, K. Kodama, S. Miyamoto, Y. Aoyagi, T. Ito, J. Magae, H. Sasaki, T. Nagashima, M. Miyazaki, and A. Ochiai, Effect of differences in cancer cells and tumour growth sites on recruiting bone marrow-derived endothelial cells and myofibroblasts in cancer-induced stroma. Int J Cancer, 2005. 115(6): p. 885-92.

176. Santos AM, Jung J, Aziz N, Kissil JL, Puré E, Targeting fibroblast activation protein inhibits tumour stromagenesis and growth in mice. Clin Invest. 2009 Dec; 119(12):3613-25. doi: 10.1172/JCI38988

177. Sasaki S, Yamamoto H, Kaneto H, Ozeki I, Adachi Y, Takagi H, Matsumoto T, Itoh H, Nagakawa T, Miyakawa H, et al. Differential roles of alterations of p53, p16, and SMAD4 expression in the progression of intraductal papillary-mucinous tumours of the pancreas. Oncol Rep. 2003;10:21–25

178. Sato N, Maehara N, Goggins M. Gene expression profiling of tumour stromal interactions between pancreatic cancer cells and stromal fibroblasts. Cancer Res 2004 Oct 1; 64(19):6950-6.

179. Schutte M, Rozenblum E, Moskaluk CA, Guan X, Hoque AT, Hahn SA, da Costa LT, de Jong PJ, Kern SE. An integrated high-resolution physical map of the DPC/BRCA2 region at chromosome 13q12. *Cancer Res* 1995; **55**: 4570-4574

180. Shi C, Daniels JA, Hruban RH. Molecular characterization of pancreatic neoplasms. *Adv Anat Pathol*. Jul 2008;15(4):185-95

181. Shinawi M, Cheung Sau Wai. The array CGH and its clinical applications. Drug discoveries today, Volume 13, Issues 17–18, September 2008, 760–770

182. Sieben NL, ter Haar NT, Cornelisse CJ, Fleuren GJ, Cleton-Jansen AM. PCR artefacts in LOH and MSI analysis of microdissected tumour cells. Hum Pathol 2000; 31:1414–9.

183. Singer, C.F., D. Gschwantler-Kaulich, A. Fink-Retter, C. Haas, G. Hudelist, K. Czerwenka, and E. Kubista, Differential gene expression profile in breast cancer-derived stromal fibroblasts. Breast Cancer Res Treat, 2008. **110**(2): p. 273-81.

184. Spratlin J, Sangha R, Glubrecht D, Dabbagh L, Young JD, Dumontet C, Cass C, Lai R and Mackey JR: The absence of human equilibrative nucleoside transporter 1 is associated with reduced survival in patients with gemcitabine treated pancreas adenocarcinoma. Clin Cancer Res 10: 6956-6961, 2004.

185. Stathis, A. & Moore, M. J. advanced pancreatic carcinoma: current treatment and future challenges, *Nat. Rev. Clin. Oncol.* 7, 163–172 (2010)

186. Sobral LM, Bufalino A, Lopes MA, Graner E, Salo T, Coletta RD, Myofibroblasts in the stroma of oral cancer promote tumourigenesis via secretion of activin A, Oral Oncol. 2011 Sep; 47(9):840-6.

187. Sotgia F, Martinez-Outschoorn UE, Howell A, Pestell RG, Pavlides S, Lisanti MP. Caveolin-1 and cancer metabolism in the tumour microenvironment:

markers, models, and mechanisms. Annu Rev Pathol. 2012; 7:423-67. Epub 2011 Nov 7.

188. Soto JL, Barbera VM, Saceda M, Carrato A. Molecular biology of exocrine pancreatic cancer. *Clin Transl Oncol*. May 2006; 8:306-12.

189. Sperti C, Pasquali C, Piccoli A, Pedrazzoli S. Recurrence after resection for ductal adenocarcinoma of the pancreas. World J Surg 1997; 21:195-200.

190. Stathopoulos GP, Syrigos K, Aravantinos G, Polyzos A, Papakotoulas P, Fountzilas G, Potamianou A, Ziras N, Boukovinas J, Varthalitis J, Androulakis N, Kotsakis A, Samonis G, Georgoulias V. A multicenter phase III trial comparing irinotecan-gemcitabine (IG) with gemcitabine (G) monotherapy as first-line treatment in patients with locally advanced or metastatic pancreatic cancer. Br J Cancer. 2006 Sep 4; 95(5): 587-92.

191. Sultana, A. *et al.* Systematic review, including metaanalyses, on the management of locally advanced pancreatic cancer using radiation/ combined modality therapy. *Br. J. Cancer* 96, 1183–1190 (2007).

192. Szafranska AE, Davison TS, John J, Cannon T, Sipos B, Maghnouj A, Labourier E, Hahn SA. MicroRNA expression alterations are linked to tumorigenesis and non-neoplastic processes in pancreatic ductal adenocarcinoma. Oncogene. 2007 Jun 28;26(30):4442-52

193. Taipale J, Cooper MK, Maiti T, and Beachy PA (2002). "Patched acts catalytically to suppress the activity of Smoothened"]. *Nature* 418 (6900): 892–897.

194. Takahashi K, Okita K, Nakagawa M, Yamanaka S. Induction of pluripotent stem cells from fibroblast cultures. Nat Protoc. 2007;2(12):3081-9.

195. Tan DS, Lambros MB, Natrajan R, Reis-Filho JS. Getting it right: designing microarray (and not 'microawry') comparative genomic hybridization studies for cancer research. Lab Invest. 2007 Aug; 87(8):737-54.

196. Thayer SP, di Magliano MP, Heiser PW, et al. Hedgehog is an early and late mediator of pancreatic cancer tumourigenesis. Nature 2003; 425:851–6.

197. Tomasek, J.J., G. Gabbiani, B. Hinz, C. Chaponnier, and R.A. Brown, Myofibroblasts and mechano-regulation of connective tissue remodelling. Nat Rev Mol Cell Biol, 2002. **3**(5): p.349-63.

198. Trimboli AJ, Cantemir-Stone CZ, Li F, Wallace JA, Merchant A, Creasap N, Thompson JC, Caserta E,Wang H, Chong JL, Naidu S, Wei G, Sharma SM, Stephens JA, Fernandez SA, Gurcan MN, Weinstein MB, Barsky SH, Yee L, Rosol TJ, Stromberg PC, Robinson ML, Pepin F, Hallett M, Park M, Ostrowski MC, Leone G (2009) Pten in stromal fibroblasts suppresses mammary epithelial

199. Tumours. Nature 461:1084–1091

200. Tuhkanen H, Anttila M, Kosma VM, Heinonen S, Juhola M, Helisalmi S, et al. Frequent gene dosage alterations in stromal cells of epithelial ovarian carcinomas. Int J Cancer 2006 Sep 15; 119(6):1345-53

201. Ueda S, Hatsuse K, Tsuda H, Ogata S, Kawarabayashi N, Takigawa T, Einama T, Morita D, Fukatsu K, Sugiura Y, Matsubara O, Mochizuki H.

Potential crosstalk between insulin-like growth factor receptor type 1 and epidermal growth factor receptor in progression and metastasis of pancreatic cancer. Mod Pathol. 2006 Jun;19(6):788-96.

202. Valencia-Sanchez MA, Liu J, Hannon GJ, Parker R. Control of translation anmRNA degradation by miRNAs and siRNAs. Genes Dev. 2006 Mar 1;20(5):515-24. Review

203. Van Cutsem, E. *et al.* Phase III trial of Gemcitabine plus tipifarnib compared with Gemcitabine plus placebo in advanced pancreatic cancer. *J. Clin. Oncol.* 22, 1430–1438 (2004).

204. Vervenne W, Bennouna J, Humblett Y. A randomized double-blind, placebo (P) controlled multicenter phase III trial to evaluate the efficacy and safety of adding bevacizumab (B) to erlotinib (E) and Gemcitabine (G) in patients (pts) with metastatic pancreatic cancer. *J Clin Oncol*. 2008; 26(15S):214s (abstract 4507).

205. Von Hoff DD, Ramanathan RK, Borad MJ, Laheru DA, Smith LS, Wood TE, Korn RL, Desai N, Trieu V, Iglesias JL, Zhang H, Soon-Shiong P, Shi T, Rajeshkumar NV, Maitra A, Hidalgo M. Gemcitabine plus nab-paclitaxel is an active regimen in patients with advanced pancreatic cancer: a phase I/II trial. J Clin Oncol. 2011 Dec 1; 29(34):4548-54.

206. Vonlaufen A, Joshi S, Qu C, Phillips PA, Xu Z, Parker NR, Toi CS, Pirola RC, WilsonJS, Goldstein D, Apte Pancreatic stellate cells: partners in crime with pancreatic cancer, MV Cancer Res 2008;68:2085-2093

207. Walter K, Omura N, Hong SM, Griffith M, Goggins M. Pancreatic cancer associated fibroblasts display normal allelotypes. Cancer Biol Ther 2008 Jun; 7(6):882-8.

208. Watanabe I, Hasebe T, Sasaki S, Konishi M, Inoue K, Nakagohri T, et al. Advanced pancreatic ductal cancer: fibrotic focus and beta-catenin expression correlate with outcome. Pancreas 2003 May; 26(4):326-33.

209. F, SHen I, Fukino K et al. Total genome analysis of BRAC1/2-related invasive carcinomas of the breast identifies tumour stroma as potential landscaper for neoplastic initiation. Am J Hum Genet 2006; 78:961-72

210. Weber F, Xu Y, Zhang L et al. Microenvironmental genomic alterations and clinicopathological behaviour in head and neck squamous cell carcinomas. JAMA 2007; 297: 187-95

211. WHO Cancer";Who.int.Retrieved 2009-09-15

212. Winter JM, Brody JR, Kern SE. Multiple-criterion evaluation of reported mutations: a proposed scoring system for the intragenic somatic mutation literature. Cancer Biol Ther 2006;5:360-70

213. Xue Y, Abou Tayoun AN, Abo KM, Pipas JM, Gordon SR, Gardner TB, Barth RJ Jr,Suriawinata AA, Tsongalis GJ. MicroRNAs as diagnostic markers for pancreaticductal adenocarcinoma and its precursor, pancreatic intraepithelial neoplasm. Cancer Genet. 2013 Jun;206(6):217-21.

214. Yauch RL, Gould SE, Scales SJ, Tang T, Tian H, Ahn CP, Marshall D, Fu L, Januario T, Kallop D, Nannini-Pepe M, Kotkow K, Marsters JC, Rubin LL, de

Sauvage FJ, A paracrine requirement for hedgehog signalling in cancer**,** Nature. 2008 Sep 18; 455(7211):406-10.

215. Yen, T.W., N.P. Aardal, M.P. Bronner, D.R. Thorning, C.E. Savard, S.P. Lee, and R.H. Bell, Jr., Myofibroblasts are responsible for the desmoplastic reaction surrounding human pancreatic carcinomas. Surgery, 2002. **131**(2): p. 129-34.

216. Zavoral M, Minarikova P, Zavada F, Salek C, Minarik M. Molecular biology of pancreatic cancer. World J Gastroenterol. 2011 Jun 28; 17(24):2897-908.

217. Zhao Y, Shen S, Guo J, Chen H, Greenblatt DY, Kleeff J, Liao Q, Chen G, Friess H, Leung PS. Mitogen-activated protein kinases and chemo-resistance in pancreatic cancer cells. J Surg Res. 2006 Dec; 136(2):325-35. Epub 2006 Oct 19.

218. Zeisberg, M., and Neilson, E.G. 2009. Biomark- ers for epithelial-mesenchymal transitions. *J. Clin. Invest.* **119**:1429–1437.